EVALUATION OF UNCERTAINTIES IN MOFAT FOR TIER 3 RBCA

AMIR ALI KHAN

EVALUATION OF UNCERTAINTIES IN MOFAT FOR TIER 3 RBCA

by

©Amir Ali Khan

A Thesis submitted to the School of Graduate Studies
in partial fulfillment of the requirement for the degree of
Doctor of Philosophy in Engineering

Faculty of Engineering and Applied Science

Memorial University of Newfoundland

January 13, 2006

St. John's, Newfoundland and Labrador, Canada

Executive Summary

The description and characterization of parametric uncertainty in the modeling process is a required component of risk assessment and is of paramount importance for Tier 3 Risk Based Corrective Action (RBCA) of petroleum-contaminated sites. The parametric uncertainty associated with the modeling process is propagated through the risk assessment computations and failure to characterize this uncertainty in multi-phase multi-component flow and transport modeling outputs results in an inaccurate risk assessment.

The primary aim of this study was to improve quantification of parametric uncertainties by developing a comprehensive framework for the uncertainty and sensitivity analysis of a fate and transport model that has wide spread application in Tier 3 RBCA of petroleum contaminated sites. The fate and transport model selected for this study was the U.S. EPA two-dimensional multi-phase multi-component fate and transport model – MOFAT. It is one of the few finite element models available from the U.S. EPA to model multi-phase and multi-component fate and transport. MOFAT was selected after screening Tier 3 RBCA numerical models against four criteria that required the selected model to be a finite element multi-phase multi-component fate and transport model; a public domain code with detailed documentation; peer reviewed and validated; and identified as a Tier 3 RBCA code by the American Society of Testing and Materials.

The specific objectives of this research were: (1) to conduct a bench mark parametric uncertainty analysis of MOFAT using Random Sampling based Monte Carlo and to evaluate the applicability and performance of various uncertainty analysis techniques to MOFAT; (2) to develop the computational tools required to undertake an uncertainty analysis of MOFAT; (3) to quantify the uncertainty in estimates of exposure due to variability in input parameters; (4) to evaluate the applicability and performance of various sensitivity analysis techniques to MOFAT; (5) to identify sensitive parameters and issues that need to be addressed when using MOFAT; (6) to use the information gained from the previous five objectives to develop a framework for uncertainty and sensitivity analysis of MOFAT and; (7) to identify areas of additional research so that uncertainty in MOFAT estimates can be better understood and quantified.

To ensure that the objectives of this research study were met, a comprehensive parametric uncertainty analysis study was formulated and implemented. The uncertainty analysis techniques evaluated were Random Sampling based Monte Carlo (RS-MC), Monte Carlo with Latin Hypercube sampling (LHS-MC), Monte Carlo using a Response Surface Methodology (RSM-MC) based replacement model and Monte Carlo using a Neural Network (NN-MC) based replacement model. LHS-MC was able to accurately replicate the cumulative distribution function (*cdf*)generated by RS-MC with greater efficiency. RSM-MC and NN-MC were not able to accurately approximate MOFAT outputs for uncertainty analysis.

A set of computational tools required to undertake an uncertainty analysis of MOFAT were also developed as a part of this study. A Monte Carlo version of MOFAT called MC-MOFAT was also developed by modifying the original FORTRAN code for

MOFAT. A pre-processing FORTRAN tool was developed to allow automated generation of MOFAT input files from text files listing all MC or LHS samples. Similarly a Visual Basic based post-processing tool was developed to automatically extract the results for a specified node and time step from MC-MOFAT output files.

An extensive sensitivity analysis of MOFAT was also accomplished. Sensitive parameters were identified through the application of sampling based statistical measures on the set of LHS-MC inputs and outputs. Scatter plots of each of the twelve MOFAT outputs versus the probabilistic input parameters indicated that all the outputs displayed a monotonic dependence on the input parameters; saturated conductivity, K_{sw}, and the van Genuchten retention parameters, α, and n. A slight dependence between all the outputs and the input parameter, apparent irreducible water saturation, S_m was also apparent. Dependencies between input parameters and MOFAT outputs were also evaluated using four different measures of correlation (Pearson's r, Spearman's ρ, Partial Correlation Coefficient and Partial Rank Correlation Coefficient). While all the tests do not always concur, in general all the outputs are correlated with K_{sw}, α, n and to a lesser degree S_m. The variation in correlations as detected by the four different tests is a function of the different testing powers of the tests, complexity of MOFAT and the correlations between the probabilistic input parameters (where K_{sw} is positively correlated with S_m, α and n.)

Interactions between the input parameters were identified using RSM models. For all phases of Benzene, Toluene, Ethyl benzene, and Xylene, interactions were identified between K_{sw} and ϕ and between ϕ and α. For the gas phases of Benzene and Toluene and all phases of Ethyl-benzene and Xylene an additional interaction was identified between K_{sw} and α.

To assign priorities to the input variables for reducing uncertainties, MOFAT input variables were ranked on the relative size of the absolute value of the Partial Rank Correlation Coefficients (PRCC). They were also grouped into three categories of decreasing significance based on critical values of the PRCC analysis. Using a new approach developed in this study the input variables were first grouped into four groups on the basis of the critical values of the PRCC and then within each group they were relatively ranked based on the relative size of absolute value of the PRCC. The higher ranked inputs within the lower critical value groups will have the most influence on the calibration and predictions and should be the focus of field investigation and calibration efforts.

Drawing on the results of the uncertainty and sensitivity analysis, a comprehensive six-step framework for uncertainty and sensitivity analysis of MOFAT was developed. This study has provided the community of MOFAT users with a comprehensive framework for uncertainty and sensitivity analysis of MOFAT. This framework not only lays out a methodology for uncertainty and sensitivity analysis of MOFAT but it also provides the tools required to conduct such an analysis.

Within the context of Tier 3 RBCA the framework and supporting tools developed will make it possible for MOFAT users to conduct comprehensive uncertainty and sensitivity

analysis of their simulation scenarios. The framework is also crucial for undertaking any further uncertainty or sensitivity research on MOFAT. Additional areas of research identified in this study to address uncertainty in Tier 3 RBCA fate and transport modeling were: improving the input covariance matrix to better account for input parameter correlations; incorporating component properties as probabilistic inputs in the uncertainty analysis; evaluating the applicability of SRSM-ADIFOR as an uncertainty analysis technique for MOFAT; further study of interactions between ϕ and α and between K_{sw} and α; extending the uncertainty analysis in this study to other Tier 3 RBCA Models; and studying the effect of scaling up of input parameters in the context of uncertainty analysis of MOFAT.

Acknowledgements

I thank God Almighty, the most Gracious, the most Merciful for his blessings and guidance.

I thank my supervisor Dr. Tahir Husain for his supervision; his patience, help and support; and for introducing me to the world of risk assessment. I thank my co-supervisor Dr. Leonard Lye for his enlightening guidance on statistical issues and for initiating me to the world of simulation statistics. I also thank Dr. Cynthia Coles of my supervisory committee for her review of my thesis.

I also thank Dr. Mahmoud Haddara for his help, support and advice. Many thanks are also extended to Ed Gellately of the Department of Computing Sciences for his guidance on VMS machine constants; Dr. A. K. Katyal for sharing with me some valuable insights into MOFAT; M.J. Shortencarier for help on the LHS code; and R. F Carsel for help in trying to locate his soil database.

I thank the School of Graduate Studies and the Faculty of Engineering and Applied Science, Memorial University of Newfoundland for the financial support extended to me in the earlier years of this research work. NSERC funding in the initial stages of this research is also appreciated.

I thank the staff of the computing section of the Faculty of Engineering and Applied Science for the extensive computing resources and support that were extended to me, especially the unbridled use of the Unix workstation CRUNCH without which this work would not have been possible. I particularly thank Philip van Ulden for his help in setting up the all-critical back up system for my simulations. I also thank Randy Dodge at University Computing Services for use of the Unix workstation PLATO for some of the simulations.

I thank the Newfoundland and Labrador Department of Environment and Conservation for allowing me to pursue this research and for accommodating my research needs. I particularly thank my colleagues for their support.

I thank all my friends, who are too many to name individually here, for their support, company and advice over the years.

Lastly, but not the least, sincere thanks are due to my wife Baasra for her love, support and patience; my parents for their love and support; my son Faris for being an amazingly quiet infant; and my daughter Mahiba who sacrificed the most for this work.

Table of Contents

List of Tables

List of Figures

List of Appendices

List of Acronyms and Abbreviations

2 D	Two Dimensional
3 D	Three Dimensional
3MRA	Multimedia, Multipathway, and Multireceptor Risk Assessment
alpha	van Genuchten air-water capillary retention parameter, α
ANOVA	Analysis of Variance
ASTM	American Society for Testing and Materials
BPNN	Back Propagation Neural Network
BTEX	Benzene, Toluene, Ethyl-Benzene and Xylene
CCD	Central Composite Design
cdf	Cumulative Distribution Function Plot
FAST	Fourier Amplitude Sensitivity Test
FORM	First Order Reliability Method
G	Gas Phase
GRNN	General Regression Neural Network
K	Hydraulic Conductivity, K_{sw}
LHS	Latin Hypercube Sampling. Also used to designate the 100 sample Latin Hypercube Sample used in this study
LHS300	300 sample Latin Hypercube Sample
LHS500	500 sample Latin Hypercube Sample
LHS-c	100 sample Latin Hypercube Sample with induced correlation between Hydraulic conductivity and maximum residual oil saturation for water, S_{or}
LHS-K	100 sample Latin Hypercube Sample with vertical to horizontal Hydraulic conductivity ratio of 1:2

LHS-MC	Latin Hypercube Sampling Monte Carlo
LHS-p	100 sample Latin Hypercube Sample with induced correlation between Hydraulic conductivity and porosity,
LHS-s	35 sample Latin Hypercube Sample
LNAPL	Light Non Aqueous Phase Liquid
Max s	Apparent irreducible water saturation, S_m
MC	Monte Carlo
MC-MOFAT	Monte Carlo Version of MOFAT developed in this study
Mtheta	Maximum residual oil saturation for water, S_{or}
N	van Genuchten air-water capillary retention parameter, n
NAPL	Non Aqueous Phase Liquid
NN	Neural Network
NN-MC	Monte Carlo Neural Network
O	Oil Phase
PC	Personal Computer
PCC	Partial Rank Correlation Coefficient
PRCC	Partial Rank Correlation Coefficient
PRZM	Pesticide Root Zone Model
RBCA	Risk Based Corrective Action
RI-FS	Remedial Investigation - Feasibility Study remediation approach
RSM	Response Surface Model/ Response Surface Methodology
RS-MC	Random Sampling Monte Carlo
RSM-MC	Response Surface Model Monte Carlo
S	Solid Phase
SCS	Soil Conservation Service

SORM	Second Order Reliability Method
SRSM-ADIFOR	Stochatic Response Surface Method - Automatic DIfferentiation of FORtran
U.S. EPA	United States Environmental Protection Agency
VBA	Visual Basic for Applications
W	Water Phase

List of Symbols

$\bar{q}_p$	Absolute magnitude of the p phase velocity
η_{rp}	Absolute viscosity ratio between phase p and water
h_{ao}	Air-Oil capillary pressure head
h_{aw}	Air-Water capillary pressure head
$\mu_{\alpha p}$	Apparent first-order decay rate coefficient in phase p
$\mu_{\alpha a}$	Apparent first-order decay rate coefficient in the gaseous phase
$\mu_{\alpha o}$	Apparent first-order decay rate coefficient in the oil phase
$\mu_{\alpha s}$	Apparent first-order decay rate coefficient in the solid phase
$\mu_{\alpha w}$	Apparent first-order decay rate coefficient in the water phase
S_m	Apparent irreducible water saturation,
$\overline{\overline{S_w}}$	Apparent water saturation
x_i (and x_j)	Cartesian spatial coordinates (i,j =1,2)
$C_{\alpha p}$	Concentration of the non inert component α in p-phase
q_{pi}	Darcy velocity of phase p in the i-direction
ρ_p	Density of phase p
ρ'_w	Density of pure water
$D^o_{\alpha p}$	Diffusion coefficient of α in the bulk p-phase
$\overline{S}_t$	Effective total liquid saturation
$\overline{S}_{ot}$	Effective trapped oil saturation
$\overline{S}_w$	Effective water saturation
z	Elevation

$\Gamma_{\alpha a}$	Equilibrium partition coefficient for species α between air-water phases
$\Gamma_{\alpha o}$	Equilibrium partition coefficient for species α between oil-water phases
$\Gamma_{\alpha s}$	Equilibrium partition coefficient for species α between solid-water phases
$\Gamma_{\alpha p}$	Equilibrium partition coefficient for species α between water and organic liquid (Raoult's constant), gas (dimensionless Henry's constant), and solid phases
g	Gravitational acceleration
S_m	Irreducible water saturation
δ_{ij}	Kronecker's delta
A_L	Longitudinal dispersivity
$J_{\alpha p_i}$	Mass flux density of α in p-phase per porous medium cross-section in the i-direction
S_{or}	Maximum residual oil saturation for water
θ_m	Maximum water content
D_{pij}^{hyd}	Mechanical dispersion coefficient
$D_{\alpha p}^{dif}$	Molecular diffusion coefficient of component α in the porous medium
R_p	Net mass transfer per unit porous media volume into (+) or out of (-) phase p
$R_{\alpha p}$	Net mass transfer rate per porous medium volume of species α into or out of the p-phase
$\gamma_{\alpha p}$	Net production or decay of component α within p-phase per porous medium volume due to reactions within the p-phase.
g_{sp}	Non dilute solution correction factor
S_o	Oil phase saturation
h_{ow}	Oil-Water capillary pressure head

S_p	p- phase saturation
S_p	p- phase saturation
ϕ	Porosity
K_p	p-phase hydraulic conductivity tensor
P_p	p-phase pressure
ρ_{rp}	p-phase specific gravity
k_{rp}	Relative permeability of phase p
θ_r	Residual water content
K_{sw}	Saturated hydraulic conductivity to water
$K sw_x$	Saturated hydraulic conductivity to water in the horizontal direction
$K sw_z$	Saturated hydraulic conductivity to water in the vertical direction
$K_{sw_{ij}}$	Saturated hydraulic conductivity tensor for water
β_{ao}	Scaling coefficient approximated by the ratio of water surface tension to oil surface tension
β_{ow}	Scaling coefficient approximated by the ratio of water surface tension to oil-water interfacial tension
$c_{\alpha s}$	Solid phase concentration expressed as mass of adsorbed component α per porous medium volume
t	Time
A_T	Transverse dispersivity
U_j	Unit gravitational vector measured positive upwards
α	van Genuchten air-water capillary retention parameter
n	van Genuchten air-water capillary retention parameter
h_p	Water height-equivalent pressure head of phase
S_w	Water phase saturation

Chapter 1. Introduction

1.1 Background to Study

Numerous releases of petroleum hydrocarbons have occurred at sites all over the world. The myriad nature of the contaminants found at these sites and the lack of detailed knowledge about the contaminants poses a challenge to remediating these sites successfully and economically.

Traditionally the goal of remediation under the Remedial Investigation - Feasibility Study (RI-FS) approach has been to return contaminant levels to background, pristine or regulatory levels. The regulatory guidelines are "conservative" in their approach and in many cases are probably extreme, and over protective (Moore and Elliott, 1996; U.S. EPA, 2003). As a consequence, the enormous costs associated with the attaining of these goals have led to a rethinking of the appropriateness of the traditional goals and approaches.

Now risk based cleanups of sites based on the intended purpose of use are looked upon as being more appropriate to save time, resources and money. Risk Based Corrective Action (RBCA) involves deriving clean up goals based on risk calculations. It not only helps derive cleanup guidelines that are scientifically sound, it also offers a means of translating the risk posed into actual numbers which can be used for communicating the risk to concerned people (risk managers, regulatory agencies and the public).

There are three tiers of risk evaluation for petroleum release sites. As defined by the ASTM (1995) a Tier 1 evaluation is a risk-based analysis to develop non-site specific values for direct and indirect exposure pathways utilizing conservative exposure factors. A Tier 2 evaluation is more site specific. It applies the direct exposure values established under a Tier 1 evaluation at the points of exposure for a specific site and develops values for potential indirect exposure pathways at the points of exposure based on site-specific conditions. In contrast, a Tier 3 evaluation is a risk analysis to develop values for potential direct and indirect exposure pathways at the points of exposure based on site-specific conditions.

Essentially, in Tier 3 RBCA, less constrained assumptions are used than in Tier 2 RBCA since actual site exposure and risk scenarios are used rather than using simplified general exposure scenarios. To derive site-specific cleanup levels, sophisticated fate and transport models are used to quantify exposure concentrations and these are in turn used as input

into pathway models to derive risk estimates. These fate and transport models are often numerical models.

An aspect of fate and transport modeling that has traditionally been ignored is the uncertainty inherent in the numerical models used. This uncertainty is particularly important as all simulations are subject to uncertainty. In particular, numerical models are almost always subject to numerical errors and this introduces an element of uncertainty in the results of any fate and transport calculation (Zheng and Bennett, 1995).

Input parameters themselves are a source of uncertainty in model outputs. The uncertainty in model outputs could be due to a lack of knowledge about an input parameter, and is called uncertainty of input parameter. The uncertainty could also be due to natural variability in an input parameter. As a result, input parameters might be either largely variable or largely uncertain or subject to both. The collective effect of this variability and uncertainty is uncertainty in the fate and transport modeling output. This resultant uncertainty can significantly influence the accuracy of risk calculations and in turn result in an inappropriate and mismatched risk management program.

While most risk managers are aware of this uncertainty in the fate and transport modeling, in the absence of any quantification of it, they use safety factors to try to account for it. The safety factors are not assigned on any scientific basis and could often be over protective. Thus, in order to design more accurate risk management programs an

emerging need is to quantify uncertainty in the RBCA process. This is particularly relevant to the fate and transport-modeling component of the RBCA process since uncertainties of this component are further propagated through the subsequent components of the RBCA process.

The current U.S. EPA policy for risk characterization also requires that all risk assessment should have the core values of transparency, clarity, consistency, and reasonableness. To attain these core values, agency risk assessors and risk managers are required to have a full and open discussion of uncertainties in the body of each risk assessment, including a prominent display of critical uncertainties (U.S. EPA, 2003).

The uncertainties in the RBCA process can be formally evaluated by conducting an uncertainty analysis. A systematic uncertainty and sensitivity analysis provides insight into the level of confidence in model estimates, and can aid in assessing how model estimates should be weighed (Isukapalli, 1999). It helps identify the significant input parameters so that resources can be concentrated appropriately on the significant parameters in the data gathering process. It also identifies data and knowledge gap that help determine research priorities. For risk managers, increased confidence in the results of the modeling is important in evaluating various regulatory options. More confidence on the part of risk managers in the results of modeling outputs results in the use of less extreme safety factors and more realistic cleanup guidelines (Reckhow, 1994; Finkel, 1994).

The fate and transport models used in the Tier 3 RBCA process are typically complex numerical models that are not amenable to simple analytical uncertainty and sensitivity analysis techniques. There is limited guidance available on the selection and application of uncertainty and sensitivity analysis techniques for the uncertainty and sensitivity analysis of these models. Any guidance available (such as the 1995 ASTM "Standard Guide for Risk Based Corrective Action Applied at Petroleum Release Sites, ASTM E 1739-95"; 1997 U.S. EPA "Policy for Use of Probabilistic Analysis in Risk Assessment at the U.S. Environmental Protection Agency"; 1997 U.S. EPA " Guiding Principles for Monte Carlo Analysis. EPA 630-R-97-001"; and the 2003 U.S. EPA "Multimedia, Multipathway, and Multireceptor Risk Assessment Modeling System. Volume IV: Evaluating Uncertainty and Sensitivity. EPA 530-D-03-001d") is general in nature and not model specific.

Modelers can, in theory, use the benchmark Random Sampling based Monte Carlo (RS-MC) analysis for uncertainty analysis but this is seldom practical. RS-MC typically requires 10,000 (or more) simulations, which for a complex model can mean over 10,000 hours (approximately 417 days) in just simulation time (if each simulation is assumed to take an hour on average to assemble and execute). This is a very conservative estimate, the actual time required to assemble input files, execute and to process the outputs can be expected to be much higher especially if appropriate pre-processing and post processing tools are not available to assemble 10,000 input files and to process 10,000 output files

respectively. Due to the complexity of these models the applicability of other uncertainty techniques (such as more efficient sampling techniques with MC or replacement models with MC) are very model specific and RBCA modelers cannot directly use these techniques without model specific testing of these techniques against RS-MC to verify their accuracy and efficiency.

To execute an uncertainty analysis of a Tier 3 RBCA fate and transport model, model specific guidance is also required on variable and uncertain input parameters; significant parameters; and input parameter interactions.

Model specific guidance, such as listed in the previous two paragraphs, can only be generated by conducting a comprehensive parametric uncertainty and sensitivity analysis with the specific goal of generating a framework that can be used by all users of the model. However the analysis of parametric uncertainty and sensitivity in multi-phase multi-component numerical finite element fate and transport models used in the Tier 3 RBCA of petroleum-contaminated sites has not been explored by any published research to date.

This research study will fill that gap in the body of knowledge. This research study, entitled "Evaluation of Uncertainties in MOFAT for Tier 3 RBCA", presents a comprehensive parametric uncertainty and sensitivity analysis of the two dimensional multi-phase multi-component fate and transport model MOFAT. The objective of this

uncertainty and sensitivity analysis is not to conduct an uncertainty and sensitivity analysis of any one given site specific simulation scenario but rather the primary aim is to improve quantification of parametric uncertainties by developing a comprehensive framework for the uncertainty and sensitivity analysis of MOFAT that will provide guidance to all MOFAT users. MOFAT is one of the few finite element models available from the U.S. EPA to model multi-phase multi-component fate and transport and was chosen for its applicability to petroleum release sites. Other models that could be used for Tier 3 RBCA and the selection of MOFAT are discussed in more detail in Sections 2.2 and 3.2 respectively.

1.2 Scope and Purpose of the Research

The aim of this research study, entitled "Evaluation of Uncertainties in MOFAT for Tier 3 RBCA", is to better quantify parametric uncertainties by conducting a parametric uncertainty and sensitivity analysis of a multi-phase multi-component fate and transport model for the purpose of developing a comprehensive uncertainty and sensitivity analysis framework to be used in Tier 3 RBCA of petroleum contaminated sites. The fate and transport model that has been selected for this study is the U.S. EPA two-dimensional multi-phase multi-component fate and transport model – MOFAT (Katyal et. al., 1991).

The primary aim of this research study is to improve quantification of parametric uncertainties by developing a comprehensive framework for the uncertainty and sensitivity analysis of MOFAT.

The specific objectives of this research are:

(1) to conduct a bench mark parametric uncertainty analysis of MOFAT using Random Sampling based Monte Carlo and to evaluate the applicability and performance of various uncertainty analysis techniques to MOFAT.

(2) to develop the computational tools required to undertake an uncertainty analysis of MOFAT.

(3) to quantify the uncertainty in estimates of exposure due to variability in input parameters.

(4) to evaluate the applicability and performance of various sensitivity analysis techniques to MOFAT.

(5) to identify sensitive parameters and issues that need to be addressed when using MOFAT.

(6) to use the information gained from the previous objectives to develop a framework for uncertainty and sensitivity analysis of MOFAT.

(7) to identify areas of additional research so that uncertainty in MOFAT estimates can be better understood and quantified.

To ensure that the objectives of this research study were accomplished, a comprehensive parametric uncertainty and sensitivity analysis study was formulated and implemented. Figure 1.1 summarizes the key components of this study, each of these components are further described and addressed in the associated chapters.

Figure 1.1 Study Flow Chart

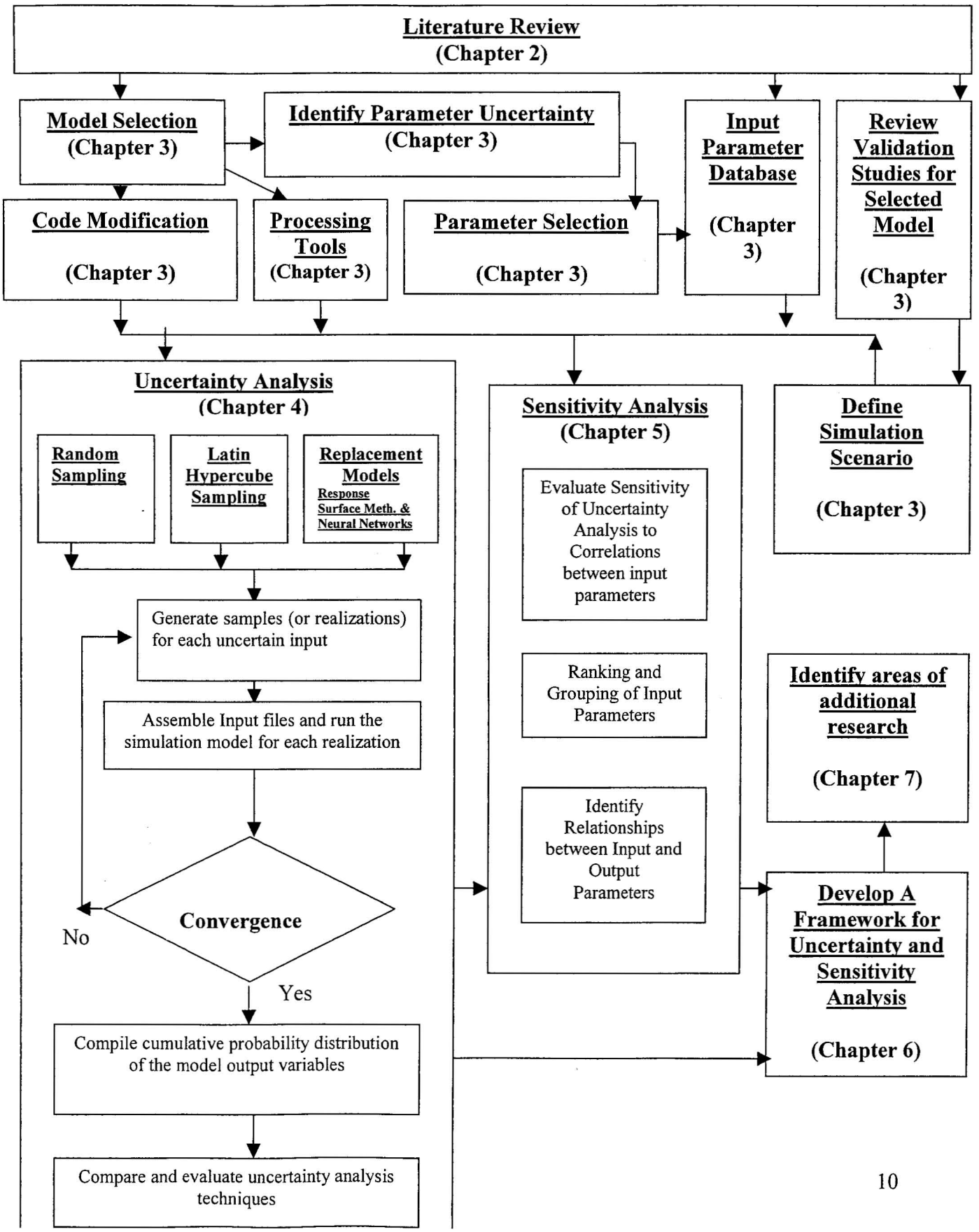

1.3 Outline of the Thesis

Chapter 1 presents a brief background to the RI-FS remediation approach, the RBCA approach and the role of uncertainty in the Tier 3 RBCA of petroleum-contaminated sites. It also presents the Scope and Purpose of the Research.

Chapter 2 presents and discusses the current state of knowledge in the four areas of transport–transformation models in RBCA; uncertainty; uncertainty analysis; and sensitivity analysis.

Chapter 3 presents the formulation and the implementation of the sensitivity and uncertainty analysis. It describes in detail the selection of the MOFAT model; the governing equations of MOFAT; identification of parameter variability; selection of input parameter database; definition of simulation scenario; modification of MOFAT; and the development of processing tools.

Chapter 4 presents the results of the uncertainty analysis of MOFAT using RS-MC, LHS-MC, RSM-MC and NN-MC. The results of 10,000 RS-MC and 935 LHS-MC simulations are summarized through cumulative distribution function *(cdf)* plots of BTEX concentrations in various phases. These *cdf* plots were used to compare the different uncertainty analysis techniques from the perspective of accuracy and efficiency.

Chapter 5 presents the results of the sensitivity analysis. To help assign priorities to the input parameters for reducing uncertainties it presents: an evaluation of relationships between input and output parameters using scatter plots and correlation analysis; a discussion of interaction effects; and a comprehensive ranking and grouping of input parameters using three different methods, including one developed as a part of this study. It also presents an evaluation of the sensitivity of the uncertainty analysis to anisotropy and to additional correlations between input parameters.

Chapter 6 presents a comprehensive six-step framework for the uncertainty and sensitivity analysis of MOFAT that is based on the results of the uncertainty and sensitivity analysis presented in Chapters 3 to 5. This provides model specific guidance on; specification of parameter uncertainty; selecting an uncertainty analysis method; generating correlated probabilistic samples and assembling input files; propagating parameter uncertainty through MC-MOFAT; post processing of MOFAT output files; and sensitivity analysis.

Chapter 7 summarizes the results of this study in the form of conclusions and presents recommendations for future research.

Chapter 8 presents a statement of originality. It presents eight aspects that define the originality of this research work.

Chapter 2. Literature Review

2.1 Introduction

This research study covers four different areas: transport–transformation models in RBCA; uncertainty in the RBCA process and in transport–transformation models; uncertainty analysis; and sensitivity analysis. This chapter reviews relevant published literature under these four areas.

2.2 Transport–Transformation Models In Tier 3 RBCA

A Tier 3 RBCA assessment is usually carried out when the results of a Tier 2 modeling exercise using an analytical model shows the existence of contaminant pathways to at-risk receptors (Zhang et. al., 2001). As a result, Tier 3 RBCA involves the derivation of site-specific target levels using relatively sophisticated statistical and contaminant transport transformation models and risk assessment models. Since petroleum release situations involve the flow of more than one contaminant or fluid and are complex, the fate and transport models used are typically numerical models.

In Tier 3 RBCA numerical methods are preferred over analytical methods since numerical methods are better at accounting for parameters that vary in space and time and are better able to describe complicated site and boundary conditions. This allows detailed replications of complex geologic and hydrologic conditions that exist in nature (National Research Council, 1990). A more detailed discussion of the advantages and limitations of analytical and numerical methods is presented in ASTM (1998). A very brief description of some numerical solution techniques is presented in Table 2.1.

The two primary numerical solution techniques are the finite difference method and the finite element method. The finite difference method requires the model domain to be discretized into blocks using an orthogonal grid whereas in the finite element method the model domain can be discretized using an irregular triangular or quadrilateral grid. This makes finite element models better suited for solving some flow and transport as they can accurately model irregular physical boundaries (ASTM, 1998). Other advantages of finite element models over finite difference models are:

- Using the flexibility in grid discretization, the grid can be oriented along the flow direction. This eliminates numerical dispersion transverse to the flow and gives the model user better control on numerical errors (Spitz and Moreno, 1996).

Table 2.1. Common Numerical Solution Techniques for Fate and Transport Models

(Adapted from National Research Council, 1990)

Solution Technique	Description of Method
Finite Difference Method	Involves the use of differential equations to approximate derivatives, resulting in a series of algebraic equations. These equations are then solved for various blocks in a finite difference grid representation of the site.
Finite Element Method	Creates an integral form of the differential equation: again discretization provides a system of linear algebraic equations. These equations are then solved for various nodes in a finite element mesh representation of the site. It is particularly useful to represent irregular shaped aquifer or geologic units.
Boundary Elements or Boundary Integral Method	Creates integral form of the governing flow equation relying on boundary rather than areal integrals. By working with the boundaries of aquifers or units this method avoids internal discretization, and thus a small number of large elements can be used instead of the finite element method.
Method of Characteristics	Breaks the advection-dispersion equation into two parts, one accounting for advection and the other accounting for dispersion. It requires the transport of reference particles.
Random Walk Method	One of the few techniques not involving a solution of the advection-dispersion equation. Simulates the migration of contaminants by moving a set of reference particles.
Integrated Finite Difference Method	A variant of the Finite Difference method, based on the concept of multi cell models, that allows for non-rectangular discretization. An efficient method used when computational time is at a premium and detailed hydraulic head information is not needed.

- The finite element formulation boundary conditions follow directly from the finite element theory (Spitz and Moreno, 1996).

- In finite element models the model user has the ability to refine the space discretization in areas where contaminant transport occurs and to maintain a coarse discretization in areas without transport (Spitz and Moreno, 1996).

A wide variety of public and proprietary models could be used in the Tier 3 RBCA modeling process. A complete description of all models is beyond the scope of this work but some numerical fate and transport models that could be used for Tier 3 RBCA at petroleum release sites are summarized in Table 2.2. Some of these are finite difference models (e.g. MODFLOW), however for the reasons presented earlier finite element models are more appropriate than finite difference models for Tier 3 RBCA.

2.3 *Uncertainty*

2.3.1 Types of Uncertainty in Transport-Transformation Models

Uncertainty is classified differently by different researchers (Morgan and Henrion, 1990; Isukapalli, 1999; Yen, 2002; U.S. EPA, 2003). Uncertainty may be classified as:

- Scenario Uncertainty
- Parameter Variability

Table 2.2. Numerical Fate and Transport Models for Tier 3 RBCA

Model	Description
Bioplume III	Public domain 2 D model for simulating multiple hydrocarbon species. Windows based only. Cannot be run on Unix. Cannot simulate flow or transport in vadose zone.
MODFLOW	Public domain finite difference 2 D, 3 D flow model.
MT3D	Public domain 3 D single species transport model Requires MODFLOW for simulating flow
RT3D	Public domain 3 D multiple species transport model Requires MODFLOW for simulating flow
MOFAT	Public domain 2 D coupled multi-phase flow and multi-component transport model
NAPL Simulator	Public domain 2 D, 3 D coupled multi-phase flow and multi-component transport model
MARS	Proprietary 2 D coupled multi-phase areal flow and LNAPL remediation simulator
MOC	Public domain 2 D solute transport finite difference model. Uses the method of Characteristics to solve the solute transport equation.
TMVOC	Public domain three-phase non-isothermal flow of water, soil gas, and a multi-component mixture of volatile organic chemical model. Uses the Integrated Finite Difference Method.

- Parameter Uncertainty
- Model Uncertainty

Scenario uncertainty is the uncertainty associated with the process of applying a model wherein a petroleum release situation is reduced to a scenario that can be modeled by a numerical model. The uncertainty is introduced by the assumptions that are made for the scenario description. Errors in specifying the boundary and initial conditions also contribute to scenario uncertainty (Isukapalli, 1999; U.S. EPA, 2003).

Parameter variability is also referred to as natural uncertainty. Many quantities are variable over time, space or number of samples and variability refers to this inherent statistical variance. Variability is sometimes referred to as "type A uncertainty". All other uncertainty is referred to as "type B uncertainty". A variable may reflect primarily variability, primarily uncertainty, or both variability and uncertainty (U.S. EPA, 1996).

Parameter uncertainty is the uncertainty due to parameter estimation. These include what are typically called data uncertainties, which are: (a) measurement errors; (b) inconsistency and non-homogeneity of data; (c) data handling and transcription errors; and (d) inadequate representativeness of data sample due to time and space limitations (Yen, 2002). Huang and Meyer (1996) state that although measurement imprecision

contributes to uncertainty, it is usually negligible relative to parameter uncertainty and variability. Another key source of parameter uncertainty is upscaling of measurements. Uncertainty is introduced when in numerical models soil parameters have to be upscaled (homogenized) to the grid or block size used by the model. Scaling can also affect the correlations between soil parameters (Dobermann et. al., 1997). Undertaking a field investigation program and appropriate review of published literature on the parameters can help reduce and quantify both parameter uncertainty and variability.

Model uncertainty is the term used to collectively describe uncertainties associated with the use of a model and is sometimes extended to include scenario uncertainty. Models are representation of processes being modeled and are based on a set of assumptions. The very process of reducing a process so as to allow it to be modeled is a source of uncertainty as no model is ever perfect. Model uncertainty thus reflects the inability of the simulation model to represent precisely the systems true physical behavior (Yen, 2002). Uncertainties include errors in model structure and errors in linking models or processes that work at different spatial and temporal scales (U.S. EPA, 2003). Numerical errors, grid size resolution and the applicability of the model at the selected grid size resolution are also contributors to uncertainty. Other sources of uncertainty are extrapolation beyond a model's intended application domain, and interpolation between point estimates of model output (Isukapalli, 1999; U.S. EPA, 2003).

Model uncertainty is generally hard to quantify. Uncertainty due to grid resolution can be analyzed by comparing the model results for different grid resolutions and can generally be kept to a minimum by using an appropriate fine grid resolution. Uncertainties in model structure can best be understood by validating the model against field studies. Model validation and peer review of models is important for ensuring model structure uncertainties are minimized. Ensuring that a model is applied within its intended domain also minimizes uncertainty.

Uncertainty may also be classified as reducible and irreducible. The irreducible uncertainty is typically the natural uncertainty. Model and parameter uncertainty consists of both reducible and irreducible components. The reducible components of model uncertainty may be reduced to an extent by improving the model resolution, ensuring the model assumptions are valid, boundary conditions are appropriate, and by sacrificing computational efficiency for precision. Parameter uncertainty may be reduced by improving sampling techniques, improving the calibration of sampling equipment, collecting representative samples, ensuring an adequate sample size, accounting for correlations and acquiring more knowledge about poorly understood parameters.

2.3.2 Uncertainty and the RBCA Process

The RBCA methodology is based on the analysis of transport and exposure between the source of contamination and the receptor (Connor et al., 1996; ASTM, 1995; U.S. EPA, 1991a; U.S. EPA, 1991b; U.S. EPA, 1989a; U.S. EPA, 1989b). However when any

analysis of transport and exposure is done using simulation models, an element of uncertainty is automatically introduced into the results due to scenario, parameter and model uncertainty and parameter variability. This makes uncertainty an intrinsic part of the RBCA process and cannot be separated from it. Various researchers (Anderson and Woessner, 1992; Konikow and Bredehoeft, 1992; Zheng and Bennett, 1995) have noted the effects of this uncertainty in post audit studies. For example, Zheng and Bennett (1995) note that the effects of uncertainty are evident in the results of post-audit studies, that compared actual field conditions with model predictions made years earlier.

The traditional approach to dealing with uncertainties has been to make the modeling exercise conservative through the use of extreme assumptions and point estimates, or large safety factors. There are, however, costs to this approach as the use of extreme assumptions and factors of safety is not without its negative consequences. An overprotective RBCA can lead to a waste of resources. Moore and Elliott (1996) observe that in regulatory programs in which worst-case assumptions are the norm, expensive risk mitigation measures may be enacted for chemicals that pose little threat to human health or the environment. Harter (1998) and the U.S. EPA (2003) also note that costly cleanup decisions could result from unrealistic or highly conservative risk assessments. Conversely, in programs that rely on best-guess values or so-called reasonable conservative values, chemicals having low likelihood of causing effects may be ignored. Maxim (1989) echoes a similar observation, "the analysis of risk involves numerous assumptions and input parameters, and if overly conservative assumptions are made for

each parameter, the result can be a grossly exaggerated risk which defies the very essence of risk assessment."

A better and increasingly popular approach to dealing with uncertainties is to formally evaluate the uncertainties in the RBCA process by conducting an uncertainty analysis. The evaluation of uncertainties does not reduce the inherent uncertainty in the modeling process but it allows for a more accurate and realistic description of risk levels. The ASTM (ASTM, 1995) guide for RBCA applied at Petroleum Release Sites lists the assessment of model accuracy and uncertainty as being one of the key steps in evaluating model results. Knowledge of the expected uncertainties in the model predictions is needed so that the risk managers can adjust their responses accordingly. More confidence on the part of risk managers in the results of modeling outputs results in the use of less extreme safety factors and more realistic cleanup guidelines (Reckhow, 1994; Finkel, 1994). Also an uncertainty analysis allows for the characterization of the impact of the variability of the relevant parameters on the estimate of risk (Hamed and Bedient, 1997). This insight and knowledge leads to a better understanding of the role of various input parameters in the modeling process and thereby helps identify avenues for reducing the uncertainty in the results. Thus, quantifying the uncertainty and accounting for it in the RBCA process allows for a more consistent RBCA process that better reflects the ground realities.

Other compelling reasons to conduct an uncertainty analysis are:

- In environmental decision-making, uncertainty analysis is needed to avoid the mistaken impression that model results are precise and well understood. The use of safety factors obscures the real issues and areas of knowledge and uncertainty. The result can be misuse of conclusions by a decision-maker who does not understand the basis of the analysis (Raiffa, 1982). Quantification of the uncertainty in a model will clearly outline the strengths and limitations of the model being used and thus prevent any wrongful interpretation of its results.

- An uncertainty analysis can highlight and pinpoint the priorities for obtaining new information, so that uncertainty can be reduced, and the decision-maker can have increased confidence in the decision ultimately taken (Reckhow, 1994; Finkel, 1994).

The need for work in this area has been reiterated repeatedly. The National Research Council, USA (1990) stated "the scope of research in the future must be broadened to formalize methods of recording subjective inputs and quantifying accuracy within the modeling process". Zheng and Bennett (1995) note that for results of predictive simulations to be of value, uncertainties must be considered and when possible their consequences should be addressed. The U.S. EPA has emphasized the importance of adequately characterizing variability and uncertainty in risk assessments in several science and policy documents. These include the 1992 U.S. Environmental Protection Agency (EPA) Exposure Assessment Guidelines, the 1992 EPA Risk Assessment

Council (RAC) Guidance, the 1995 EPA Policy for Risk Characterization, the EPA Proposed Guidelines for Ecological Risk Assessment, the EPA Region 3 Technical Guidance Manual on Risk Assessment, the EPA Region 8 Superfund Technical Guidance, the 1994 National Academy of Sciences "Science and Judgment in Risk Assessment," and the report by the Commission on Risk Assessment and Risk Management (U.S. EPA, 1997a).

As a follow up to these activities the U.S. EPA issued the "Guiding Principles for Monte Carlo Analysis" (U.S. EPA, 1997b). This is a policy and preliminary guidance on using probabilistic analysis. The policy documents the U.S. EPA's position "that such probabilistic analysis techniques as MC analysis, given adequate supporting data and credible assumptions, can be viable statistical tools for analyzing variability and uncertainty in risk assessments." The policy establishes conditions that are to be satisfied by risk assessments that use probabilistic techniques. These conditions relate to the good scientific practices of clarity, consistency, transparency, reproducibility, and the use of sound methods (U.S. EPA, 1997b).

It needs to be mentioned that, though there is the need to quantify uncertainty, it is not possible to quantitatively measure all the uncertainties associated with models and data. The U.S. EPA recognizes this and states, "the analyst should attempt to identify the full range of types of uncertainty impinging on an analysis and clearly disclose what set of uncertainties the analysis attempts to represent and what it does not. Qualitative

evaluations of uncertainty including relative ranking of the sources of uncertainty may be an acceptable approach to uncertainty evaluation, especially when objective quantitative measures are not available" (U.S. EPA, 1997b).

2.3.3 Incorporating Parameter Uncertainties

The issue of uncertainty analysis also has its origins in how fate and transport models are used. There are two approaches to using models, the deterministic and the probabilistic. The deterministic approach, also known as the point estimates approach, involves representing model inputs as a single value. The single value used to represent data could be its mean, median, highest value, lowest value or some other measure that might be deemed to be representative of the parameter.

In contrast, in the probabilistic approach an attempt is made to more thoroughly represent each data set by capturing the variability in it. Representing the input variability as a distribution captures the data variability.

The deterministic approach to modeling is easy to implement and has been the traditional approach to modeling. However the process of representing data by a single descriptor results in a loss of information. The probabilistic approach on the other hand is harder to implement as the input distributions have to be known, but the output is a better representation of the situation being modeled. This output gives an estimate of the

uncertainty associated with using the model. Thus the probabilistic approach to representing data sets is intrinsically linked to uncertainty analysis.

In the published literature there is much comparison of deterministic and probabilistic approaches. Various researchers have emphasized the need for a probabilistic approach to RBCA. Amongst them Paustenbach (1989), Finkel (1990) and Burmastar and Lehr (1991) have suggested that the exposure assessment procedure could be refined if probability density functions rather than point exposure estimates were incorporated into the exposure analysis. Similarly Anderson and Woessner (1992) conclude that post audits of modeling projects clearly point to the need for simulations of many different possible scenarios. This is because the probabilistic approach places the point estimate into a full and proper context, and provides more information to the risk managers and the public (Finley et al., 1992).

At the U.S. EPA workshop on MC analysis (U.S. EPA, 1996), panelists speculated that the results of probabilistic risk assessment could conceivably lead to reduced risk management costs. For example, when a full distribution of risk is available to risk managers, they may be able to establish more cost-effective cleanup levels. Incremental improvements in decision-making provided by probabilistic risk assessment versus deterministic risk assessment could sometimes make a big difference in the real world (U.S. EPA, 1996).

The differences between the deterministic and probabilistic approaches are highlighted in the following points:

- A dataset can be represented by several different point "best estimates" (e.g. mean, median etc.). Representing data by "best estimates" always results in a loss of information. The loss of information is different for different "best estimates" so "best estimates" can differ markedly from each other. This can lead to diametrically different choices (Finkel, 1994). In contrast, probability density outputs from a probabilistic approach present a more complete picture because no "best estimates" are used to represent the input data.

- Point estimates are derived from combinations of exposure factors that sometimes may be unrealistic. In contrast, in probabilistic analysis the impact of assumptions is explicit as a full description of exposure is provided (U.S. EPA, 1996).

- Deterministic risk assessment does not account for the dependency structure between the model input parameters. Whereas, probabilistic risk assessment not only provides distribution shapes, but also takes into account the dependency structure between the model input parameters (U.S. EPA, 1996).

- Deterministic risk assessment tends to focus on known data and ignore other influential factors. A probabilistic risk assessment, on the other hand, ideally will

at least consider, clearly acknowledge, and attempt to capture as many influential factors as possible (U.S. EPA, 1996).

- Probabilistic methods also have an advantage over deterministic methods in the ranking of sites according to risk. The ranking of waste areas using deterministic methods yields disparate rankings because risk assessment results are very user-specific and depend on the user's selection of models, parameter values and uncertainty about important model parameters. This results in large inconsistencies in the amount of conservatism used to quantify model parameters for specific contaminant and exposure pathways. Through the use of uncertainty analyses on the risk assessment of the waste sites, it is possible to rank the waste areas in a more reliable manner (Shevenell and Hoffman, 1993).

The probabilistic approach is not without its shortcomings. There is the potential for misuse and errors. A possible error can be inaccurate characterization of the input data. This can lead to a faulty probabilistic analysis. Another possible source of error is when correlations between input variables are ignored and modelers assume independence between variables that are mechanistically related for the sake of mathematical convenience (Scott and Tucker, 2003). Conversely it is important for risk managers to be wary of attaching a false sense of certainty to the results of a probabilistic analysis (U.S. EPA, 1996).

The probabilistic approach is generally harder to implement and is computationally more intensive. This is especially true for complex fate and transport models. Typically a large amount of data is required to characterize properly the distribution of the input parameters. This kind of data is not always available for all inputs especially in the environmental engineering area. Deriving from this is the concern that the value added by probabilistic analysis techniques may not always be enough to justify the additional costs compared to point estimates (U.S. EPA, 1996). In recognition of this the U.S. EPA (2003) recommends that uncertainty analysis be used only on projects where the risk estimates are at or slightly below the acceptable level of risk and where remedial actions may require substantial resources. This makes Tier 3 RBCA situations appropriate candidates for uncertainty analysis.

2.4 Uncertainty Analysis

2.4.1 Monte Carlo (MC)

Uncertainty analysis techniques can be broadly classified into two groups; analytical techniques and Monte Carlo (MC) simulation based techniques.

Analytical methods are very popular because they are easy to implement and are not computationally intensive. Hamed and Bedient (1997) evaluated the performance of computational methods for the assessment of risk from ground water contamination and they noted that first and second order reliability methods could be of major benefit in

probabilistic analysis in risk assessment. However the application of moment techniques is limited to linear or nearly linear systems, for which the coefficient of variation of model parameters is much less than one (Peck et al., 1988). Thus when the transport equations are complex and non-linear, first and second order reliability methods (FORM and SORM) and other analytical methods cannot be applied in some cases and in other cases are not very easy to apply because the problem becomes computationally complex.

MC refers to the traditional method of sampling random variables in simulation modeling. Samples are chosen completely randomly across the range of the distribution, thus necessitating large numbers of samples for convergence for highly skewed or long tailed distributions (Palisade, 1992). The earliest documented uses of random sampling occurred in the late 1700s, when French scientists used the technique to define a solution to an integral (U.S. EPA, 1996). The term "Monte Carlo" was introduced by von Neumann and Ulam during World War II, as a code word for secret work at Los Alamos. The MC method was then applied to problems related to the atomic bomb (Rubinstein, 1981).

In contrast to analytical methods, the MC analysis method is not limited by the non-linearity of the transport equations. It is a robust method and has been proposed by many as the method of choice. Examples include the work of Finkel (1990), Meeks and Salhotra (1990), Ahlfeld (1991), Burmaster and Lehr (1991), Paustenbach et al. (1991), Salhotra et al. (1991), McKone and Bogen (1991), Finley et al. (1992), Thompson et al.

(1992), Keenan et al. (1994), Goodrich and McCord (1995), Bright et. al. (2002) and Brewer et. al. (2003). As a result random sampling based MC (RS-MC) simulation is one of the most widely used methodologies to account for parameter variability in groundwater flow and contaminant transport. It is easy to program and apply, amenable to analytical and numerical models, and it is theoretically convergent (i.e. RS-MC output statistics will converge if a sufficiently large sample RS size is used). A statistical advantage of random sampling is that it produces unbiased estimates of the mean and variance of the output variables (Saltelli et. al., 2004).

A major disadvantage of RS-MC, however, is that it is very computationally intensive when the simulated event is of very low probability (Hamed and Bedient, 1997). It is this computational intensiveness of RS-MC that has lead to a lot of research into examining whether the results of the RS-MC method could be achieved by less intensive analytical methods. However where analytical methods cannot be used, RS-MC is usually the method of choice.

Another shortcoming of RS-MC is that for complex transport problems in large heterogeneous domains (Freeze et al., 1990) or for high order systems (Helton and Davis, 2000) RS-MC analysis may be computationally prohibitive especially since it is important to ensure that the RS-MC simulations converge. If the number of RS-MC simulations are less than those needed for convergence RS-MC simulation can potentially over and under sample from various points of the distribution (U.S. EPA, 2003).

There are various modifications of the RS-MC technique that have been developed over the years with the aim of reducing the computational effort of the RS-MC technique. These modifications work on modifying the simulation procedure. Modifying the sampling techniques that are used to select realizations (possible values) of the various parameters from their probabilistic distributions can reduce the computational intensity of the RS-MC method by minimizing the required sample size. The procedures are generally called variance reduction techniques. Variance reduction can be viewed as a means to use the known characteristics of a situation to reduce the required sample size. This makes the efficiency of variance reduction techniques directly proportional to what is known about a problem (Rubinstein, 1981). Since the various variance reduction techniques are related they are not always distinct and there is a lot of overlapping. They have been classified in many different ways by different researchers. McGrath and Irving (1975) have classified the various variance reduction techniques as listed in Table 2.3.

In addition to the above techniques some other techniques have been suggested for reducing the number of realizations required by the MC method. Among them are the Rackwitz-fiessler algorithm (Veneziano et al., 1989) and the Gauss-Hermite Scheme (Levy, 1993).

Of the above listed techniques one of the best-known techniques is stratified sampling. It has been recommended, amongst others, by Hillier and Lieberman (1990), and it has been described as a combination of the systematic and importance sampling schemes. The

Table 2.3. Categorization of Variance Reduction Techniques

Category	Category Name	Variance Reduction Techniques
1	Modification of the Sampling Process	Importance sampling Russian roulette and splitting Systematic sampling Stratified sampling
2	Use of Analytical Equivalence	Expected values Statistical estimation Correlated sampling History reanalysis Control variates Antithetic variates Regression
3	Specialized Techniques	Sequential sampling Adjoint function Transformations Orthonormal functions Conditional Monte Carlo

systematic sampling technique works by modifying the selection from the sample space in a structured manner. The importance sampling technique works by concentrating the distribution of the sample points in the parts of the region that are of most "importance" instead of spreading them out evenly (Marshall, 1956). Under this scheme the sampling distributions that would be used in the direct simulation are replaced with ones that force the sampling into more interesting or important regions. Thus the sampling is structured such that the more important regions of interest are sampled more frequently. Lu and Zhang (2003) have shown when an importance density function is chosen appropriately, importance sampling techniques may be orders of magnitude more efficient than RS-MC simulations for flow and transport modeling in porous media. However importance sampling is more appropriate for rare events (i.e. high quantiles) and requires detailed prior knowledge of a model's sensitivity. The stratified sampling technique does not require detailed prior knowledge of a model's sensitivity and works by first dividing the input distribution space into strata and then directs the sampling to these strata. This works to ensure that the input distribution space is covered more quickly.

Alternatively stratified sampling may also be viewed as a special case of systematic sampling where optimal distribution of each distribution of samples is attempted. It tends to force convergence of a sampled distribution in fewer samples (Palisade, 1992).

2.4.2 Latin Hypercube Sampling (LHS)

One stratified sampling technique that has been very successfully used is Latin Hypercube Sampling (LHS). LHS is a relatively new stratified sampling technique used in simulation modeling (Palisade, 1992). It was developed by McKay, Conover, and Beckman (1979). It uses stratified sampling without replacement to reduce variance (Helton and Davis, 2003). A detailed description of the method and its application for uncertainty analysis of complex systems, which has been in use in Sandia National Laboratories since 1975, is available in Helton and Davis (2003).

Using stratified sampling techniques like LHS instead of random sampling, can reduce the computational intensity of MC analysis, as fewer samples are needed to cover the whole range of possible realizations. Helton and Davis (2000) state that compared to random sampling which may require 1000's or 10,000's of samples, LHS can often be completed using only 10's to 100's of samples. LHS is generally recommended over simple random sampling when the model is complex or when time and resource constraints are an issue (U.S. EPA, 1997b). The LHS forces the MC sampling to select values over the whole range of a model parameter, thereby reducing the total number of MC samples required to preserve the probability distributions. This significantly improves the computational efficiency of the MC analysis. There is much discussion to be found in published literature on the benefits of using LHS-MC versus RS-MC sampling. The U.S. EPA (2003) draws upon various sources to offer the following points regarding the benefits and limitations of LHS from a computational efficiency viewpoint:

- A primary benefit of LHS is that the technique ensures each of the inputs is represented in a fully stratified manner, no matter which might turn out to be important (Campolongo et al., 2000; Helton and Davis, 2003; Saltelli et. al., 2004).

- Desirable features of LHS include [comparatively] unbiased estimates of means and distribution functions [for small sample sizes] (McKay et al., 1979; Helton and Davis, 2000, 2003).

- When the output is a monotonic function of its inputs, LHS is proven to be better than random sampling in describing the mean and the population distribution function (McKay et al., 1979; Campolongo et al., 2000; Helton and Davis, 2003).

- Asymptotically, LHS is proven to be better than random sampling in that it provides an estimator (of the expectation of the output function) with lower variance. The closer the output function is to being additive (i.e. linear) in its input quantities, the greater is the reduction in variance (Stein, 1987; Campolongo et al., 2000; Helton and Davis, 2003; Saltelli et. al., 2004).

- Although LHS can sometimes still be more efficient, in cases dealing with non – additive and non–monotonic input functions, LHS has been shown to be

equivalent to or worse than random sampling (Stein, 1987; Camoplongo et al., 2000).

- LHS is particularly practical and useful in dealing with the aspect of computational limitations in performing random sampling for long running models (e.g. single model run of hours, days, etc.). If computational capacity is sufficient to handle random sampling, there is little reason to use LHS (Helton and Davis, 2003).

- Due to their computational complexity and expense, long-running models do not constitute convenient vehicles for comparing differences between random sampling and LHS (Helton and Davis, 2003).

- Another aspect of LHS is that it performs better than random sampling when the output is dominated by a few components of the input factors (Camoplongo et al., 2000; Saltelli et. al., 2004).

While LHS can impart bias in estimates of output distribution statistics (U.S. EPA, 2003; Saltelli et. al., 2004), in many cases the bias maybe found to be insignificant (Helton and Davis, 2003). Further, LHS is typically not to be used when the estimation of high fractiles (e.g. 0.99, 0.999 etc) is required. The more subjective stratified sampling

technique "importance sampling" is used for such situations (Helton and Davis, 2000; Helton and Davis, 2003).

While no comprehensive RS-MC or LHS-MC uncertainty study of a complex Tier 3 RBCA multi-phase and multi-component fate and transport model or scenario has been reported in literature, a RS-MC uncertainty analysis using MODFLOW, MODPATH and MT3DMS of two plumes (a trichloroethene (TCE) plume and a strontium-90 plume) in South Carolina has been reported by Brewer et. al. (2003). The uncertainty analyses of the two plumes are the most comprehensive RS-MC uncertainty analyses of groundwater fate and transport model reported in published literature. However the study does not advance scientific knowledge as the study is specific to the Savannah River Site being studied; does not account for correlations between input parameters; and does not evaluate any realization reducing techniques. Consequently while the analyses for the two plumes were both successful at assisting project decision in managing uncertainty for the specific sites, the results do not add to scientific knowledge and cannot be used to develop any general framework that will help better quantify parametric uncertainties.

2.4.3 Response Surface Model (RSM)

For computationally complex models it is sometimes useful to replace the model with an approximate version just for the purpose of uncertainty analysis. In this "Replacement Model" technique, a replacement model is used as a proxy for the original model and is then subjected to the uncertainty analysis that the original model would have been

subjected to. This approach of uncertainty analysis helps to overcome the computational intensity and complexity of applying the MC approach to the original model. For complex models with outputs that have spatial and temporal components the replacement models are usually only valid for a specific spatial location and a specific time and are used for the uncertainty analysis of model results for only that specific location and time.

A Response Surface Model (RSM) is a commonly used replacement model. RSM is a collection of mathematical and statistical techniques that are useful for modeling and analysis of problems in which a response of interest is influenced by several variables and the objective is to optimize this response (Montgomery, 2001). The mathematical expression that models the response of interest is called the response surface (RS) model.

The use of RSM in the uncertainty and sensitivity analysis of complex models is aimed at deriving a RS model to be used as a substitute for the complex model. Responses surfaces are fitted on the responses generated by a few selected simulations of the complex model. If a fitted surface is an adequate approximation of the true response function, then analysis of the fitted surface will be approximately equivalent to analysis of the actual system (Montgomery, 2001).

To ensure the effective computation of model parameters for the RS the model simulations are planned using experimental design based RS designs. The RS designs are typically factorial designs as factorial designs are widely used in experiments involving

several factors where it is necessary to investigate the joint effects of the factors on a response variable.

The most popular RS design is the central composite design (CCD), which was introduced by Box and Wilson (1951). The CCD is an efficient design that is ideal for sequential experimentation and allows a reasonable amount for testing lack of fit while not involving an unusually large number of design points (Montgomery, 2001).

There are two parameters that need to be specified in the design: the distance of the axial points and the number of center points. For computer simulation experiments, only one center point is specified since simulated responses are always the same. The choice of the axial distance depends on the degree of rotatability desired in the design. A rotatable design is one in which the variance of the predicted response is the same at all points that are the same distance from the design center (Montgomery, 2001). Designs with complete rotatability are called spherical CCD. A spherical CCD requires each factor to be varied over five levels; two axial points, two factorial points and one center point.

While rotatability is usually a desired property, exact rotatability is not important for having a good design and there are situations when the region of interest is cuboidal rather than spherical (Montgomery, 2001). A cuboidal CCD, where the axial distance is equal to one, is called the face centered CCD. It is a non-rotatable design and requires only three levels of each factor.

The CCD may use full factorial or fractional factorial (of resolution V) design points. Fractional factorial designs are used when resources or the complexity of a model limit the number of experiments or simulations that can be executed. They are however efficient and can be used to obtain information on the main effects and low order interactions.

After a RS model is fitted on the responses generated by selected simulations of the complex model, the RS model is evaluated to meet parametric requirements;

(a) Compliance with least squares regression assumptions. Examining the normal probability plot of the residuals checks the normality assumption. The residuals are also plotted against the predicted responses to verify that the variance of the original observations is constant. Residuals are similarly plotted against the run order and each of the independent variables. These are examined for non-randomness, as non-randomness would indicate model inadequacy (Myers and Montgomery, 1995).

(b) Statistical significance using ANOVA. In addition to the ANOVA, other model diagnostic statistics (R^2, adjusted R^2, Predicted R^2 and Adequate Precision statistic) are used to evaluate the fit and appropriateness of the RS.

The RSM approach has been used for uncertainty analysis of some very large computer codes in the nuclear reactor field (Vario, 1982). No attempt to replace a complex multi-phase and multi-component fate and transport model by a response surface model for the purpose of uncertainty analysis has been reported in literature.

When dealing with complex models that are computationally intensive replacing them with a RS has several advantages. There is some literature available (Cox and Baybutt,1981; Iman and Helton, 1988) on the comparison of RS-MC or LHS-MC and RSM-MC. Due to the different models used in the studies, Cox and Baybutt (1981) concluded that in comparison to RS-MC the RSM-MC is more general and flexible while Iman and Helton (1988) rated LHS-MC as being more flexible and adaptable. This demonstrates that while the two methods have their distinct advantages and disadvantages the applicability of the two methods is model specific.

2.4.4 Neural Network (NN)

Another replacement model could be a Neural Network (NN) derived replacement model. NNs have their origins in 1940s, when the first mathematical model of a biological neuron was published by Warren McCulloch and Walter Pitts in 1943 (Picton, 1994). NNs are an attempt at modeling the information processing capabilities of nervous systems (Rojas, 1996). NNs work on the principle of pattern recognition and classification and the basic function of NNs is to produce an output pattern when presented with an input pattern (Picton, 1994). A NN learns from a set of input and

output patterns (called the training set) and generalizes this training to give correct responses for other similar input pattern sets that the NN has not been shown before.

NN are called a network because it is a network of interconnected elements. The basic building block of neural network technology is the simulated neuron, which is depicted in Figure 2.1 as a black circle. The neurons are connected by weights, depicted as lines in Figure 2.1, which are applied to values passed from one neuron to the next. A group of neurons is called a slab. Neurons are also grouped into input or output layers on the basis of whether they are connected to the input or output patterns. Neurons in between the input and output layers are in the hidden layer (s). A layer may contain one or more slabs of neurons (Ward Systems Group Inc., 1993).

A network "learns" by adjusting the interconnection weights between layers. The answers the network is producing are repeatedly compared with the testing set, and each time the connecting weights are adjusted slightly in the direction of the correct answers. Eventually, if the problem can be learned, a stable set of weights adaptively evolves and will produce good answers for all of the sample decisions or predictions (Ward Systems Group Inc., 1993).

NNs can be implemented using different architectures or algorithms. A learning algorithm is an adaptive method by which a network of computing units self organizes to implement desired behavior (Rojas, 1996). Some examples of NN architectures are Back

Figure 2.1 Neural Network Structure (adapted from Ward Systems Group Inc., 1993)

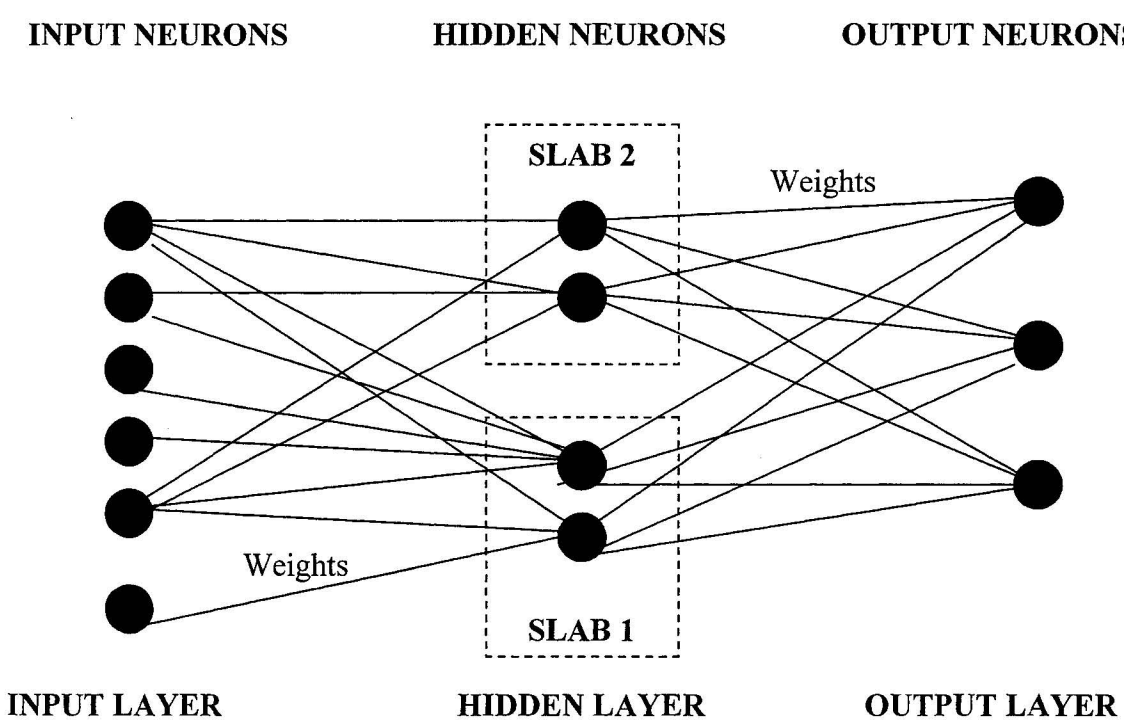

propagation Neural Networks (BPNN) and General Regression Neural Networks (GRNN).

Back propagation is a gradient descent system that tries to minimize the mean squared error of the system by moving down the gradient of the error curve (Rojas, 1996). BPNN are used for the vast majority of working neural network applications and are known for their ability to generalize well on a wide variety of problems (Ward Systems Group Inc., 1993). NeuroShell 2 offers several different variations of back propagation networks: (a) each layer connected to the immediately previous layer (with either 3, 4, or 5 layers); (b) each layer connected to every previous layer (with either 3, 4, or 5 layers); (c) recurrent networks with dampened feedback; and (d) Ward Networks. Ward Networks are three different BPNN architectures with multiple hidden layers invented by Ward Systems Group (Ward Systems Group Inc., 1993). In Ward Networks different hidden slabs are given different activation functions.

GRNN are known for their ability to train quickly on sparse data sets. GRNN is a type of supervised network that is useful for continuous function approximation and is able to produce continuous valued outputs. GRNN networks evaluate each output independently of the other outputs and thus may be more accurate than BPNN when there are multiple outputs. GRNN is a three-layer network where there must be one hidden neuron for each training pattern (Ward Systems Group Inc., 1993).

NN have been used by a number of researchers for a variety of groundwater applications. Najjar and Basheer (1995) successfully used NN with backpropagation to contour map the spatial distribution of boron in an aquifer due to contamination from a chemical waste site. Morshed and Kaluarachchi (1998) developed a one dimensional unsaturated flow and transport scenario and used backpropagation NN to simulate the effects of specific input parameters. Tansel et. al. (1999) also used NN to develop subsurface contaminant profiles with limited data from monitoring studies conducted for small potable water wells in Dade County, Florida. Krom and Rosjerg (2000) investigated the use of backpropagation NN as a tool for the simulation of contaminant loss and recovery in three-dimensional heterogeneous groundwater flow and contaminant transport. Variable pumping withdrawal rates were used as inputs to the NN. Hassan and Hamed (2001) used NN to map the relationship between particle trajectories in a two dimensional domain and the physical properties of the domain. Solute mass flux and mean concentrations predicted by the trained network agreed closely with results from RS-MC simulations. NN have also been used to identify non-point (from farming) contamination flux to groundwater inversely from monitored data (Hiramatsu et. al., 2001).

However no attempt to replace a complex multi-phase and multi-component fate and transport model by a NN model for the purpose of uncertainty analysis has been reported in published literature. The use of NN to replace a model for the purposes of uncertainty analysis has been reported by Zou et. al. (2002) but this application was for uncertainty

and risk analysis of a phosphorous water quality model for the Tridelphia reservoir in Maryland.

2.4.5 Selecting Uncertainty Analysis Techniques

The review presented in the previous section illustrates that the choice of which probabilistic approach is appropriate is clearly model specific. While generalizations can be made as to which approach would be best for a given model based on the model type (linear, complex, periodic etc.) the performance of any given uncertainty analysis technique for complex models cannot be evaluated until the technique is actually applied to the model.

Analytical methods cannot be implemented for non-linear and relatively complex models such as MOFAT. Model runs of MOFAT can run into hours so a RS-MC exercise with 10,000 random samples is neither practical nor feasible for most Tier 3 RBCA investigations. In the interest of computational efficiency, the pairing of MC with stratified sampling (LHS) or with a replacement model (RSM or NN) needs to be evaluated for the development of an uncertainty analysis framework for MOFAT. This evaluation will be from the twin perspectives of accuracy and efficiency. Based on this literature review the applicable uncertainty analysis techniques for this study are RS-MC, LHS-MC, RSM-MC or NN-MC. Within NN-MC both BPNN and GRNN are applicable architectures for this study.

A detailed elaboration of the implementation and evaluation of these uncertainty analysis techniques within this research study is presented in Chapter 4.

2.5 Sensitivity Analysis

Sensitivity analysis is the study of how the variation in the output of a model can be apportioned either qualitatively or quantitatively to different sources of variation (Saltelli, 2000). Sensitivity analysis are conducted for various reasons including the need to determine (Hamby, 1994; Saltelli et. al., 2004):

1. Which inputs correlate highly with other inputs.
2. Which inputs contribute most to output variability.
3. Which parameters require additional research for strengthening the knowledge base thereby reducing output uncertainty.
4. Once the model is in use what consequence result from changing a given input parameter.
5. Which inputs interact with each other.

Sensitivity analysis is closely linked to uncertainty analysis. By providing an understanding of how a model responds to changes in input parameters, sensitivity analysis helps to foster an increased level of confidence in the model and its predictions (Saltelli, 2000). Conversely, it also identifies parameters for uncertainty analysis (Spitz

and Moreno, 1996). The identification of important input parameters driving most of the variation in the output is also a means of quality assurance (Saltelli et. al., 2004). From a calibration perspective, sensitivity analysis is important for identifying the elements that are mostly responsible for model realizations in the acceptable range (Saltelli et. al., 2004).

2.5.1 Techniques

There are several publications on sensitivity analysis techniques. Hamby's (1994) review of techniques for parameter sensitivity analysis for environmental models is a comprehensive review of more than a dozen techniques. The U.S. EPA's workshop (U.S. EPA, 1996) on MC analysis also reviewed some sensitivity analysis techniques. Saltelli et. al. (2000) present a comprehensive guide to sensitivity analysis techniques and applications, while Saltelli et. al. (2004) present a practitioners guide to sensitivity analysis of scientific models.

Sensitivity analysis techniques are classified in different ways by different researchers. They may be generally grouped into the following categories:

- Differential Sensitivity Analysis
- Reliability Techniques
- Variance Based Methods
- Response Surface Methodology

- Sampling Based Methods

Differential sensitivity analysis methods are ideally suited for homogeneous systems and they work on the principle of approximating a model by a Taylor series that is then used as a surrogate for the original model in sensitivity studies (Campolongo et al., 2000). Differential sensitivity analysis techniques are only valid for small variability in parameter values and require that the partials be recalculated for each change in the base-case scenario (U.S. EPA, 1997b).

Reliability techniques are approximate methods. First Order and Second Order reliability methods (FORM and SORM) seek to find a point in the space of all possible realizations of the uncertain variables that defines the likely point of failure. Once the most likely failure point has been determined using an optimization scheme, a first or second order surface is fitted to that point to evaluate a probability of failure (Cawlfield, 2000).

Variance based methods work on the principle of using variance as an indicator of input parameter importance. These include the methods of correlation ratio, Sobol, and Fourier amplitude sensitivity test (FAST). The concept of variance also underlies other techniques such as standardized regression coefficients and correlation coefficients (Chan et. al., 2000).

Response surface methodology methods work on the principle of approximating a model by a response surface. These methods usually also include factorial designs, design of experiments and regression analysis as these are often used in conjunction with response surfaces. Regression analysis is commonly used to investigate parameter sensitivity and to build response surfaces that approximate complex models (Hamby, 1994).

Sampling based methods, also known as Monte Carlo analysis techniques, are based on generating multiple realizations of model outputs and then using the outputs for sensitivity analysis. A number of sensitivity analysis procedures can be used to examine the outputs from the sampling based technique. These include scatter plots, pattern identification, correlation coefficients, and regression analysis. A detailed comparison of 10 sampling based statistical measures for sensitivity analysis is presented in Helton and Davis (2002). The methods compared are linear (correlation coefficients, partial correlation coefficients and standardized regression coefficients), rank transformation based (rank correlation coefficients, partial rank correlation coefficients, standardized rank regression coefficients), and non-random pattern detection (common means, common locations, common medians, and statistical independence) based methods.

Scatter plots are the simplest sensitivity analysis technique (Saltelli et. al., 2004). When the relationships are nonlinear, scatter plots of the output against each of the model inputs are a very effective tool for identifying sensitivities (U.S. EPA, 1997b). Patterns and dependencies in scatter plots are usually identified visually. However Kleijnen and

Helton (1999a) present a review and comparison of statistical techniques that are particularly relevant for identifying patterns in scatter plots generated in LHS-MC and RS-MC sensitivity analyses. These pattern identification techniques are based on attempts to detect increasingly complex patterns in scatter plots and correlations between input and output through the identification of:

- Linear relationships with correlation coefficients,
- Monotonic relationships with rank correlation coefficients,
- Trends in central tendency as defined by means, medians and the Kruskal Wallace statistic,
- Trends in variability as defined by variances and inter-quartile ranges, and
- Deviations from randomness as defined by the chi-square statistic.

Kleijnen and Helton (1999a, 1999b) recommend using a sequence of the above tests as there is a high probability that at least one of the above tests will be appropriate for a given dependent variable and will correctly identify the factors affecting this variable. They further conclude that the smaller samples associated with LHS-MC are better for identifying important variables as with increasing sample size there is a greater resolution of the effects associated with less important variables.

Widely used measures for correlation analysis include the linear correlation coefficient (also called the product-moment correlation coefficient or Pearson's correlation

coefficient), and such non-parametric measures as Spearman rank-order correlation coefficient, and Kendall's tau. When input parameters are correlated the correlation analysis of outputs is usually done using the Partial Correlation Coefficient (PCC). The PCC gives the strength of relationship between the inputs and outputs after adjusting for the effect of correlations between the input parameters (Saltelli et. al., 2004). The non-parametric equivalent of the PCC is the Partial Rank Correlation Coefficient (PRCC). The PRCC is the PCC test computed on ranks (Saltelli et. al., 2004). When the data are nonlinear, non-parametric correlation is generally considered to be more robust than linear correlation (U.S. EPA, 1997a).

2.5.2 Selecting Sensitivity Analysis Techniques

The different sensitivity analysis techniques presented in the previous section are valid for different situations. Each technique has its strengths and weaknesses and the choice of which technique to use is a function of the problem that is being addressed, the characteristics of the model under study, and the computational cost that the investigator can afford (Saltelli, 2000).

In this research study, the problem being addressed is the development of a framework for uncertainty and sensitivity analysis of MOFAT in the context of Tier 3 RBCA of petroleum release sites. MOFAT is a complex model that is computationally intensive and has correlated inputs (e.g. hydraulic conductivity is positively correlated with the van Genuchten water retention parameters α and n). Correlation between input parameters is

a critical issue in sensitivity analysis (Uhl and Sullivan, 1982). Correlation between input parameters strongly affects the applicability of many sensitivity analysis techniques and this has to be taken into account when selecting an appropriate technique.

Practitioners involved in the analysis of risk most often use sampling based MC methods in conjunction with various sampling strategies for sensitivity analysis (Saltelli et. al., 2004). MC procedure results are ideally suited for sensitivity studies. They are widely used as a part of sensitivity studies to develop a mapping (scatter plot) between uncertain model inputs and the associated model results that then can be analyzed to identify dependencies between the inputs and outputs (Kleijnen and Helton, 1999a). As discussed in Section 2.4.2, and with these considerations, sampling based sensitivity analysis was chosen for this research study.

A major advantage of sampling based sensitivity analysis is that when used with sampling based uncertainty analysis the same simulations can be used for both the uncertainty and sensitivity analysis. Other advantages are (Helton and Davis, 2000):

1. Conceptual simplicity
2. Ease and flexibility in adaptation to different analysis
3. Stratification over the range of each uncertain variable
4. Direct estimation of model uncertainty through cdfs. Can be used directly for uncertainty analysis.

5. Availability of a wide variety of sensitivity analysis techniques such as scatter plots and correlation coefficients
6. The correlation structure of the inputs is incorporated into the sampling process

A detailed elaboration of the implementation of sampling based sensitivity analysis within this research study is presented in Chapter 5.

Chapter 3. Study Formulation and Implementation

3.1 Introduction

A parametric uncertainty analysis simulation study is as complex and intricate as any field or laboratory study and requires careful planning and implementation to ensure that the study objectives are met. The computer workstation used for this study was a Compaq Alphaserver DS10 running TRu64 Unix 5.1.

This chapter presents the formulation and implementation of this study. The components of the study have been presented earlier in Figure 1.1. This chapter includes a description of the screening and selection of the numerical fate and transport model. The model selected for this study is described along with its development and validation history. The governing equations of the selected model are presented to identify input parameters and to identify the type and degree of uncertainty associated with each of these input parameters. The use of this analysis to identify input parameters that were to be modeled as variable inputs in the parametric uncertainty study is also described.

The chapter describes in detail how parametric variability and correlations, for parameters being modeled as variable inputs, were defined using the best available data. A comprehensive soil properties database was used to ensure that parametric uncertainty was at a minimum and that consequently parametric variability and correlations were accurately captured. Similarly a parametric uncertainty analysis requires meticulous design of a simulation scenario that minimizes other sources of variability and uncertainty. The design of such a simulation scenario based on a review of the model's validation studies is also described.

Random Sampling based Monte Carlo (RS-MC) of a complex model is a computationally intensive task and is typically very time intensive. The manual execution of a RS-MC uncertainty analysis is neither practical nor is it efficient. RS-MC uncertainty analysis requires the ability to process input files in a semi automated mode using batch processing. It also requires the use of appropriate pre and post-processing tools to assemble input files and to process output files. To accomplish this, the modification of the selected model code for Monte Carlo simulation was undertaken and a set of pre and post processing tools were developed. These are described in this chapter.

3.2 Model Selection

When selecting a model for a study or application, the primary features of the model such as the type of contaminants to be modeled and the transport mechanism, need to be

examined to ensure that the model is appropriate (Clark and Richardson, 1998). To select a model for this study, four criteria were used to screen models. The first criterion was that the model was to be applicable to petroleum release sites. For a model to be applicable for petroleum release it should be a finite element code capable of simulating multi-phase multi-component flow and transport. Johnson and Marx (2003) have demonstrated that the simulation of a mixture through the use of pure component modeling will not always provide accurate predictions. They also note that one of the most difficult problems in consequence modeling is the prediction of the multi-phase behavior of a multi-component mixture like petroleum. Thus, the use of a multi-phase multi-component flow and transport model for petroleum release sites is crucial for ensuring accurate exposure assessments. The preference of finite element models over finite difference models is based on the strengths that finite element models have over finite difference models for fate and transport modeling. These have been explained earlier in Section 2.2.

The second criterion was that the model was to be a public domain code with detailed documentation. A public domain code allows scientific scrutiny of the model since public domain codes are reviewed and studied by many researchers. This ensures that models have been reviewed for coding and numerical errors. The second criterion was also necessary to allow the model's input and output modules to be modified so as to develop a MC version of the model to allow MC analysis of the model. Most numerical models are compiled with input and output modules that are not suitable for MC analysis. For

public domain codes model documentation tends to be more detailed since there is no effort to protect proprietary components. Model documentation is crucial for understanding of the input parameters and how they are used within the model (Clark and Richardson, 1998).

The third criterion required the model to be both peer reviewed and validated so that experts had screened the model for any errors in model concepts, model structure and theory. This was aimed at ensuring that there were no mathematical and conceptual errors associated with the model. Conceptual errors are the most difficult to identify (Spitz and Moreno, 1996) and review by peers is the most efficient way to identify them. Similarly code errors are the most difficult to solve (Spitz and Moreno, 1996) and validation studies are the most efficient way to identify them. Validation has been described by Spitz and Moreno (1996) as " a shortcut to gaining greater confidence in model predictions in the absence of uncertainty analysis". These criteria are summarized in Table 3.1.

The fourth criterion was that the model had been identified as a Tier 3 RBCA fate and transport model in the 1998 "ASTM RBCA Fate and Transport Models: Compendium and Selection Guidance". This comprehensive screening of models used in the RBCA process was utilized to ensure that the model selected for this study was a model that was actually being used as a Tier 3 RBCA model. At the time of initiation of this study this was the most comprehensive model selection guidance available.

Table 3.1. Criteria for Selecting a NAPL Simulation Model

Criteria	Remarks
Applicability to Petroleum Contaminated sites	The model should be a finite element code capable of simulating multi-phase multi-component flow and transport.
Public Domain Code with Detailed Documentation	The model should have an open source code available for scientific scrutiny and possible modification if needed.
Validated and Peer Reviewed	The model should have been validated and the results published in peer-reviewed publications.
Identified as a Tier RBCA model in ASTM RBCA Fate and Transport Models: Compendium and Selection Guidance (ASTM, 1998).	The model should have established use as a Tier 3 RBCA model.

Following a preliminary literature review (Figure 1.1), many candidate models were screened and evaluated against the criteria in Table 3.1. The results of the evaluation are summarized in Table 3.2. Based on the evaluation presented in Table 3.2, MOFAT was selected as the candidate model for this study. MOFAT is a two-dimensional finite element U.S. EPA model for coupled multi-phase flow and multi-component transport in planar or radially symmetric vertical sections.

The program can simulate flow only or coupled flow and transport. The flow module can be used to analyze two-phase flow of water and NAPL or explicit three-phase flow of water, NAPL and gas at variable pressure. The transport module can handle up to five non-inert chemical components which partition among water, NAPL, gas and solid phases. Governing equations are solved using an efficient upstream- weighted finite element scheme. MOFAT achieves a high degree of computational efficiency by using an adaptive solution domain algorithm that confines the mathematical solution domain to a sub-domain within which transient oil flow occurs. Three phase permeability-saturation-capillary pressure relations are defined by an extension of the van Genuchten model, which considers effects of oil entrapment (Katyal et. al., 1991).

Required input for flow analyses consists of initial conditions, soil hydraulic properties, fluid properties, time integration parameters, boundary condition data and mesh geometry. For transport analyses, additional input data are porous media dispersivities, initial water phase concentrations, equilibrium partition coefficients, component

Table 3.2. Summary Results of the Model Evaluation

Model	Results	Primary Reason for Screening Out
Bioplume III	Screened Out	Did not meet Criterion 2. It is Windows based only and cannot be modified to run on Unix for MC analysis.
BioSVE	Screened Out	Did not meet Criterion 2 and 4. Limited simulation capability in terms of simulating multi-phase multi-component flow and transport.
MT3D	Screened Out	Did not meet Criterion 2. Limited simulation capability in terms of simulating multi-phase multi-component flow and transport.
MARS	Screened Out	Did not meet Criterion 2 and 4. Code is not available in the public domain.
BIOSLURP	Screened Out	Did not meet Criterion 2 and 4. Code is not available in the public domain.
MODFLOW coupled with RT3D	Screened Out	Did not meet Criterion 1 and 4. RT3D (1999) was publicly released after the ASTM model selection guidance was published in 1998. While a promising model, when this study was initiated in 1999 RT3D was a recently released model and was in a state of improvement as a revised version was anticipated. Consequently this was screened out. However, as of the time of writing this thesis in 2005, MODFLOW with RT3D is a recognized international standard for ground water modeling at petroleum release sites.
MOFAT	Was Not Screened Out	Meets all Criteria
NAPL Simulator	Screened Out	Did not fully meet Criterion 3. Also did not meet Criterion 4. A promising candidate model. However at the time of initiation of this study the model was undergoing revision to improve its computational efficiency and had yet to be tested at field scale.
MOC	Screened Out	Did not meet Criterion 1. It is not applicable for all complex boundary situations due to its being a finite difference model.
T2VOC	Screened Out	Did not meet Criterion 4. Belongs to the TOUGH family of codes. A new TOUGH code TMVOC was released in 2002. TOUGH codes can be used for non-rectangular discretization as they use the Integrated Finite Difference Method.

diffusion coefficients, first-order decay coefficients, mass transfer coefficients (for non equilibrium analyses) and boundary condition data.

Time-dependent boundary conditions for the flow analysis may involve user-specified phase heads at nodes or phase fluxes along a boundary segment with zero-flux as the default condition. For transport analyses, initial conditions are specified in terms of equilibrium water phase concentrations of each partitionable component. Time-dependent boundary conditions may be stipulated as equilibrium water phase concentrations in the porous medium as prescribed fluxes defined in terms of a specified concentration in the influent liquid, or with zero dispersive flux specified.

Program output consists of basic information on input parameters, mesh details and initial conditions plus pressure heads, saturation and velocities for each phase at every node for specified output intervals. For transport analyses, the phase concentrations at each node are output at each print-out interval.

3.3 Development and Validation History of MOFAT

MOFAT was initially developed as a multi-phase flow code. The initial development and testing of MOFAT is described in Kaluarachchi and Parker (1989). Kaluarachchi and Parker (1989) presented a formulation for liquid flow in a three fluid phase porous media system and tested the effect of different iteration schemes on the formulation using

different numerical experiments to validate the model and demonstrate the effects of the iteration schemes on efficiency. Picard and Newton-Raphson iteration schemes were tested. While both schemes demonstrated similar accuracy, the Picard method was more efficient. The governing equations were solved using an upstream finite element implementation, developed by Huyakorn and Nikuha (1979), that has been demonstrated to be better than the standard Galerkin technique from the perspective of accuracy and stability of simulations.

In Kaluarachchi and Parker (1990) this multi-phase flow model was extended to include multi-component constituent transport. The transport model utilizes a parametric model developed by Parker et. al. (1987) for relative permeability-saturation-pressure relationships in three fluid phase systems. These have been modified to account for NAPL entrapment. The relationships can be calculated using measurements of two-phase pressure-saturation relations.

MOFAT and its constitutive components have been tested, validated and presented in a series of studies by Parker et. al. (1987), Parker (1989), Lenhard et. al. (1988), Kaluarachchi and Parker (1989), Kaluarachchi and Parker (1990), and Kaluarachchi and Parker (1992). Helweg (1992) successfully used MOFAT to study the impact of an oil pipeline rupture in the recharge area of a West Tennessee aquifer. Similarly Tyagi and Martell (1993) successfully used MOFAT to predict the plume migration of p-cymene. Lenhard et. al. (1995) used MOFAT to test STOMP, a subsurface flow and transport

simulator for investigating remediation technologies. Steffy et al. (1998) successfully tested modifications to MOFAT to improve its simulation of LNAPL displacement and entrapment in response to a fluctuating water table. The modifications include a linear LNAPL trapping estimate and a new scaling technique for the inhibition portion of the fluctuation (water table rise).

3.4 Identifying Uncertainty

The identification of uncertain and variable input parameters is an integral component of parametric uncertainty analysis. It identifies those parameters that would need to be modeled as probabilistic inputs rather than deterministic inputs.

The identification of uncertain input parameters for MOFAT requires a careful examination of its mathematical formulation. The mathematical formulation for MOFAT consists of governing equations for describing multi-phase flow and governing equations for describing multi-component transport. These equations are presented in the next two sub-sections with the intention of identifying the input parameters and for categorizing the type of uncertainty associated with each input parameter. As new input parameters are encountered in the formulation they are underlined and the level of variability associated with the input parameter is discussed.

3.4.1 Governing Equations for Multi-Phase Flow

The mass conservation equations for water (w), organic liquid (o) and air (a), assuming an incompressible porous medium, incompressible liquid phases and compressible gas phase, may be written in summation convention for a two dimensional Cartesian domain as (Parker, 1989):

$$\phi \frac{\partial \rho_p s_p}{\partial t} = -\frac{\partial \rho_p q_{p_i}}{\partial x_i} + R_p \qquad [1]$$

Where

ϕ = porosity. Porosity is a soil property that is inherently variable.

S_p = p- phase saturation

x_i (and x_j) = Cartesian spatial coordinates ($i,j = 1,2$)

q_{pi} = Darcy velocity of phase p in the i-direction

ρ_p = density of phase p

R_p = net mass transfer per unit porous media volume into (+) or out of (-) phase p

t = time

Darcy velocities in the p-phase are defined by:

$$q_{p_i} = -K_{p_{ij}} \left\{ \frac{\partial h_p}{\partial x_j} + \rho_{rp} u_j \right\} \qquad [2]$$

Where

$\boldsymbol{K_p}$ is the p-phase conductivity tensor. Hydraulic conductivity is a soil property that is also inherently variable. The vertical hydraulic conductivity is a function of soil type. Typically horizontal conductivities are higher than vertical conductivities (Spitz and Moreno, 1996). The horizontal hydraulic conductivity however is a function of soil formation and can vary from being equal to the vertical hydraulic conductivity to being up an order of magnitude or more higher than the vertical hydraulic conductivity.

$h_p = P_p / g\rho'_w$ is the water height-equivalent pressure head of phase p

Where

P_p = p-phase pressure

g = gravitational acceleration

ρ'_w = density of pure water

ρ_p = density of phase p

$\rho_{rp} = \rho_p/\rho'_w$ is the p-phase specific gravity. Specific gravities are fluid properties, are constants by definition and do not display variability. The bulk fluid density is however dependent on fluid composition.

$U_j = \partial Z / \partial X_j$ is a unit gravitational vector measured positive upwards where z is elevation.

Combining [1] and [2] yields

$$\phi \frac{\partial \rho_p s_p}{\partial t} = \frac{\partial}{\partial x_i}\left[\rho_p K_{p_{ij}} \left\{\frac{\partial h_p}{\partial x_j} + \rho_{rp} u_j\right\}\right] + R_p \qquad [3]$$

If fluid saturations are treated as implicit functions of the phase pressures, equations [3] may be solved directly with phase pressures as primary variables. To solve equation 3 the following constitutive relations were described by Parker et al. (1987), Kaluarachchi and Parker (1989) and Katyal et. al. (1991):

P- Phase Saturations

Water and oil saturations may be calculated as follows (Parker et al., 1987):

$$S_w = (1 - S_m)(\overline{\overline{S_w}} - \overline{S}_{ot}) + S_m \qquad [4]$$

$$S_o = (1 - S_m)\overline{S}_t + S_m - S_w \qquad [5]$$

Where

S_o = Oil phase saturation

S_w = Water phase saturation

S_m = Irreducible water saturation. This is the water content at which no additional water will flow. This is also known as the residual water saturation.

$\overline{\overline{S_w}}$ = Apparent water saturation

$\overline{S}_{ot}$ = Effective trapped oil saturation

$\overline{S}_t$ = Effective total liquid saturation

Apparent Water Saturation

Relationships between phase permeabilities, saturations and pressures are described by a 3-phase extension of the van Genuchten model that takes into account effects of NAPL entrapment (Parker et al., 1987):

$$\overline{\overline{S}}_w = [1 + (\alpha\beta_{ow}h_{ow})^n]^{-m} \qquad [6]$$

Where

β_{ow} = Scaling coefficient approximated by the ratio of water surface tension to oil-water interfacial tension. This is a fluid property. It is the ratio of two constants and thus does not display variability.

h_{ow} = Oil-Water capillary pressure head = h_o-h_w

α = van Genuchten porous medium parameter. This is a soil property and like most soil properties is inherently variable.

n = van Genuchten porous medium parameter. This is a soil property and like most soil properties is inherently variable. van Genuchten parameters can be estimated fairly accurately from grain size distribution data as described by Mishra et. al. (1989). However, analyses of laboratory core samples are desirable for more accurate determinations (Katyal et. al., 1991).

$$m = 1 - \frac{1}{n}$$

$$\overline{\overline{S_w}} = \overline{S}_w + \overline{S}_{ot}$$

Where

$\overline{S}_w$ = Effective Water Saturation

Effective Water Saturation

Prior to the occurrence of oil at a given location, the system is treated as a two-phase air-water system described by the van Genuchten (1980) function:

$$\overline{S}_w = [1 + (\alpha h_{aw})^n]^{-m} \qquad [7]$$

Where

α and n = van Genuchten porous medium parameters

h_{aw} = Air-Water capillary pressure head = h_a-h_w

Effective Total Liquid Saturation

$$\overline{S}_t = [1 + (\alpha \beta_{ao} h_{ao})^n]^{-m} \qquad [8]$$

Where

β_{ao} = Scaling coefficient approximated by the ratio of water surface tension to oil surface tension. This is a fluid property. It is the ratio of two constants and thus does not display variability.

h_{ao} = Air-Oil capillary pressure head = h_a-h_o

α and n = van Genuchten porous medium parameters.

Effective Trapped Oil Saturation

The effective trapped oil saturation is estimated using an empirical equation given by Land (1968). The empirical equation relates the effective trapped oil saturation to the maximum effective residual oil saturation S_{or}. The maximum effective residual oil saturation S_{or} varies from 0.3 to 0.5 (Katyal et. al., 1991).

The P-Phase Conductivity Tensors

Phase conductivities are described by Kaluarachchi and Parker (1989) as:

$$K_{p_{ij}} = \frac{k_{rp} K_{sw_{ij}}}{\eta_{rp}} \qquad [9]$$

Where

$K_{sw_{ij}}$ = Saturated tensor for water

k_{rp} = relative permeability of phase p

η_{rp} = absolute viscosity ratio between phase p and water. This is a fluid property that is dependent on fluid composition. It is the ratio of two constants and thus does not display variability for a given fluid composition.

Kaluarachchi and Parker (1989) assumed that the coordinate system is oriented with the conductivity tensor, or otherwise that off-diagonal components may be disregarded, so that $K_{sw_{ij}} = 0$ for $i \neq j$.

Relative permeability relationships corresponding to the 3-phase van Genuchten model have been derived by Parker et al. (1987). These may be modified to account for effects of NAPL entrapment:

$$k_{rw} = \bar{S}_w^{0.5}(1-(1-\bar{S}_w^{1/m})^m)^2$$
$$k_{ro} = (\bar{S}_t - \bar{\bar{S}}_w)^{0.5}[(1-\bar{\bar{S}}_w^{1/m})^m - (1-\bar{S}_t^{1/m})^m]^2 \qquad [10\text{-}12]$$
$$k_{ra} = (1-\bar{S}_t)^{0.5}(1-\bar{S}_t^{1/m})^{2m}$$

Based on a review of equations 1-12 the MOFAT input parameters for multi-phase flow are the soil properties and bulk fluid properties shown in Figure 3.1.

3.4.2 Governing Equations for Multi-Component Transport

The MOFAT multi-component transport model is based on the work of Parker (1989) and Kaluarachchi and Parker (1990). Kaluarachchi and Parker (1990) state that the mass conservation of species α in the ρ phase requires that:

$$\phi \frac{\partial C_{\alpha p} S_P}{\partial t} = -\frac{\partial J_{\alpha p_i}}{\partial x_i} + R_{\alpha p} + \gamma_{\alpha p} \qquad [13]$$

Where

$C_{\alpha p}$ = concentration of the non inert component α in p-phase

S_p = p- phase saturation

$J_{\alpha p_i}$ = mass flux density of α in p-phase per porous medium cross-section in the i-direction

Figure 3.1 MOFAT Input Parameters

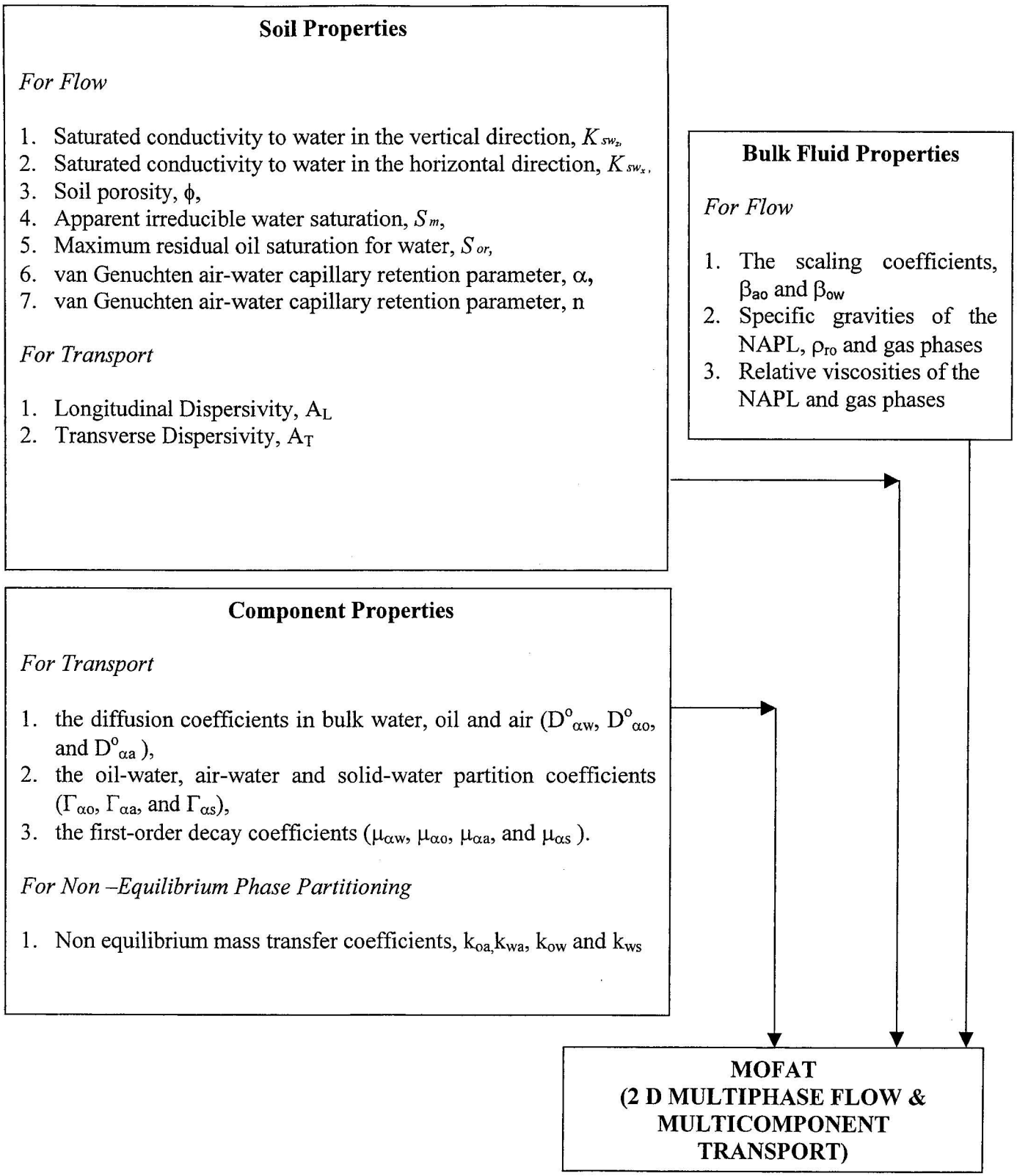

$R_{\alpha p}$ = net mass transfer rate per porous medium volume of species α into or out of the p-phase

$\gamma_{\alpha p} = -\mu_{xp} c_{\alpha p} =$ net production or decay of α within p-phase per porous medium volume due to reactions within the p-phase.

Where

μ_{xp} is an apparent first-order decay rate coefficient. This is called a component property, as it is required for each of the NAPL components being simulated. This is called an apparent decay rate coefficient, as it is representative of the decay due to a number of chemical and biological processes. As a result this parameter is difficult to quantify and is associated with significant uncertainty. This is essentially a parameter that needs to be calibrated for each individual site. Without calibration at a site these would be subject to considerable uncertainty (Katyal et. al., 1991).

Kaluarachchi and Parker (1990) describe the mass flux density of component α in p-phase due to convection, diffusion and mechanical dispersion as:

$$J_{\alpha p_i} = c_{\alpha p} q_{p_i} - \phi S_p D_{\alpha p_{ij}} \frac{\partial c_{\alpha p}}{\partial x_j} \qquad [14]$$

where $D_{\alpha p_{ij}}$ is a dispersion tensor given by:

$$D_{\alpha p_{ij}} = g_{sp}(D^{dif}_{\alpha p} + D^{hyd}_{pij}) \qquad [15]$$

Where

$D^{dif}_{\alpha p}$ = molecular diffusion coefficient of α in the porous medium

D^{hyd}_{pij} = mechanical dispersion coefficient

g_{sp} = non dilute solution correction factor

The molecular diffusion coefficient of α in the porous medium is described by Millington and Quirk (1959) as

$$D^{dif}_{\alpha p} = \phi^{1/3} S_p^{7/3} D^{o}_{\alpha p} \qquad [16]$$

Where

$D^{o}_{\alpha p}$ = diffusion coefficient of α in the bulk p-phase. This is a component property. This has been tabulated for many common industrial chemicals or may be estimated using semi-empirical estimation methods (Katyal et. al., 1991). This is not associated with any significant variability.

The mechanical dispersion coefficient, D^{hyd}_{pij}, has the form (Bear, 1972):

$$D^{hyd}_{pij} = \frac{1}{\phi S_p}\left[A_T \bar{q}_p \delta_{ij} + (A_L - A_T)\frac{|q_{pi} q_{pj}|}{\bar{q}_p} \right] \qquad [17]$$

Where

$\mathbf{A_L}$ and $\mathbf{A_T}$ = longitudinal and transverse dispersivities. The dispersivities are soil properties. The dispersivities are controlled largely by porous

media heterogeneity that typically increases with the scale of observation (Katyal et. al., 1991). Katyal et. al. (1991) note that A_L is typically on the order of 1-10% of the scale of the maximum plume dimension and A_T is several times smaller than A_L.

q_{pi} and q_{pj} = p-phase Darcy velocities

$\bar{q}_p$ = absolute magnitude of the p phase velocity

δ_{ij} = Kronecker's delta

Combining equations [13] and [14] yields:

$$\phi \frac{\partial C_{\alpha p} S_P}{\partial t} = \frac{\partial}{\partial x_i}\left[\phi S_p D_{\alpha p_{ij}} \frac{\partial c_{\alpha p}}{\partial x_j}\right] - \frac{\partial c_{\alpha p} q_{pi}}{\partial x_i} + R_{\alpha p} - \mu_{\alpha p} c_{\alpha p} \qquad [18]$$

Expanding the first and third terms, employing the bulk p phase continuity equation and assuming density derivative terms to be of second order importance yields:

$$\phi S_p \frac{\partial C_{\alpha p}}{\partial t} = \frac{\partial}{\partial x_i}\left[\phi S_p D_{\alpha p_{ij}} \frac{\partial c_{\alpha p}}{\partial x_j}\right] - q_{pi} \frac{\partial c_{\alpha p}}{\partial x_i} + R_{\alpha p} - (\mu_{\alpha p} + \frac{R_p}{\rho_p}) c_{\alpha p} \qquad [19]$$

The following continuity equation is required to describe the adsorption of α by the solid phase:

$$\frac{\partial c_{\alpha s}}{\partial t} = R_{\alpha s} - \mu_{\alpha s} c_{\alpha s} \qquad [20]$$

Where

$c_{\alpha s}$ = Solid phase concentration expressed as mass of adsorbed component α per porous medium volume

$\mu_{\alpha s}$ = First-order decay term in the solid phase.

$R_{\alpha s}$ = Mass transfer rate per porous medium volume

Inter-phase transfer terms provide coupling between the phase transport equations. To avoid the explicit consideration of inter-phase transfer kinetics, Kaluarachchi and Parker (1990) assume phase transfer to be equilibrium controlled and introduced the following thermodynamic relation:

$$c_{\alpha p} = \Gamma_{\alpha p} c_{\alpha w} \qquad [21]$$

Where

$\Gamma_{\alpha p}$ = equilibrium partition coefficient for species α between water and organic liquid (Raoult's constant), gas (dimensionless Henry's constant), and solid phases. These are component properties and are constants. They do not exhibit significant parameter variability.

The water-air partition coefficient is also known as Henry's Law Constant. It is the ratio of the aqueous solubility of substance to the saturated vapor concentration of the pure phase of the substance (Baehr, 1987). Compounds such as the BTEX compounds which have a high water-air

partition coefficient favor the aqueous phase. This selective partitioning allows the BTEX compounds to reach the water table via infiltration of capillary water before other components of a gasoline spill (Fetter, 1992). This is why the BTEX compounds are of concern during an oil spill.

Using the equilibrium relations in equation 21 to eliminate oil, gas and solid phase concentrations from equation 19 and summing the equations so that $R_{\alpha w} + R_{\alpha o} + R_{\alpha a} + R_{\alpha s} = 0$, leads to the following phase-summed transport equation for species α:

$$L(c_{\alpha w}) \equiv \Phi^*_{\alpha} \frac{\partial c_{\alpha w}}{\partial t} - \frac{\partial}{\partial x_i}\left[D^*_{\alpha ij} \frac{\partial c_{\alpha w}}{\partial x_j} \right] + q^*_{\alpha j} \frac{\partial c_{\alpha w}}{\partial x_i} + \mu^*_{\alpha} c_{\alpha w} = 0 \qquad [22]$$

Where

$$\Phi^*_{\alpha} = \Phi S_W + \Phi S_o \Gamma_{\alpha o} + \Phi S_a \Gamma_{\alpha a} + \Gamma_{\alpha s}$$

$$D^*_{\alpha ij} = \Phi S_w D_{\alpha w ij} + \Phi S_o D_{\alpha o ij} \Gamma_{\alpha o} + \Phi S_a D_{\alpha a ij} \Gamma_{\alpha a}$$

$$q^*_{\alpha i} = q_{\alpha w i} + q_{\alpha o i} \Gamma_{\alpha o} + q_{\alpha a i} \Gamma_{\alpha a}$$

$$\mu^*_{\alpha} = \mu^*_{\alpha} + \mu_o \Gamma_{\alpha o} + \mu_a \Gamma_{\alpha a} + \mu_s \Gamma_{\alpha s} + \frac{R_w}{\rho_w} + \frac{R_o \Gamma_{\alpha o}}{\rho_o} + \frac{R_a \Gamma_{\alpha a}}{\rho_a}$$

$L(c_{\alpha w})$= Differential operator describing phased-summed transport.

For non-equilibrium transport, apparent equilibrium partition coefficients are used instead of the equilibrium partition coefficients used in equation 21. These are dependent on concentration and non-equilibrium mass transfer rate coefficients, k_{oa}, k_{wa}, k_{ow} and k_{ws}.

This introduces non-linearity in the phase summed transport equation and an iterative solution procedure described in section 3.4.3 is required to solve this.

Based on a review of equations 13-22 the MOFAT input parameters for multi-component transport are the component properties shown in Figure 3.1. Soil properties and bulk fluid properties are primarily input parameters for multi-phase flow simulation while component properties are input parameters for modeling multi-component transport.

3.4.3 Solution Approach

The solution of the governing equations for flow and those for transport impacts how uncertainty is propagated through MOFAT. An understanding of the solution approach further helps identify which input parameters should be modeled as probabilistic inputs.

In MOFAT the fluid flow equations are highly coupled with each other due to the dependence of saturation and permeability of each phase on pressures in other phases. The inter phase mass transfer terms couple the flow equations with the transport equations. There is also coupling due to the dependence of fluid density and viscosity on fluid composition. While the dependence of the flow equations on transport is limited over short time spans the transport equations are highly dependent on the solution of the flow equations due to the occurrence of fluid velocity and phase saturation terms directly in the transport equations and in the functional forms for the dispersion coefficients (Kaluarachchi and Parker, 1990). Kaluarachchi and Parker (1990) present the following

solution approach in which the transport equations are solved serially with the flow equations for equilibrium mass transfer conditions:

- Solve the fluid flow equations simultaneously for the current time step using time lagged densities and inter-phase mass transfer rates.
- Solve phase summed transport equations serially for species 1, 2...n using time lagged phase densities and inter-phase mass-transfer rates for the same time step.
- Back calculate inter-phase mass transfer rates and update phase densities for current time step.
- Proceed to the next time step.

For non-equilibrium mass transfer a modified solution approach is used (Katyal et. al., 1991):

- Solve the fluid flow equations simultaneously for the current time step using time lagged phase densities and inter-phase mass transfer rates.
- Solve the phase summed transport equation using current values of apparent partition coefficients, inter-phase mass transfer rates and phase densities.
- Back calculate inter-phase mass transfer rates, update phase densities and apparent partition coefficients and repeat step 2 until transport solution converges.
- Proceed to the next time step.

The numerical implementation for the above solution approaches is presented and described in detail in Kaluarachchi and Parker (1989), Kaluarachchi and Parker (1990) and Katyal et. al (1991).

An examination of the solution approaches clearly illustrates that the solution of the multi-component transport equations is highly dependent on the solution of the flow equations. The uncertainty in soil properties also directly affects the solution of the multi-component transport equations as the p-phase Darcy velocities are required for the solution of the mechanical dispersion equation (Equation 14). Consequently the input parameters associated with the flow component would be expected to have a greater impact than the input parameters associated with the transport component, on the propagation of uncertainty through MOFAT.

3.5 Parameter Selection

Based on the discussion presented in Sections 3.4.1 and 3.4.2, the soil properties are the primary source of parameter variability in the model inputs and hence are the primary source of uncertainty in model outputs. Spitz and Moreno (1996) note that in a hydro geological context uncertainty in the model predictions is largely related to heterogeneity in the system.

Heterogeneity primarily affects soil properties and this is why they are the primary source of parameter variability in the model inputs. Conductivity in the vertical and horizontal directions are affected by heterogeneity and are subject to a high degree of variability. The ratio of horizontal conductivity to vertical conductivity can vary from 1 to 10. However, the relative ratio is a function of geological formation of the sub strata and hence is a site-specific factor. For this study the soil medium was assumed to be isotropic throughout the simulated domain i.e. conductivity in the vertical and horizontal direction were assumed to be equal for this study. Dispersivity is a soil property that is important for modeling transport. The need to model dispersivity as an input subject to uncertainty was emphasized by Medina et al. (1989) though it was not attempted by them. Dispersivities are site-specific properties that are controlled largely by porous media heterogeneity that typically increases with the scale of observation (Katyal et. al., 1991). There are few methods to predict the magnitude of dispersion for a previously unstudied field situation. These are typically sourced from tracer tests or other field-tested models and are fitted values in most model applications (Spitz and Moreno, 1996). Thus, while dispersitivities are subject to a high degree of uncertainty, in the absence of more detailed information on longitudinal and transverse dispersivities these are best modeled as deterministic point inputs in this study.

The bulk fluid properties are also generally not a major source of variability as they are mostly constants by definition. Moreover when simulating coupled flow and transport, MOFAT computes the phase specific gravities internally as a function of the current

phase compositions. NAPL viscosity also varies with fluid composition. MOFAT assumes these effects are comparatively minor and does not update viscosity for temporal phase composition changes. Bulk phase viscosity may be determined experimentally for the fluid of concern, or an estimate may be made from the phase composition (Katyal et. al., 1991). Capillary pressure curve scaling parameters can be estimated from surface tension and interfacial tension data however Katyal et. al. (1991) also present other approaches for computing the scaling parameters from NAPL composition or NAPL specific gravity. Since the NAPL composition can be known accurately, bulk phase viscosity and scaling coefficients can be determined relatively accurately. The results of a literature review did not identify any studies in which the bulk fluid properties exhibited a high coefficient of variation. Consequently the bulk fluid properties were modeled as deterministic inputs (fixed values).

Most component properties are generally not a major source of variability as they are mostly constants by definition, e.g. air-water partition coefficient (Henry's constant), oil-water partition coefficient (Raoult's constant), etc. The apparent first-order decay rate coefficient is subjective to considerable uncertainty for reasons presented earlier in section 3.4.2. However this is not a well-defined parameter as it is representative of the decay due to a number of chemical and biological processes. It needs specific calibration at a site. In the absence of more detailed information on first-order decay rate coefficient in the parametric uncertainty study these are best modeled as being equal to zero. The component properties were thus modeled as deterministic point inputs. This screened the

list of probabilistic parameters required for simulating multi-phase multi-component flow down to the seven soil parameters listed in Table 3.3. Table 3.3 also lists how each of the MOFAT input parameters was modeled in this parametric uncertainty study.

3.6 Defining Parameter Uncertainties and Correlations

A parametric uncertainty analysis is the process of propagating parameter variability through a model to quantify the uncertainty introduced in the model output by input parameter variability. Input parameter variability is described by statistical distributions.

The variability in model output, also called uncertainty, is typically captured through a statistical representation (typically *cdf* plot) of the model output.

It is important that the parameter database used to quantify parameter variability be as extensive as possible to ensure that the parameter variability has been accurately determined from as large a sample set as possible. This reduces parameter uncertainty. A second requirement for the parameter database is the documentation of correlations between the input parameters. One of the goals of this study being the development of a framework for uncertainty analysis that would be widely applicable, a third requirement for the parameter database was coverage of as many soil types as possible.

Table 3.3 Categorization of MOFAT Input Parameters as Probabilistic or Deterministic and Listing of any Associated Assumptions Used in this Study

MOFAT Input Parameters	Input Type	Assumptions
Soil Parameters		
For Flow		
Saturated conductivity to water in the vertical direction, $K\,sw_z$,	Probabilistic	Isotropy
Saturated conductivity to water in the horizontal direction, $K\,sw_x$,	Probabilistic	Isotropy
Soil porosity, ϕ,	Probabilistic	
Apparent irreducible water saturation, $S\,m$,	Probabilistic	
Maximum residual oil saturation for water, $S\,or$,	Probabilistic	
van Genuchten air-water capillary retention parameter, α,	Probabilistic	
van Genuchten air-water capillary retention parameter, n	Probabilistic	
For Transport		
Longitudinal Dispersivity, A_L	Deterministic	
Transverse Dispersivity, A_T	Deterministic	
Bulk Fluid Properties		
For Flow		
The scaling coefficients,		
β_{ao}	Deterministic	
β_{ow}	Deterministic	
Specific gravities of the NAPL, ρ_{ro} and gas phases	Deterministic	
Relative viscosities of the NAPL and gas phases	Deterministic	
Component Properties		
For Transport		
Diffusion coefficients in bulk water, oil and air ($D^{o}_{\alpha w}$, $D^{o}_{\alpha o}$, and $D^{o}_{\alpha a}$),	Deterministic	
Oil-water, air-water and solid-water partition coefficients ($\Gamma_{\alpha o}$, $\Gamma_{\alpha a}$, and $\Gamma_{\alpha s}$),	Deterministic	
First-order decay coefficients ($\mu_{\alpha w}$, $\mu_{\alpha o}$, $\mu_{\alpha a}$, and $\mu_{\alpha s}$).	Deterministic	Modeled as being equal to zero
For Non –Equilibrium Phase Partitioning		
Non equilibrium mass transfer coefficients, k_{oa},k_{wa}, k_{ow} and k_{ws}	Deterministic	Not applicable

Keeping these three requirements in sight, a search was made for an extensive database of soil distributional and correlational properties that had all or most of the soil properties selected in Table 3.3. A database that met all three requirements was found to have been compiled by Robert Carsel of the U.S. EPA. This database was compiled using SCS Soil Survey Information reports from 42 states and was used to characterize input parameters for a Monte Carlo uncertainty analysis of pesticide leaching using the unsaturated zone Pesticide Root Zone Model (PRZM) (Carsel et. al., 1988).

The SCS Soil Survey Information reports were used to obtain bulk density, sand and clay contents for the 12 SCS textural classifications (Carsel and Parrish, 1988). The saturated water contents, the sand contents and the clay contents reported for each of the SCS classifications were used to compute saturated hydraulic conductivity and water retention parameters for the van Genuchten model using a multiple regression equation developed by Rawls and Brakensiek (1985).

The computed saturated hydraulic conductivity and van Genuchten water retention parameters for each of the 12 soil textural classifications was then used as the basis for characterization of probability distributions for these variables. Empirical *cdf* were derived for all of these variables and hypothesized distributions were fitted (Carsel and Parrish, 1988).

Within each of the 12 different SCS soil textural classifications, after Johnson family transformations to normal distribution were selected and distributions were fitted for all variables, sample Pearson product-moment correlations and covariances were calculated for saturated hydraulic conductivity, residual water content and van Genuchten water retention parameters α and n. This database has also been incorporated into commercial software SOILPARA (Scientific Software Group, 2005) that is used to estimate hydraulic parameters in the van Genuchten constitutive model for variably saturated soils.

For this study, joint probability distributions published by Carsel and Parrish (1988) were used to model K_{sw}, θ_r, α and n. Table 3.4 summarizes the probability distributions and the distribution parameters used to describe the variability of K_{sw}, θ_r, α and n for the SCS textural classification "loam". The "loam" soil classification was selected as an illustration for this study

The apparent irreducible water saturation, S_m, was calculated from the maximum water content, θ_m, and residual water content, θ_r, as follows (Katyal et. al, 1991):

$$S_m = \frac{\theta_r}{\theta_m}$$

Table 3.4 Input parameters, probability distributions and the distribution statistics

Parameter	Distribution	Distribution Statistics	Source
K_{sw}	Normal	Johnson Transformed Variable 0.001 quantile –9.2106 0.999 quantile 1.7906	Carsel and Parrish (1988)
ϕ	Uniform	Untransformed Variable Minimum 0.15 Maximum 0.35	Katyal et. al. (1991)
θ_r *(used to calculate* S_m*)*	Normal	Johnson Transformed Variable 0.001 quantile -0.8659 0.999 quantile 2.1439	Carsel and Parrish (1988)
S_{or}	Uniform	Untransformed Variable Minimum 0.3 Maximum 0.5	Katyal et. al. (1991)
α	Normal	Johnson Transformed Variable 0.001 quantile -3.6989 0.999 quantile 1.1589	Carsel and Parrish (1988)
n	Normal	Johnson Transformed Variable 0.001quantile 0.2261 0.999 quantile 0.8379	Carsel and Parrish (1988)

The maximum residual oil saturation for water, S_{or}, and soil porosity, ϕ, were modeled as uniform distributions based on the ranges presented in the users manual for MOFAT (Katyal et. al., 1991).

The Pearson product-moment correlations for the "loam" SCS soil textural classification are presented in Table 3.5. K_{sw} is positively correlated with θ_r, α and n. The correlations between K_{sw} and the van Genuchten water retention parameters α and n are especially strong. K_{sw} and α are also empirically related as follows:

$$\alpha \approx \left(\frac{K_{SW}}{0.5} \right)^{0.5}$$

θ_r shows a strong negative correlation with n. It is also negatively correlated with α but the correlation coefficient is a mere -0.0860. α and n show a strong positive correlation.

3.7 Code Modification

To accomplish a Monte Carlo based uncertainty analysis of any model it is important to have the ability to run the model in a batch mode where the model sequentially processes different input files and directs the output to different output files. MOFAT as distributed by the U.S. EPA and other commercial vendors does not allow batch processing of input files. It requires a single input file that defines the initial conditions, boundary conditions, soil hydraulic properties, fluid properties, time integration parameters, and mesh

Table 3.5 Pearson Product Moment Correlation Matrix

K_{sw}	1.0000			
θ_r	0.2040	1.0000		
α	0.9820	-0.0860	1.0000	
n	0.6320	-0.7480	0.5910	1.0000
	K_{sw}	θ_r	α	n

geometry. Program output consists of an output file and an auxiliary data file that defines the conditions for a restart problem. For restart problems MOFAT requires this auxiliary data file in addition to the input file.

To execute this study the FORTRAN code for MOFAT was modified and the code was compiled to run in a Unix environment to accept batch inputs. The code is attached in Appendix B. This code shall henceforth be referred to as the MC-MOFAT code in this study. The MC-MOFAT code reads in the names of input files and their corresponding output and auxiliary data files from a text file called "control". Figure 3.2 shows a sample control file. The first column lists the name of the input file, the second column lists the name of the output file, the third column lists the name of the auxiliary restart file to use if this is a restart simulation and the last column lists the name of the auxiliary data file to be created.

3.8 Processing Tools

In addition to modifying the FORTRAN code for MOFAT to allow batch processing, a set of pre and post processing tools were developed as a part of this research.

Figure 3.2 Sample Control File

```
lhshc090  lhshc090.o    lhs090.x  lhshc090.x
lhshc091  lhshc091.o    lhs091.x  lhshc091.x
lhshc092  lhshc092.o    lhs092.x  lhshc092.x
lhshc093  lhshc093.o    lhs093.x  lhshc093.x
lhshc094  lhshc094.o    lhs094.x  lhshc094.x
lhshc095  lhshc095.o    lhs095.x  lhshc095.x
lhshc096  lhshc096.o    lhs096.x  lhshc096.x
lhshc097  lhshc097.o    lhs097.x  lhshc097.x
lhshc098  lhshc098.o    lhs098.x  lhshc098.x
lhshc099  lhshc099.o    lhs099.x  lhshc099.x
```

MC analysis requires the generation of several thousand input files that represent parameter variability. The manual generation of these input files for MOFAT is very tasking and can be a source of formatting errors that would cause the data to be misread from the input file. To alleviate this a pre-processing tool was developed as a part of this research. This FORTRAN pre-processing tool allows the automated generation of MOFAT input files from a text file listing all MC or LHS samples. The tool reads in a text file that lists all MC or LHS samples and then searches for and replaces the corresponding data line in a MOFAT input file to sequentially create a new MOFAT input file for each MC or LHS sample. This tool is able to create 10,000 MOFAT input files in minutes. If done manually this task would take months. The process flow chart for this tool is shown in Figure 3.3.

When the several thousand input files generated for MC analysis are processed through the model the end result are an equal number of output files. To represent the variability of output parameters as a *cdf,* the output results for a user specified time step and node have to be extracted from each of these output files. MOFAT output files may be as large as 50 MB and several hundred pages long. To manually extract the output results for any given node and time step is time consuming so a post processing tool had to be developed to automatically extract the results for a specified node and time step from MOFAT output files.

Figure 3.3 MOFAT Pre Processor Flow Chart

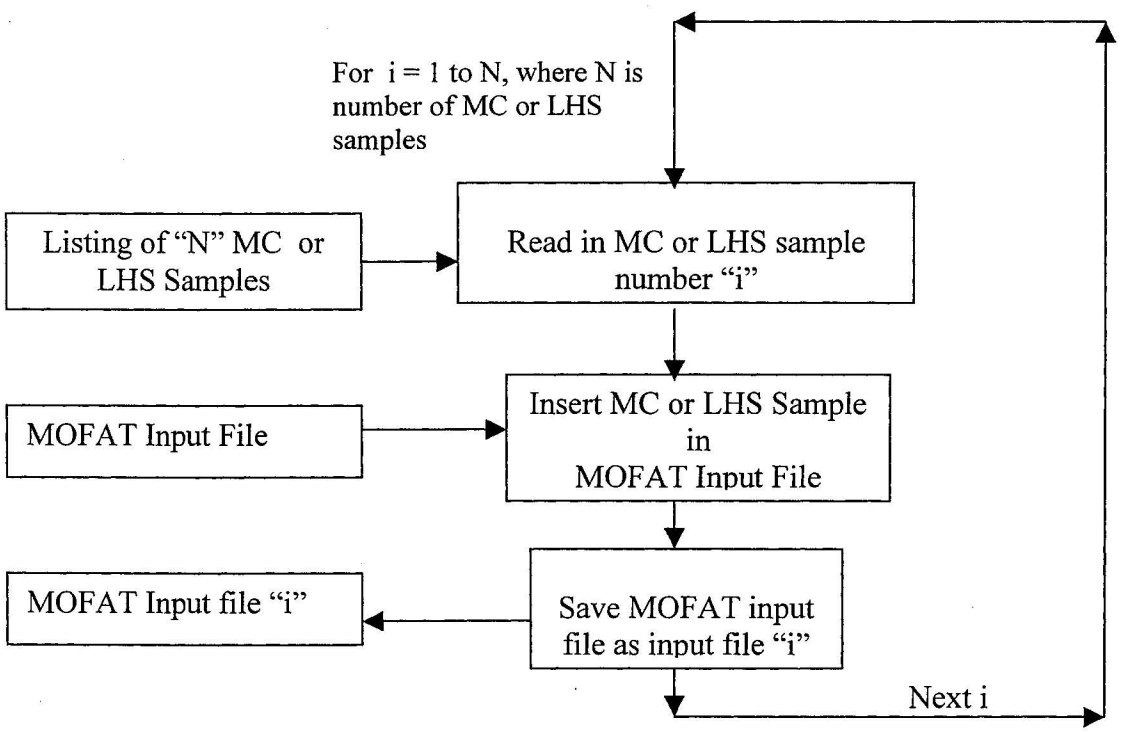

The post-processing tool is a Visual Basics for Applications (VBA) code that runs from within Microsoft Word. It sequentially opens all MOFAT output files in a specified folder, extracts the output results for the user specified time step and node and then copies the results to a text file. The text file is formatted so that it can be opened in any spreadsheet or statistical program for further analysis and plotting of *cdfs*. This tool is able to accurately extract the output results for 10,000 MOFAT output files in approximately a fortnight. If done manually this task would take months. The process flow chart for this tool is shown in Figure 3.4.

3.9 Defining Simulation Scenario and Boundary Conditions

To undertake a parametric uncertainty analysis of MOFAT a simulation scenario with appropriate boundary conditions is required to be the simulation domain for the simulation runs. This scenario could be based on an actual site specific spill scenario or a hypothetical spill scenario.

For a parametric uncertainty analysis it is also important that scenario and model uncertainties are kept at a minimum. The best way of ensuring this is to use a simulation scenario that has been validated for the model. In using a validated scenario there is assurance that the initial and boundary conditions are appropriate. The initial and boundary conditions describe the distribution of heads and concentrations in the model domain (Spitz and Moreno, 1996) and errors in these significantly affect all simulations.

Figure 3.4 MOFAT Post Processor Macro Flow Chart

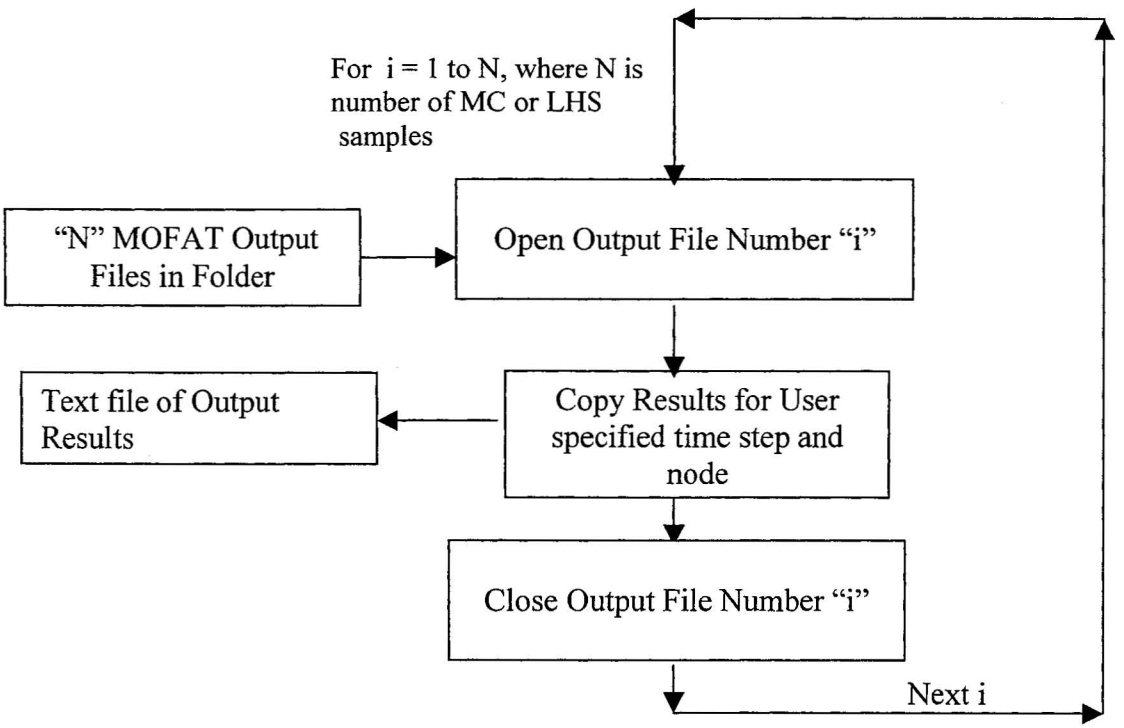

In using a validated scenario there is also added assurance that the model is being used in its intended application domain; model theory errors are at a minimum; code errors are not a factor; and that sources of model uncertainties such as numerical errors and grid size resolution are being kept at a minimum or an acceptable level.

To ensure that scenario and model uncertainties are kept at a minimum the site scenario developed for this study is based on hypothetical site scenarios used in the peer reviewed validation studies (Parker, 1989; Kaluarachchi and Parker, 1989; Kaluarachchi and Parker, 1990; and Kaluarachchi and Parker, 1992) for MOFAT. The scenarios used by Sleep and Sykes (1989) to model the transport of volatile organics in variably saturated media were also part of the comparison group used to develop the site scenario for this study. That these validation studies, and hence the hypothetical spill scenarios used in them, have been peer reviewed makes them more appropriate than any other actual spill scenario for use in the parametric uncertainty analysis of MOFAT.

The spill scenario used in this study and those used in the validation studies are compared in Table 3.6. The physical domain simulated is a 24 m long vertical slice through an aquifer with a distance of 10 m from the soil surface to the aquifer bottom. As depicted in Figure 3.5, a finite element mesh of 1029 nodes with an inter-nodal spacing of 0.5 m represents it. A slightly finer grid resolution, as opposed to the coarser ones used in the validation studies, was adopted to further minimize any potential contributions to model uncertainties due to the grid size.

Figure 3.5 Finite Element Mesh Representation of the Physical Domain Used For Simulations in This Study

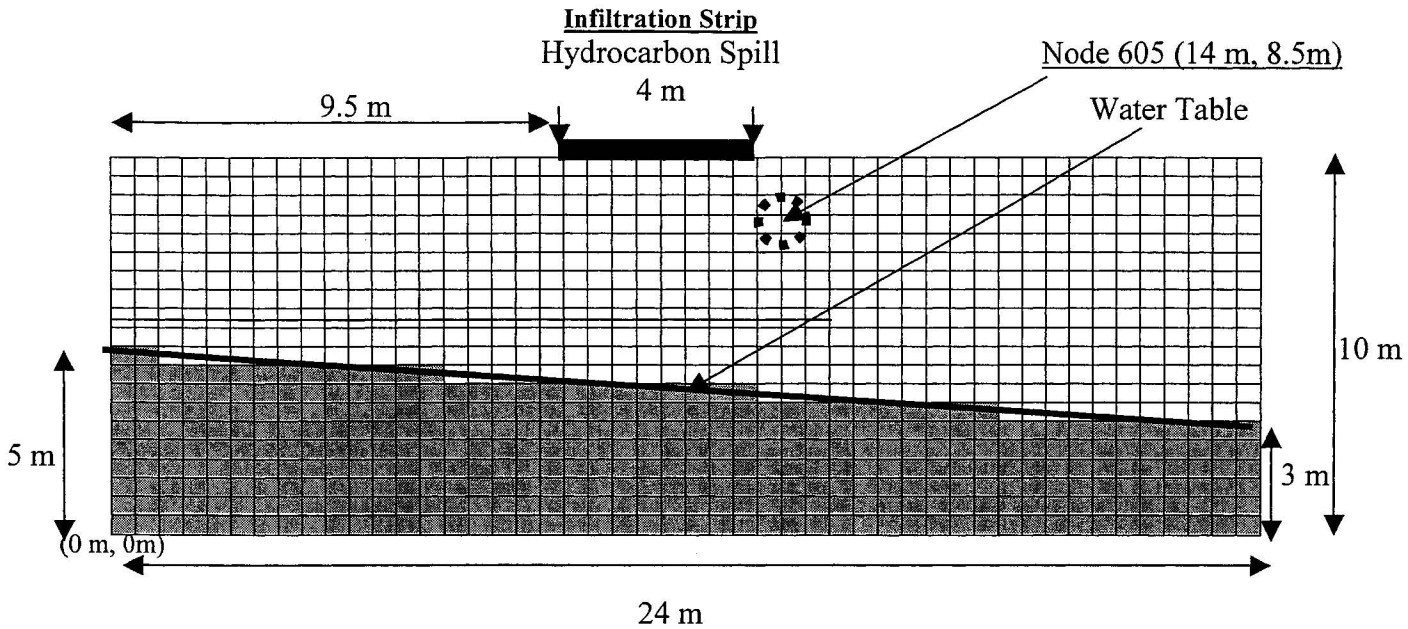

Table 3.6 Comparison of Simulation Scenarios

	No. of Elements	No. of Nodes*	Length (m)	Depth (m)	No. of Oil Components	Infiltration Strip Width (m)
Kaluarachchi and Parker (1992)	232	270	17	4	1	0.5
Kaluarachchi and Parker (1990)	513		25	12	3	3
Kaluarachchi and Parker (1989)	308	345	23	10	4	5
Parker (1989)			23	15	4	5
Sleep and Sykes (1989)	640			10		6
This Study	930	1029	24	10	4	4

* The maximum number of nodes in MOFAT must not exceed 1500 and the maximum difference between node numbers of adjacent nodes must not exceed 50.

Aspects of this scenario and the validation scenarios that contribute to minimizing numerical errors are: orienting the discretization grid along the main flow direction; using constant space discretization; and keeping cell aspect ratio within the same order of magnitude.

A water table occurs at a depth of five metres on the left boundary and a depth of three metres on the right boundary, which is maintained throughout the simulation, resulting in continuous groundwater flow to the right. A hydrocarbon spill on a four metre wide strip source at the upper surface is simulated by permitting infiltration of a prescribed volume of one cubic meter under a head of 0.1 m. Once the hydrocarbon has infiltrated into the soil (infiltration stage), the inter-phase mass transfer and transport (re-distribution stage) of the hydrocarbon is simulated while subject to zero boundary flux. The hydrocarbon simulated is a Benzene, Toluene, Ethyl benzene and Xylene (BTEX) mixture consisting of equal volumes of each component.

The results were evaluated at node 605, which is located at a X coordinate of 14 m and a Y coordinate of 8.5 m. The origin (coordinates 0 m, 0 m) of the coordinate system is the lower left corner of the grid. The results were evaluated at node 605 at time step of 3.1 days, as it was the most common time for the maximum number of simulations. The effect of parametric variability was reflected in the simulation time steps, which varied from 0.6 day to 57.8 days for the infiltration stage and from 1 day to 28.4 days for the re-distribution stage.

Chapter 4. Uncertainty Analysis

4.1 Introduction

The uncertainty analysis of MOFAT consisted of several stages. While the general layout of the study has been presented earlier in Figure 1.1, the stages specific to the uncertainty analysis component are expanded and illustrated in Figure 4.1. The preliminary stages of spill scenario selection, code modification, identification of variable inputs and compilation of the input parameter database have been described earlier in Chapter 3.

The first stage of the uncertainty analysis itself was the execution of a Monte Carlo analysis of MOFAT using random sampling (RS-MC). RS-MC refers to the traditional method of sampling variables in simulation modeling where samples for each input parameter are chosen completely randomly across the range of each distribution. RS-MC is considered the benchmark of uncertainty analysis and all other techniques are compared to the results of RS-MC to establish their accuracy and effectiveness. The aim of this exercise was to establish the uncertainty in model outputs that results from the

Figure 4.1 Uncertainty Analysis Flow Chart

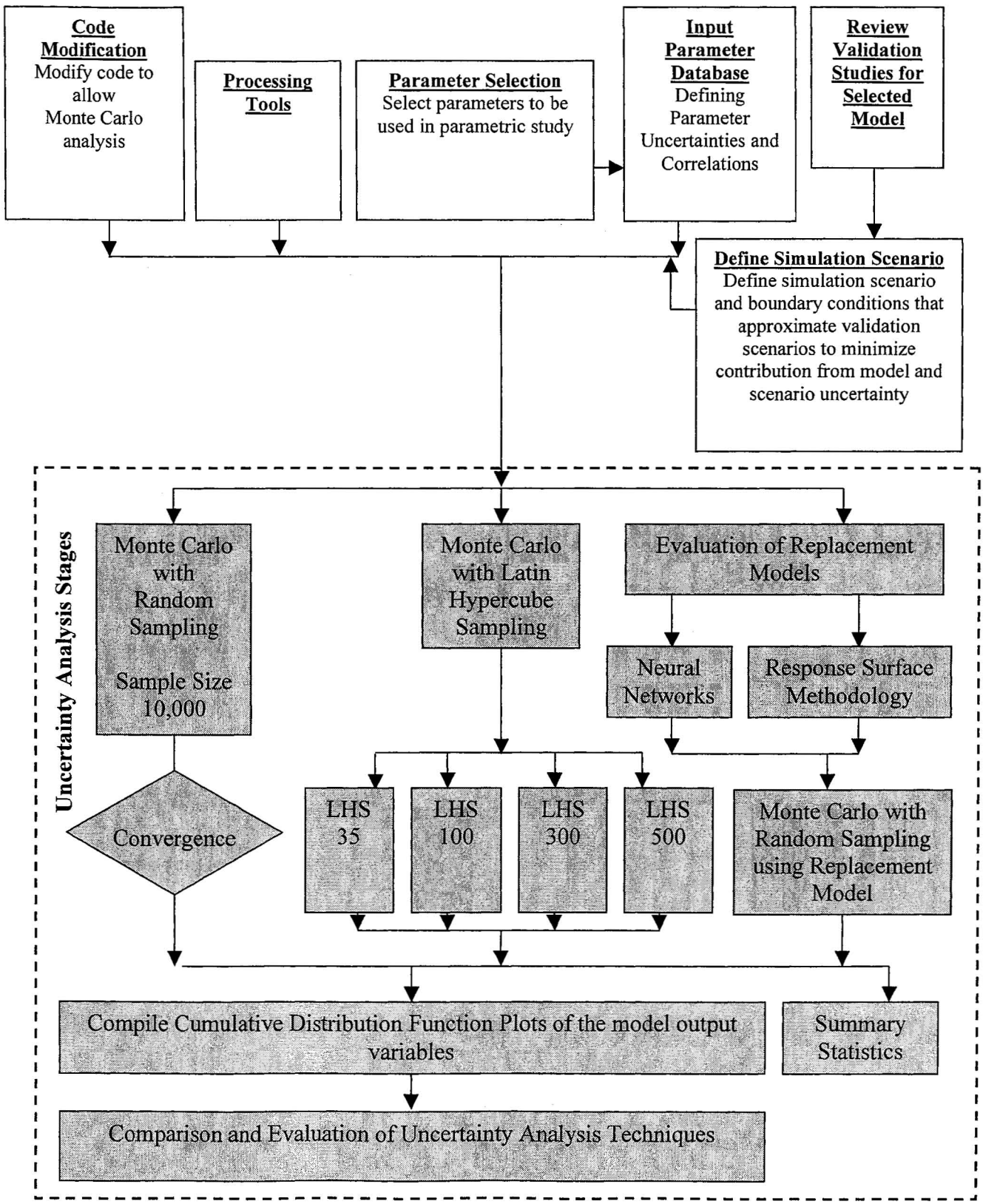

propagation of parameter variability through MOFAT. *cdf* plots for each of the 12 model outputs (concentrations of Benzene, Toluene, Ethyl benzene and Xylene in the soil, water and gaseous phases) were plotted to capture the uncertainty in model outputs.

The second stage was the execution of an uncertainty analysis using the more economical Latin Hypercube Sampling (LHS) with MC to evaluate if LHS-MC could be used as a replacement for RS-MC. LHS- MC was significantly more economical than the RS-MC simulations; RS-MC simulations consisted of 10,000 simulations whereas the simulation required for LHS-MC were only 35. The uncertainty analysis was conducted using four different LHS sample sizes of 35, 100, 300 and 500 to evaluate the effect of sample size.

The third stage was the evaluation of the two model replacement techniques to evaluate if an alternate model, for the purpose of uncertainty analysis, could replace MOFAT. Two model replacement techniques; Response Surface Methodology (RSM) and Neural Networks (NN) were evaluated. As discussed earlier in Section 2.4.1, for complex models with outputs that have spatial and temporal components the replacement models are usually only valid for a specific spatial location and a specific time. Consequently, the two replacement models were evaluated at the finite element mesh node 605 (X coordinate of 14 m,Y coordinate of 8.5 m) at time step of 3.1 days. The rationale for selecting this node location and time step has been presented earlier in Section 3.9.

If a RSM based or a NN based model could successfully replace MOFAT, the next step was to use the replacement model to conduct an uncertainty analysis using RS-MC. Replacement models can be programmed into spreadsheets so the advantage of using a replacement model is that RS-MC analysis of the replacement model can be executed more efficiently.

The final stage of this analysis was a comparison of the various uncertainty analysis techniques with RS-MC from the perspective of accuracy and efficiency. This was to evaluate if any of the alternate uncertainty analysis techniques (LHS-MC, RSM-MC or NN-MC) could be used in lieu of RS-MC for any uncertainty analysis of MOFAT. This would be possible only if any of the alternate uncertainty analysis techniques are able to accurately replicate the results of RS-MC uncertainty analysis with greater efficiency.

4.2 Random Sampling Monte Carlo (RS-MC)

4.2.1 Generating Correlated Random Samples

The first task in executing a RS-MC is the generation of random samples of the input parameters. When correlations exist between the input parameters then the random samples need to reflect the correlations.

Random samples of correlated input parameters were generated using the Iman and Shortencarier's (1984) LHS program presented in the report entitled "Fortran 77 program

and User's Guide for the Generation of Latin Hypercube and Random Samples for use with Computer Models". This LHS program can generate both LHS and random samples. The primary reason for selecting Iman and Shortencarier's (1984) LHS program is that it is a public domain code that includes a unique restricted pairing technique that protects the samples from undesirable pair wise correlations in the sample. Due to the random pairing in the sample generation process there is the possibility of inducing undesirable pair wise correlations among some of the variables in the sample. The restricted pairing technique developed by Iman and Conover (1982) and implemented in Iman and Shortencarier's LHS computer program avoids this by restricting the interval pairings so that all the pair wise rank correlations among the input variables are very close to zero. This ensures no unwanted large pair wise correlations will exist between input variables. Conversely, this technique also allows the user to induce any desired rank correlation among the variables. It is a distribution free technique that maintains the original structure of the underlying sampling scheme (U.S. EPA, 2003). For many uncertainty and sensitivity analysis problems rank correlation is probably a more natural measure of congruent model input behavior than is the more traditional sample correlation (U.S. EPA 2003). A more detailed discussion of the restricted pair wise correlation technique, the LHS program and LHS method is found in Iman and Conover (1982), Iman and Shortencarier (1984) and Iman and Helton (1985) respectively.

Iman and Shortencarier's LHS program was written for a VMS environment and has random number generator sub routines that are dependent on the machine as well as

machine dependent constants. Various setting of its machine code dependent sub routines had to be tested to ensure that LHS samples generated, on the Compaq Alphaserver DS10 running TRu64 Unix 5.1 used in this study, were accurate. The reconfigured code was compiled and run on the Unix system to generate random and LHS samples for this study. The modified code is attached as Appendix B. The Pearson product-moment correlations for the "loam" SCS soil textural classification, presented earlier in Table 3.2, was used to generate the correlated random samples. Table 3.2 has been reproduced in Table 4.1.

The input rank correlation matrix generated using the Pearson Product Moment correlation matrix presented in Table 4.1 was not "positive definite" so Iman and Shortencarier's (1984) LHS program used an iterative procedure to produce a substitute rank correlation matrix listed in Table 4.2. This compares well to the matrix in Table 4.1. A matrix is positive definite if all its eigenvalues are positive. A positive definite matrix has exactly one matrix square root and is of computational importance since a linear system of equations with a positive definite matrix can be efficiently solved using the Cholesky decomposition (Weisstein, 1999).

The LHS program generated 10,000 random correlated samples of the input parameters K_{sw}, ϕ, S_m, S_{or}, α and n listed as parameters 2 to 7 in Table 3.3. Isotropy was assumed and consequently the vertical hydraulic conductivity was assumed to be equal to the horizontal conductivity. These samples were processed using the FORTRAN pre-

Table 4.1 Pearson Product Moment Correlation Matrix

K_{sw}	1.0000			
θ_r	0.2040	1.0000		
α	0.9820	-0.0860	1.0000	
n	0.6320	-0.7480	0.5910	1.0000
	K_{sw}	θ_r	α	n

Table 4.2 Adjusted Rank Correlation Matrix

K_{sw}	1.0000			
θ_r	0.1441	1.0000		
α	0.9373	-0.0544	1.0000	
n	0.5688	-0.7035	0.6243	1.0000
	K_{sw}	θ_r	α	n

processor tool (described earlier in Section 3.8) to assemble MOFAT input files for each random sample.

4.2.2 Execution and Convergence of Simulations

Each RS-MC MOFAT input file was sequentially used as an input in the MC-MOFAT code (described earlier in Section 3.7) and executed.

In RS-MC simulations since the random sampling process is unsupervised it is important to ensure an adequate number of random samples have been used. As discussed earlier in Section 2.4 if the number of RS-MC simulations is less than those needed for convergence, RS-MC simulation can potentially over and under sample from various points of the distribution (U.S. EPA, 2003). Since the statistics of simulation outputs start to converge when the random samples have adequately sampled the complete range of the input probabilities, convergence of the RS-MC simulations was manually tracked by comparing the mean and standard deviation for all the simulation outputs after each simulation with the same statistics for the previous simulation using a 1% convergence criterion. Summary statistics for the RS-MC outputs are presented in Appendix A.

As can be seen from the flat lining of the curves in Figures 4.2, the means for Benzene started to converge after approximately 2500 RS-MC simulations. The means for Toluene, Ethyl benzene and Xylene (Figures 4.3, 4.4, and 4.5 respectively) converged earlier after approximately 1000 RS-MC simulations Similarly the standard deviations for

Benzene (Figures 4.6) showed a much higher degree of variability and took longer to converge. They started to converge after approximately 2500 RS-MC simulations. The standard deviations for Toluene (Figures 4.7) started to converge after approximately 2000 RS-MC simulations while the Ethyl benzene and Xylene standard deviations converged earlier after approximately 1000 RS-MC simulations (Figures 4.8 and 4.9 respectively). Figures 4.2 to 4.9 illustrate that the random sample size of 10,000 used in this study was adequate.

4.2.3 RS-MC Outputs

The concentrations of the various components (BTEX) in the water, gas, and solid phases as computed by MC-MOFAT for the 10,000 RS-MC input samples are summarized using logged box plots in Figure 4.10.

The means and standard deviations for the RS-MC simulations are presented in Table 4.3. Further summary statistics for the RS-MC simulations are presented in Appendix A. For the RS-MC simulations the Benzene concentration for the water and gas phases displays the highest standard deviation with the standard deviation for the water phase being an order of magnitude higher than the corresponding standard deviation for the water phase concentration of Toluene and two orders of magnitude higher than corresponding standard deviations for the water phases concentrations of Ethyl benzene and Xylene. The standard deviations for the solid phase concentrations of all BTEX components are the same order of magnitude. The standard deviations for the water, gas

Figure 4.2 Means for Untransformed RS-MC Benzene

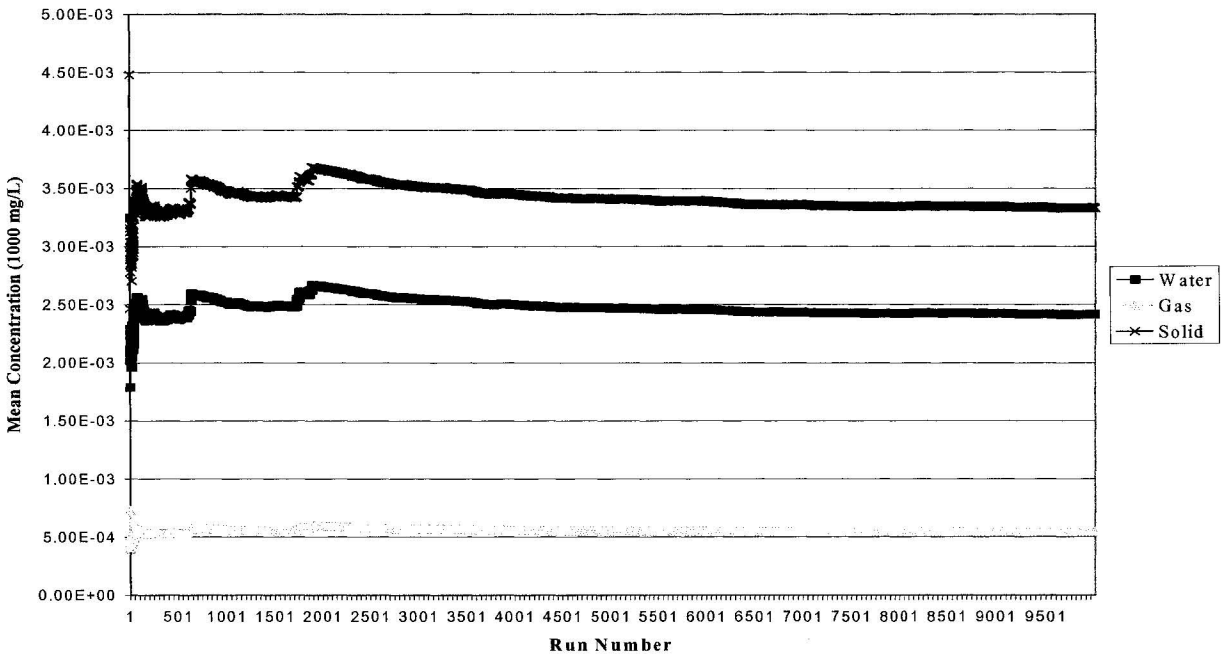

Figure 4.3 Means for Untransformed RS-MC Toluene

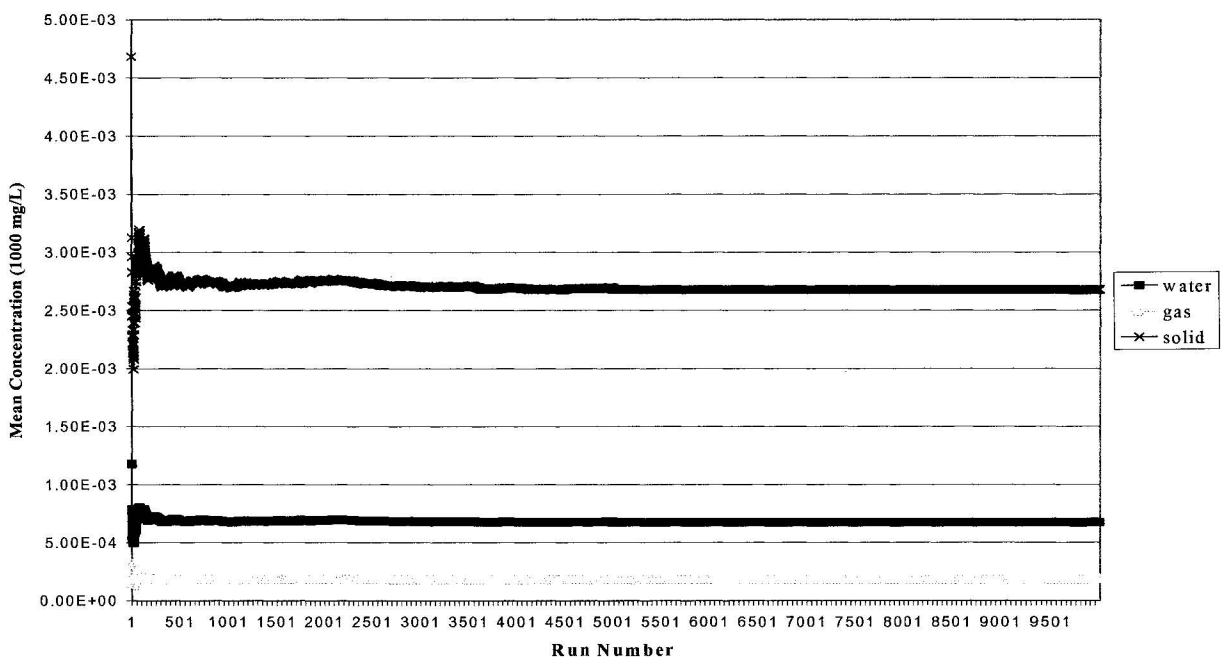

Figure 4.4 Means for Untransformed RS-MC Ethyl Benzene

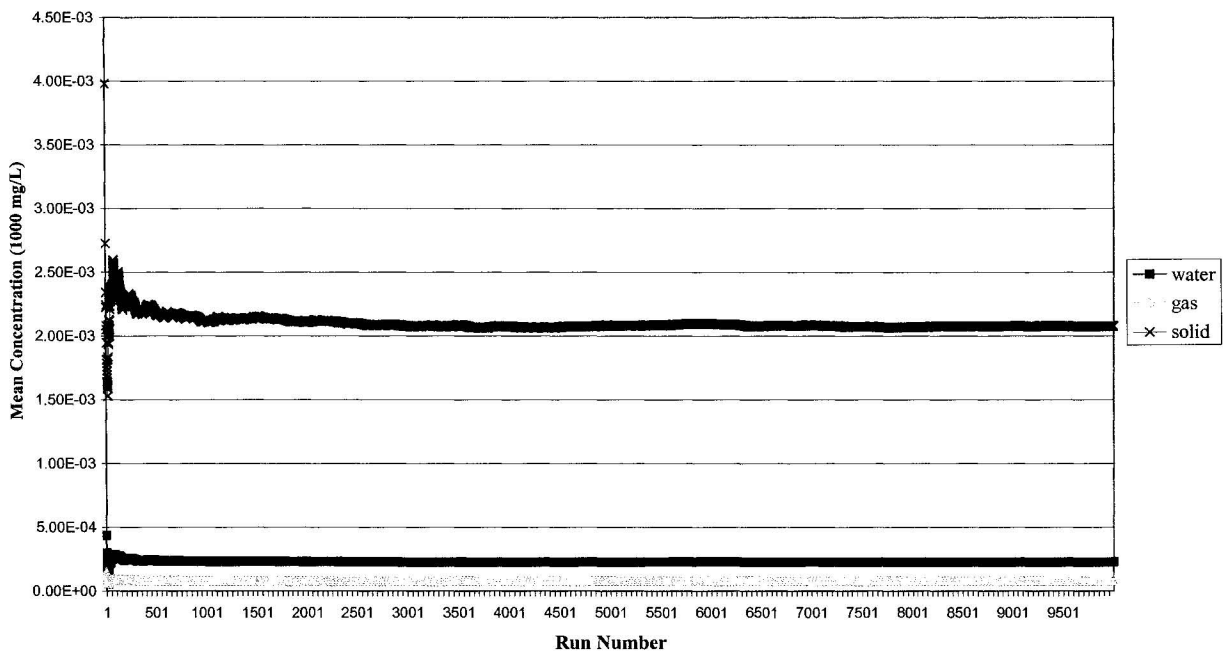

Figure 4.5 Means for Untransformed RS-MC Xylene

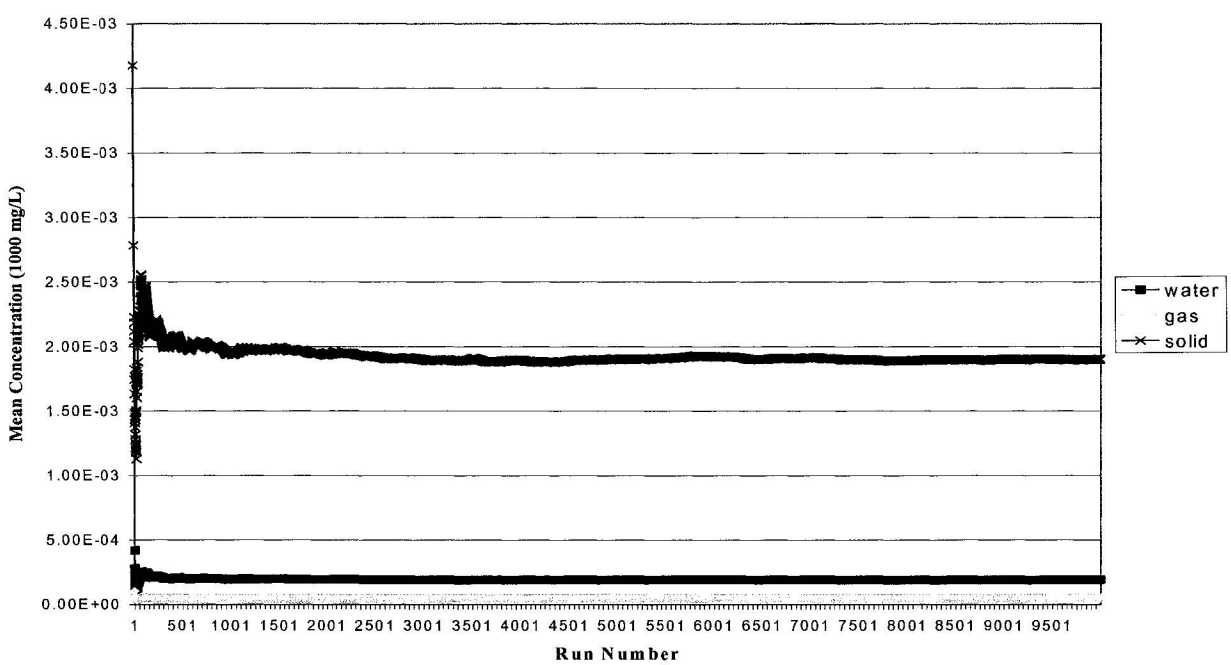

Figure 4.6 Standard Deviations for Untransformed RS-MC Benzene

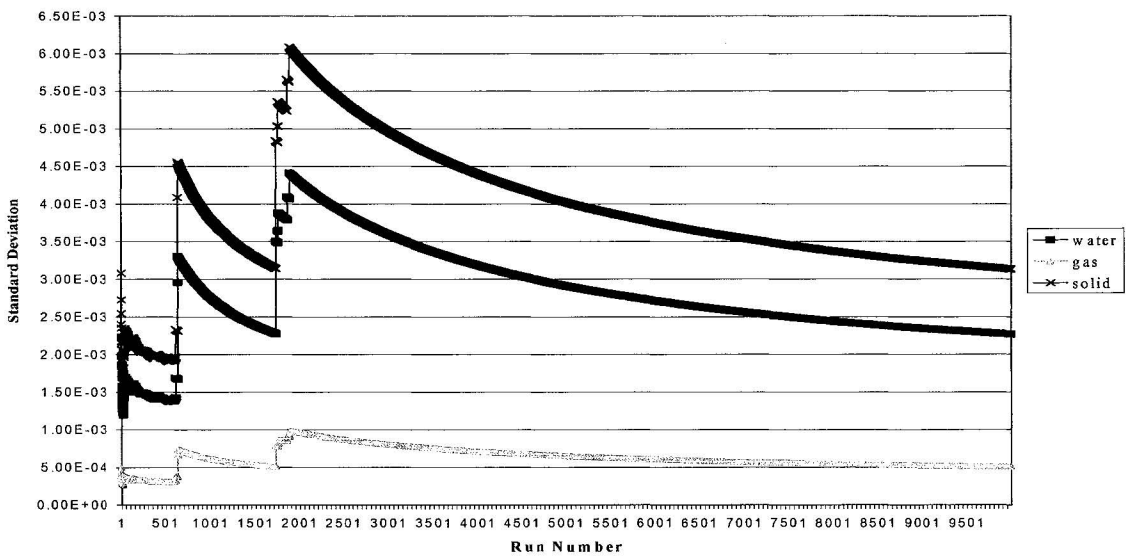

Figure 4.7 Standard Deviations for Untransformed RS-MC Toluene

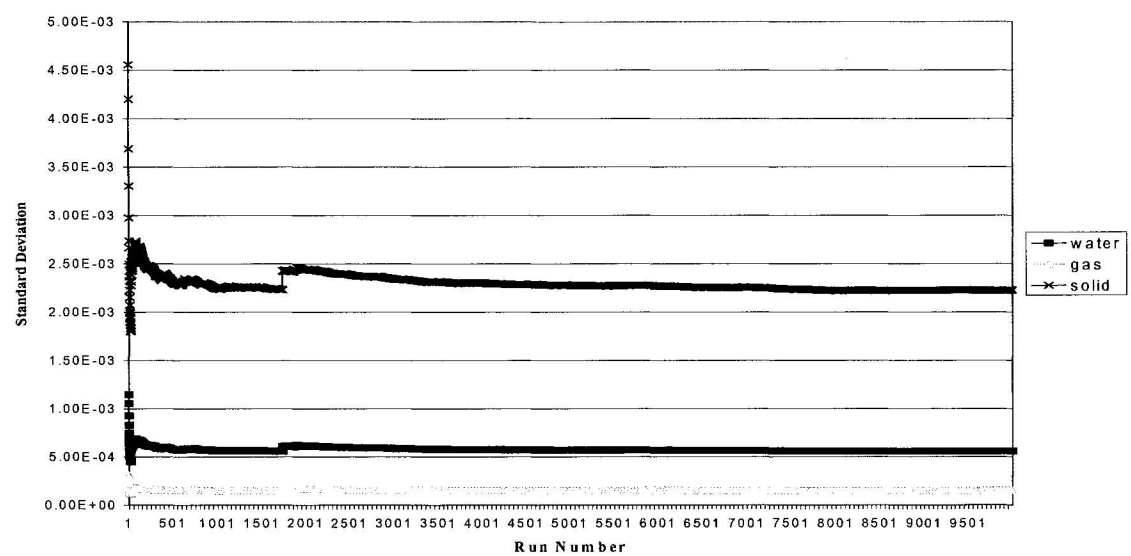

Figure 4.8 Standard Deviations for Untransformed RS-MC Ethyl Benzene

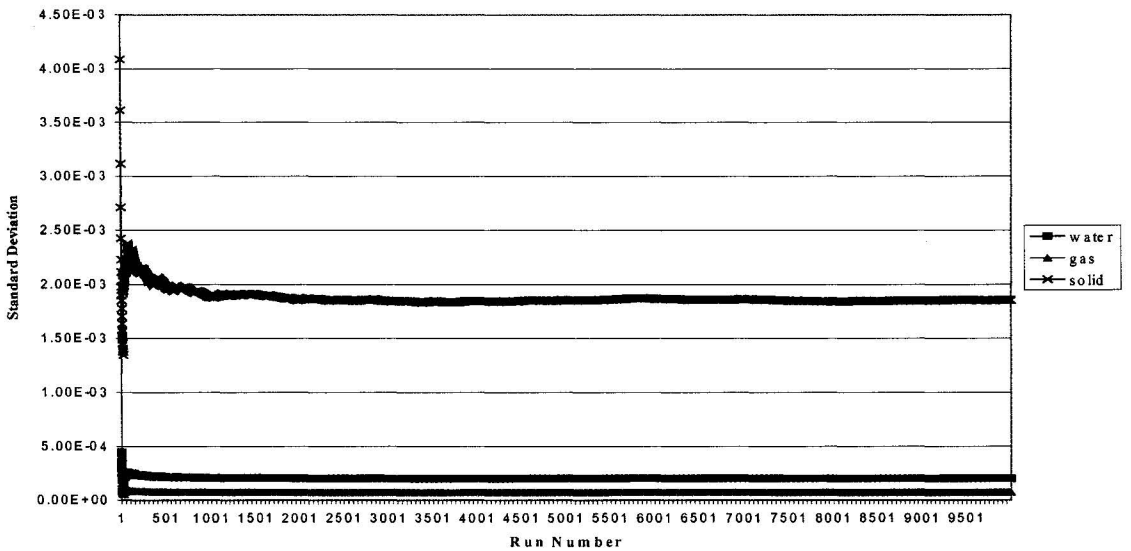

Figure 4.9 Standard Deviations for Untransformed RS-MC Xylene

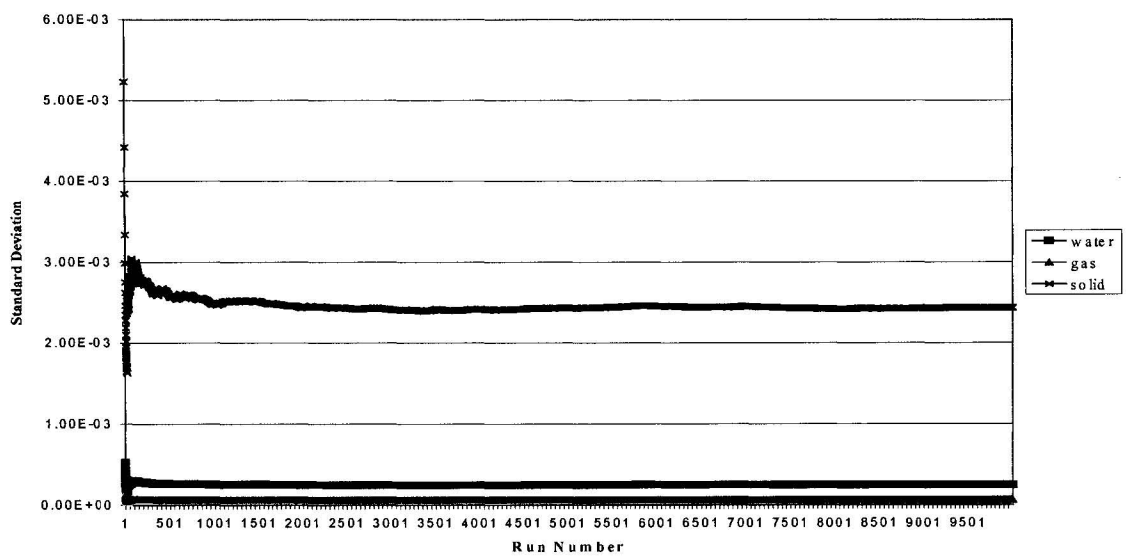

Figure 4.10 Box plots of BTEX Concentrations for RS-MC Simulations

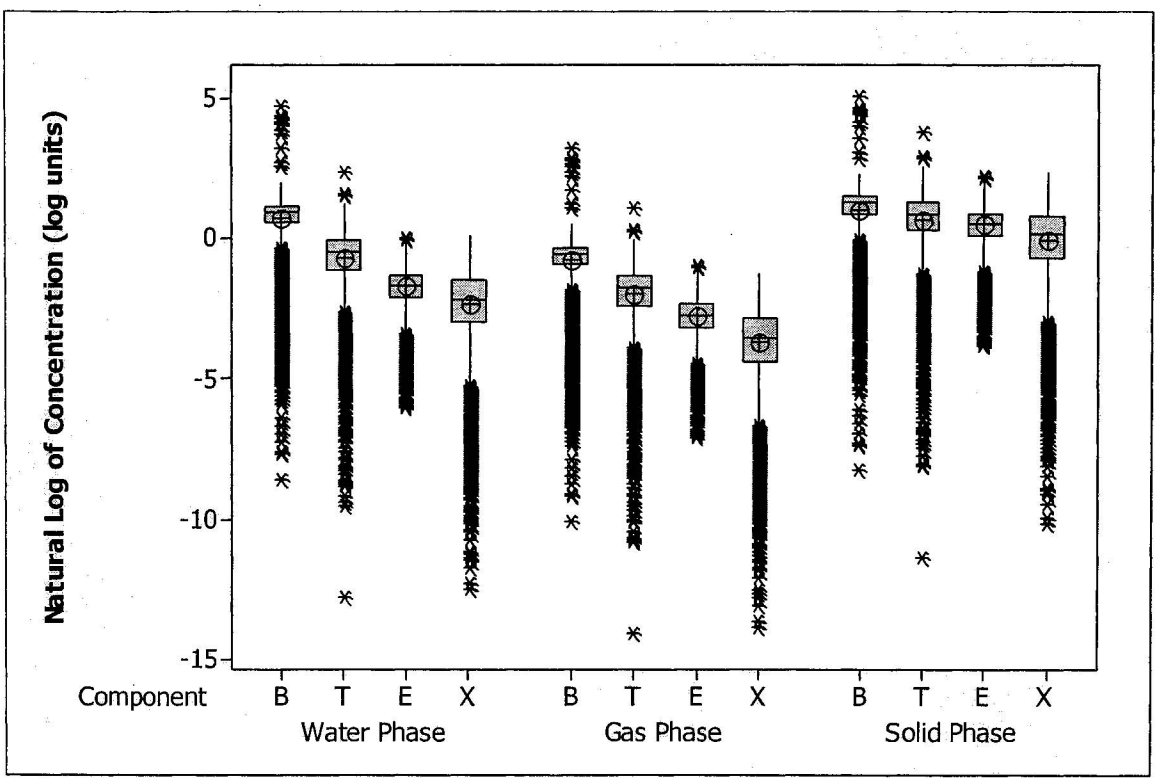

Table 4.3 Simulation Means and Standard Deviations

Component	Phase	Statistics	RS-MC*	LHS*	LHS-s*
Benzene	Water	Mean	2.41E-03	2.33E-03	2.36E-03
Benzene		Standard Deviation	2.27E-03	1.47E-03	1.38E-03
Benzene	Gas	Mean	5.43E-04	5.24E-04	5.33E-04
Benzene		Standard Deviation	5.10E-04	3.31E-04	3.10E-04
Benzene	Solid	Mean	3.33E-03	3.21E-03	3.27E-03
Benzene		Standard Deviation	3.13E-03	2.03E-03	1.90E-03
Toluene	Water	Mean	6.73E-04	6.54E-04	6.55E-04
Toluene		Standard Deviation	5.59E-04	5.65E-04	4.84E-04
Toluene	Gas	Mean	1.84E-04	1.79E-04	1.79E-04
Toluene		Standard Deviation	1.53E-04	1.54E-04	1.32E-04
Toluene	Solid	Mean	2.67E-03	2.60E-03	2.60E-03
Toluene		Standard Deviation	2.22E-03	2.24E-03	1.92E-03
Ethyl-Benzene	Water	Mean	2.27E-04	2.38E-04	2.14E-04
Ethyl-Benzene		Standard Deviation	2.03E-04	2.37E-04	1.71E-04
Ethyl-Benzene	Gas	Mean	8.15E-05	8.43E-05	7.67E-05
Ethyl-Benzene		Standard Deviation	7.28E-05	8.05E-05	6.12E-05
Ethyl-Benzene	Solid	Mean	2.07E-03	2.11E-03	1.95E-03
Ethyl-Benzene		Standard Deviation	1.85E-03	1.95E-03	1.56E-03
Xylene	Water	Mean	1.90E-04	1.88E-04	1.81E-04
Xylene		Standard Deviation	2.44E-04	2.48E-04	2.02E-04
Xylene	Gas	Mean	4.80E-05	4.80E-05	4.57E-05
Xylene		Standard Deviation	6.16E-05	6.37E-05	5.09E-05
Xylene	Solid	Mean	1.90E-03	1.87E-03	1.81E-03
Xylene		Standard Deviation	2.43E-03	2.46E-03	2.01E-03

* Units = 1000 mg/L = 1 Kg/m^3

and solid phase concentrations of Ethyl benzene and Xylene are of the same order of magnitude.

To understand if parametric statistics can be used to analyze and summarize the RS-MC outputs the RS-MC simulation outputs were tested for normality. Environmental parameters and outputs of computer simulations rarely follow the normal distribution and the RS-MC simulation results echo this. The concentrations of the various components (BTEX) in the water, gas, and solid phases are positively skewed and do not follow the normal distribution. This is highlighted in the histograms of Benzene, Toluene, Ethyl-benzene and Xylene concentrations presented in Figures 4.11 to 4.14. Consequently non-parametric statistics are more appropriate for analyzing RS-MC outputs.

4.3 Latin Hypercube Sampling Monte Carlo (LHS-MC)

4.3.1 Generating Correlated LHS Samples

As discussed earlier in Section 2.4.1 one stratified sampling technique that has been very successful is a relatively new technique called Latin Hypercube Sampling (LHS). Developed by McKay, Conover and Beckman (1979) it is a variance reduction technique that works by modifying the MC sampling process.

In the LHS-MC sampling process, n different values are selected from each of k variables $X_1, \ldots X_k$ by dividing the range of each variable into n overlapping intervals on the basis

Figure 4.11 Histograms of 10,000 RS- MC Benzene (B) Outputs

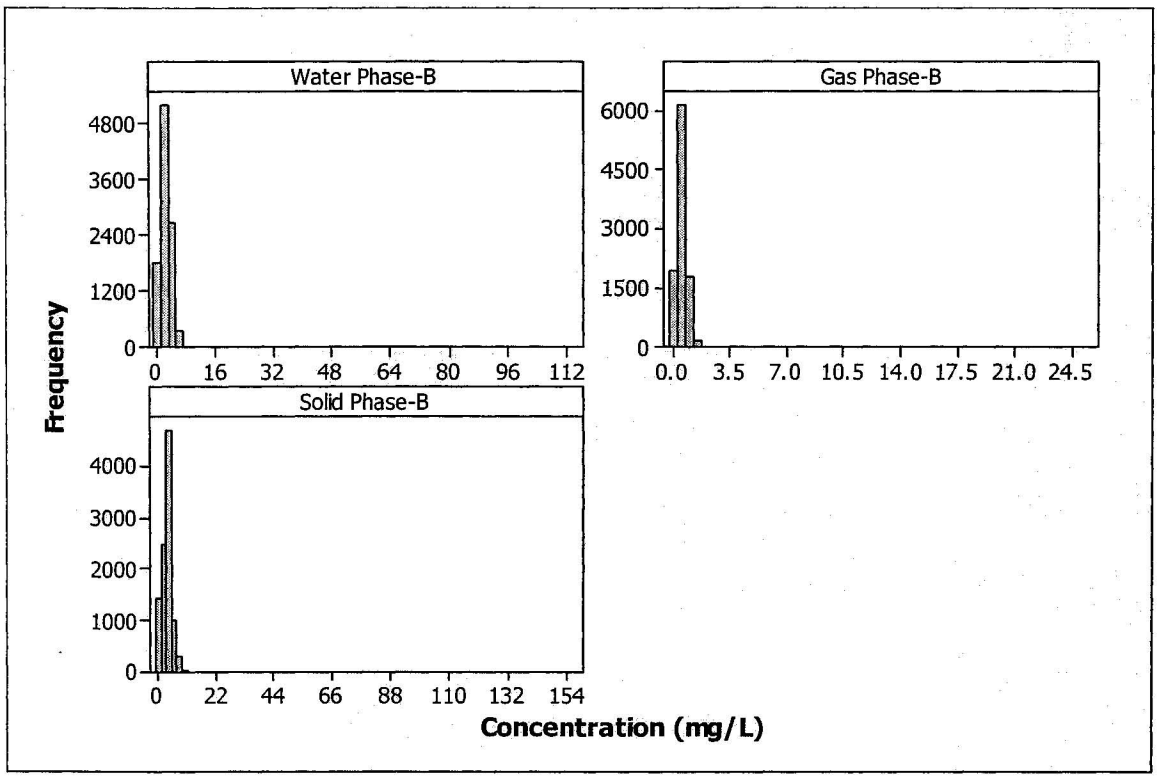

Figure 4.12 Histograms of 10,000 RS- MC Toluene (T) Outputs

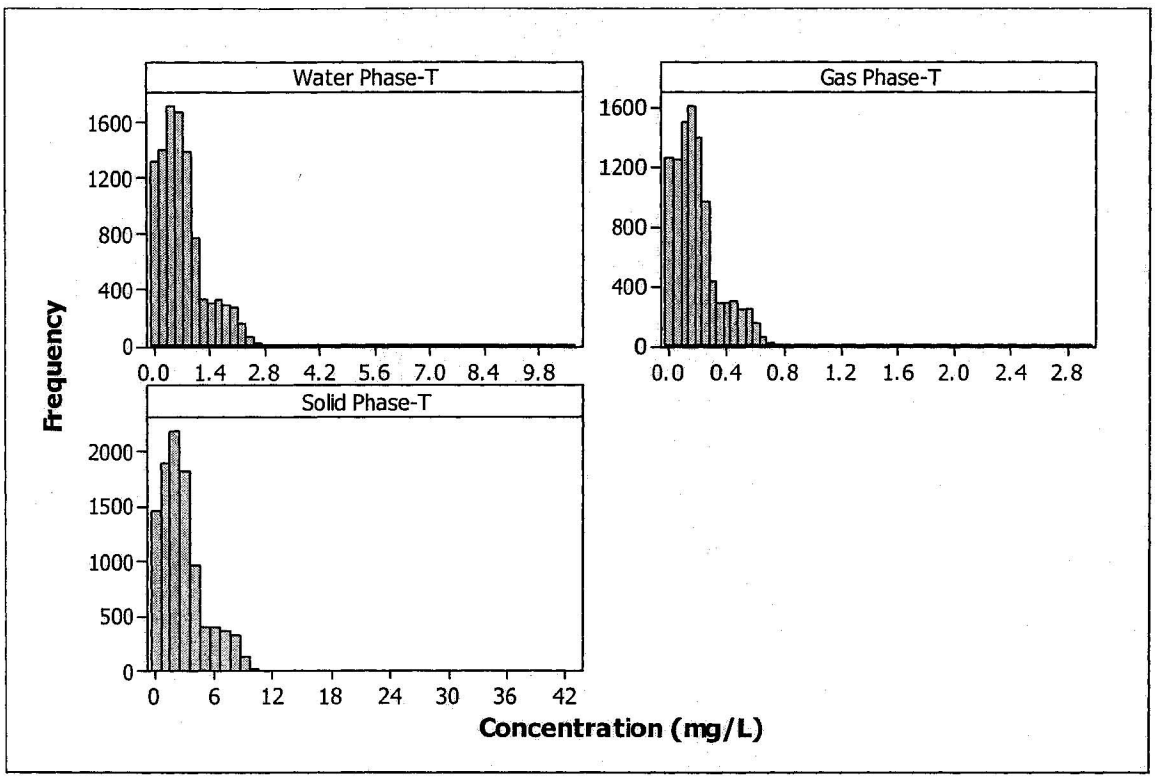

Figure 4.13 Histograms of 10,000 RS- MC Ethyl Benzene (E) Outputs

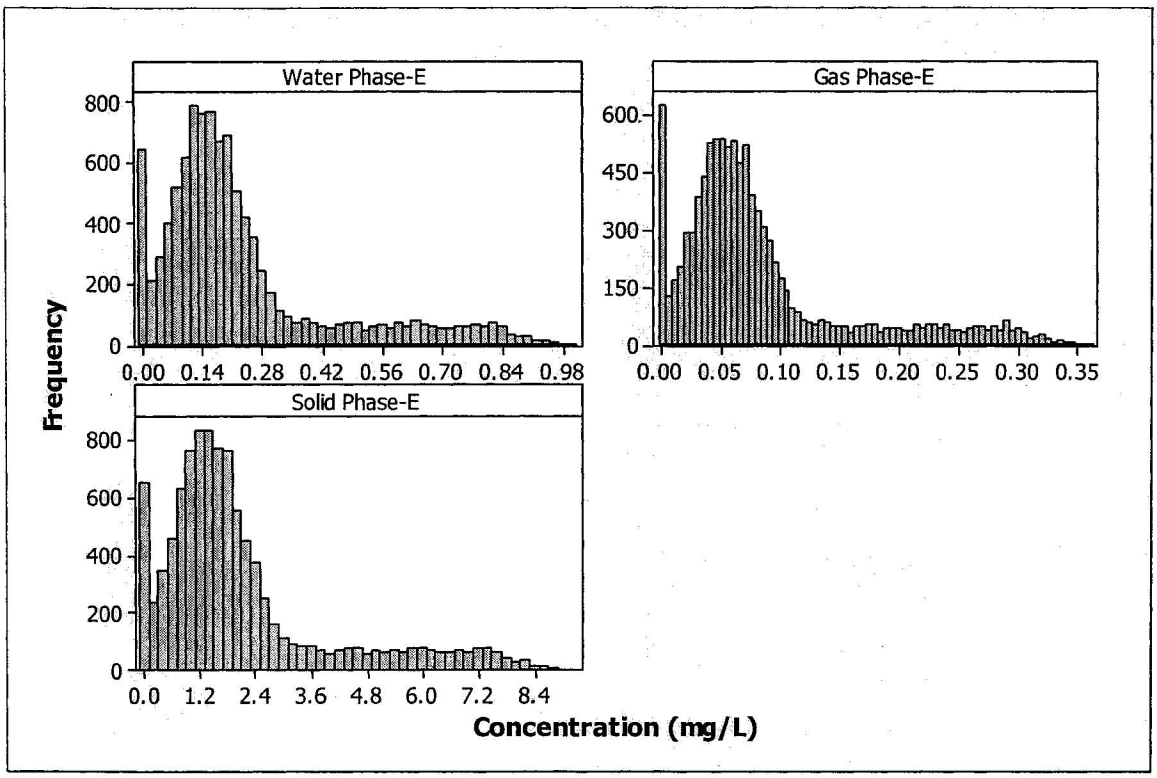

Figure 4.14 Histograms of 10,000 RS- MC Xylene (X) Outputs

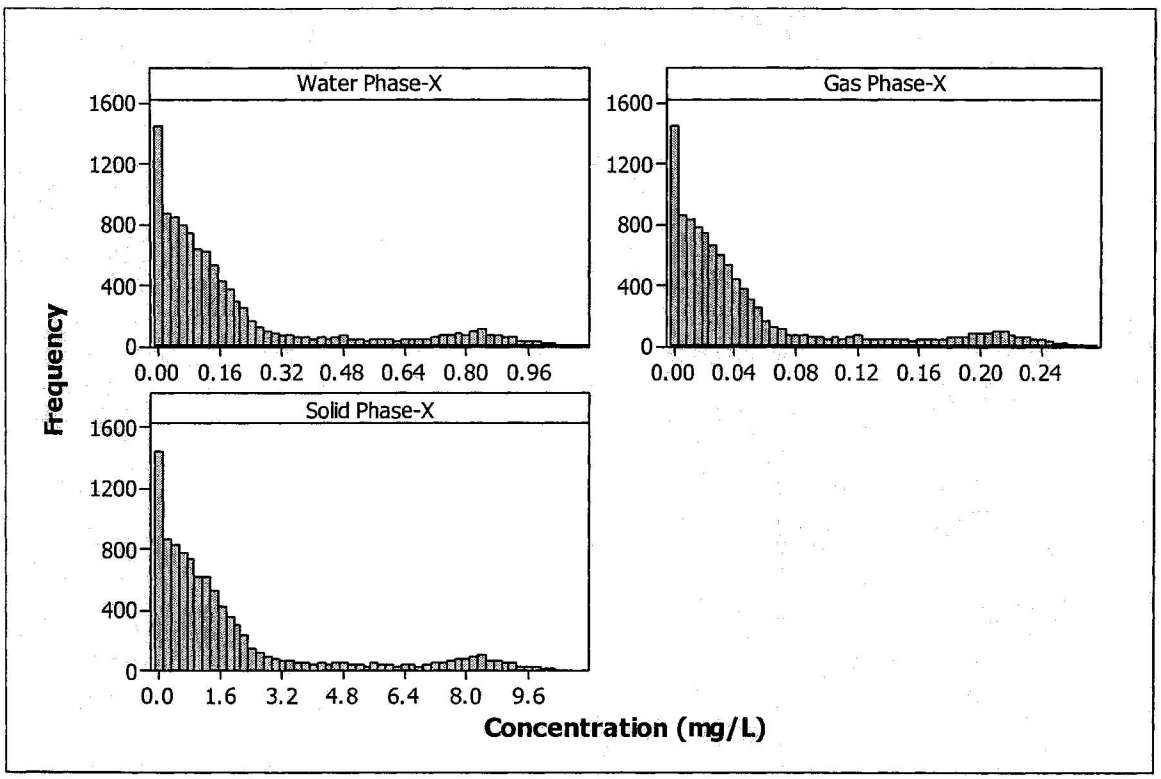

of equal probability. One value of variable from each interval is selected at random with respect to the probability density in the interval. The n values thus obtained for X_1 are paired in random order with the n values of X_2. These n pairs are combined in a random manner with the n values of X_3 to form n triplets, and so on, until n k-tuplets are formed. This is the LHS sample. The LHS-MC method is described in detail by Iman and Shortencarier (1984) and Iman and Helton (1985).

When the number of variables is large, Iman and Helton (1985) recommend that good results can be obtained if the LHS-MC sample size is between (4/3)*(number of variables) to 5*(number of variables). The appropriate LHS-MC sample size to be used in an uncertainty analysis also depends on the quantiles that are to be estimated in the uncertainty analysis. For estimating the 0.95 quantile, which is the quantile of interest in risk assessment studies, a LHS-MC sample size of at least 20 is required. A sample size of 20 ensures that each variable is divided into 20 intervals having a probability of 0.05 each. As discussed earlier in Section 2.4.1, LHS is not to be used when the estimation of very high quantiles is required, the more subjective stratified sampling technique "importance sampling" is used for such situations (Helton and Davis, 2000; Helton and Davis, 2003).

Using the recommended sample size of 5*(number of variables), a sample size of 35 was selected for this study since we have seven probabilistic variables. A sample size of 35 is adequately large to estimate the 0.95 quantile. This LHS-MC sample was designated as

LHS-s. To evaluate the effect of LHS-MC sample size, three more sample sizes of 100, 300 and 500 were also selected. These samples were designated as LHS, LHS300 and LHS500 respectively. The correlated LHS-MC samples (LHS-s, LHS, LHS300 and LHS500) were generated using Iman and Shortencarier's (1984) LHS program. The sample correlations specified earlier in Table 4.1 were induced in the samples.

These samples were processed using the FORTRAN pre-processor tool (described earlier in Section 3.8) to assemble MOFAT input files for each LHS-s, LHS, LHS300 and LHS500 sample.

4.3.2 Execution and Convergence of Simulations

Each LHS-s, LHS, LHS300 and LHS500 MOFAT input file, assembled using the LHS-s, LHS, LHS300 and LHS500 samples generated in the previous section, was sequentially used as an input in the MC-MOFAT code (described earlier in Section 3.7) and executed.

In LHS-MC simulations since the sampling process is supervised and is designed to cover the range of each input variable the convergence of simulations is not tracked.

4.3.3 LHS-MC Outputs

The concentrations of the various components (BTEX) in the water, gas, and solid phases for the LHS and LHS-s simulation outputs are summarized using log box plots in Figure 4.15. The results from the LHS and LHS-s simulations for each BTEX component within

Figure 4.15 Box plots of BTEX Concentrations for LHS and LHS-s Simulations

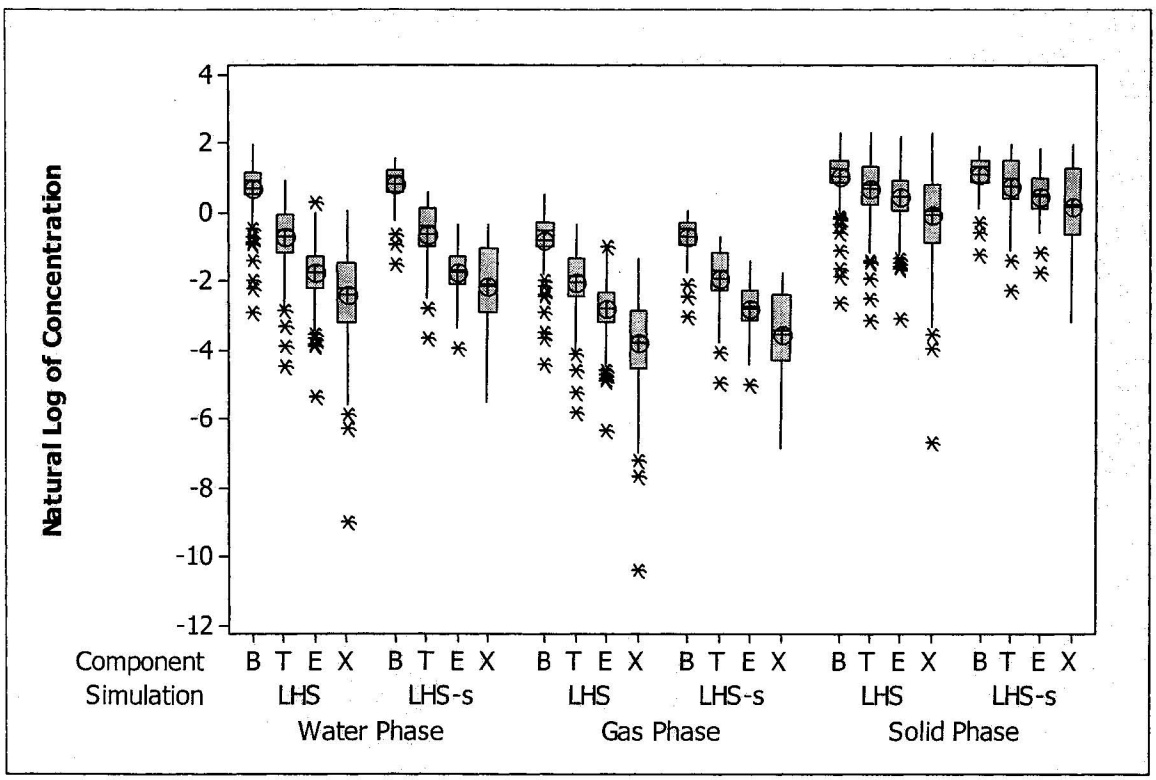

each phase are similar but the LHS simulations display a higher number of outliers in each case. The LHS300 and LHS500 simulation outputs displayed a similar trend with the number of outliers increasing with sample size.

The means and standard deviations for the LHS and LHS-s LHS-MC simulations have been presented earlier in Table 4.3. Further summary statistics for the LHS and LHS-s LHS-MC simulations are presented in Appendix A. Echoing the trend observed in the RS-MC simulations, in the LHS and LHS-s simulations the Benzene concentration for the water and gas phases displays the highest standard deviation with the standard deviation for the water phase being an order of magnitude higher than the corresponding standard deviation for the water phase concentration of Toluene. This is similarly two orders of magnitude higher than corresponding standard deviations for the water phases concentrations of Ethyl benzene and Xylene. The standard deviations for the solid phase concentrations of all BTEX components are the same order of magnitude. The standard deviations for the water, gas and solid phase concentrations of Ethyl benzene and Xylene are of the same order of magnitude.

To understand if parametric statistics can be used to analyze and summarize the LHS-MC outputs, the LHS-MC simulation outputs were tested for normality. However, in keeping with the earlier noted observation that environmental parameters and outputs of computer simulations rarely follow the normal distribution, the concentrations of the various components (BTEX) in the water, gas, and solid phases for the LHS-MC simulations do

not follow the normal distribution. This is highlighted in the normal probability plots for untransformed LHS output data (i.e. Sample size is 100) presented in Figures 4.16 to 4.19. Probability plots for untransformed LHS-s, LHS300 and LHS500 output data have not been presented but are similar. Consequently non–parametric statistics should be used to analyze all LHS-MC outputs.

4.4 Response Surface Methodology (RSM)

As described earlier in Section 2.4.1, the use of RSM in the uncertainty and sensitivity analysis of complex models is aimed at deriving a RSM to be used as a substitute for the complex model. A RSM is fitted on the responses generated by a few selected simulations of the complex model and then this RSM is evaluated as a proxy for the original model.

4.4.1 Response Surface Model Design

To develop a RS model for MOFAT the RS design selected was a six factor half fractional factorial face centered central composite design (FC-CCD). The design consists of 45 model runs with one center point run. A half fractional factorial was selected to conserve the number of model runs. A six factor full factorial CCD design would have consisted of 86 model runs.

Figure 4.16 Normal Probability Plot and 95 % Confidence Intervals for Water, Gas and Solid Phase Concentrations of Benzene from LHS Outputs

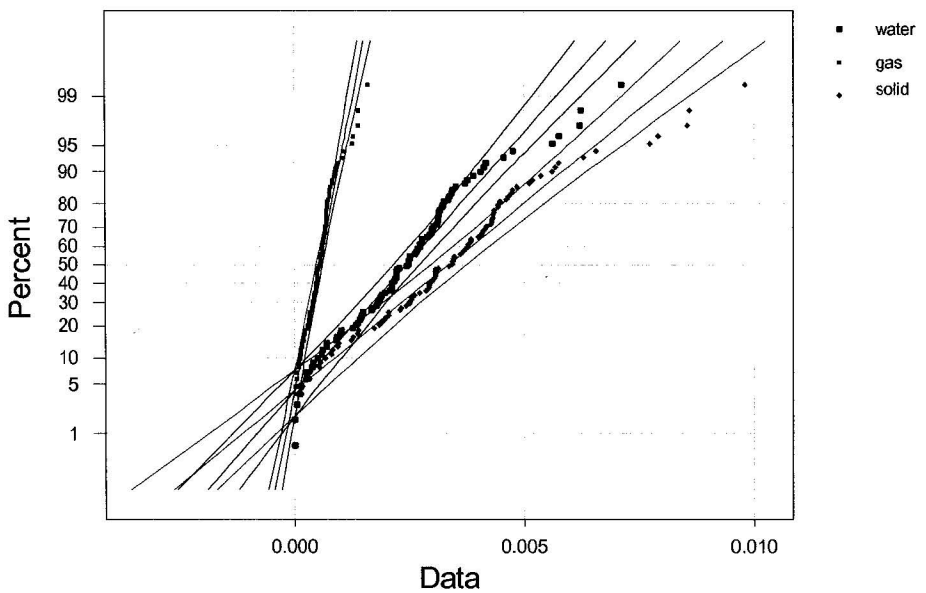

Figure 4.17 Normal Probability Plot and 95 % Confidence Intervals for Water, Gas and Solid Phase Concentrations of Toluene from LHS Outputs

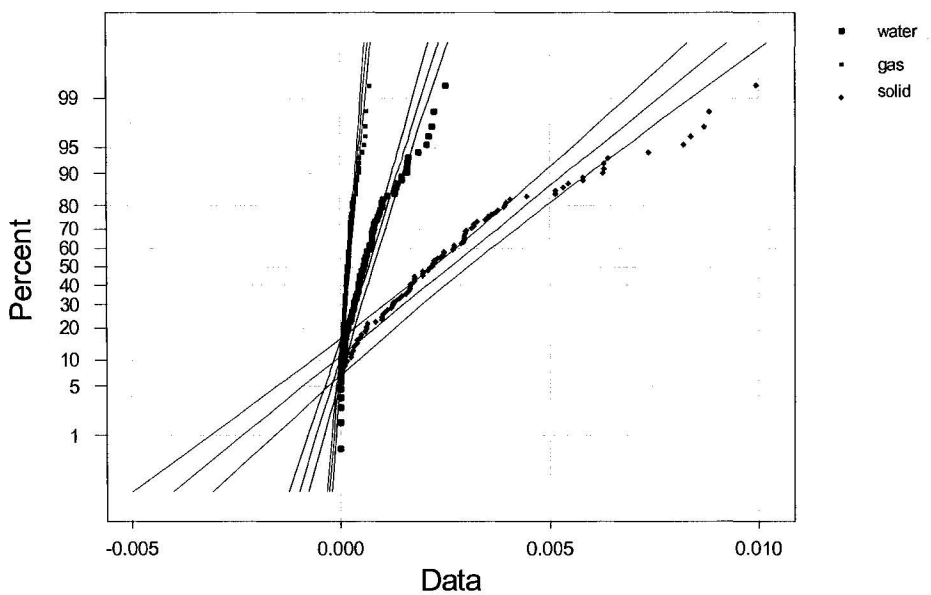

Figure 4.18 Normal Probability Plot and 95 % Confidence Intervals for Water, Gas and Solid Phase Concentrations of Ethyl Benzene from LHS Outputs

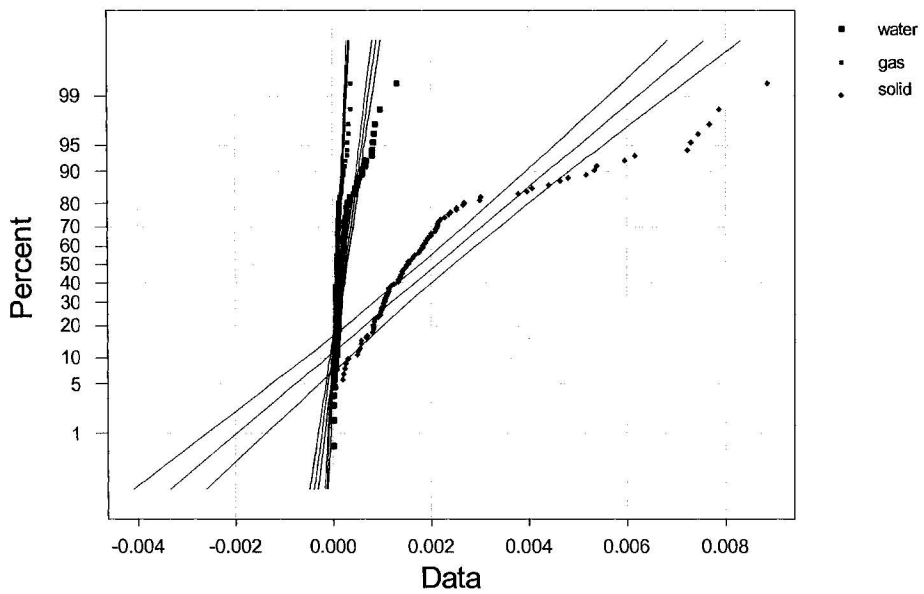

Figure 4.19 Normal Probability Plot and 95 % Confidence Intervals for Water, Gas and Solid Phase Concentrations of Xylene from LHS Outputs

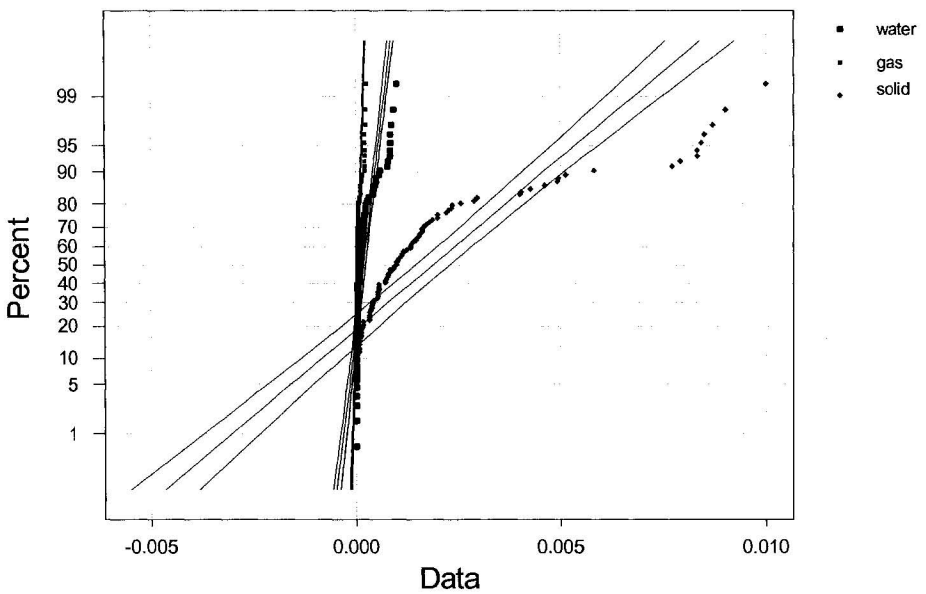

The FC-CCD design was selected because it only requires three levels of each factor. The design is not rotatable but as discussed in Section 2.4.1, while rotatability is usually a desired property, rotatability is not important for having a good design

The CCD design like all RS designs is orthogonal, that is they are based on the assumption that the input parameters are not correlated. Hence the correlations between the six input parameters could not be accommodated in the RS design.

The input files corresponding to the 45 CCD runs were assembled and simulated using MC-MOFAT. The input parameters and the corresponding responses were analyzed using the Design Expert 6 software from Stat-Ease Inc. The input parameters $K\,sw$, ϕ, S_m, S_{or}, α, and n were coded as A, B, C, D, E and F respectively. Separate response surfaces were fitted for all phases of Benzene, Toluene, Ethyl benzene and Xylene.

4.4.2 Evaluation of Response Surface Models

As described by Montgomery (2001), response surfaces are evaluated by:

1. Examining the statistical significance of the fitted models to ensure that they provide an adequate representation of the system being modeled (i.e. no difference is expected between the fitted model and the system being modeled).
2. Verifying that none of the least squares regression assumptions are violated.

4.4.2.1 Examining the statistical significance of the fitted models

All 12 response surfaces (one for each of the three phases of each BTEX component) were evaluated for statistical significance using ANOVA. In addition to the ANOVA, other model diagnostic statistics (R^2, adjusted R^2, Predicted R^2 and Adequate Precision statistic) were used to evaluate the fit and appropriateness of the responses surfaces.

The R^2 statistic is a measure of the fit of the model. It quantifies the percentage of the total variability that can be explained by the ANOVA model. The R^2 statistic is sensitive to the number of factors and is increased merely by increasing the number of factors (Montgomery, 2001).

The adjusted R^2 statistic is a variation of the R^2 statistic that desensitizes the statistic to the number of factors as it takes into account the number of factors in the model (Montgomery, 2001). The predicted R^2 is a measure of how well the model will predict the responses in a new experiment. It is based on the Prediction Error Sum of Squares (PRESS) (Montgomery, 2001).

The Adequate Precision is another measure of the predictive accuracy of the RS model. It is computed by dividing the difference between the maximum predicted response and the minimum predicted response by the average standard deviation of all predicted responses (Montgomery, 2001). Models with an Adequate Precision statistic greater than four perform well in prediction and can be used to navigate the design space.

The Adjusted R-Squared and Predicted R-Squared should be within approximately 0.20 of each other to be in "reasonable agreement." If they are not, this indicates a possible problem with either the data or the model (Montgomery, 2001).

A summary of the ANOVA, RS model statistics and the significant variables for the water, gas and solid phases of all four BTEX components are presented in Table 4.4.

For all three phases of all BTEX components the Model F-values imply that the respective RS models are significant since the "**Prob > F**" values are less than 0.001. The "Pred R-Squared" statistic is in reasonable agreement with the "Adj R-Squared" statistic for 11 responses surfaces, the exception being the RS model for the solid phase of Ethyl-benzene. The "adequate precision" statistic for all 12 RS models is above four indicating the designs can be used to navigate the design space. In general the significant model terms are A, B and E, (i.e. K sw_z, ϕ, and α) and their interactions.

The "Pred R-Squared" statistic range from 0.4496 to 0.7277. This indicates that while the RS models are generally good approximations of the design space they can at best account for up to only 72.77 % of the total variability. Consequently, while the RS models can be used to study the effects of various factors they cannot be used as replacement models for the uncertainty analysis of MOFAT.

Table 4.4 ANOVA and RSM Summary

Component	Phase	Transformation	F Value	Prob > F	R-Squared	Adjusted R-Squared	Pred R-Squared	Adeq Precision	Significant Model Terms*
Benzene	Water	Inverse sqrt	9.53	< .0001	0.6007	0.5377	0.4496	11.195	A, B, AB, BE
Benzene	Gas	Inverse sqrt	22.02	< .0001	0.7766	0.7414	0.6732	17.258	A, B, E, AB, AE, BE
Benzene	Solid	Inverse sqrt	9.90	< .0001	0.6098	0.5482	0.4618	11.468	A, B, AB, BE
Toluene	Water	Inverse	11.23	< .0001	0.6799	0.6193	0.5493	10.093	A, B, A^2, AB, BE
Toluene	Gas	Inverse sqrt	20.82	< .0001	0.8223	0.7828	0.7065	16.574	A, B, E, AB, AE, BE
Toluene	Solid	Inverse sqrt	12.73	< .0001	0.7388	0.6808	0.5832	12.607	A, B, A^2, AB, BE
Ethyl-Benzene	Water	Inverse	24.55	< .0001	0.7949	0.7625	0.7075	18.114	A, B, E, AB, AE, BE
Ethyl-Benzene	Gas	Inverse	20.67	< .0001	0.8212	0.7815	0.7078	16.704	A, B, E, AB, AE, BE
Ethyl-Benzene	Solid	Inverse	8.98	< .0001	0.7711	0.6853	0.4577	9.515	A, B, A^2, C^2, E^2, AB, AE, BE
Xylene	Water	Inverse sqrt	26.98	< .0001	0.8099	0.7799	0.7277	18.711	A, B, E, AB, AE, BE
Xylene	Gas	Inverse sqrt	22.35	< .0001	0.8324	0.7952	0.7231	17.062	A, B, E, AB, AE, BE
Xylene	Solid	Inverse	13.74	< .0001	0.8375	0.7765	0.6179	10.197	A, B, A^2, C^2, D^2, E^2, AB, AE, BE.

* input parameters K_{sw}, ϕ, S_m, S_{or}, α, and n have been coded as A, B, C, D, E and F respectively.

4.4.2.2 Verifying the least squares regression assumptions

All 12 RS models were evaluated for compliance with least squares regression assumptions. Normal probability plots of the residuals were used to check the validity of the normality assumption. All of the normal probability plots indicated problems with normality. As an illustration the normal probability plot of the residuals for the water phase of Benzene is shown in Figure 4.20. Normal probability plots of residuals were similar for other phases and other BTEX components. Transformations (inverse, inverse square root, log, and exponential) to the response variables do not remedy the problems with normality. Figure 4.21 shows the normal probability plot of the residuals for water phase of Benzene after the responses were transformed using an inverse transformation.

The residuals were also plotted against the predicted responses to verify that the variance of the original observations is constant. These residual plots indicated that the variance of the original observations was not constant for all responses. As an illustration Figure 4.22 shows the plot of residuals versus predicted responses for the water phase of Toluene. The residuals are not randomly scattered and this indicates that the variance of the original observations is not constant for all responses. Plot of residuals versus predicted responses were similar for other phases and other BTEX components. Transformation of the response variables does not remedy the problems with normality. Figure 4.23 shows the plot of residuals versus the transformed predicted responses for the water phase of Toluene. Despite the transformation the residuals are still not randomly scattered.

Figure 4.20 Normal Probability Plot of Residuals

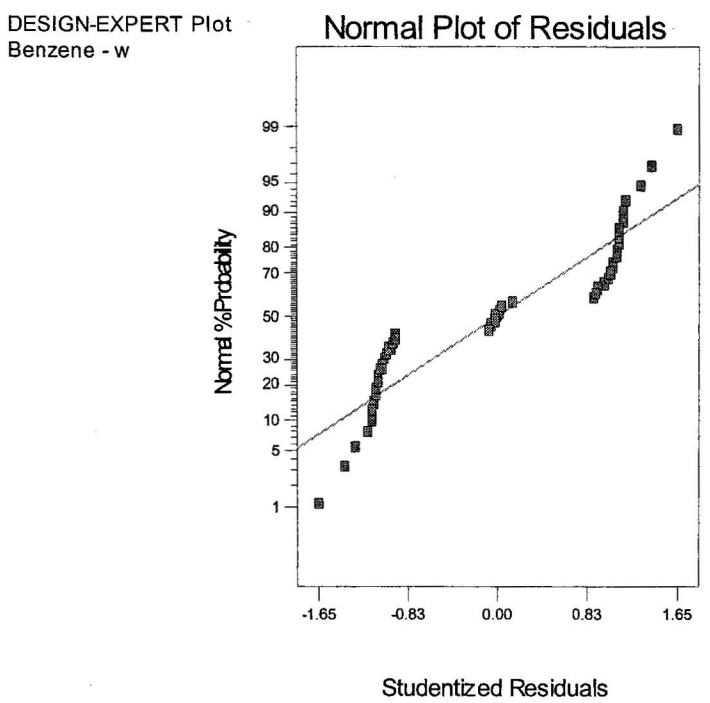

Figure 4.21 Normal Probability Plot of Residuals for Transformed Responses

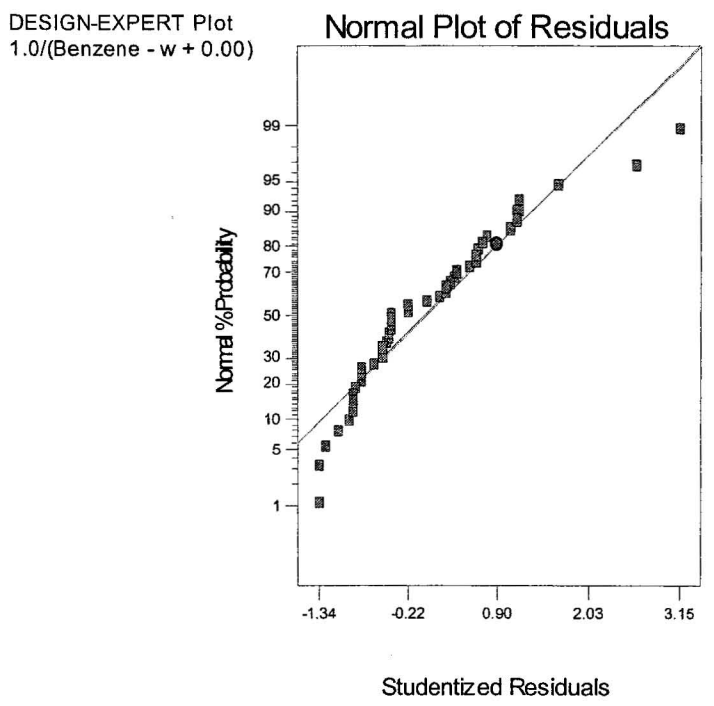

Figure 4.22 Plot of Residuals versus Predicted Responses

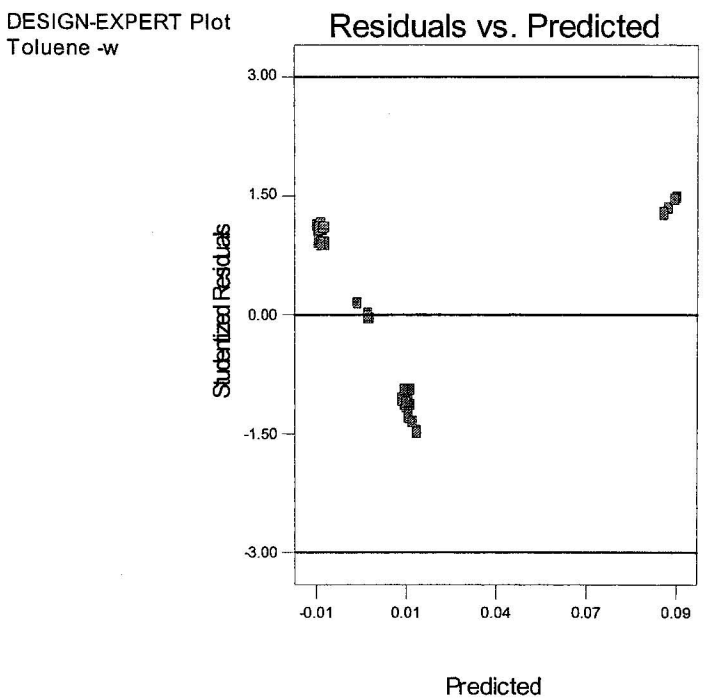

Figure 4.23 Plot of Residuals versus Transformed Predicted Responses

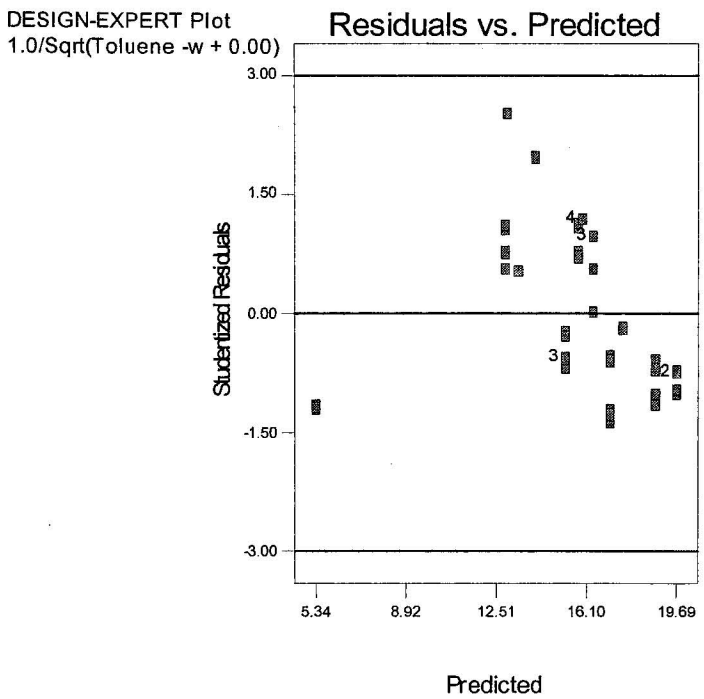

Residuals were similarly plotted against the run order and each of the independent variables. All of these plots for all phases of all the BTEX components exhibited the expected randomness. As an illustration the plot of residuals against run order for the gas phase of Ethyl-benzene is shown in Figure 4.24. Similarly, as an illustration, the plot of residuals versus the independent variable C (i.e. S_m) for the solid phase of Xylene is presented in Figure 4.25. Both these plots highlight the randomness of the residuals and indicate that there are no problems with model adequacy.

The problems with normality observed in the normal probability plots of the residuals and the non-constant variance observed in the plots of residuals versus predicted responses clearly establishes that the least squares regression assumptions were violated.

4.4.3 Monte Carlo Analysis of Response Surface Models

As discussed in the previous sections 4.4.2.1 and 4.4.2.2, the RS models fitted for the BTEX components can at best account for only 72.77 % of the total variability and they violated the least squares assumptions. Consequently, the RS models cannot be used as replacement models for MOFAT.

The response surface models still provide valuable qualitative information for MOFAT users on the interactions between the input variables. This is discussed in greater detail in the next section.

Figure 4.24 Plot of Residuals versus Run order

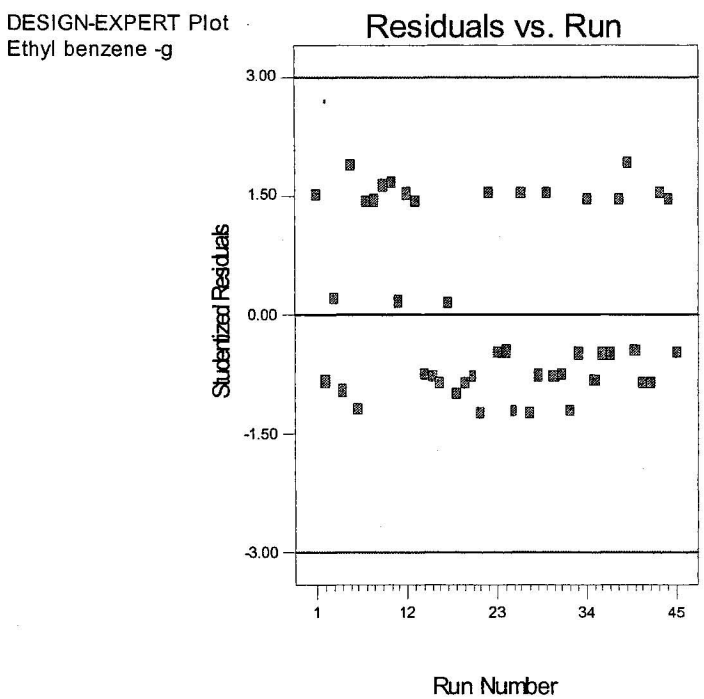

Figure 4.25 Plot of Residuals versus Independent Factor C

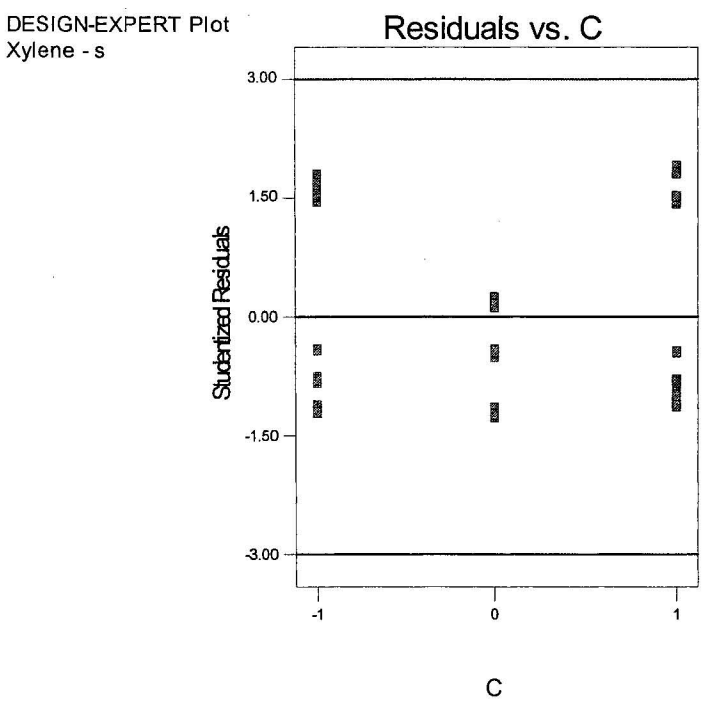

4.4.4 Identifying Interactions

An interaction is the failure of one factor to produce the same effect on the response at different levels of another factor (Montgomery, 2001). Simulation based methods like RS-MC and LHS-MC do not provide any information on interactions between input variables, however the fractional factorial design used for fitting the response surfaces does identify and provide information on interactions. This is because the fractional factorial design tests the effects of a factor at several levels of the other factors.

From the list of significant model terms presented in Table 4.4, it is apparent that for all phases of the BTEX components the AB and BE interactions are significant. The AE interaction is significant for the gas phases of Benzene and Toluene and all phases of Ethyl-benzene and Xylene.

The AB interaction is the interaction between K_{sw} and ϕ. The AB interaction for the gas phase of Benzene is presented in Figure 4.26. Though the RS model was fitted on an inverse square root transformed response (gas phase concentrations of Benzene), the responses have been shown in original scale in Figure 4.26. The AB interaction is qualitatively the same for all other 11 responses (BTEX concentrations) i.e. the magnitude of the effect on the response varies but the interaction is the same. The effect of the AB interaction on the response (water phase concentrations of Benzene) is best illustrated through the 3-D response surface plot shown in Figure 4.27. At the high levels of ϕ, the level of K_{sw} does not have an effect. However at the low levels of ϕ, there is a

Figure 4.26 K_{sw} and ϕ Interaction Graph for Gas Phase Concentrations of Benzene

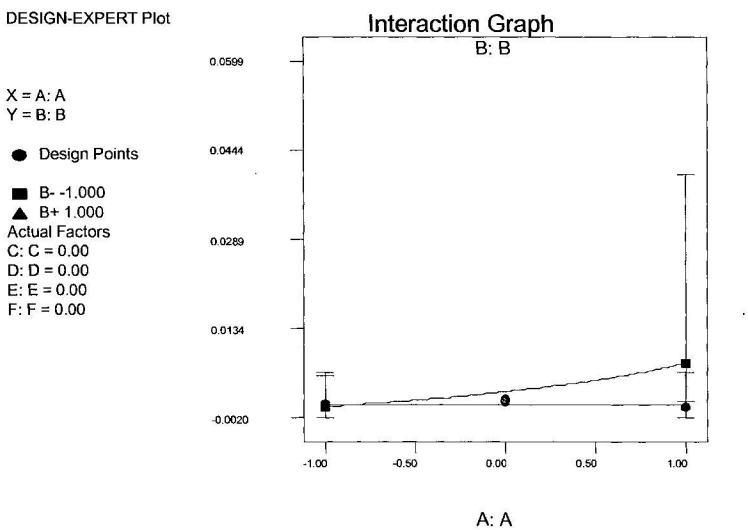

Figure 4.27 3-D Surface Plot of the K_{sw} and ϕ Interaction

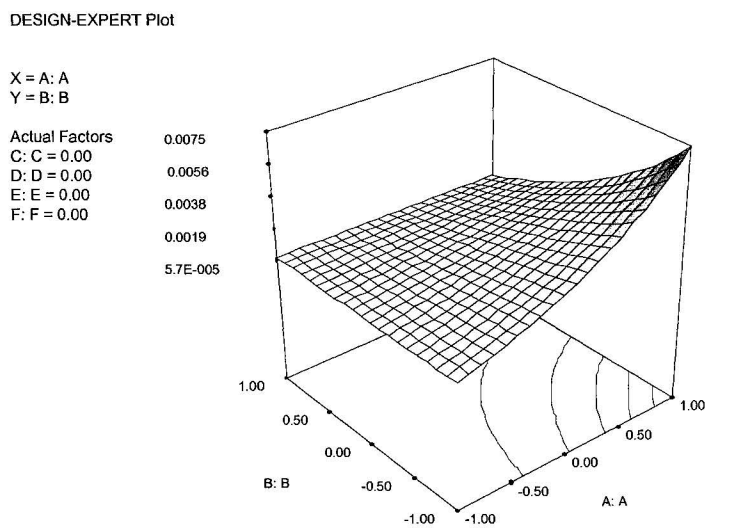

positive interaction between K_{sw} and ϕ, i.e. as the level of K_{sw} increases the response increases. The physical significance of this interaction is explained in Section 5.2.3.

The BE interaction is the interaction between ϕ and α. The BE interaction for the water phase of Toluene is presented in Figure 4.28. Again the response has been shown in original scale. The BE interaction is qualitatively the same for all other 11 responses. At the high levels of α, the level of ϕ does not have an effect. However at the low levels of α, there is a negative interaction between ϕ and α, i.e. as the level of ϕ increases the response decreases. Figure 4.29 shows the 3-D response surface plot. The physical significance of this interaction is explained in Section 5.2.3.

The AE interaction is the interaction between K_{sw} and α. The AE interaction for the gas phase of Toluene is presented in Figure 4.30. Again the response has been shown in original scale. The AE interaction is qualitatively the same for other responses. At the high levels of α, the level of K_{sw} does not have an effect. However at the low levels of α, there is a positive interaction between K_{sw} and α, i.e. as the level of K_{sw} increases the responses increases. The effect of the AE interaction on the response (gas phase concentrations of Toluene) is best illustrated through the 3-D response surface plot shown in Figure 4.31. The physical significance of this interaction is explained in Section 5.2.3.

Figure 4.28 ϕ and α Interaction Graph for Water Phase Concentrations of Toluene

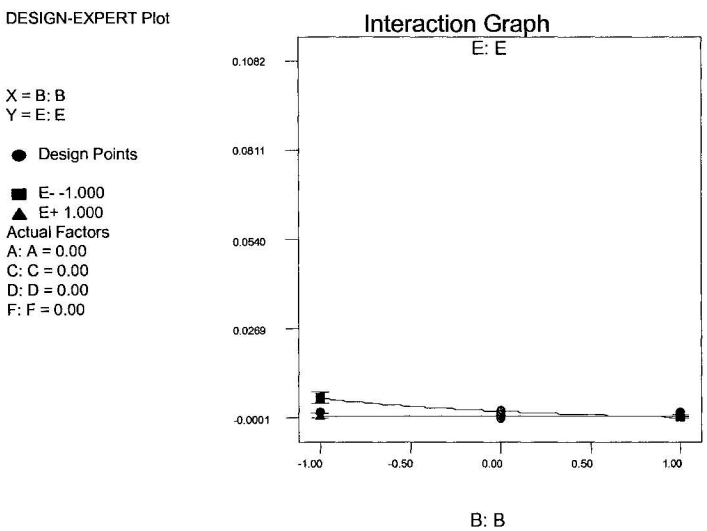

Figure 4.29 3-D Surface Plot of the ϕ and α Interaction

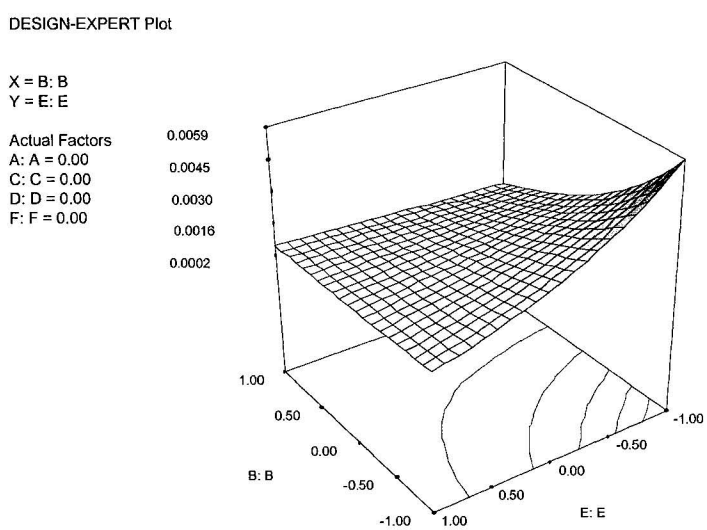

Figure 4.30 K_{sw} and α Interaction Graph for Gas Phase Concentrations of Toluene

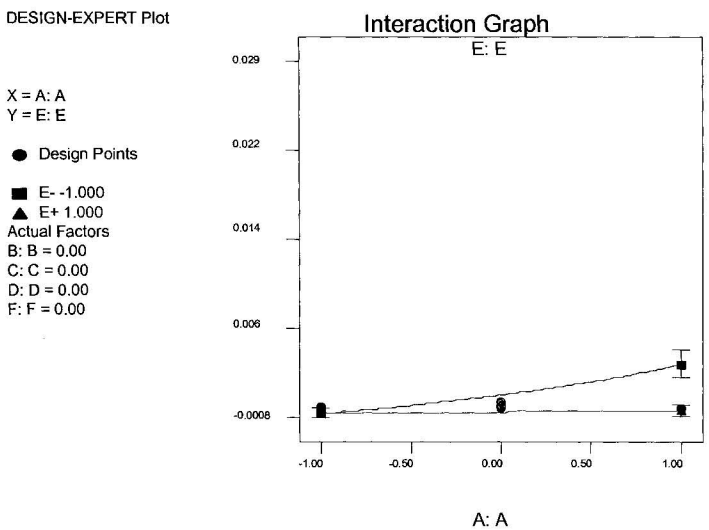

Figure 4.31 3-D Surface Plot of the K_{sw} and α Interaction

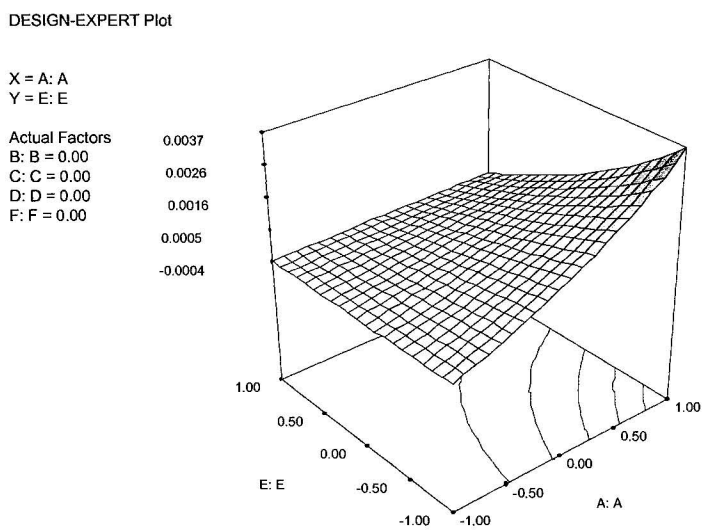

4.5 Neural Networks (NN)

The NeuroShell 2 program (Ward Systems Group Inc., 1993) was used as the Neural Networks (NN) training software. Since it is important for a training set to span the total range of input patterns sufficiently well so that the trained network can generalize from the training set (Rojas, 1996), LHS-MC sets were used as the training sets. To test the effect of the training set size the NN were trained using two different training set sample sizes. The LHS-MC sets LHS (sample size 100) and LHS300 were used as the training sets. NeuroShell 2 further splits each training set into a training and a test set. Another LHS-MC set consisting of 100 LHS samples was generated and used as an alternate test set.

4.5.1 Training and Evaluation of Neural Network Models

Both Back Propagation and General Regression based Neural Networks were evaluated in this study. As discussed earlier in Section 2.4.1, Back Propagation Neural Networks (BPNN) are used for the vast majority of working neural network applications and are known for their ability to generalize well on a wide variety of problems (Ward Systems Group Inc., 1993). The General Regression based Neural Networks (GRNN) is a type of supervised network that is useful for continuous function approximation and is known for its ability to train quickly on sparse data sets.

NeuroShell 2 offers several different variations of BPNN:

(a) each layer connected to the immediately previous layer (with either 3, 4, or 5 layers);

(b) each layer connected to every previous layer (with either 3, 4, or 5 layers);

(c) recurrent networks with dampened feedback; and

(d) Ward Networks. Ward Networks are three different BPNN architectures with multiple hidden layers invented by Ward Systems Group (Ward Systems Group Inc., 1993). In Ward Networks different hidden slabs are given different activation functions.

GRNN is a three-layer network where there must be one hidden neuron for each training pattern (Ward Systems Group Inc., 1993).

All four variations of the BPNN available in the NeuroShell 2 software and the GRNN were applied to the training set using with various combinations of scale functions, activation factors, learning rates, number of hidden layers and neurons. NeuroShell 2's NET-PERFECT was used in some schemes to optimize the network and prevent over training of the neural network. NeuroShell 2 uses NET-PERFECT to optimize the network by applying the current network to an independent test set during training. NET-PERFECT finds the optimum network for the data in the test set by computing the mean squared error between actual and predicted for all outputs over all patterns (Ward Systems Group Inc., 1993).

For all NN schemes tested and for both training set sample sizes while excellent correlations were obtained on the training set, correlation coefficients for the test set were poor for the smaller training set of 100 LHS simulations. The correlation coefficient r is a statistical measure of the strength of the relationship between the actual versus predicted outputs. The r coefficient can range from -1 to +1. The closer r is to 1, the stronger the positive linear relationship, and the closer r is to -1, the stronger the negative linear relationship.

A better predictor is the statistic; R squared (Ward Systems Group Inc., 1993), the coefficient of multiple determination, which is a statistical indicator usually applied to multiple regression analysis. It compares the accuracy of the model to the accuracy of a trivial benchmark model wherein the prediction is simply the mean of all of the samples. A perfect fit would result in an R squared value of 1, a very good fit near 1, and a very poor fit near 0 (Ward Systems Group Inc., 1993). A R squared value of 0.00 indicates that the neural model predictions are worse than that would predicted by just using the mean of the test set outputs. For the test set, the R squared values for the NN schemes were again poor for the smaller training set of 100 LHS simulations.

As an illustration, Tables 4.5, 4.6 and 4.7 summarize the results of the application of two different BPNN and a GRNN respectively. The networks configurations are illustrated in Figures 4.32 to 4.34 respectively.

Table 4.5 Summary of Application of a Standard Back Propagation Neural Network

Training Set Size	Evaluation Statistic	Training Portion of Training Set	Test Portion of Training Set	Complete Training Set	100 Sample LHS Test Set
100 LHS Samples	R Squared	0.6168	0.4863	0.5874	0.0796
	Correlation Coefficient r	0.785	0.728	0.767	0.520
300 LHS Samples	R Squared	0.6643	0.7906	0.6773	0.6293
	Correlation Coefficient r	0.816	0.900	0.824	0.794

Table 4.6 Summary of Application of a Ward Back Propagation Neural Network

Training Set Size	Evaluation Statistic	Training Portion of Training Set	Test Portion of Training Set	Complete Training Set	100 Sample LHS Test Set
100 LHS Samples	R Squared	0.6992	0.8044	0.7231	0.1133
	Correlation Coefficient r	0.862	0.899	0.866	0.644
300 LHS Samples	R Squared	0.8124	0.8334	0.8145	0.7106
	Correlation Coefficient r	0.902	0.918	0.903	0.847

Table 4.7 Summary of Application of a GRNN Neural Network

Training Set Size	Evaluation Statistic	Training Portion of Training Set	Test Portion of Training Set	Complete Training Set	100 Sample LHS Test Set
100 LHS Samples	R Squared	0.9756	0.2962	0.7529	0.4563
	Correlation Coefficient r	0.990	0.564	0.868	0.687
300 LHS Samples	R Squared	0.9636	0.7419	0.9408	0.4928
	Correlation Coefficient r	0.984	0.872	0.971	0.707

As shown in Figure 4.32, the first BPNN used consists of five layers with standard connections, i.e. each layer is connected to only the previous layer. Each layer has only one slab. The five slabs have 6,4,4,4 and 1 neurons respectively. Neurons are depicted as black circles. The learning rate, momentum and initial weights were 0.1, 0.1 and 0.3 respectively. The scaling function for slab 1 is linear. The activation function for slabs 2, 3, 4 and 5 are logistic.

As shown in Figure 4.33, the second BPNN used is a Ward network and it consists of four layers with a variety of connections. The second layer has two slabs, while all the other layers have only 1 slab each. The five slabs have 6,4,4,4 and 1 neurons respectively. The learning rate, momentum and initial weights were 0.1, 0.1 and 0.3 respectively. The scaling function for slab 1 is linear. The activation function for slabs 2, 3, 4 and 5 are gaussian, tanh, gaussion and logistic respectively.

As shown in Figure 4.34, the GRNN used consists of three layers with a single slab in each layer. The slabs have 1, 100 (300 for 300 sample training set) and 6 neurons respectively. The second slab has 100/300 neurons as in GRNN there must be one hidden neuron for each training pattern. The scaling function for slab 1 is linear.

For all three neural networks applications it is clear from Tables 4.5, 4.6 and 4.7 that for the smaller training set of 100 LHS simulations, the neural networks are able to train well

Figure 4.32 Structure of Standard BPNN

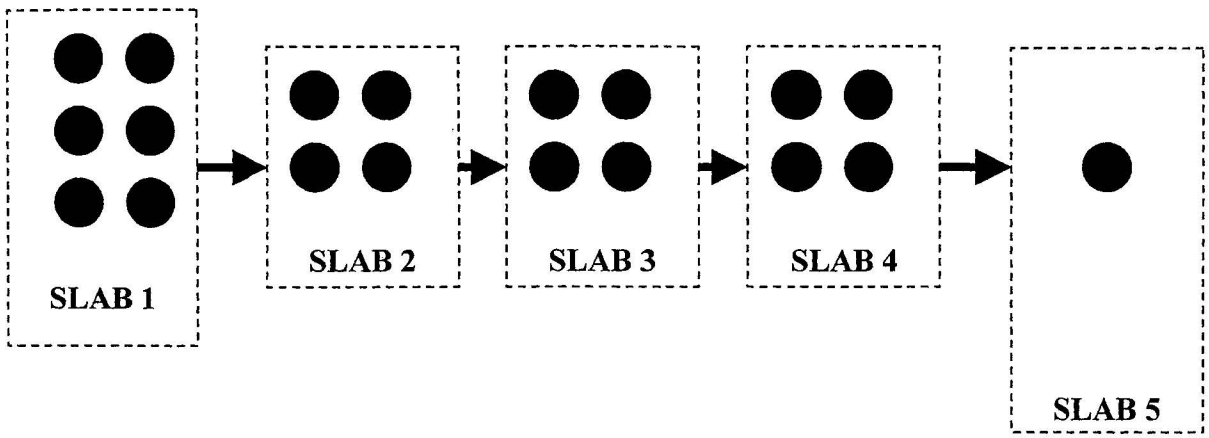

Figure 4.33 Structure of Ward BPNN

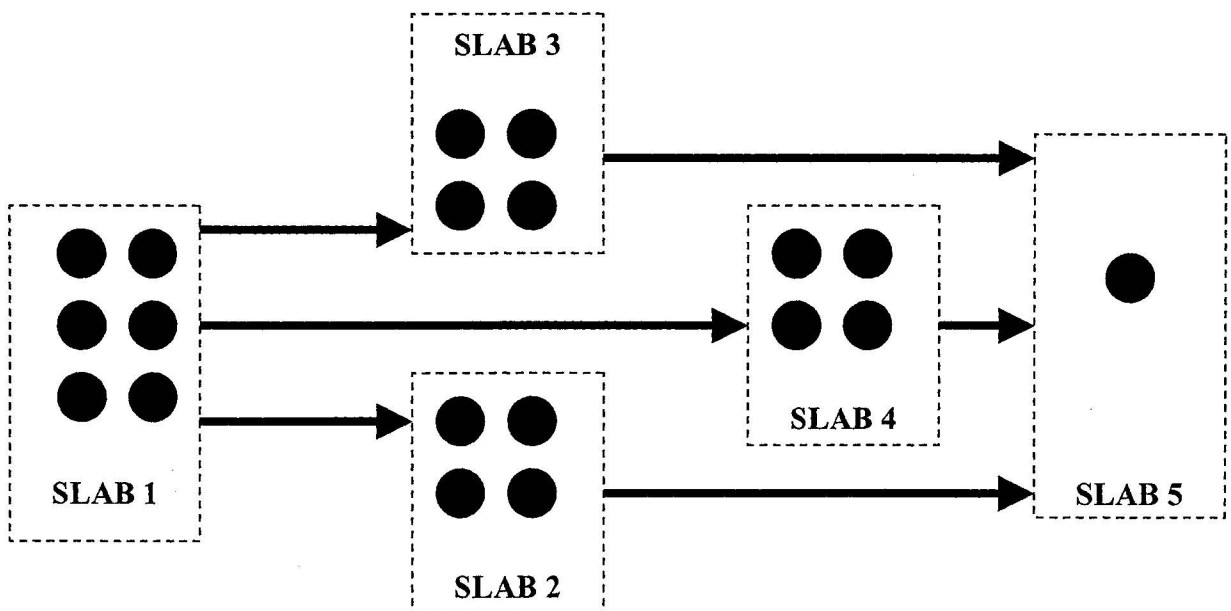

Figure 4.34 Structure of GRNN

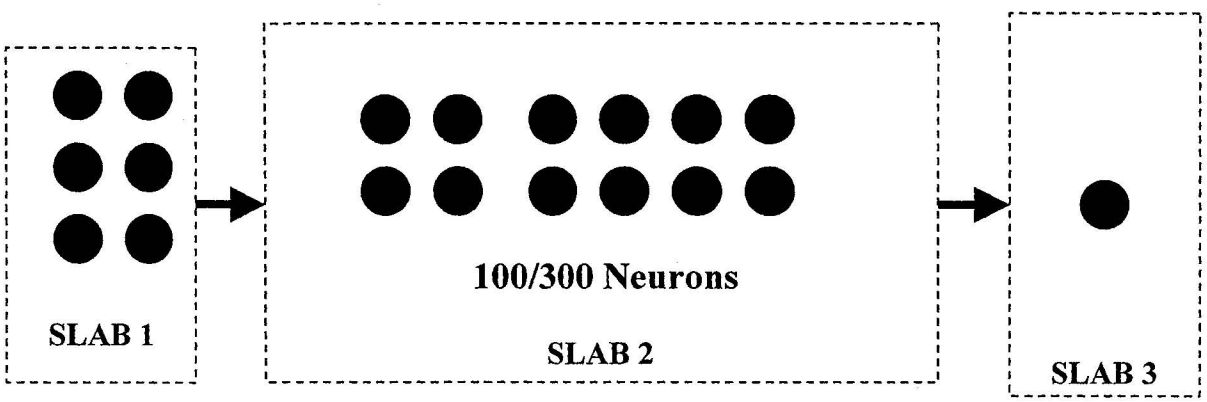

on the training sets (R Squared ranged from 0.5874 to 0.7529) but are not able to predict well on the alternate test set (R Squared ranged from 0.0796 to 0.4563). However using the larger training set of 300 LHS simulations, the neural networks are able to predict better on the alternate test set (R Squared ranged from 0.4928 to 0.7106). The best prediction was obtained using the Ward BPNN. This indicates that the MOFAT outputs are highly non linear and consequently the neural networks in general need bigger training sets to learn the non-linear patterns.

The objective of this study was to evaluate if a neural network model for the purpose of efficiently conducting an uncertainty analysis could replace MOFAT. In keeping with this objective the neural networks were not retrained using larger training sets since the results presented in the next section (Section 4.6) indicate that an uncertainty analysis of MOFAT could be executed more efficiently (i.e. with fewer simulations) using Latin Hypercube Sampling based Monte Carlo.

4.5.2 Monte Carlo Analysis of Neural Network Models

The results of the application of NN to test files clearly demonstrated that the NN models could not efficiently replicate the output results of MOFAT. The highly non-linear outputs of MOFAT require large (i.e. greater than 300 LHS simulations) training sets to train. Consequently MC analysis of the NN models was not undertaken.

4.6 Comparison and Evaluation of Uncertainty Analysis Techniques

As stated earlier in the introduction to this chapter, uncertainty analysis techniques are evaluated by comparing the outputs of each uncertainty analysis technique with the outputs of RS-MC from the perspective of accuracy of convergence of *cdfs* and efficiency of the convergence.

Figures 4.35, 4.37, 4.39 and 4.41 present the empirical *cdfs* of BTEX concentrations for the water, gas and solid phases as estimated from the outputs of the RS-MC, LHS and LHS-s simulations. Figures 4.36, 4.38, 4.10 and 4.42 present the empirical *cdfs* of BTEX concentrations for the water, gas and solid phases as estimated from the outputs of the RS-MC, and the larger sample LHS300 and LHS500 simulations. The Cunane plotting position was used to plot the *cdfs*.

In Figures 4.35, 4.37, 4.39 and 4.41, the LHS *cdfs* and LHS-s *cdfs* converge well with the RS-MC *cdfs* for all oil components and all phases. The LHS *cdfs* display a slightly higher degree of convergence to the RS-MC *cdfs* than the LHS-s *cdfs*. This is especially so at the higher quantiles. While the RS-MC, LHS and LHS-s *cdfs* converge, the LHS and LHS-s *cdf* estimates were generated with greater efficiency using only 100 and 35 simulations respectively against the 10,000 simulations used for the RS-MC *cdfs*.

Figure 4.35 Empirical cdf Plots of Uncertainty in Benzene Concentrations – MC, LHS, and LHS-s Runs

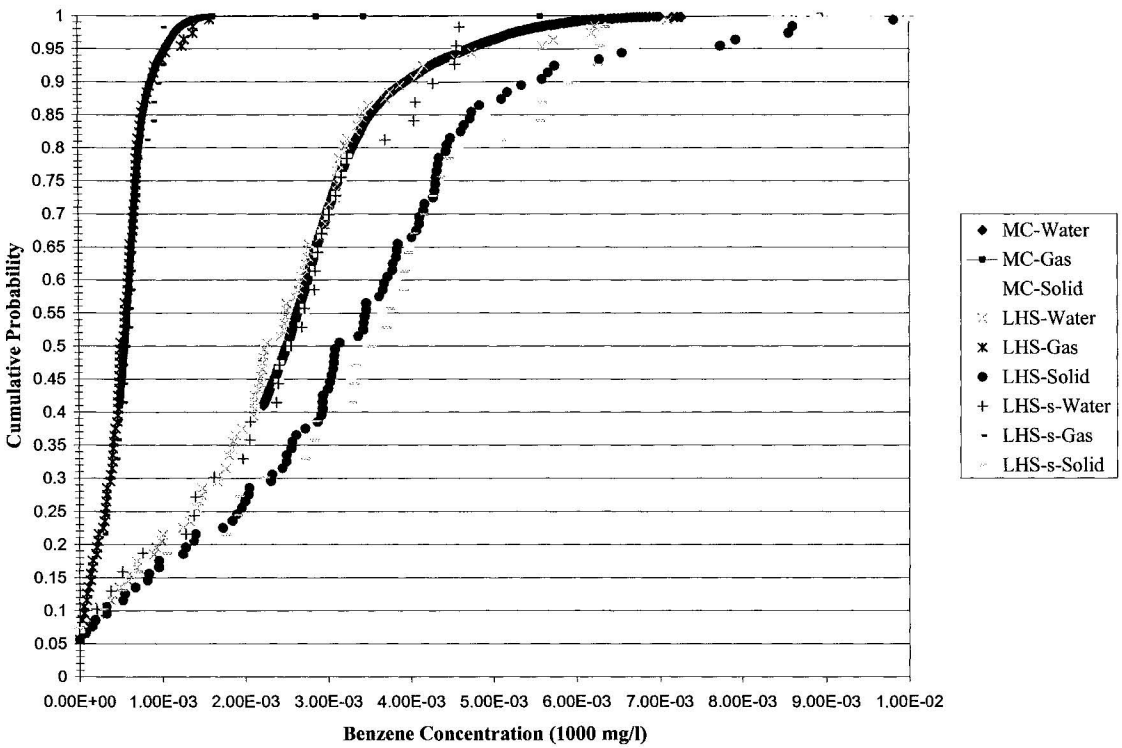

Figure 4.36 Empirical cdf Plots of Uncertainty in Benzene Concentrations – MC, LHS300, and LHS500 Runs

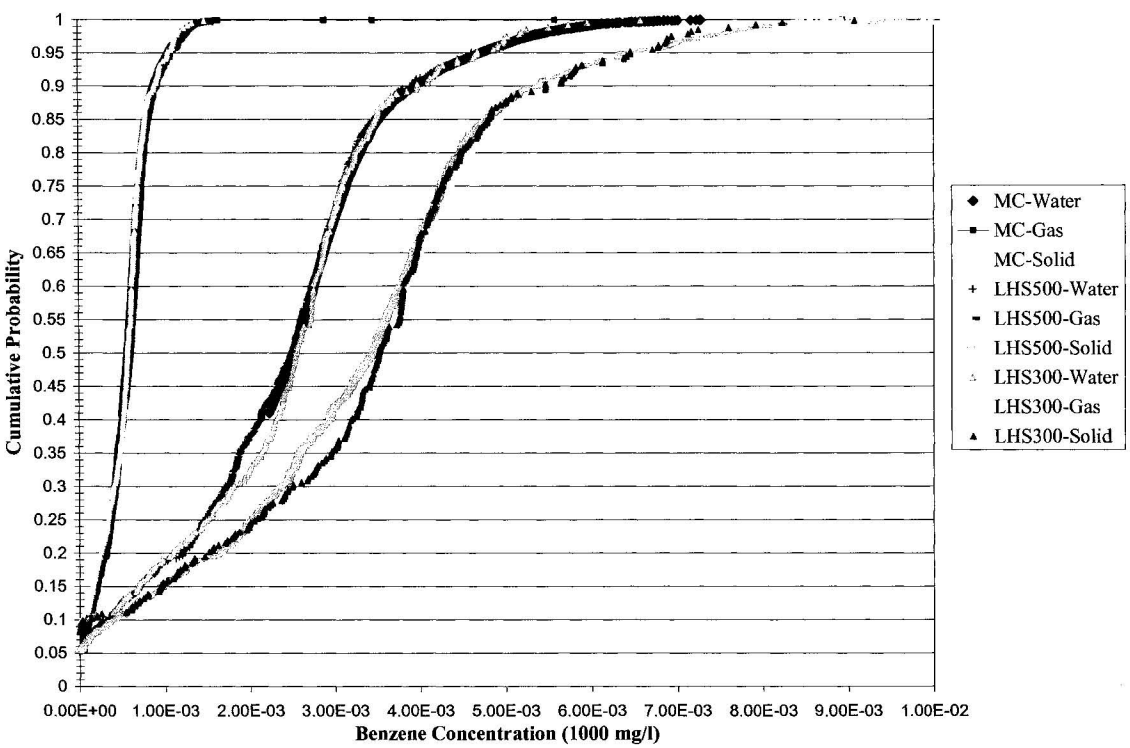

Figure 4.37 Empirical cdf Plots of Uncertainty in Toluene Concentrations – MC, LHS, and LHS-s Runs

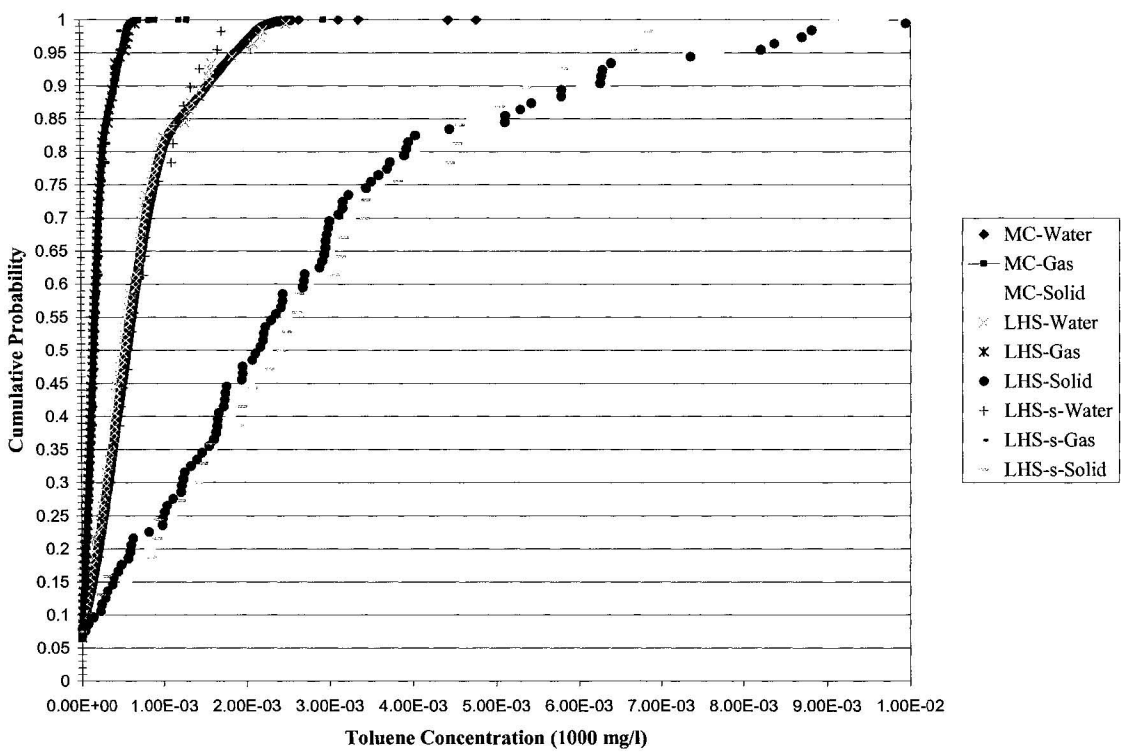

Figure 4.38 Empirical cdf Plots of Uncertainty in Toluene Concentrations – MC, LHS300, and LHS500 Runs

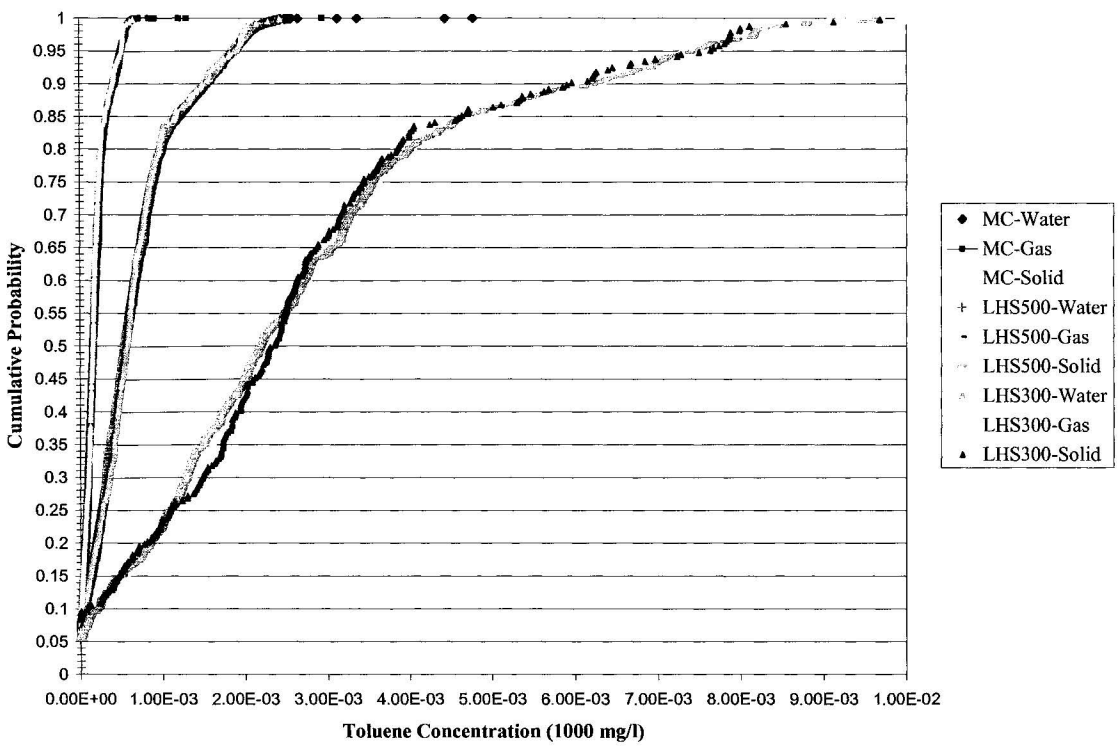

Figure 4.39 Empirical cdf Plots of Uncertainty in Ethyl benzene Concentrations – MC, LHS, and LHS-s Runs

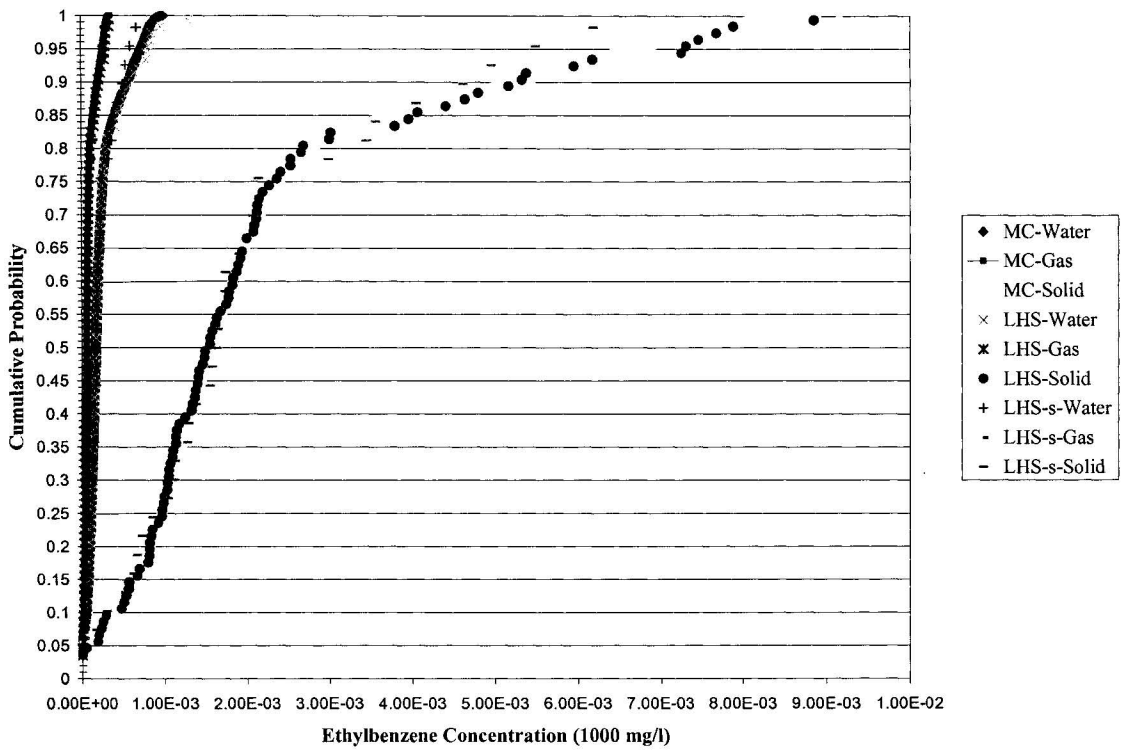

Figure 4.40 Empirical cdf Plots of Uncertainty in Ethyl benzene Concentrations – MC, LHS300, and LHS500 Runs

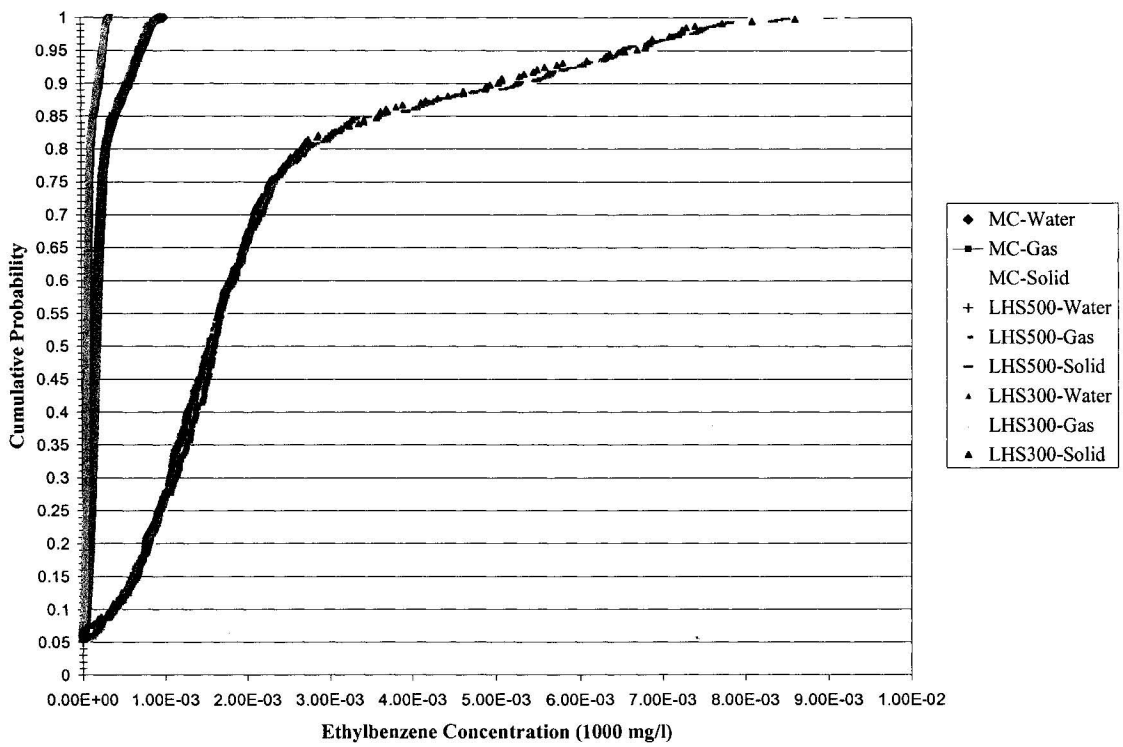

Figure 4.41 Empirical cdf Plots of Uncertainty in Xylene Concentrations – MC, LHS, and LHS-s Runs

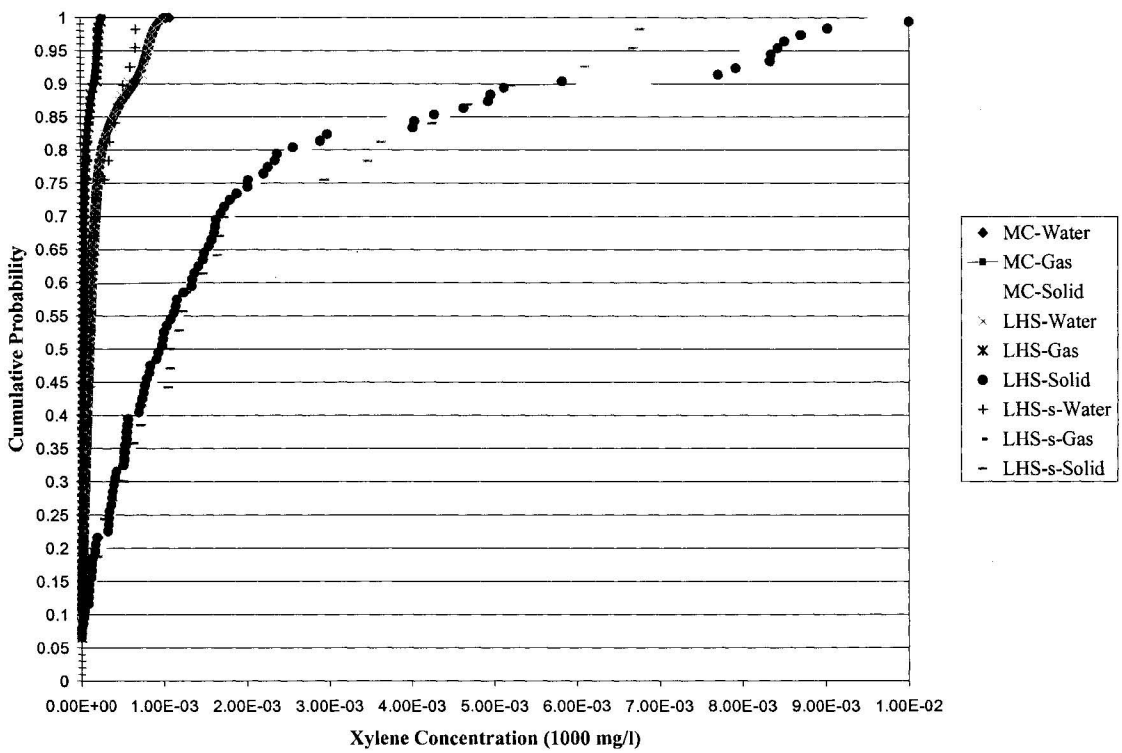

Figure 4.42 Empirical cdf Plots of Uncertainty in Xylene Concentrations – MC, LHS300, and LHS500 Runs

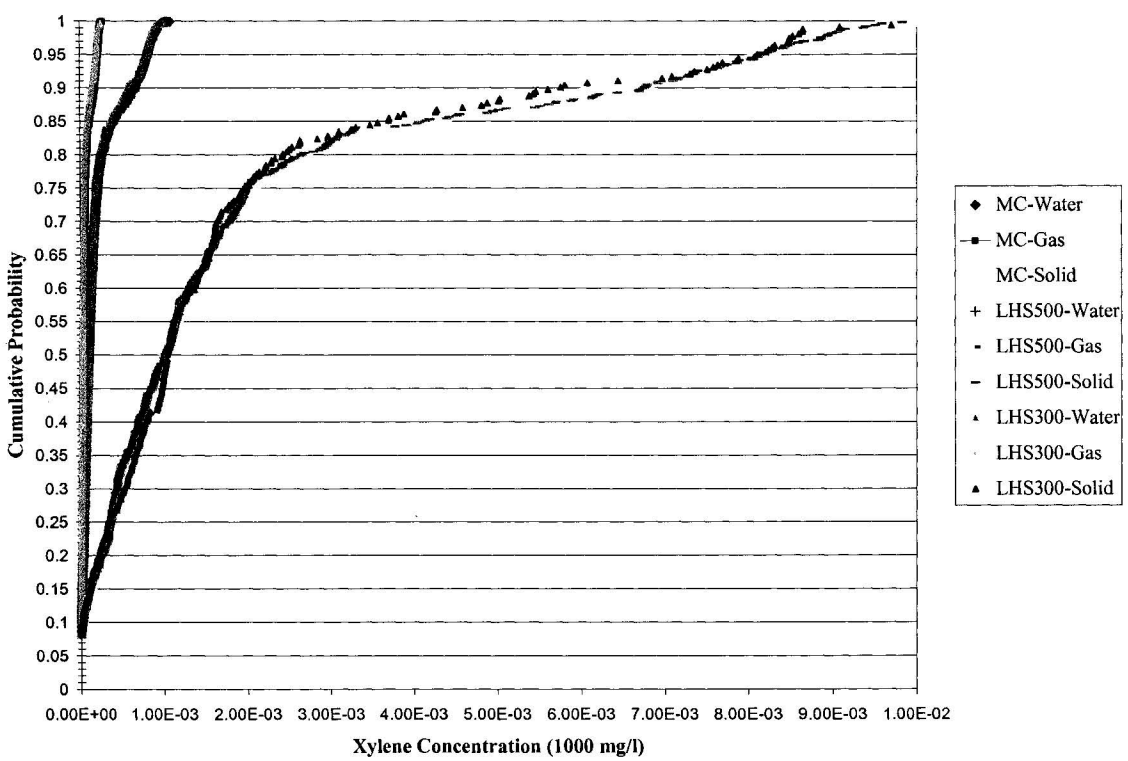

In Figures 4.36, 4.38, 4.10 and 4.42, the LHS300 *cdfs* and LHS500 *cdfs* converge very closely with the RS-MC *cdfs* for all oil components and all phases. The LHS-300 and the LHS-500 *cdfs* in Figures 4.36, 4.38, 4.10 and 4.42, display a much higher degree of convergence to the RS-MC *cdfs* than the LHS-100 *cdfs* in Figures 4.35, 4.37, 4.39 and 4.41. Since the convergence of both the LHS300 and LHS500 sample sizes to the RS-MC *cdfs* is excellent, improvement in convergence when moving from the LHS300 sample to the LHS500 sample is not significant. The LHS300 and LHS500 *cdfs* are almost identical for the water and gas phase concentrations. For the solid phase concentrations the LHS300 and LHS500 *cdfs* are not identical but the differences between them are negligible.

Based on the analysis presented in this chapter it can be concluded that a parametric uncertainty analysis of MOFAT can be accurately and efficiently undertaken using Monte Carlo with LHS sampling. As demonstrated in this study the recommended Iman and Helton (1985) LHS sample size of 5*(number of variables) would be able to replicate the RS-MC *cdfs,* however a larger sample size of up to 15 *(number of variables) would be more accurate at the higher probabilities. For yet higher accuracies an LHS sample size of 45*(number of variables) can be used. However using an LHS sample size greater than 45*(number of variables) will not provide any appreciable increase in convergence as the *cdfs* produced using an LHS sample size of 45*(number of variables) are already very similar to the RS-MC *cdfs.*

The model replacement techniques of NN and RSM were not able to successfully replace MOFAT for the purpose of uncertainty analysis.

Chapter 5. Sensitivity Analysis

5.1 Introduction

This chapter describes the sensitivity analysis of MOFAT. Sensitivity analysis is an essential component of model assessment and application (Kleijnen and Helton, 1999a). Amongst the many aims of sensitivity analysis are priority setting, the determination of which factors needs better quantification and the identification of variance propagating weak links in the assessment chain (Saltelli et. al., 2004).

The selection of sampling based Monte Carlo sensitivity analysis as the sensitivity analysis technique for this study has been presented earlier in Section 2.5.2. As discussed, sampling based MC methods are ideally suited for sensitivity studies and practitioners involved in the analysis of risk most often use them for sensitivity analysis (Saltelli et. al., 2004).

For this sensitivity analysis the LHS-MC simulation results were used instead of the RS-MC simulation results. The smaller samples associated with LHS-MC are better for

identifying important variables since with the increasing sample sizes associated with the RS-MC simulation there is a greater resolution of the effects associated with less important variables (Kleijnen and Helton 1999a, 1999b).

The staging of the sensitivity analysis process within this research study has been presented earlier in Figure 1.1. The steps of the sensitivity analysis component are further expanded and illustrated in Figure 5.1.

As presented earlier in Section 2.5, while the primary aim of sensitivity studies is to identify key input variables other reasons include the need to determine (Hamby, 1994; Saltelli et. al., 2004):

1. Which inputs correlate highly with other inputs.
2. Which inputs contribute most to output variability.
3. Which parameters require additional research for strengthening the knowledge base thereby reducing output uncertainty.
4. Once the model is in use what consequence result from changing a given input parameter.
5. Which inputs interact with each other.

Figure 5.1 The Sensitivity Analysis Process

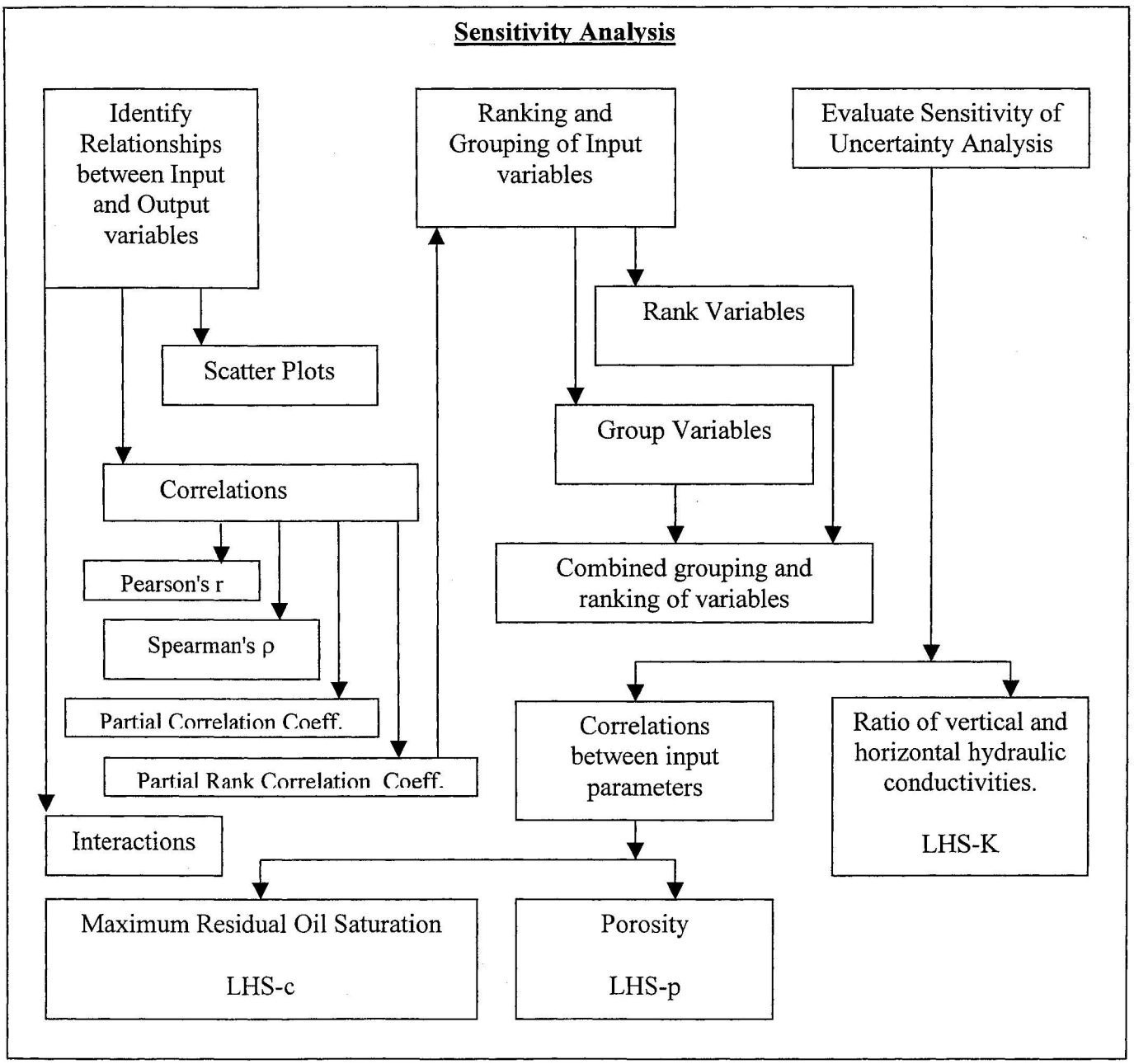

Of these five sensitivity goals, since the first sensitivity goal "Which inputs correlate highly with other inputs" is already known (See Table 3.5), the aim of this study was to primarily determine the latter four goals.

To accomplish the second sensitivity analysis goal of determining "which inputs contribute most to output variability", the first step was to identify relationships (correlations and interactions) between input parameters and the output parameters. These were examined using scatter plots, four different types of correlation coefficients and regression analysis. The second step was to gauge the relative contribution of input parameters to the model's output parameters. This was accomplished by using two different methods to respectively rank and group the input parameters based on the relative contribution of input parameters to the model's output parameters. The two methods were further amalgamated to create a new approach for ranking and grouping the input parameters.

This ranking and grouping of the input parameters based on the their relative contribution to output variability also accomplished the third sensitivity analysis goal of identifying "Which parameters require additional research for strengthening the knowledge base thereby reducing output uncertainty". The higher ranked parameters should be the focus of additional research since these parameters contribute the most to output variability and reducing uncertainty in the higher ranked parameters will reduce output uncertainty.

The fourth sensitivity goal of determining "Once the model is in use what consequence result from changing a given input parameter" cannot be explicitly determined for complex models where the input parameters are correlated. The correlated structure of the inputs does not allow the modeler to independently change input parameters one at a time while the complex structure prevents the application of first order sensitivity techniques. An attempt has been made to address this sensitivity analysis goal through the computation of partial correlation coefficients, partial rank correlation coefficients and an examination of the results of the regression analysis that was used to build response surfaces approximations of the MOFAT model.

The fifth sensitivity analysis goal of "Which inputs interact with each other" was accomplished by using the RSM models, developed earlier in Section 4.4, to identify interactions between input parameters.

Another aim of the sensitivity analysis was to evaluate the sensitivity of the uncertainty analysis undertaken in this study to:

- correlations between input parameters that were not addressed in the Pearson Product Moment Correlation Matrix presented in Table 3.5, and
- anisotropy (ratio of vertical and horizontal hydraulic conductivities).

5.2 *Identifying Relationships between Inputs and Outputs*

5.2.1 Scatter Plots

Scatter plots are an effective means of visually identifying sensitivities in simulation data. Scatter plots of each of the twelve MOFAT outputs (three phases of each of the BTEX components) versus the probabilistic input parameters were plotted to identify any obvious dependence between the input and output parameters and to identify the type of dependence between the parameters. The scatter plot for the water phase concentration of Benzene is shown in Figure 5.2. The remaining scatter plots are provided in Appendix C.

Dependencies are identified by visually screening scatter plots for some form of deviation from randomness. Deviations from randomness in scatter plots indicate the presence of dependences. Where dependences were apparent from the scatter plots these were examined to determine if the dependences were monotonic or non-monotonic. Monotonic dependencies being those in which there are no reversals in slope. Monotonic dependencies were further scrutinized to identify if they were linear or non-linear. Linear dependences being those monotonic dependences that have a constant slope. The nature of dependence between the input and output variables is an important factor in quantifying correlations as it determines the applicability of various correlation measures.

Examination of the scatter plots, indicates that in general all the outputs display a monotonic dependence on the inputs K_{sw}, α, and n. The relationships between the inputs

Figure 5.2 Scatter Plots for the Water Phase Concentration of Benzene Plotted against the Input Parameters *K sw* (K), ϕ (Porosity), S_m (Max s), S_{or} (Mtheta), α (alpha), and *n(N)*

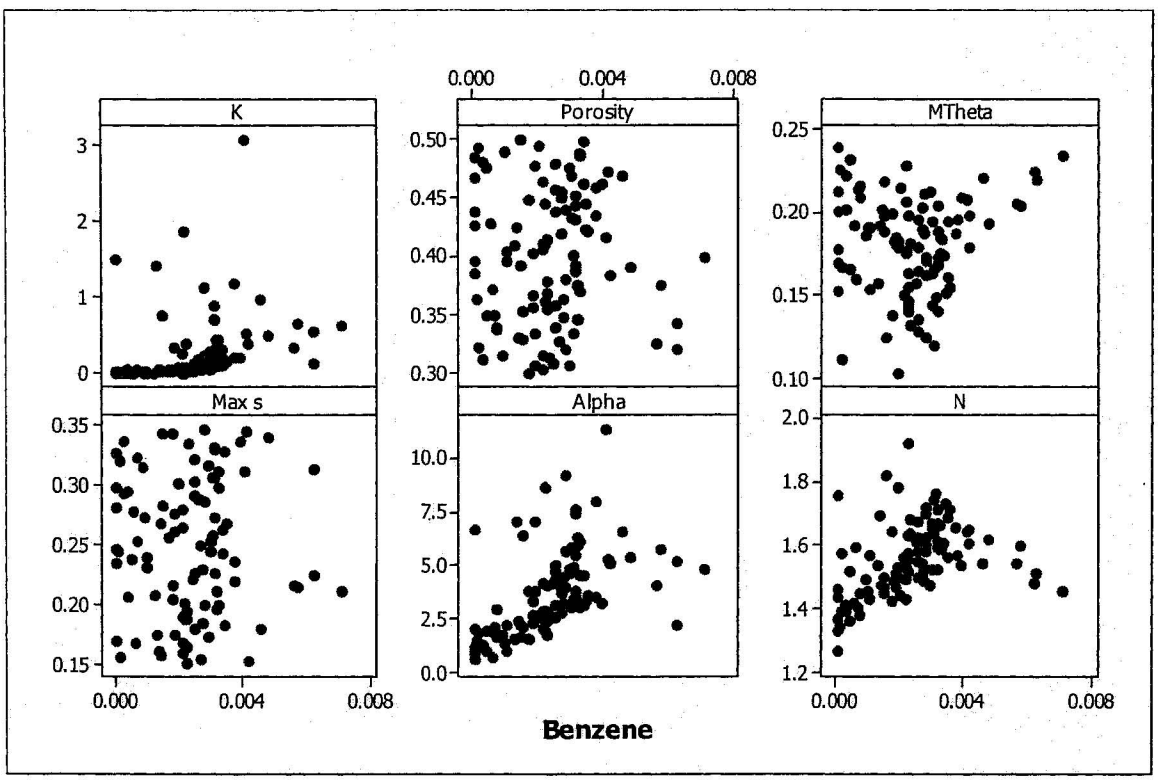

(K_{sw}, α, and n) and the outputs seem to be linear at the lower concentrations with increasing non-linearity at higher concentrations. There also seems to be a slight dependence between all the outputs and the input S_m.

5.2.2 Measures of Correlation

Correlation is a quantification of the strength of the relationship between two variables. There are several measures of correlation however they are all scaled to report in the –1 to 1 range.

Pearson's r, one of the most widely used measures of correlation, is a measure of linear correlation. Spearman's ρ is a measure of correlation that is calculated on the ranks of the data for the two variables and not on the actual data unlike the Pearson's r. This makes the Spearman's ρ more robust as it makes it less sensitive to linearity.

When input parameters are correlated to each other LHS-MC simulation runs are made with many input variables changing simultaneously and this makes it difficult to isolate the sensitivity of the output variables to specific individual variables (Iman and Helton, 1985). Iman and Helton (1985) suggest that one way of quantifying such sensitivity can be by calculating another measure of correlation called partial correlation coefficient (PCC).

The PCC is a measure of correlation between two variables after accounting for the influence of other variables. The PCC does not provide a reliable measure of sensitivity when the relationship between the variables is monotonic but non linear or if there are outliers present. By using the ranks in the PCC test the PCC becomes less sensitive to linearity and outliers in a manner similar to the Spearman's ρ. This is called the Partial Rank Correlation Coefficient (PRCC).

Based on the analysis presented in the previous section all four measures of correlations can be applied to the results of the LHS-MC simulation. However due to indications of non-linearity at higher concentrations, the Spearman's ρ and PRCC seem to be more applicable. Each of the correlation measures provides a different perspective on the correlations between the parameters. As a result correlations between input and outputs of the LHS runs were measured by computing Pearson's r, Spearman's ρ, PCC, and PRCC. The Pearson's r and Spearman's ρ are presented in Tables 5.1 and 5.2.

From the results presented in Tables 5.1 and 5.2, at a 5% significance level both the Pearson and Spearman correlation coefficients indicate there is significant positive correlation between the simulated oil components and K_{sw}, α, and n. The Pearson's r for K_{sw}, α, and n are slightly higher for Toluene, and even higher for Ethyl benzene and Xylene than they are for Benzene. They however do not show any significant variation between the water, gas and solid phases for each BTEX component. The Spearman's ρ

Table 5.1 Pearson Correlations between Inputs and Outputs

Component	Phase		K_{sw}	ϕ	S_m	S_{or}	α	n
Benzene	Water	Pearson's r	0.31	-0.002	0.091	-0.001	0.521	0.379
Benzene		p	0.002	0.987	0.366	0.995	0	0
Benzene	Gas	Pearson's r	0.31	-0.001	0.092	-0.001	0.521	0.379
Benzene		p	0.002	0.99	0.364	0.992	0	0
Benzene	Solid	Pearson's r	0.31	-0.002	0.092	-0.001	0.521	0.379
Benzene		p	0.002	0.985	0.364	0.993	0	0
Toluene	Water	Pearson's r	0.543	0.011	0.046	-0.032	0.636	0.503
Toluene		p	0	0.911	0.646	0.753	0	0
Toluene	Gas	Pearson's r	0.543	0.011	0.046	-0.032	0.636	0.503
Toluene		p	0	0.912	0.647	0.749	0	0
Toluene	Solid	Pearson's r	0.543	0.011	0.046	-0.032	0.636	0.503
Toluene		p	0	0.912	0.647	0.75	0	0
Ethyl-Benzene	Water	Pearson's r	0.652	-0.008	0.113	-0.12	0.603	0.471
Ethyl-Benzene		p	0	0.933	0.264	0.236	0	0
Ethyl-Benzene	Gas	Pearson's r	0.65	-0.025	0.12	-0.107	0.616	0.473
Ethyl-Benzene		p	0	0.807	0.234	0.29	0	0
Ethyl-Benzene	Solid	Pearson's r	0.626	-0.049	0.129	-0.085	0.618	0.461
Ethyl-Benzene		p	0	0.627	0.202	0.401	0	0
Xylene	Water	Pearson's r	0.652	-0.008	0.113	-0.12	0.603	0.471
Xylene		p	0	0.933	0.264	0.236	0	0
Xylene	Gas	Pearson's r	0.65	-0.025	0.12	-0.107	0.616	0.473
Xylene		p	0	0.807	0.234	0.29	0	0
Xylene	Solid	Pearson's r	0.626	-0.049	0.129	-0.085	0.618	0.461
Xylene		p	0	0.627	0.202	0.401	0	0

Table 5.2 Spearman Correlations between Inputs and Outputs

Component	Phase		K_{sw}	ϕ	S_m	S_{or}	α	n
Benzene	Water	Spearman's ρ	0.725	0.078	-0.006	0.044	0.679	0.515
Benzene		p	0	0.439	0.955	0.661	0	0
Benzene	Gas	Spearman's ρ	0.725	0.078	-0.005	0.044	0.679	0.515
Benzene		p	0	0.441	0.961	0.665	0	0
Benzene	Solid	Spearman's ρ	0.725	0.078	-0.006	0.044	0.679	0.515
Benzene		p	0	0.442	0.957	0.667	0	0
Toluene	Water	Spearman's ρ	0.836	0.091	-0.096	0.002	0.788	0.655
Toluene		p	0	0.37	0.341	0.987	0	0
Toluene	Gas	Spearman's ρ	0.836	0.091	-0.096	0.001	0.788	0.654
Toluene		p	0	0.367	0.343	0.989	0	0
Toluene	Solid	Spearman's ρ	0.835	0.091	-0.097	0.002	0.788	0.655
Toluene		p	0	0.369	0.339	0.988	0	0
Ethyl-Benzene	Water	Spearman's ρ	0.93	0.037	-0.031	-0.04	0.854	0.673
Ethyl-Benzene		p	0	0.718	0.761	0.692	0	0
Ethyl-Benzene	Gas	Spearman's ρ	0.93	0.037	-0.031	-0.04	0.854	0.673
Ethyl-Benzene		p	0	0.718	0.759	0.694	0	0
Ethyl-Benzene	Solid	Spearman's ρ	0.928	0.031	-0.029	-0.036	0.852	0.669
Ethyl-Benzene		p	0	0.763	0.777	0.722	0	0
Xylene	Water	Spearman's ρ	0.93	0.037	-0.031	-0.04	0.854	0.673
Xylene		p	0	0.718	0.761	0.692	0	0
Xylene	Gas	Spearman's ρ	0.93	0.037	-0.031	-0.04	0.854	0.673
Xylene		p	0	0.718	0.759	0.694	0	0
Xylene	Solid	Spearman's ρ	0.928	0.031	-0.029	-0.036	0.852	0.669
Xylene		p	0	0.763	0.777	0.722	0	0

for K_{sw}, α, and n are similarly slightly higher for Toluene, and even higher for Ethyl benzene and Xylene than they are for Benzene. The Spearman's ρ coefficients are however higher than the Pearson's r coefficients for all BTEX components.

The PCC and PRCC are presented in Tables 5.3 and 5.4 respectively. After adjusting for the effects of other variables, through the computation of PCC, the correlation coefficients change significantly. From the results presented in Table 5.3, at a 5% significance level there is significant positive correlation between all BTEX components and S_m and n. There is also significant negative correlation between K_{sw} and Benzene and significant positive correlation between α and Benzene. The water and gas phase concentrations of Ethyl benzene and Xylene are also positively correlated with K_{sw}. When the PCC are made less sensitive to non-linearity through the computation of the PRCC, as shown in Table 5.4, at a 5% significance level there are significant correlations between α and n and all phases of the oil components Ethyl benzene and Xylene.

The correlations with α are negative. There is also significant positive correlation between K_{sw} and all phases of the oil components Toluene, Ethyl benzene and Xylene. At the 5 % significance none of the input parameters are significantly correlated with Benzene. However at the 10 % significance level there is an additional significant positive correlation between K_{sw} and all Benzene phases and also significant negative correlation between α and Toluene.

Table 5.3 Partial Correlations between Inputs and Outputs

Component	Phase		K_{sw}	ϕ	S_m	S_{or}	α	n
Benzene	Water	pcc	-0.383	0.023	0.485	0.008	0.304	0.452
Benzene		p	0	0.824	0	0.934	0.002	0
Benzene	Gas	pcc	-0.383	0.023	0.485	0.008	0.304	0.452
Benzene		p	0	0.82	0	0.938	0.002	0
Benzene	Solid	pcc	-0.383	0.022	0.485	0.008	0.304	0.452
Benzene		p	0	0.827	0	0.936	0.002	0
Toluene	Water	pcc	-0.071	-0.014	0.487	-0.009	0.131	0.505
Toluene		p	0.48	0.887	0	0.93	0.192	0
Toluene	Gas	pcc	-0.071	-0.015	0.487	-0.01	0.131	0.505
Toluene		p	0.481	0.885	0	0.925	0.193	0
Toluene	Solid	pcc	-0.071	-0.015	0.487	-0.009	0.131	0.505
Toluene		p	0.481	0.885	0	0.925	0.193	0
Ethyl-Benzene	Water	pcc	0.284	-0.088	0.552	-0.116	-0.172	0.566
Ethyl-Benzene		p	0.004	0.386	0	0.249	0.087	0
Ethyl-Benzene	Gas	pcc	0.253	-0.112	0.564	-0.099	-0.139	0.572
Ethyl-Benzene		p	0.011	0.267	0	0.327	0.169	0
Ethyl-Benzene	Solid	pcc	0.185	-0.141	0.556	-0.066	-0.078	0.554
Ethyl-Benzene		p	0.065	0.163	0	0.511	0.441	0
Xylene	Water	pcc	0.284	-0.088	0.552	-0.116	-0.172	0.566
Xylene		p	0.004	0.386	0	0.249	0.087	0
Xylene	Gas	pcc	0.253	-0.112	0.564	-0.099	-0.139	0.572
Xylene		p	0.011	0.267	0	0.327	0.169	0
Xylene	Solid	pcc	0.185	-0.141	0.556	-0.066	-0.078	0.554
Xylene		p	0.065	0.163	0	0.511	0.441	0

Table 5.4 Partial Rank Correlations between Inputs and Outputs

Component	Phase		K_{sw}	ϕ	S_m	S_{or}	α	n
Benzene	Water	prcc	0.166	0.080	0.070	0.070	-0.033	0.150
Benzene		p	0.099	0.426	0.489	0.488	0.741	0.136
Benzene	Gas	prcc	0.167	0.080	0.069	0.070	-0.034	0.149
Benzene		p	0.096	0.429	0.495	0.492	0.737	0.139
Benzene	Solid	prcc	0.166	0.080	0.070	0.069	-0.033	0.150
Benzene		p	0.098	0.430	0.492	0.495	0.744	0.138
Toluene	Water	prcc	0.379	0.120	-0.064	0.020	-0.176	0.132
Toluene		p	0.000	0.235	0.528	0.846	0.079	0.191
Toluene	Gas	prcc	0.378	0.121	-0.063	0.019	-0.175	0.133
Toluene		p	0.000	0.229	0.536	0.851	0.081	0.188
Toluene	Solid	prcc	0.377	0.120	-0.062	0.019	-0.175	0.134
Toluene		p	0.000	0.232	0.542	0.848	0.082	0.183
Ethyl-Benzene	Water	prcc	0.657	0.005	-0.060	-0.112	-0.414	0.257
Ethyl-Benzene		p	0.000	0.958	0.555	0.267	0.000	0.010
Ethyl-Benzene	Gas	prcc	0.656	0.005	-0.060	-0.111	-0.413	0.257
Ethyl-Benzene		p	0.000	0.958	0.554	0.272	0.000	0.010
Ethyl-Benzene	Solid	prcc	0.652	-0.017	-0.070	-0.093	-0.412	0.237
Ethyl-Benzene		p	0.000	0.866	0.489	0.355	0.000	0.018
Xylene	Water	prcc	0.657	0.005	-0.060	-0.112	-0.414	0.257
Xylene		p	0.000	0.958	0.555	0.267	0.000	0.010
Xylene	Gas	prcc	0.656	0.005	-0.060	-0.111	-0.413	0.257
Xylene		p	0.000	0.958	0.554	0.272	0.000	0.010
Xylene	Solid	prcc	0.652	-0.017	-0.070	-0.093	-0.412	0.237
Xylene		p	0.000	0.866	0.489	0.355	0.000	0.018

The variation in correlations as detected by the four different tests is a function of the different testing powers of the tests and also of the complexity of MOFAT. The signage of the correlations presented in Tables 5.1 to 5.4 is summarized in Table 5.5. While all the tests do not always concur, in general all the outputs are correlated with K_{sw}, α, n and to a lesser degree S_m. These correlations correspond with the dependences that were observed in the scatter plots.

5.2.3 Interactions

When used as screening tools the RS models developed earlier in Section 4.4 provide valuable qualitative information on the interactions between the input parameters. The RS models do not incorporate the correlation structure of the inputs but for screening purposes it is advantageous to drop the correlation structure to avoid needless complexity in the analysis (Saltelli et. al., 2004).

As presented in Section 4.4.4, for all phases of the BTEX components there are interactions between K_{sw} and ϕ and between ϕ and α. The interaction between K_{sw} and α is significant for the gas phases of Benzene and Toluene and all phases of Ethyl-benzene and Xylene.

At high levels of ϕ, the level of K_{sw} does not have an effect on the responses (BTEX concentrations). However at the low levels of ϕ, there is a positive interaction between K_{sw} and ϕ. The physical significance of this interaction is that at low porosities the

Table 5.5 Summary of Correlations

Component	Phase	K_{sw}				ϕ				S_m				S_{or}				α				n			
		Pearson's r	Spearman's ρ	PCC	PRCC	Pearson's r	Spearman's ρ	PCC	PRCC	Pearson's r	Spearman's ρ	PCC	PRCC	Pearson's r	Spearman's ρ	PCC	PRCC	Pearson's r	Spearman's ρ	PCC	PRCC	Pearson's r	Spearman's ρ	PCC	PRCC
Benzene	Water	+	+	-	+							+						+	+	+		+	+	+	
Benzene	Gas	+	+	-	+							+						+	+	+		+	+	+	
Benzene	Solid	+	+	-	+							+						+	+	+		+	+	+	
Toluene	Water	+	+		+							+						+	+		-	+	+	+	
Toluene	Gas	+	+		+							+						+	+		-	+	+	+	
Toluene	Solid	+	+		+							+						+	+		-	+	+	+	
Ethyl-Benzene	Water	+	+	+	+							+						+	+		-	+	+	+	+
Ethyl-Benzene	Gas	+	+	+	+							+						+	+		-	+	+	+	+
Ethyl-Benzene	Solid	+	+	+	+							+						+	+		-	+	+	+	+
Xylene	Water	+	+	+	+							+						+	+		-	+	+	+	+
Xylene	Gas	+	+	+	+							+						+	+		-	+	+	+	+
Xylene	Solid	+	+	+	+							+						+	+		-	+	+	+	+

+/- = Positive or negative correlation at the 10 % significance level
+/- = Positive or negative correlation at the 5 % significance level
Blank = No significant correlations at either of the 5 % and 10 % significance levels

hydraulic conductivity has a positive effect on the responses since porosity is playing a limiting role in mass conservation (Equation 1, Section 3.4.1). This interaction however will not be applicable in an actual Tier 3 RBCA scenario since low porosities with high hydraulic conductivity are a characteristic of porous media with fractures. MOFAT is not applicable for simulating in a fractured media environment and would not be used for Tier 3 RBCA scenarios involving fractured media.

At the high levels of α, the level of ϕ does not have an effect on the responses. However at low levels of α, there is a negative interaction between ϕ and α. The van Genuchtan α affects the p phase saturations (Equations 4,5,6 and 7, Section 3.4.1), which affect the governing equations for both flow and transport at several levels (Equations 4, 5, 6 and 7, in Section 3.4.1, equations 13, 14, 16, 17, 18 and 19 in Section 3.4.2). Due to the complexity of the equations it is not possible to explicitly describe why this interaction occurs.

At the high levels of α, the level of K_{sw} does not have an effect on the responses. However at the low levels of α, there is a positive interaction between K_{sw} and α, i.e. as the level of K_{sw} increases the responses increases. Again, since van Genuchtan α affects the governing equations for both flow and transport at several levels it is not possible to explicitly describe why this interaction occurs due to the complexity of the equations.

5.2.4 Effects of Input Parameter Correlations on Sensitivity Analysis

The presence of correlations between probabilistic input parameters can greatly complicate the interpretation of sensitivity analysis results (Helton and Davis, 2000). To correctly interpret the results of the correlations presented in Tables 5.1 to 5.5 the results should be reviewed in conjunction with information on the correlations between the probabilistic input parameters. The U.S. EPA guidelines on MC analysis recommends that the presence or absence of moderate to strong correlations or dependencies between the input variables is to be discussed and accounted for in sensitivity analysis, along with the effects that these have on the output distribution (U.S. EPA, 1997b).

Information on the correlations between the probabilistic input parameters has been presented earlier in Table 3.5 and discussed earlier in Section 3.6. K_{sw} is positively correlated with θ_r (and hence S_m), α and n. These are the same input parameters that are in general correlated with all of the outputs as seen in Tables 5.1 to 5.5. It was also noted earlier that these correlations correspond with the dependences that were observed in the scatter plots.

The correlations between K_{sw} and the van Genuchten water retention parameters α and n are especially strong. This explains why the output parameters in general were distinctly correlated with K_{sw}, α and n. θ_r (and hence S_m) shows a strong correlation with n. This might be the explanatory cause as to why in the PCC test, S_m showed a significant correlation with all outputs.

5.3 Ranking and Grouping of Input Parameters

An aim of sensitivity studies is to obtain a ranking of the input parameters based on their contribution to the output variance. This is primarily for the purpose of identifying the inputs that contribute most to output variability and to consequently identify which parameters require additional research or more focus for reducing output uncertainty. The aim of the ranking is not to obtain an absolute ranking of parameter importance. This is more a prioritization exercise to provide model users with guidance on relative parameter importance. This ranking is important for assigning priorities to variables for reducing uncertainties. These higher ranked inputs typically have the most influence on the calibration and predictions and should be the focus of field investigation and calibration efforts.

5.3.1 Ranking Based on the Absolute Value of the PRCC

One approach for identifying important input variables is to rank the input parameters on the relative size of the absolute value of the PRCC (Iman and Helton, 1985). The PRCC have been presented earlier in Table 5.4. The absolute value of the PRCC is a quantification of the strength of the relationship between two parameters. The higher the absolute value of the PRCC the greater is the strength of the correlation between the input and output parameter. As the strength of the correlation increases the importance of the input parameter increases so the absolute value of the PRCC can be used to rank input

parameters. The input parameters have been ranked on the relative size of the absolute value of the PRCC as shown in Table 5.6.

5.3.2 Grouping Based on Critical "p" Values

Another approach for identifying important input variables is to divide the variables into groups on the basis of critical values (Kleijnen and Helton, 1999a). The p values are a useful tool for distinguishing between parameters that appear to have a substantial effect on predicted parameters and parameters that appear to have little or no effect (Kleijnen and Helton, 1999a). The critical values or p values are the probability that a larger coefficient value would occur owing to chance variation. A small critical value indicates that under the assumptions of the test, an outcome equal to or greater than the observed value of the statistic is unlikely to occur owing to chance (Kleijnen and Helton, 1999a). The importance of a parameter goes up as the p value goes down so the p value can be used to rank input parameters. The p values are a function of sample size and it is important to compare p values based on the same sample size. Since the LHS-MC simulation results were used for this sensitivity study, the sample size used in this study is 100. Using the critical values of the PRCC the input variables have been grouped in Table 5.7 into three groups in decreasing order of significance as follows:

Group 1	Variables with p less than 0.01
Group 2	Variables with p equal to or greater than 0.01 but less than 0.05
Group 3	Variables with p equal to or greater than 0.05

Table 5.6 Ranking of Inputs Based on the Absolute Value of the PRCC

Component	Phase	K_{sw}	ϕ	S_m	S_{or}	α	n
Benzene	Water	1	3	4	4	6	2
Benzene	Gas	1	3	5	4	6	2
Benzene	Solid	1	3	4	5	6	2
Toluene	Water	1	4	5	6	2	3
Toluene	Gas	1	4	5	6	2	3
Toluene	Solid	1	4	5	6	2	3
Ethyl-Benzene	Water	1	6	5	4	2	3
Ethyl-Benzene	Gas	1	6	5	4	2	3
Ethyl-Benzene	Solid	1	6	5	4	2	3
Xylene	Water	1	6	5	4	2	3
Xylene	Gas	1	6	5	4	2	3
Xylene	Solid	1	6	5	4	2	3

*Table 5.7 Grouping of Inputs Based on the Basis of Critical Values of PRCC**

Component	Phase	K_{sw}	ϕ	S_m	S_{or}	α	n
Benzene	Water	3	3	3	3	3	3
Benzene	Gas	3	3	3	3	3	3
Benzene	Solid	3	3	3	3	3	3
Toluene	Water	1	3	3	3	3	3
Toluene	Gas	1	3	3	3	3	3
Toluene	Solid	1	3	3	3	3	3
Ethyl-Benzene	Water	1	3	3	3	1	2
Ethyl-Benzene	Gas	1	3	3	3	1	2
Ethyl-Benzene	Solid	1	3	3	3	1	2
Xylene	Water	1	3	3	3	1	2
Xylene	Gas	1	3	3	3	1	2
Xylene	Solid	1	3	3	3	1	2

*based on a sample size of 100.

5.3.3 Combined Grouping and Ranking

The two previous approaches both use the PRCC results for identifying important input variables. The ranking approach is based on a measure of absolute correlation while the grouping approach is based on the significance of results. A shortcoming with the measure of absolute correlation approach is that even those correlations that are not significant are included in the ranking. Similarly while the grouping approach takes into account the significance of a correlation it does not provide an indication of the absolute value of the correlation coefficient. Moreover the grouping presented in Table 5.7 is not very useful for prioritizing variables since too many of the variables have the same rank.

A more relevant approach for identifying important input variables would be to merge the two approaches so that the input variables are first grouped on the basis of the critical values of the PRCC and are then ranked within each group based on the relative size of the absolute value of the PRCC. The grouping can be further improved by including a fourth category based on the 10% significance level as shown below:

Group A	Variables with p less than 0.01
Group B	Variables with p equal to or greater than 0.01 but less than 0.05
Group C	Variables with p equal to or greater than 0.05 but less than 0.1
Group D	Variables with p equal to or greater than 0.1

The addition of a fourth category essentially presents four groups based on the 1%, 5% and 10 % significance levels. This approach has been implemented on the PRCC results and the resulting grouping and ranking are presented in Table 5.8. An alphanumeric character indicates the significance of each variable for each phase of each BTEX component. The alphabetic character indicates the group based on the critical p values of the PRCC while the numeric portion indicates the relative rank within that group based the absolute value of the PRCC.

5.4 Sensitivity to Additional Correlations between Input Parameters

Of the seven probabilistic input parameters the Pearson Product Moment Correlation Matrix used for this study accounted for correlations between four of the input parameters; K_{sw}, θ_r, α and n. The correlation matrix was developed by Carsel and Parrish (1988) for use in the uncertainty analysis of the leaching potential of the pesticide aldicarb using the PRZM model. Consequently, S_{or} and ϕ were not included in the correlation matrix as they are not inputs for the PRZM model.

The sensitivity analysis presented earlier in Section 5.2 showed that the MOFAT outputs parameters are not significantly correlated to either S_{or} or ϕ. To further test the sensitivity of the uncertainty analysis conducted in Chapter 4, to the omission of the S_{or}

*Table 5.8 Grouping and Ranking of Inputs Based on PRCC**

Component	Phase		K_{sw}	ϕ	S_m	S_{or}	α	n
Benzene	Water	LHS	C1	D2	D4	D3	D5	D1
Benzene	Gas	LHS	C1	D2	D4	D3	D5	D1
Benzene	Solid	LHS	C1	D2	D3	D4	D5	D1
Toluene	Water	LHS	A1	D2	D3	D4	C1	D1
Toluene	Gas	LHS	A1	D2	D3	D4	C1	D1
Toluene	Solid	LHS	A1	D2	D3	D4	C1	D1
Ethyl-Benzene	Water	LHS	A1	D3	D2	D1	A2	B1
Ethyl-Benzene	Gas	LHS	A1	D3	D2	D1	A2	B1
Ethyl-Benzene	Solid	LHS	A1	D3	D2	D1	A2	B1
Xylene	Water	LHS	A1	D3	D2	D1	A2	B1
Xylene	Gas	LHS	A1	D3	D2	D1	A2	B1
Xylene	Solid	LHS	A1	D3	D2	D1	A2	B1

*based on a sample size of 100.

and ϕ from the correlation matrix, the next two sections test the effect of individually incorporating S_{or} and ϕ into the correlation matrix.

5.4.1 Maximum Residual Oil Saturation

A LHS-MC sample consisting of 100 simulations was generated and simulated to test the sensitivity of the uncertainty analysis to correlation between saturated conductivity, K_{sw}, and maximum residual oil saturation for water, S_{or}.

As listed in Table 5.9, in the absence of any information on the magnitude of correlation between K_{sw} and S_{or} a correlation of 0.5 was assumed between the two parameters for this LHS-MC sample. The sample was labeled as LHS-c. The adjusted rank correlation matrix generated by the LHS program is presented in Table 5.10. The empirical *cdfs* for the 12 MOFAT responses were plotted against the corresponding *cdfs* from LHS-MC simulation LHS set (described earlier in Section 4.3) to evaluate the sensitivity of the uncertainty analysis.

Figure 5.3 shows that the *cdfs* for Benzene generated using the LHS and the LHS-c samples match up very closely for the water and gas phases. There is a slight deviation between the *cdf* plots for the water and solid phases at the higher probabilities starting at the 95% probability level.

Table 5.9 Pearson Product Moment Correlation Matrix

K_{sw}	1.0000				
θ_r	0.2040	1.0000			
α	0.9820	-0.0860	1.0000		
n	0.6320	-0.7480	0.5910	1.0000	
S_{or}	0.5000	0.0000	0.0000	0.0000	1.0000
	K_{sw}	θ_r	α	n	S_{or}

Table 5.10 Adjusted Rank Correlation Matrix

K_{sw}	1.0000				
θ_r	0.1175	1.0000			
α	0.8907	-0.0373	1.0000		
n	0.5417	-0.6995	0.6418	1.0000	
S_{or}	0.4353	0.0346	0.0365	0.0361	1.0000
	K_{sw}	θ_r	α	n	S_{or}

Figure 5.3 LHS and LHS-c cdf comparison for Water, Gas and Solid Phase Concentrations of Benzene

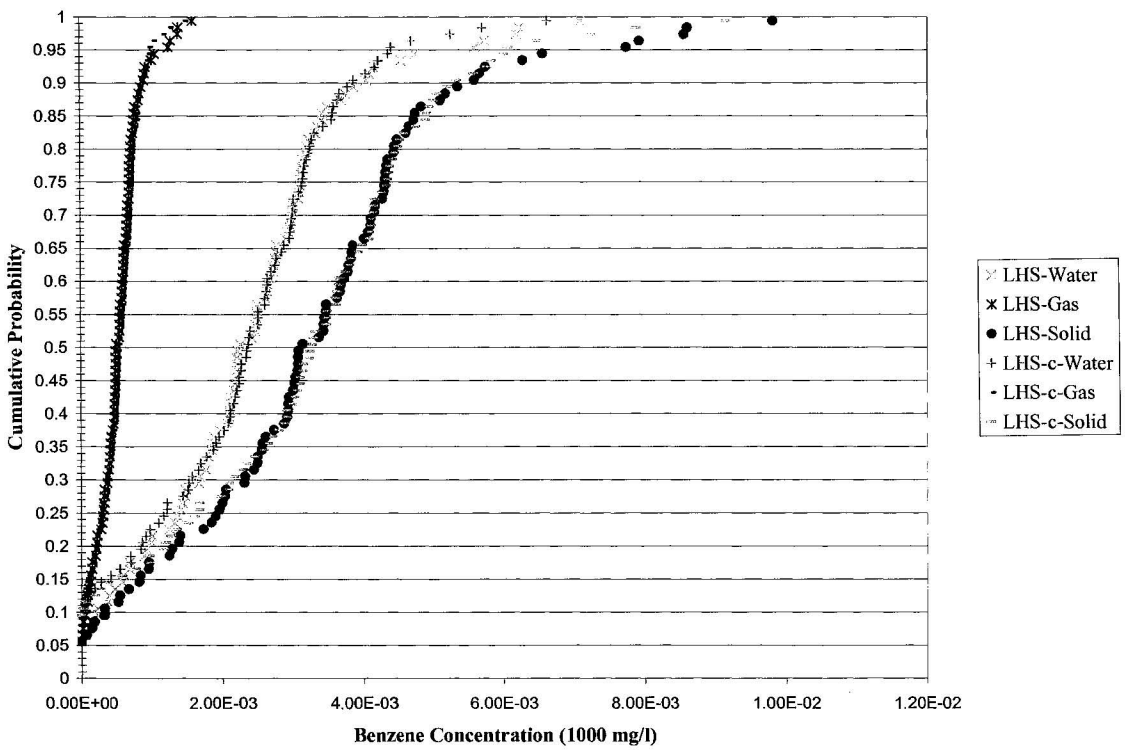

Figure 5.4 shows that the *cdfs* for Toluene generated using the LHS and the LHS-c samples match up very closely for the water and gas phases. There is a slight deviation between the *cdf* plots for the solid phases at the higher probabilities starting at the 85% probability level.

Figure 5.5 shows that the *cdfs* for Ethyl benzene generated using the LHS and the LHS-c samples match up very closely for the water and gas phases. There is a slight deviation between the *cdf* plots for the solid phase at the higher probabilities starting at the 90 % probability level.

Figure 5.6 shows that the *cdfs* for Xylene generated using the LHS and the LHS-c samples match up very closely for all three phases. In Figures 5.3 to 5.6, the closeness of the LHS and LHS-c *cdf* plots, especially for the water and gas phases of all four BTEX components, implies that the output responses are not sensitive to S_{or} values. The deviation between the *cdf* plots for the solid phase for all BTEX components at the higher probabilities are largely negligible and it can be reasonably concluded that the exclusion of S_{or} from the correlation matrix does not significantly affect the accuracy of the uncertainty analysis.

Figure 5.4 LHS and LHS-c cdf comparison for Water, Gas and Solid Phase Concentrations of Toluene

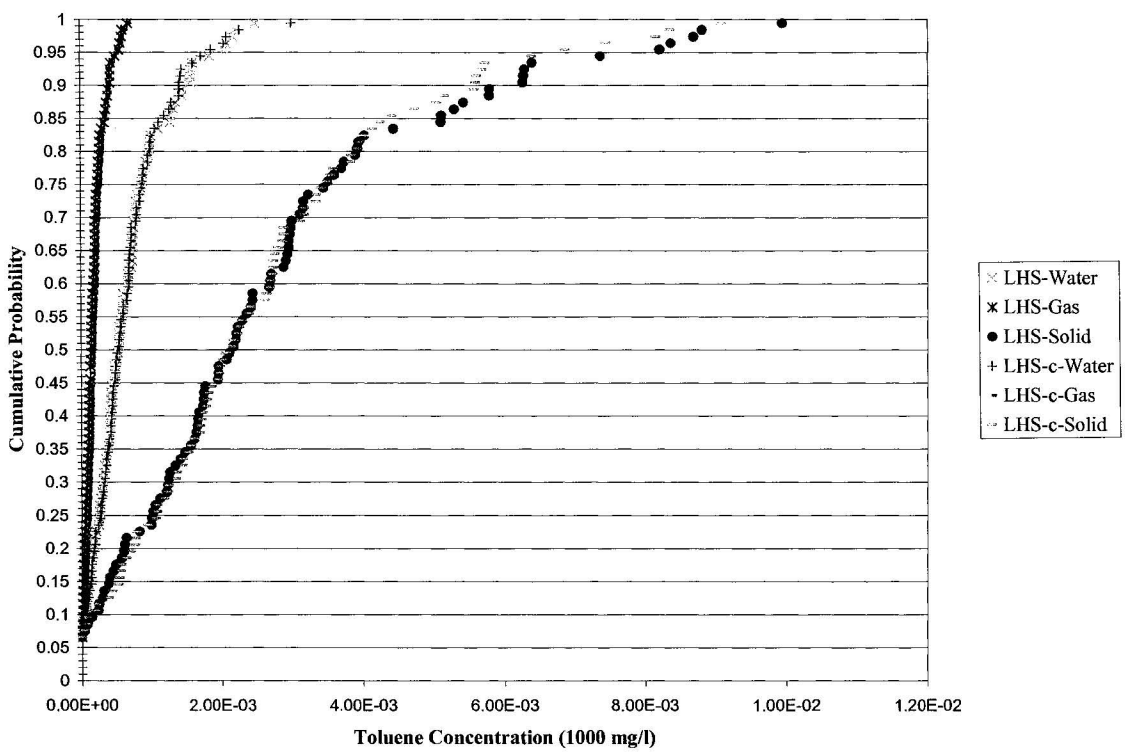

Figure 5.5 LHS and LHS-c cdf comparison for Water, Gas and Solid Phase Concentrations of Ethyl benzene

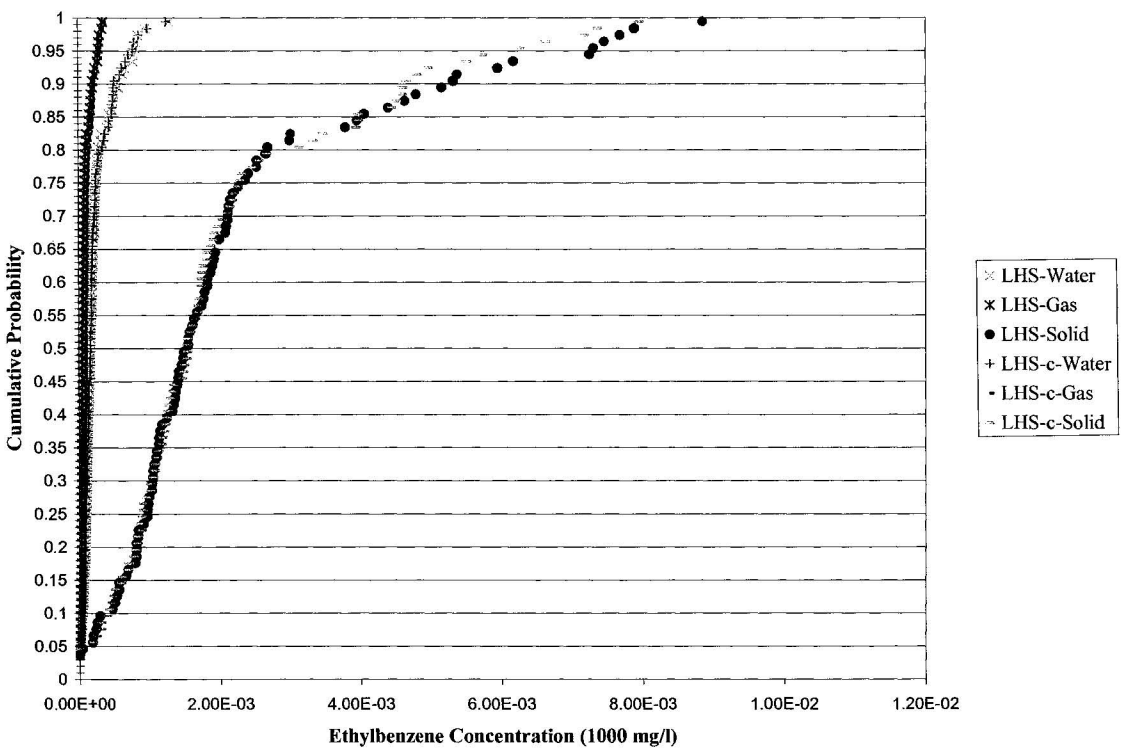

Figure 5.6 LHS and LHS-c cdf comparison for Water, Gas and Solid Phase Concentrations of Xylene

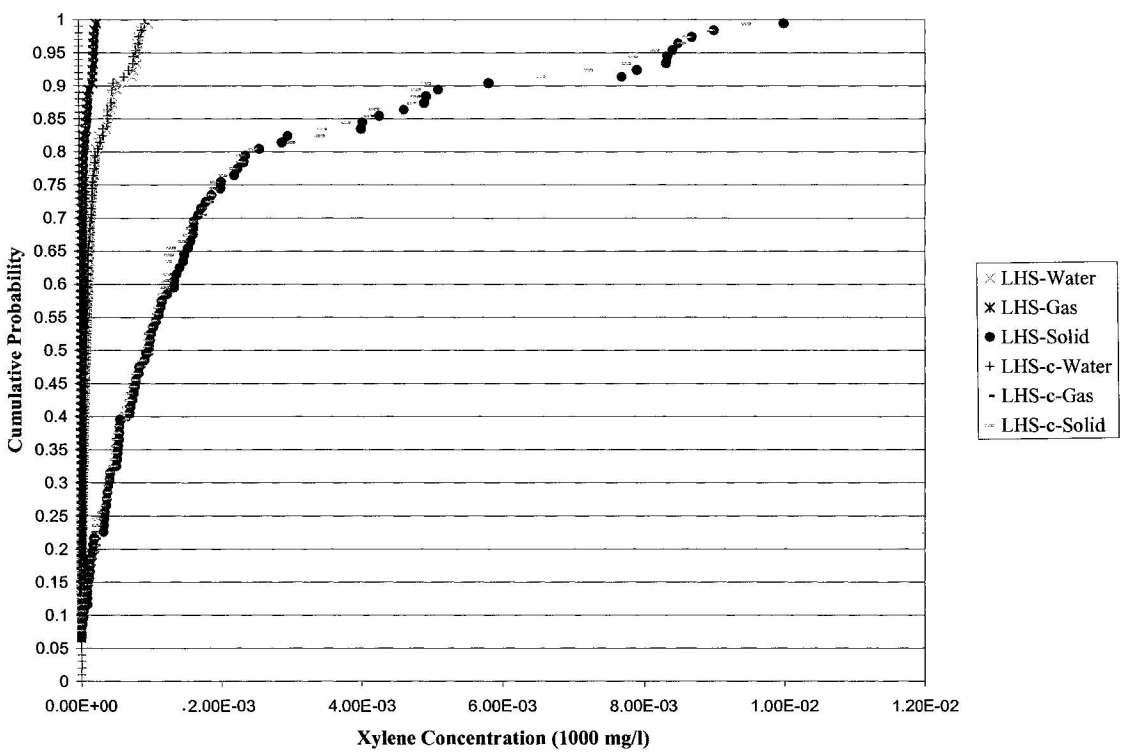

5.4.2 Porosity

A LHS-MC sample consisting of 100 simulations was generated and simulated to test the sensitivity of the uncertainty analysis to correlation between saturated hydraulic conductivity, K_{sw} and porosity, ϕ..

These two parameters are generally correlated. There is no strict relationship between porosity and saturated hydraulic conductivity but generally as long as the influence of molecular attraction is on the second order, hydraulic conductivity increases with an increase in porosity (Spitz and Moreno, 1996). As listed in Table 5.11, in the absence of any information on the magnitude of correlation between K_{sw} and, ϕ a correlation of 0.5 was assumed between the two parameters for this LHS sample. The sample was labeled as LHS-p.

The adjusted rank correlation matrix generated by the LHS program is presented in Table 5.12. The empirical *cdfs* for the 12 responses were plotted against the corresponding *cdfs* to evaluate the sensitivity of the uncertainty analysis.

Figure 5.7 shows that the *cdfs* for Benzene generated using the LHS and the LHS-p samples match up very closely for the gas phase. There is a very slight deviation between the *cdf* plots for the water and solid phases at the higher probabilities.

Table 5.11 Pearson Product Moment Correlation Matrix

K_{sw}	1.0000				
θ_r	0.2040	1.0000			
α	0.9820	-0.0860	1.0000		
n	0.6320	-0.7480	0.5910	1.0000	
ϕ	0.5000	0.0000	0.0000	0.0000	1.0000
	K_{sw}	θ_r	α	n	ϕ

Table 5.12 Adjusted Rank Correlation Matrix

K_{sw}	1.0000				
θ_r	0.1175	1.0000			
α	0.8907	-0.0373	1.0000		
n	0.5417	-0.6995	0.6418	1.0000	
ϕ	0.4353	0.0346	0.0365	0.0361	1.0000
	K_{sw}	θ_r	α	n	ϕ

Figure 5.7 LHS and LHS-p cdf comparison for Water, Gas and Solid Phase Concentrations of Benzene

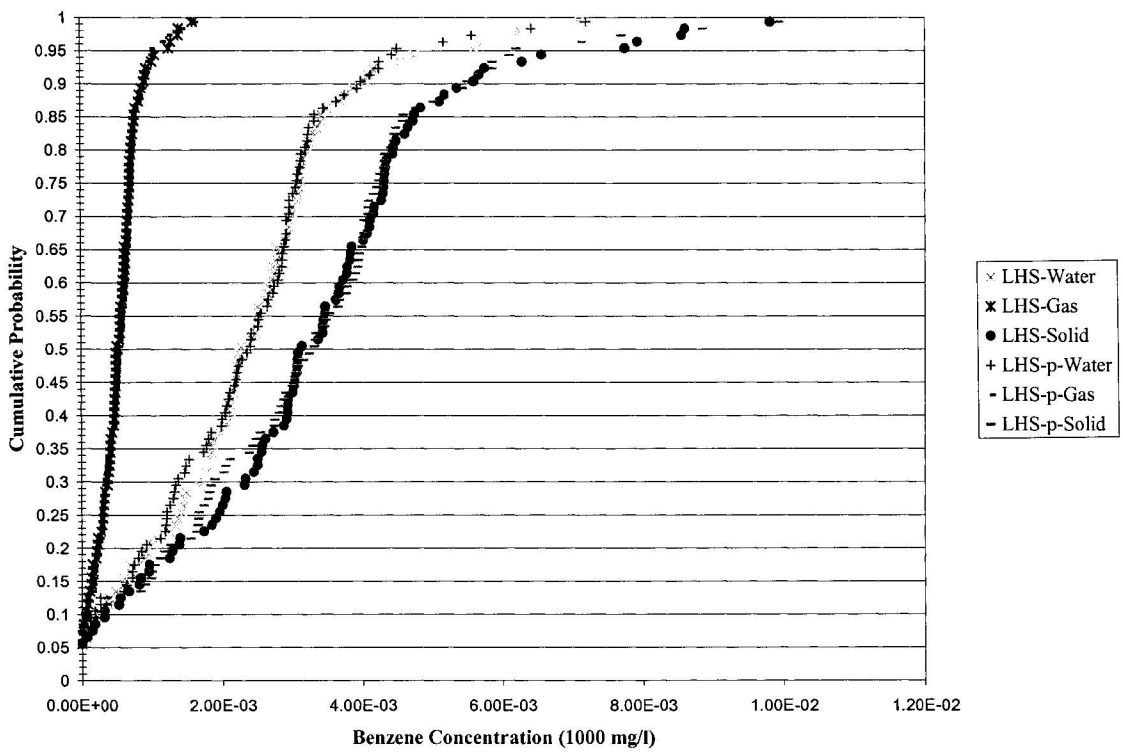

Figure 5.8 shows that the *cdfs* for Toluene generated using the LHS and the LHS-p samples match up very closely for all three phases.

Figure 5.9 shows that the *cdfs* for Ethyl benzene generated using the LHS and the LHS-p samples match up very closely for the water and gas phases. There is a slight deviation between the *cdf* plots for the solid phase at the higher probabilities.

Figure 5.10 shows that the *cdfs* for Xylene generated using the LHS and the LHS-p samples match up very closely for all three phases.

In Figures 5.7 to 5.10, the closeness of the LHS and LHS-p *cdf* plots, especially for the water and gas phases of all four BTEX components, implies that the output responses are not sensitive to the inclusion of ϕ in the correlation matrix. The deviation between the *cdf* plots for the solid phase for all BTEX components at the higher probabilities are largely negligible and it can be reasonably concluded that the exclusion of ϕ from the correlation matrix does not significantly affect the accuracy of the uncertainty analysis.

5.5 Sensitivity to Anisotropy

For anisotropic soil mediums the ratio of horizontal to vertical hydraulic conductivity can vary from one to much higher values like 10. Typically horizontal conductivities are

Figure 5.8 LHS and LHS-p cdf comparison for Water, Gas and Solid Phase Concentrations of Toluene

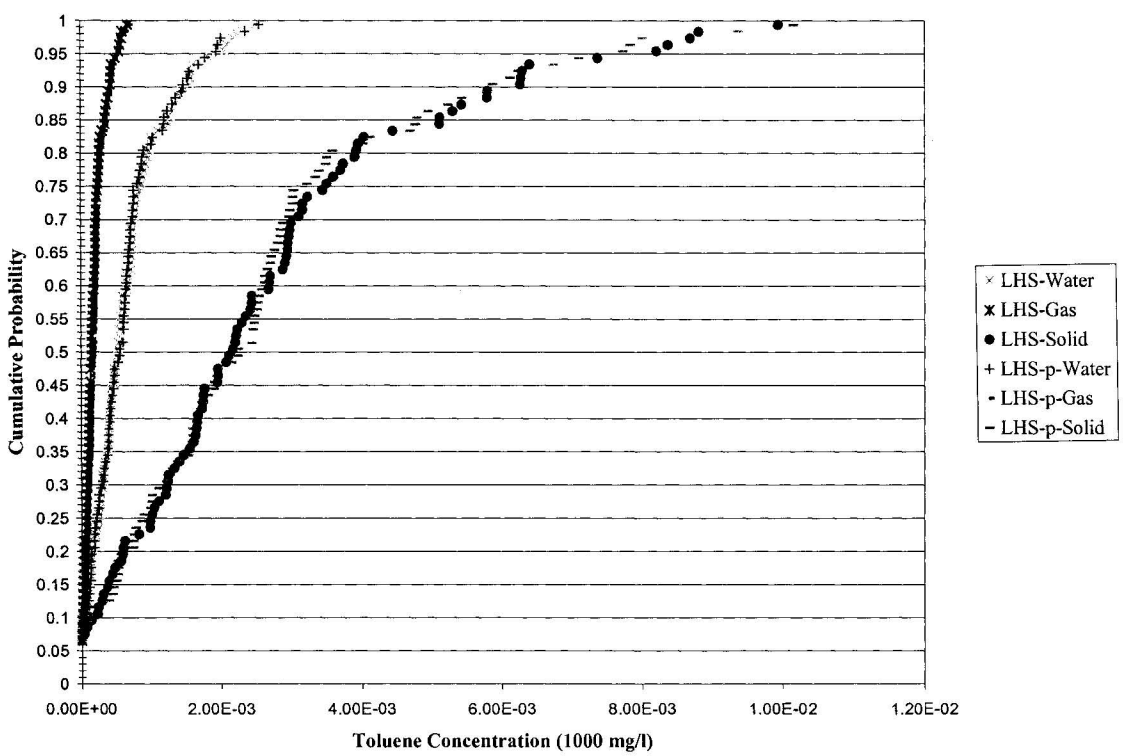

Figure 5.9 LHS and LHS-p cdf comparison for Water, Gas and Solid Phase Concentrations of Ethyl benzene

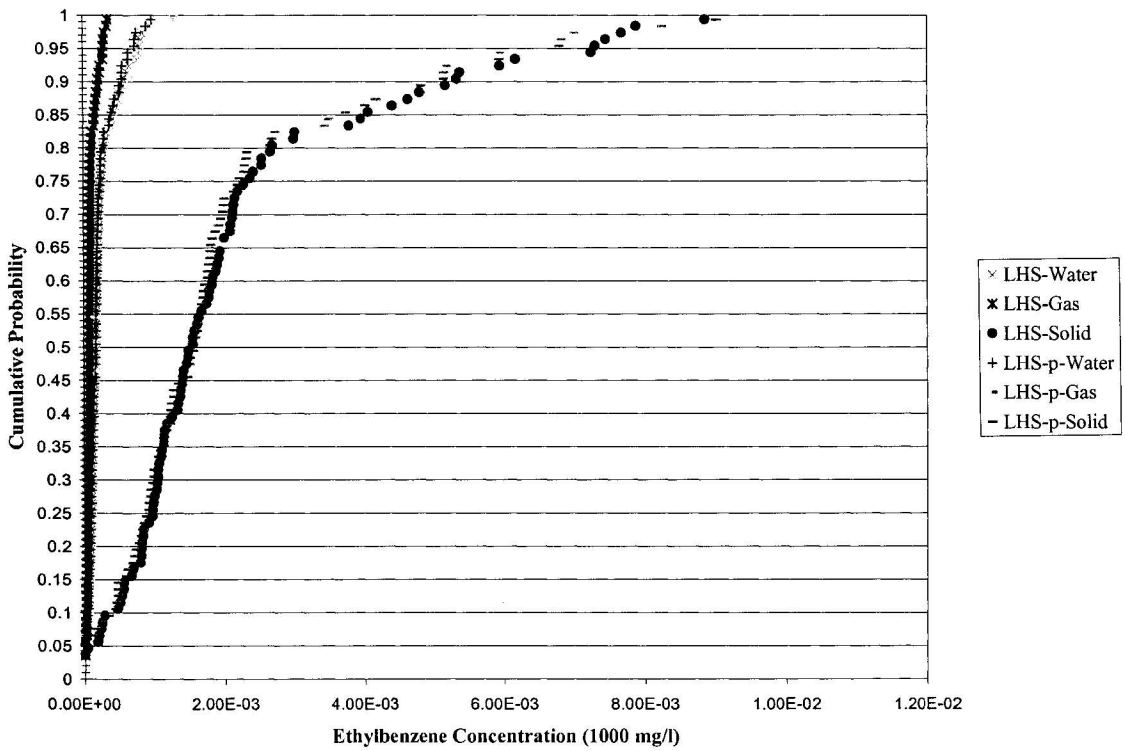

Figure 5.10 LHS and LHS-p cdf comparison for Water, Gas and Solid Phase Concentrations of Xylene

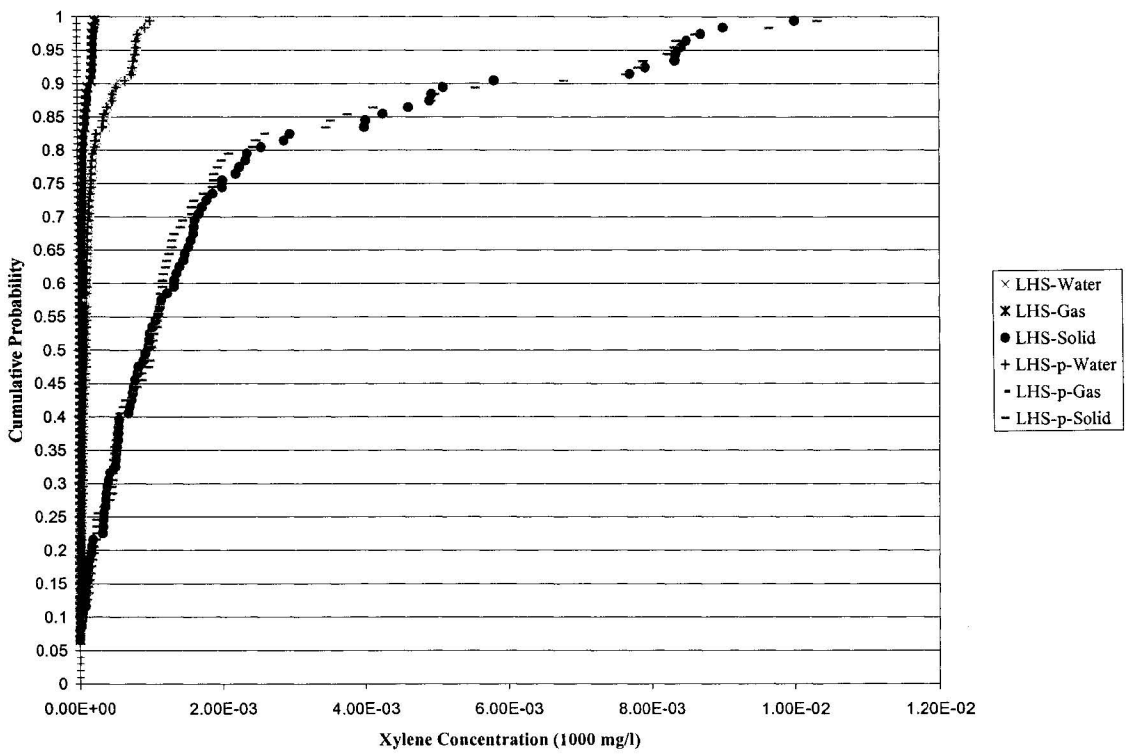

higher than vertical conductivities (Spitz and Moreno, 1996). For the uncertainty analysis presented in this study isotropic conditions were assumed and the vertical and horizontal hydraulic conductivity were assumed to be equal for the RS-MC, LHS, LHS-s, LHS-c, and LHS-p simulations. To test the sensitivity of the uncertainty analysis to the ratio of horizontal to vertical hydraulic conductivity, a sixth LHS-MC sample was generated. This sample was labeled as LHS-K. For this LHS sample the horizontal hydraulic conductivity was assumed to be twice the vertical conductivity.

The empirical *cdfs* for the 12 responses were plotted against the corresponding *cdfs* to evaluate the sensitivity of the uncertainty analysis.

Figure 5.11 shows that the *cdfs* for Benzene generated using the LHS and the LHS-K samples match up very closely for the gas phase. There is a clear deviation between the *cdf* plots for the water and solid phase starting right at the lower probabilities. However at the higher probabilities the LHS and the LHS-K *cdf* plots for the water and solid phase match very closely.

Figure 5.12 shows that the *cdfs* for Toluene generated using the LHS and the LHS-K samples match up very closely for the water and gas phases. There is a slight deviation between the *cdf* plots for the solid phase starting right at the lower probabilities but again at the higher probabilities the LHS and the LHS-K *cdf* plots for the solid phase match very closely.

Figure 5.11 LHS and LHS-K cdf comparison for Water, Gas and Solid Phase Concentrations of Benzene

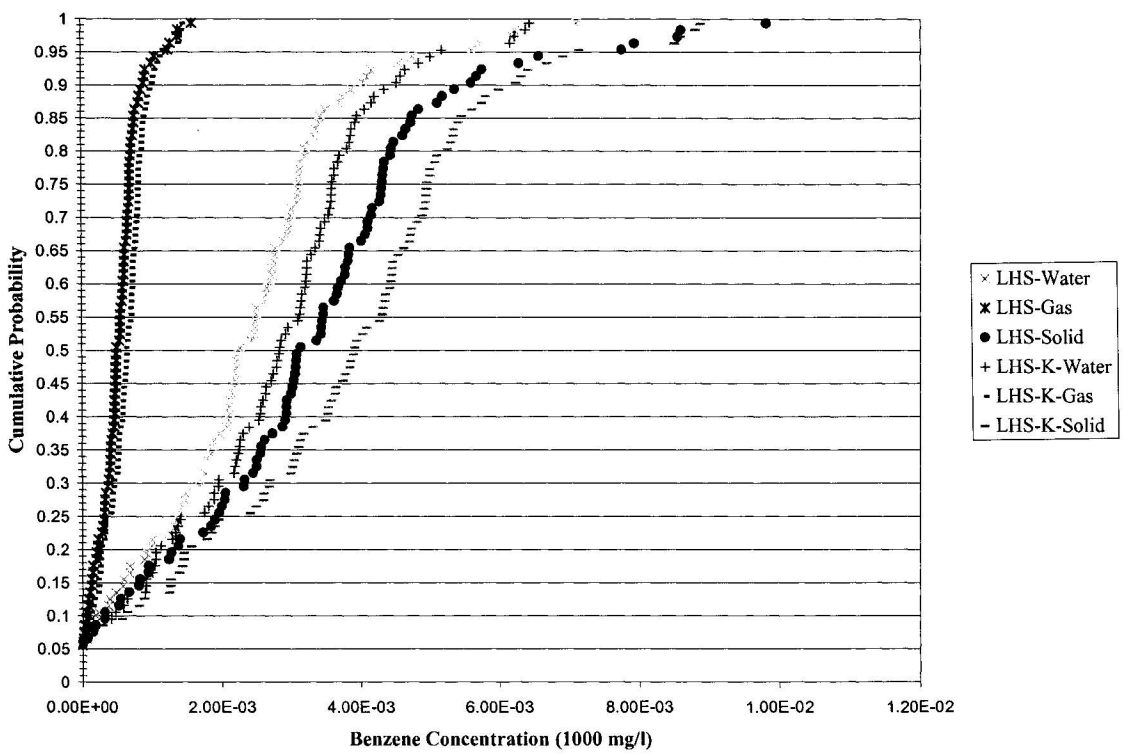

Figure 5.12 LHS and LHS-K cdf comparison for Water, Gas and Solid Phase Concentrations of Toluene

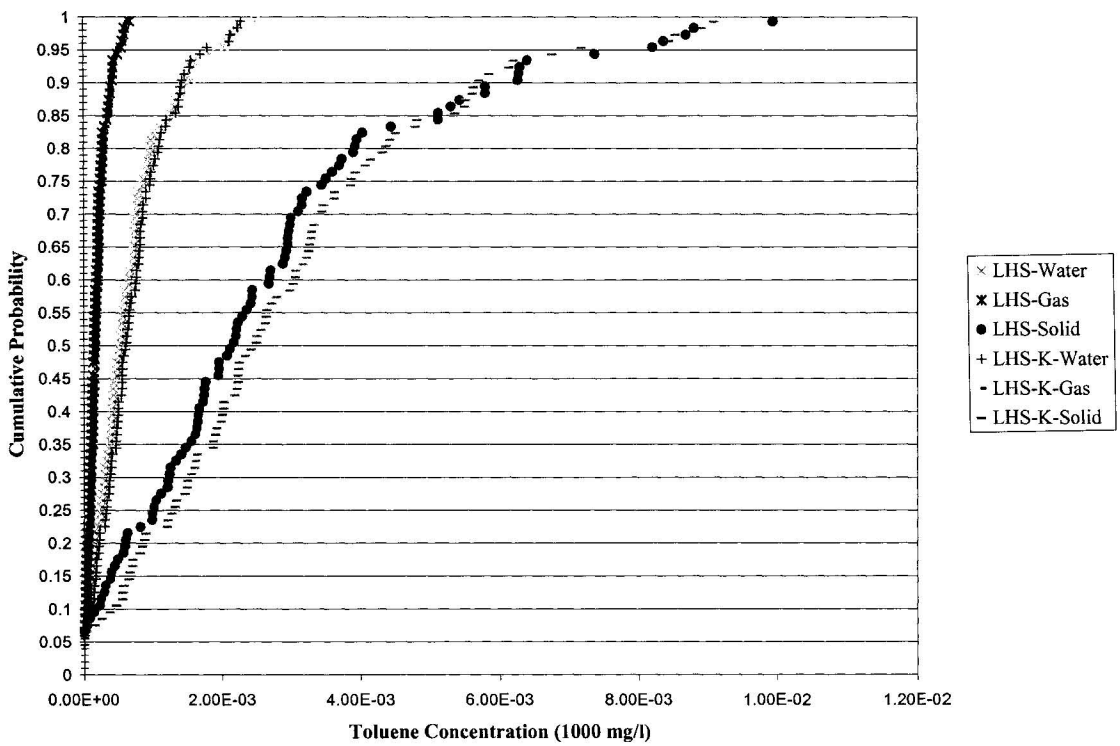

Figure 5.13 shows that the *cdfs* for Ethyl benzene generated using the LHS and the LHS-K samples match up very closely for the water and gas phases. There is a slight deviation between the *cdf* plots for the solid phase at the higher probabilities.

Figure 5.14 shows that the *cdfs* for Xylene generated using the LHS and the LHS-K samples match up very closely for all three phases. In Figures 5.11 to 5.14, the closeness of the LHS and LHS-p *cdf* plots, especially for the water and gas phases of all four BTEX components, implies that the output responses are not overtly sensitive to the ratio of horizontal to vertical hydraulic conductivity. While there is slight sensitivity in the solid phase concentrations of all four BTEX components to the ratio of horizontal to vertical hydraulic conductivity these results establish that the uncertainty analysis presented earlier in Chapter 4 was not significantly affected by the ratio of horizontal to vertical hydraulic conductivity.

Figure 5.13 LHS and LHS-K cdf comparison for Water, Gas and Solid Phase Concentrations of Ethyl benzene

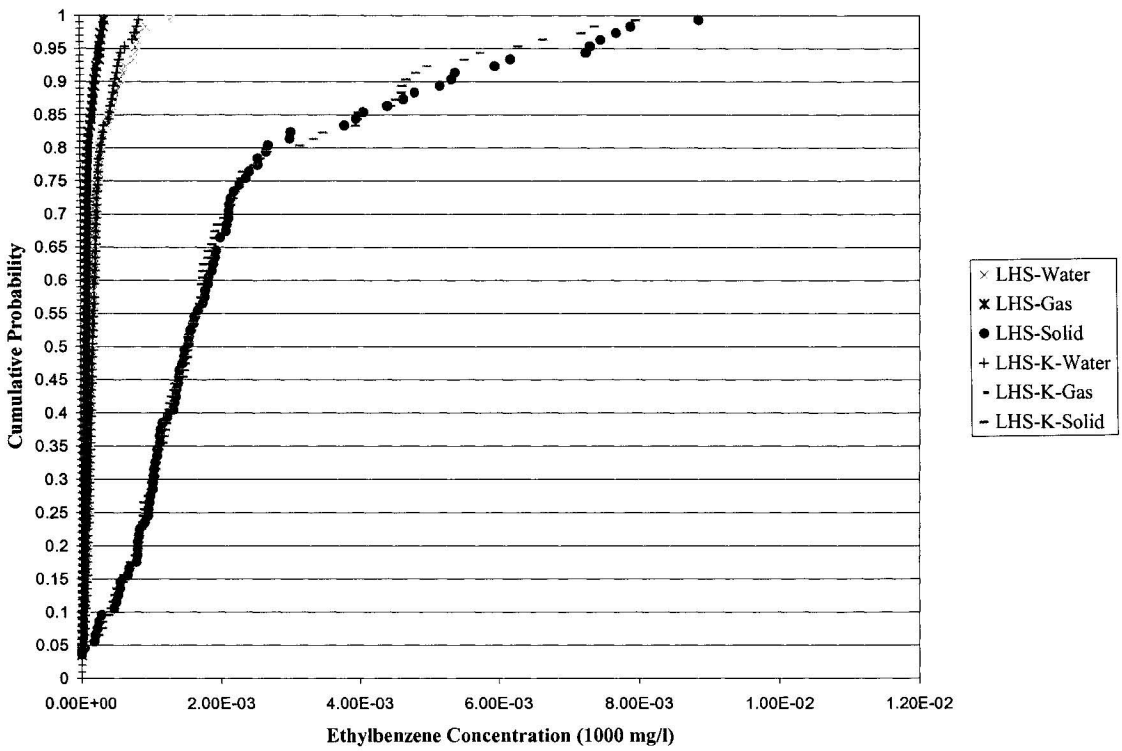

Figure 5.14 LHS and LHS-K cdf comparison for Water, Gas and Solid Phase Concentrations of Xylene

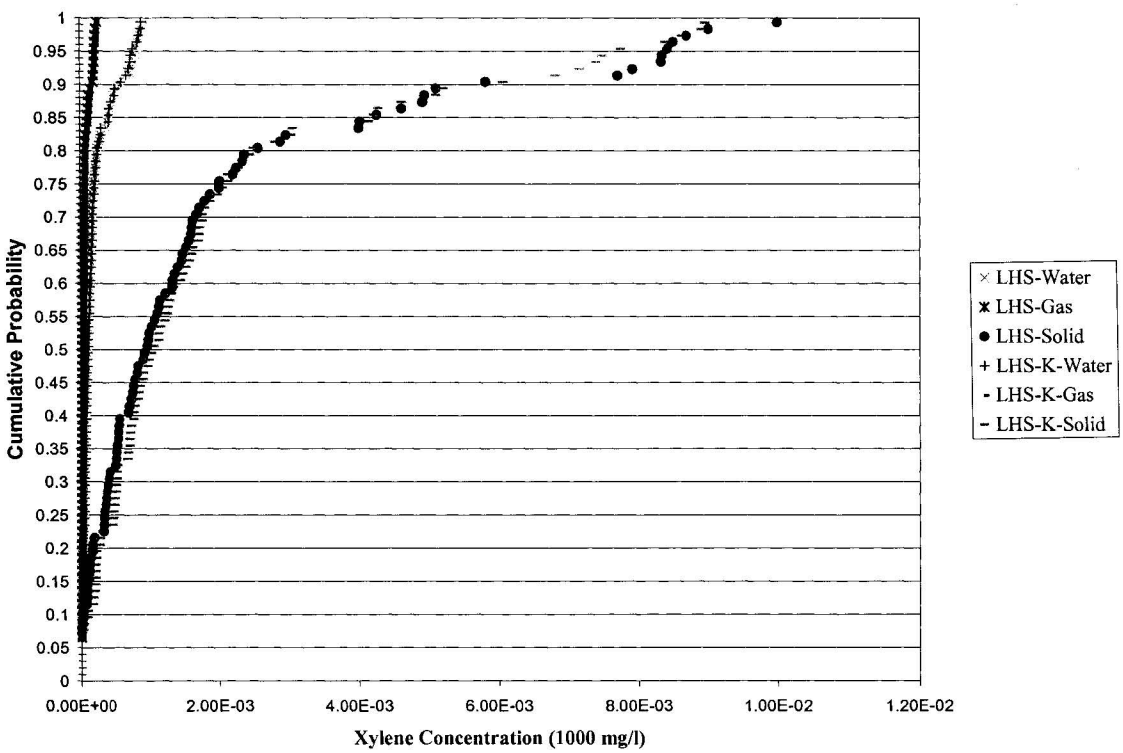

Chapter 6. A Framework for Uncertainty and Sensitivity Analysis of MOFAT

6.1 Introduction

Saltelli et. al. (2004) note "uncertainty and sensitivity analysis are more often mentioned than practiced". This is reflected in that when this research study was initiated no published guidance was available (and is still not available) on the parametric uncertainties associated with MOFAT or for that matter any multi-phase multi-component fate and transport model that could be used for Tier 3 RBCA of petroleum release sites. Similarly no published framework was available (and is still not available) on how to undertake an uncertainty and sensitivity analysis of MOFAT (or other any multi-phase multi-component fate and transport model that could be used for Tier 3 RBCA of petroleum release sites) to estimate parametric uncertainties and identify sensitive parameters.

One reason for the absence of quantification of parametric uncertainties (and an associated framework) is that the area of quantitative uncertainty analysis for RBCA is a relatively recent development that has primarily come of age in the last decade. Institutional and regulatory policy and guidance, which is a strong impetus for development, in the form of the 1995 ASTM "Standard Guide for Risk Based Corrective Action Applied at Petroleum Release Sites, ASTM E 1739-95"; 1997 U.S. EPA "Policy for Use of Probabilistic Analysis in Risk Assessment at the U.S. Environmental Protection Agency"; 1997 U.S. EPA " Guiding Principles for Monte Carlo Analysis. EPA 630-R-97-001" and the 2003 U.S. EPA "Multimedia, Multipathway, and Multireceptor Risk Assessment (3MRA) Modeling System. Volume IV: Evaluating Uncertainty and Sensitivity. EPA 530-D-03-001d" have only become available in the last decade. More over it is only in the more recent of these documents that the impetus has shifted from a qualitative to a quantitative assessment of uncertainty and sensitivity.

Another reason for the absence of such a framework is that development of such a framework for a complex model is in itself a complex and resource intensive endeavor that essentially requires comparison of various uncertainty analysis techniques with the benchmark Random Sampling Monte Carlo technique (RS-MC). Due to their computational complexity and expense, complex models like MOFAT do not constitute convenient vehicles for comparing differences between benchmark RS-MC and other more computationally efficient uncertainty analysis techniques. As discussed in Section 1.1 the simulation time itself for RS-MC could be prohibitive. Another restricting factor

is that specialized processing tools (a MC version of model, a pre processor and a post processor) are required. The 10,000 RS-MC simulations conducted in this research study took approximately two years to complete. This was using the MC-MOFAT version developed in this study, which allowed batch processing. Without the batch processing abilities of the MC-MOFAT code this would have taken significantly longer. Similarly the manual compilation of 10,000 MOFAT input files is time consuming task. The pre-processing tool developed as a part of this study allowed the assembly of 10,000 MOFAT input files in minutes. If done manually this task would take at least 20.8 days if done continuously without a break. This is based on the assumption that to manually assemble one MOFAT input file it would take approximately three minutes and hence 30,000 minutes (20.8 days) to assemble 10,000 input files.

The processing of the 10,000 output data files generated due to RS-MC is also an overwhelming task. The post-processing tool developed as a part of this study is able to accurately extract the output results for 10,000 MOFAT output files in approximately a fortnight. If done manually this task would take at least 41.6 days if done continuously without a break. This is based on the assumption that to manually extract the results of one MOFAT output file to a text file it would take on an average six minutes and hence 60,000 minutes (41.6 days) to manually extract the output results for 10,000 MOFAT output files.

As presented in Chapter 1, with an aim of addressing this gap in published literature the objectives of this research study were; (1) to conduct a benchmark uncertainty analysis of MOFAT using Random Sampling based Monte Carlo and to evaluate the applicability and performance of various uncertainty analysis techniques to MOFAT. The uncertainty analysis techniques evaluated were Random Sampling based Monte Carlo (RS-MC), Monte Carlo with Latin Hypercube sampling (LHS-MC), Monte Carlo using a Response Surface Methodology (RSM-MC) based replacement model and Monte Carlo using a Neural Network (NN-MC) based replacement model; (2) to develop the computational tools required to undertake an uncertainty analysis of MOFAT. These tools were a Monte Carlo version of MOFAT called MC-MOFAT, a pre processing tool to compile MC-MOFAT input files and a post processing tool to process MC-MOFAT output files; (3) to quantify the uncertainty in estimates of exposure due to variability in input parameters; (4) to evaluate the applicability and performance of various sensitivity analysis techniques to MOFAT; (5) to identify sensitive parameters and issues that need to be addressed when using MOFAT; (6) to use the information gained from the previous objectives to develop a framework for uncertainty and sensitivity analysis of MOFAT (7) to identify areas of additional research so that uncertainty in MOFAT estimates can be better understood and quantified.

This chapter presents the sixth objective. This chapter draws on the experiences acquired in conducting the uncertainty and sensitivity analysis of MOFAT, presented in Chapters 3 to 5, to formulate a framework designed specifically for undertaking an uncertainty and

sensitivity analysis of MOFAT. As illustrated in Figure 6.1, this is a six-step framework consisting of the following steps, which are discussed in further detail in Section 6.2:

Step 1: Specification of Parameter Uncertainty

This component of the framework provides guidance on which parameters to give particular attention to when specifying parameter uncertainty and in developing a field investigation program. It also provides guidance on how to use, for preliminary and planning level model runs and uncertainty analysis, Robert Carsel's database of soil properties to establish good approximations to empirical distributions for many soil parameters and to account for correlations between input parameters.

Step 2: Selecting an Uncertainty Analysis Method

This component of the framework provides guidance on which uncertainty analysis technique to use and the appropriate sample size to use.

Step 3: Generating Correlated Probabilistic Samples and Assembling Input Files

This component of the framework provides guidance on how to incorporate dependencies when generating probabilistic (LHS-MC or RS-MC) samples. It also provides guidance on assembling MOFAT input files from these samples using the pre-processing tool developed in this study.

Figure 6.1 A Framework for the Uncertainty and Sensitivity Analysis of MOFAT

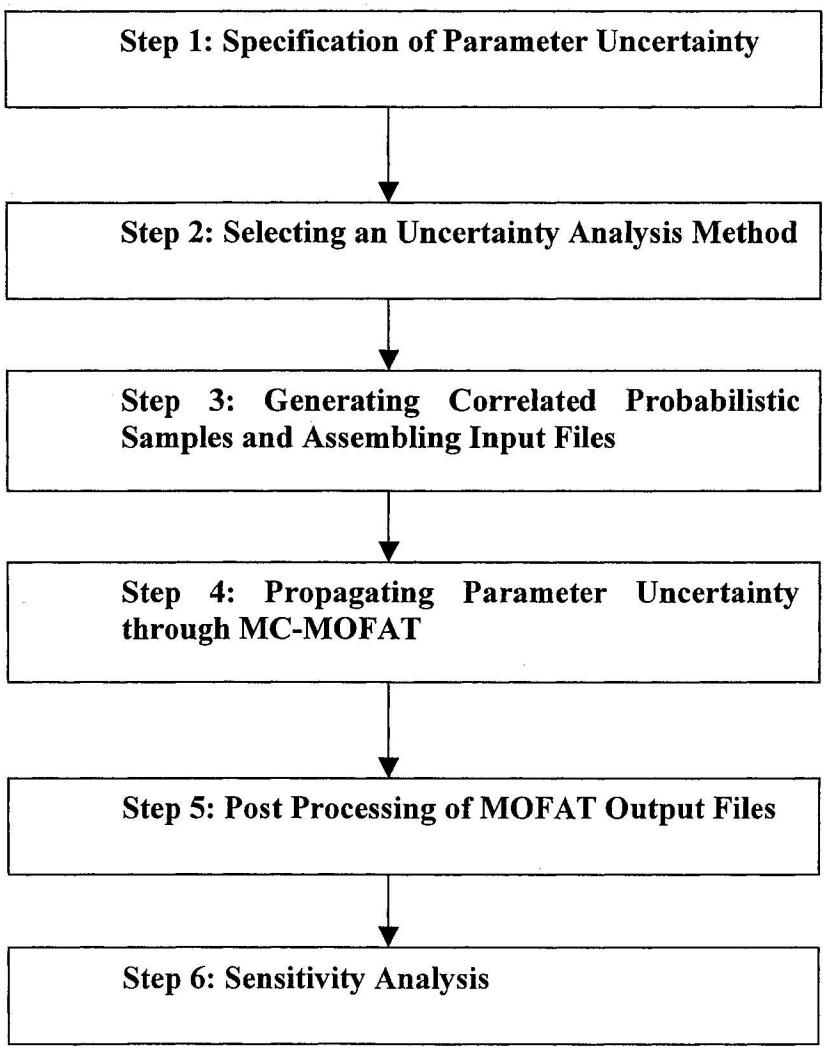

Step 4: Propagating Parameter Uncertainty through MC-MOFAT

This component of the framework provides guidance on the processing of the MOFAT input files using MC-MOFAT.

Step 5: Post Processing of MOFAT Output Files

This component of the framework provides guidance on the post processing of the MOFAT output files using the post-processing tool developed in this study.

Step 6: Sensitivity Analysis

This component of the framework provides guidance on how to conduct a sensitivity analysis of the uncertainty analysis results. For identifying important input parameters, it provides guidance on techniques for ranking and grouping input parameters.

The uncertainty analysis techniques (RS-MC, LHS-MC, RSM-MC, and NN-MC) that comprise the framework are not new but prior to this research study they had never been tested and benchmarked for MOFAT or for any multi-phase multi-component fate and transport model that could be used for Tier 3 RBCA of petroleum release sites. The need for this MOFAT specific framework arises from the discussion presented earlier in Section 1.1 and the literature review presented earlier in Section 2.4 where it was observed that for complex models like MOFAT the applicability and performance of various uncertainty analysis techniques is very model specific.

The framework not only lays out a methodology for uncertainty and sensitivity analysis for MOFAT that can be used by all users of MOFAT, it also provides the tools required to conduct such an analysis. Tools developed to support this methodology include a pre-processor to generate MOFAT input files, a MC version of MOFAT (MC-MOFAT) and a post processor to automatically extract results from a batch of MOFAT output files. The framework and supporting tools will for the first time enable MOFAT users to conduct comprehensive uncertainty and sensitivity analysis of their simulation scenarios. This will provide them with invaluable insight into the uncertainty associated with their simulations and will help them meet growing regulatory requirements for uncertainty and sensitivity analysis. It will also be invaluable in helping MOFAT users study the impact of various input parameters on their simulations and help them direct field resources to where they would most useful in reducing uncertainty in model outputs. For preliminary and planning level model runs and uncertainty analysis the framework also directs the modeler to a comprehensive database of soil properties and correlation coefficients. The use of this comprehensive soil database compiled from soil survey reports from 42 states in the United States to define parametric variability and correlations ensures that uncertainty in defining parameter variability and correlations is kept at a minimum.

The primary strength of the framework is that it is based on a comprehensive evaluation of uncertainty analysis techniques using a simulation scenario based on MOFAT's validation studies. This ensured that various sources of model uncertainty were kept at a minimum and that the uncertainty analysis was not carried for a site-specific problem.

The use of the comprehensive soil database mentioned in the previous paragraph also ensured that uncertainty in defining parameter variability was kept at a minimum. The framework provides detailed guidance on which uncertainty analysis technique best replicates the results of the benchmark uncertainty analysis technique RS-MC with greater efficiency. It also alerts the MOFAT user to problems associated with using any Replacement model based MC uncertainty analysis technique. It further provides guidance on the effect of various LHS sample sizes.

This framework was developed specifically for MOFAT but the steps in this framework may be used in developing a framework for other complex fate and transport models. This framework is also of direct use for further research and can be used to further extend the uncertainty and sensitivity analysis presented earlier in Chapter 4.

6.2 A Six Step Framework for Uncertainty and Sensitivity Analysis of MOFAT

While a brief outline of the framework and a discussion of its highlights have been presented in the previous section, a detailed description of the specific steps of the framework is presented in the following sections:

6.2.1 Step 1: Specification of Parameter Uncertainty

The first step of this six step framework is illustrated in Figure 6.2. In specifying parameter uncertainty and in developing a field investigation program it is very important to give particular attention to those parameters that were closely correlated to the outputs and those that were identified as being significant in the sensitivity analysis. Based on the results of this study, the model was most sensitive to the soil properties; saturated conductivity to water, K_{sw}, van Genuchten air-water capillary retention parameter, α, and van Genuchten air-water capillary retention parameter, n. The model also displayed a lesser degree of sensitivity to the apparent irreducible water saturation, S_m. These have been highlighted in Chapter 5.

Also fundamental to the use of Monte Carlo numerical simulations in the flow and solute transport area is the need to establish good approximations to empirical distributions for many soil parameters and to account for the correlation between input parameters. As discussed earlier in Section 3.6, the most comprehensive published source for specification of parameter uncertainty and correlations is a database of soil properties compiled by Robert Carsel of the U.S. EPA using SCS Soil Survey Information reports from 42 states. Consequently this is being sold as a commercial package SOILPARA.

Figure 6.2 Step 1 of Framework - Specification of Parameter Uncertainty

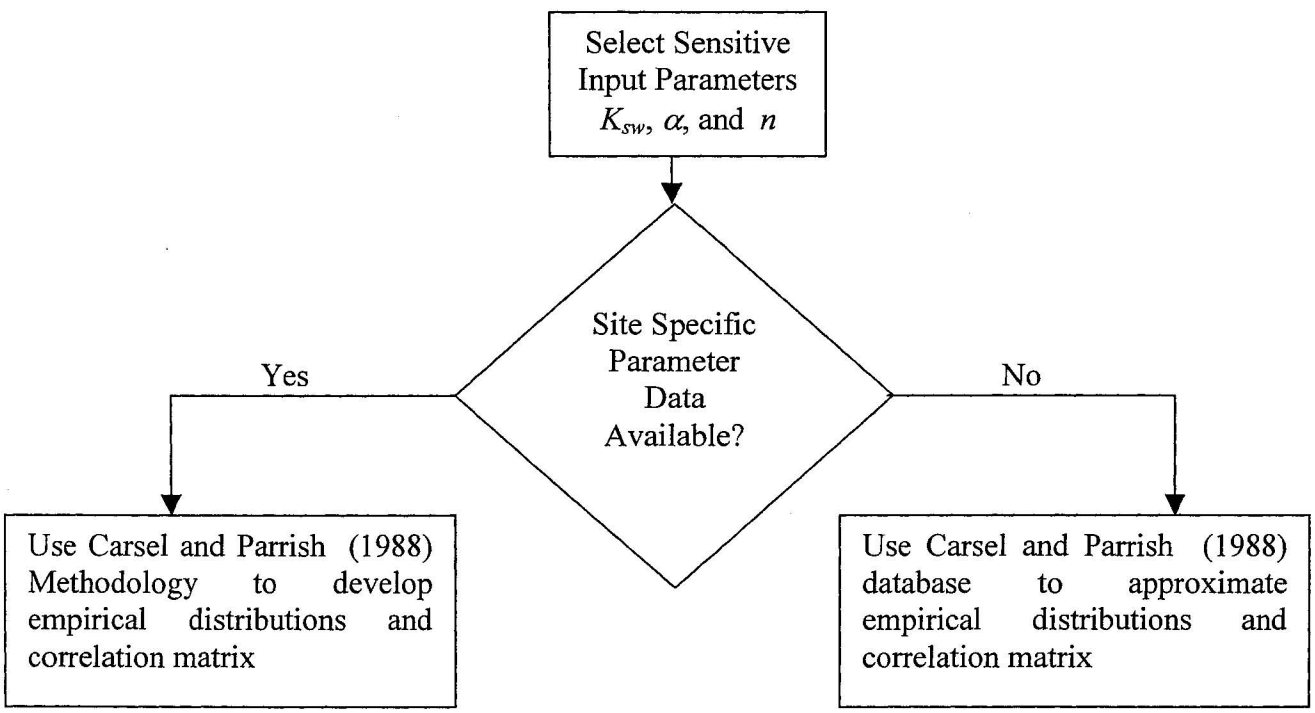

The distribution approximations and factored covariance matrices developed by Carsel and Parrish (1988) can be used directly for preliminary and planning level model runs and uncertainty analysis to gauge the sensitivity of the simulation scenario. The results can then be used to direct the field investigation and sampling program to focus on those parameters that would reduce uncertainty most.

Following an extensive field investigation and sampling program the approach used by Carsel and Parrish (1988) can be used to cross check and develop distribution approximations and obtain a site-specific covariance matrix. The SCS classification is widely used in soil survey reports across the world (including Canada) so the approach can be easily extended to other soil survey databases.

While a detailed description of Carsel and Parrish's approach can be found in their paper (Carsel and Parrish, 1988), the approach can be summarized as follows:

> Using Carsel's database to obtain bulk density, sand and clay contents for the 12 SCS textural classifications, Carsel and Parrish (1988) have estimated the covariance matrix for saturated hydraulic conductivity, residual water content and van Genuchten water retention parameters α and n for 12 different SCS soil textural classifications. The saturated water contents, the sand contents and the clay contents reported for each of the SCS classifications were used to compute saturated hydraulic conductivity and water retention parameters for the van

Genuchten model using a multiple regression equation developed by Rawls and Brakensiek (1985). This database of computed saturated hydraulic conductivity and van Genuchten water retention parameters for each of the 12 soil textural classifications was then used as the basis for characterization of probability distributions for these variables. Empirical *cdf* were derived for all of these variables and hypothesized distributions were fitted. Within each soil textural class, after Johnson family transformations to normal were selected and distributions were fitted for all variables, sample Pearson product-moment correlations and covariances were calculated for the transformed variables.

If Carsel and Parrish's approach is used to develop distribution approximations and obtain a site-specific covariance matrix, the approach can potentially be improved in two ways:

- Including porosity in the covariance matrices could strengthen the covariance matrices. Porosity is one of the fundamental soil characteristics that affects flow and solute transport in the soil. By its very nature porosity is generally correlated to other parameters such as saturated hydraulic conductivity and is a key source of uncertainty in groundwater modeling.

- The Carsel and Parrish approach could also be further improved if an attempt is made to use a transformation to normal that does not need the estimation of the

ranges of variation for each water retention parameter as was needed by the Johnson family of distribution. The estimation of the limits of variation, as needed in the Carsel and Parrish (1988) study, via initial screening and theoretical considerations is time consuming and is a possible source of error. The use of a normal transformation such as the Box-Cox transformation could potentially avert this problem.

6.2.2 Step 2: Selecting an Uncertainty Analysis Method

This step of the framework is illustrated in Figure 6.3. As demonstrated in Chapter 4 an uncertainty analysis of MOFAT can be accurately and efficiently conducted using LHS-MC. *Cdfs* of MOFAT outputs generated using LHS-MC were able to accurately converge with *cdfs* generated using the benchmark RS-MC. The efficiency of the LHS-MC sampling method over RS-MC has been demonstrated in this study. Model replacement techniques RSM and NN were evaluated in this study and were found not to be suitable for uncertainty analysis of MOFAT.

The Iman and Helton (1985) recommended LHS-MC sample size of 5*(number of variables) has been demonstrated in this study to accurately converge to the RS-MC *cdfs*. However, it has also been demonstrated in this study that a LHS-MC sample size that is approximately three times the recommended LHS-MC sample size of 5*(number of variables) displays a slightly higher degree of convergence to the RS-MC *cdfs*. A yet higher degree of convergence to the RS-MC *cdfs* is achieved by using an LHS-MC

Figure 6.3 Step 2 of Framework - Selecting an Uncertainty Analysis Method

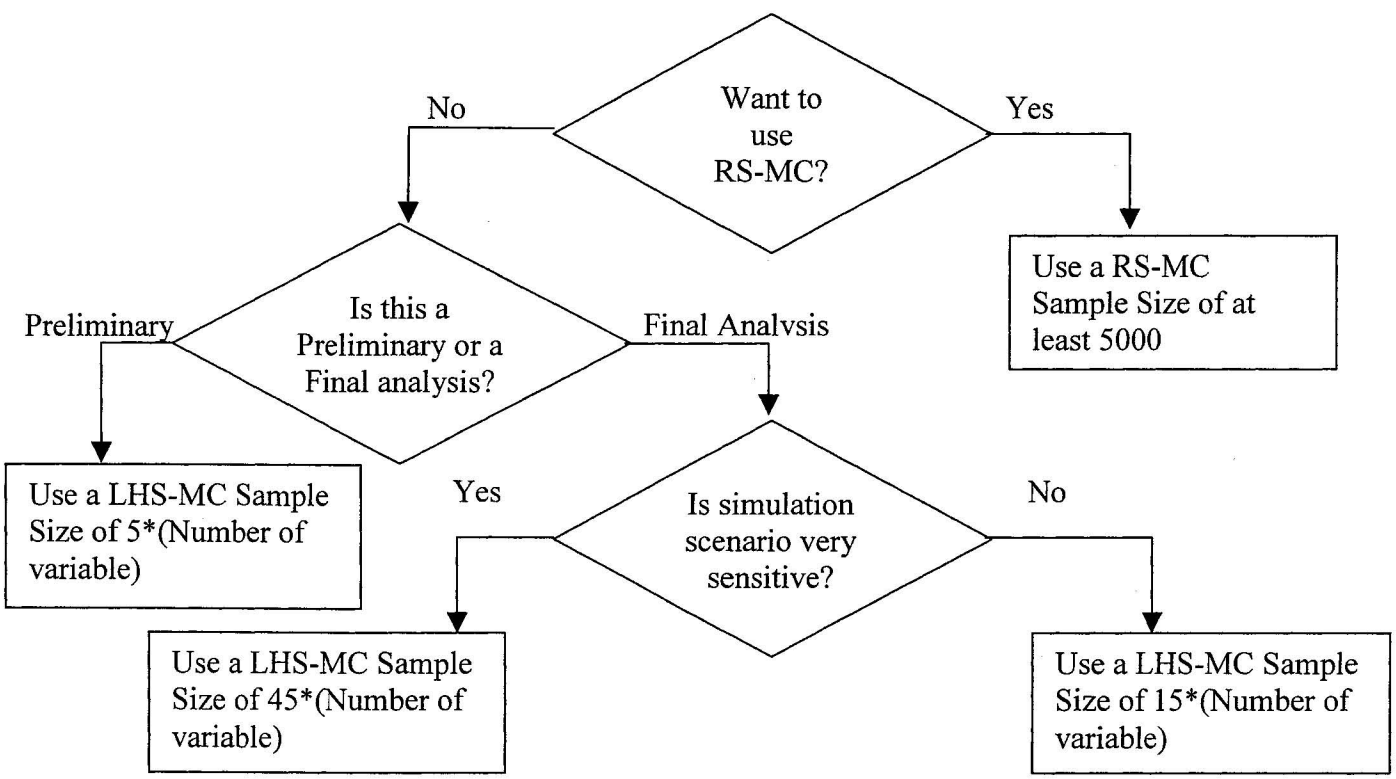

sample size of 45*(number of variables). However using an LHS-MC sample size greater than 45*(number of variables) does not result in any significant increase in convergence since the convergence of the 45*(number of variables) LHS-MC samples is already excellent.

Based on the results of this study the ideal LHS–MC sample size is one with 15*(number of variables) runs. However for preliminary or screening level uncertainty and sensitivity analysis it would be more efficient to use the smaller LHS-MC sample size of 5*(number of variables). For highly sensitivity scenarios an LHS-MC sample size equal to 45*(number of variables) may be used to ensure an excellent convergence to RS-MC outputs. The use of an LHS-MC sample size greater than 45*(number of variables) will not result in any significant additional gain in convergence.

If a RS-MC uncertainty analysis of MOFAT is to be conducted then a sample size of greater than 3000 random samples would be sufficient for convergence of the RS-MC outputs. However it is highly recommended that a sample size of at least 5000 be used. As described in section 4.2.2 the means and standard deviations for all components had converged after approximately 2500 simulations.

6.2.3 Step 3: Generating Correlated Probabilistic Samples and Assembling Input Files

This step of the framework is illustrated in Figure 6.4. A key component of generating probabilistic (LHS-MC or RS-MC) samples is accounting for dependencies between the probabilistic inputs. Typically analysts and modelers assume independence between variables that are mechanistically related for the sake of mathematical convenience and this makes the resulting risk assessments unreliable (Scott and Tucker, 2003). The Iman and Shortencarier (1984) FORTRAN LHS code is an excellent tool for accounting for dependencies and it does so by using a restricted pairing technique to generate rank correlated samples for LHS-MC and RS-MC simulations. Iman and Conover's restricted pairing technique has been explained in Chapter 3. The code has been configured for Unix and is available on the compact disc in Appendix B. If being compiled for a PC the results would need to be verified against the sample files provided by Iman and Shortencarier (1984).

Once LHS-MC (or RS-MC) samples have been generated, MOFAT input files have to be compiled for each sample. A FORTRAN program for automatically compiling MOFAT input files for the various LHS-MC (or RS-MC) samples was developed as a part of this study. The code is attached as Appendix B. This can be compiled in either a Unix or PC environment. Further details about the code are available in Appendix B.

Figure 6.4 Steps 3, 4 and 5 of Framework - Generating Correlated Probabilistic Samples and Assembling Input Files; Propagating Parameter Uncertainty through MC-MOFAT; and Post Processing of MOFAT Output Files

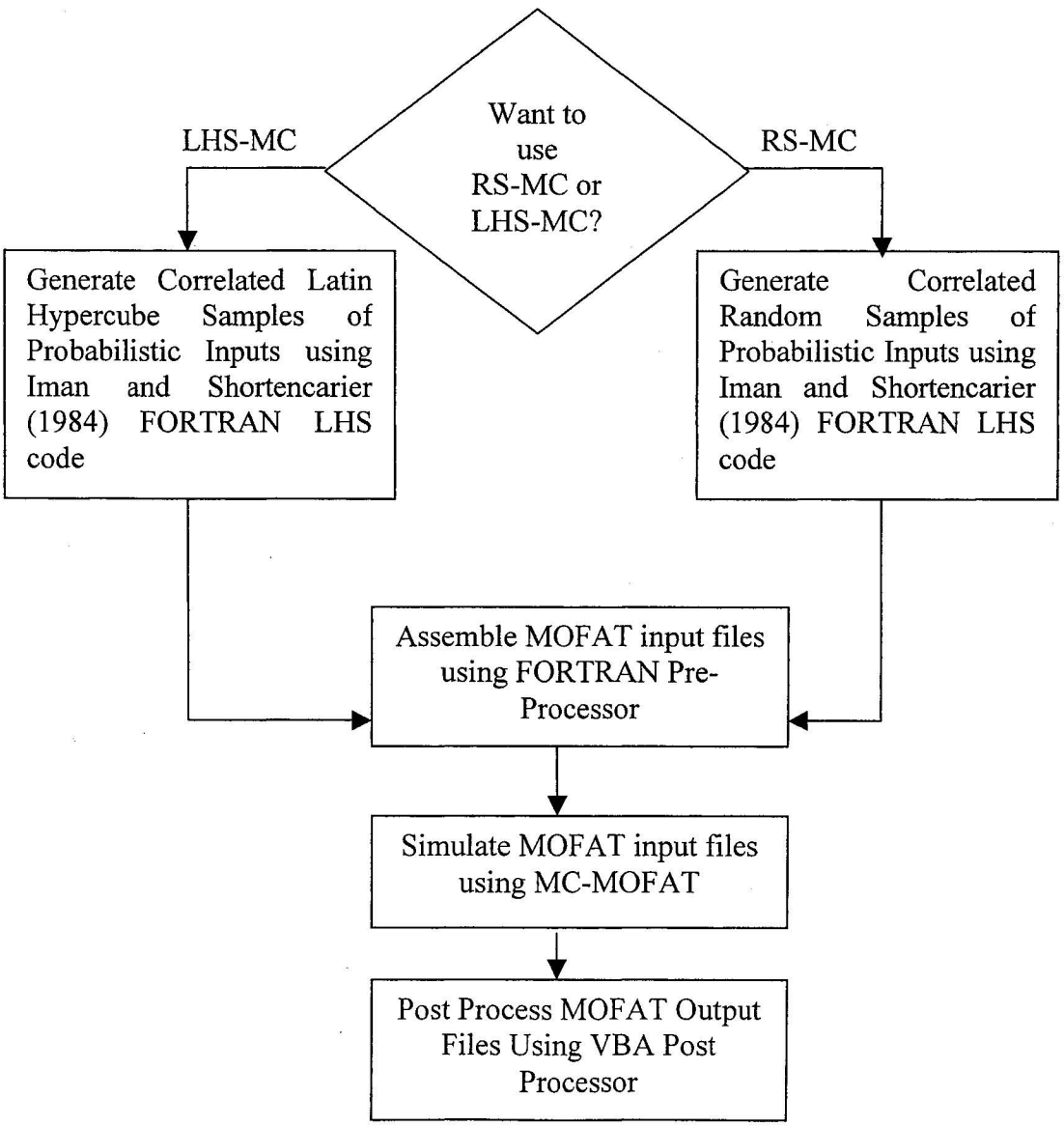

For dependencies between the probabilistic inputs it is best to acquire these from site-specific studies. In the absence of site-specific data, for preliminary and planning level uncertainty analysis, Carsel and Parrish (1988) provide an excellent source for these correlations. This is better than assuming independence between probabilistic inputs that are mechanistically related. As described in Section 3.6 and 6.2.1, Carsel and Parrish (1988) have estimated the covariance matrix for saturated hydraulic conductivity, residual water content and van Genuchten water retention parameters α and n for 12 different SCS soil textural classifications. The comprehensiveness of this soil database ensures that the uncertainty in defining dependencies between the probabilistic inputs parameter is kept at a minimum. To use Carsel and Parrish's covariance matrix, the initial fieldwork should be focused on identifying the SCS classifications of the soil media at the study site.

Where the contaminant travel path crosses different soil types probabilistic correlated samples of the soil properties would have to be generated for all soil types. MOFAT allows the user to designate a maximum of 10 soil types.

6.2.4 Step 4: Propagating Parameter Uncertainty through MC-MOFAT

This step of the framework is illustrated in Figure 6.4. For LHS-MC and RS-MC simulations it is necessary to have the ability to process input files through MOFAT as a batch. As a part of this study the MOFAT code was modified to allow batch input and is attached as MC-MOFAT in Appendix B. This allows the batch processing of specified

input files through MOFAT with the output directed to user-defined files. The modified code can be compiled in either a Unix or PC environment. Further details about the code are available in Appendix B.

6.2.5 Step 5: Post Processing of MOFAT Output Files

This step of the framework is illustrated in Figure 6.4. Post processing primarily involves extracting specific information from the output files to allow analysis of the information. MOFAT output files can be quite large and the manual extraction of data from these files is time consuming. As described in Section 3.8 an automated post-processing tool developed as part of this study sequentially copies from MOFAT output files the results for a specified time step and node number to a text file. This file can then be opened in any spreadsheet or statistical program for subsequent data analysis and plotting of *cdfs*. This tool is able to accurately extract the output results for 10,000 MOFAT input files in approximately a fortnight. If done manually this task would take months. The automated post-processing tool is attached in Appendix B.

6.2.6 Step 6: Sensitivity Analysis

This step of the framework is illustrated in Figure 6.5. As described in Chapter 5, MC procedure results are ideally suited for sensitivity studies. In uncertainty analysis the use of LHS-MC as a substitute for RS-MC also positively impacts the sensitivity analysis process. The smaller samples associated with LHS-MC simulation are better for identifying important input parameter as with the increasing sample sizes associated with

Figure 6.5 Step 6 of Framework - Sensitivity Analysis

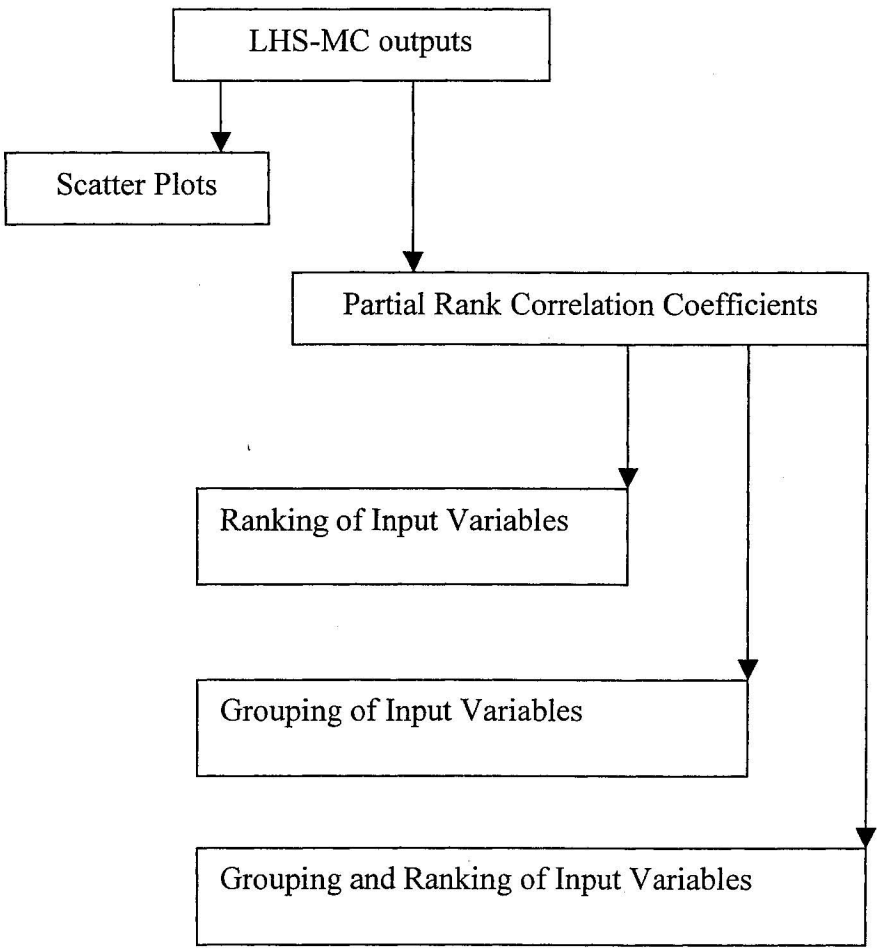

the RS-MC simulation there is a greater resolution of the effects associated with less important parameters (Kleijnen and Helton 1999a, 1999b).

In addition to scatter plots, for identifying important input parameters two techniques for ranking and grouping input parameters based on the Partial Rank Correlation Coefficient (PRCC) proposed by Iman and Helton (1985) and Kleijnen and Helton (1999a) respectively can be used directly with LHS-MC simulation results.

Iman and Helton's (1985) technique ranks the input parameters on the relative size of the absolute value of the PRCC. The absolute value of the PRCC is a quantification of the strength of the relationship between two parameters. The higher the absolute value of the PRCC the greater is the strength of the correlation between the input and output parameter. Since the importance of the input parameter increases as the strength of the correlation increases the absolute value of the PRCC is used to rank input parameters.

Kleijnen and Helton's (1999a) technique identifies important input variables by dividing the variables into groups on the basis of critical values of the PRCC test statistic. The critical values or p values are the probability that a larger coefficient value would occur owing to chance variation. This can used to group input parameters into those that appear to have a significant effect on predicted parameters and those that appear to have little or no effect.

A third technique that draws on the strengths of these two ranking and grouping techniques to collectively group and rank input parameters has been proposed and used in this study. This is a more relevant approach for identifying important input variables that first groups input parameters on the basis of the critical values of the PRCC and then within each group relatively ranks the input parameters based on the relative size of absolute value of the PRCC.

Chapter 7. Conclusions and Recommendations

7.1 Conclusions

To quantity parametric uncertainties, to address an area of increasing concern in the use of numerical models for Tier 3 RBCA of petroleum contaminated sites and to address a significant gap in the published literature, a comprehensive parametric uncertainty and sensitivity analysis of the multi-phase multi-component fate and transport model MOFAT was successfully accomplished in this research study. The research examined the applicability of various uncertainty and sensitivity analysis techniques to MOFAT and developed a comprehensive framework for the uncertainty and sensitivity analysis of MOFAT.

This uncertainty analysis of MOFAT provides a quantification of output variability over a whole range of possible inputs. It allows confidence limits to be placed on the output results and this helps place the results of MOFAT in correct perspective. The sensitivity analysis improves the understanding of which parameters are most important for reducing

uncertainty in the simulation results. This pinpoints the priorities for obtaining new information and helps devise more appropriate field sampling programs.

A distinguishing feature of this research study is that it is extensive in its scope in terms of the number of input parameters that have been reviewed in it. Most published groundwater studies have concentrated primarily on the variability of hydraulic conductivity while this study examined the variability of seven soil parameters.

Undertaking an uncertainty analysis simulation study is as complex and intricate as any field or laboratory study and requires careful planning and implementation. To ensure that the objectives of this research study were met a comprehensive uncertainty analysis study was formulated and implemented. The tools required to undertake this study were also developed. The original FORTRAN code for MOFAT was modified as MC-MOFAT to allow compilation of the MOFAT model to accept batch inputs, a feature that is needed to undertake MC analysis of the model. A pre-processing FORTRAN tool was developed to allow automated generation of MOFAT input files from a text file listing all MC samples. A VBA based post-processing tool was also developed to automatically extract the results for a specified step and time step from MOFAT output files. In this study, the machine constants in the original VAX11/780 based LHS sub routines have been adjusted to run in an Unix operating environment.

The governing equations of MOFAT were used to identify seven input parameters subject to variability. These were the soil properties; saturated conductivity to water in the vertical direction *($K\ sw_z$);* saturated conductivity to water in the horizontal direction (*$K\ sw_x$);* soil porosity (ϕ); apparent irreducible water saturation (S_m); maximum residual oil saturation for water (S_{or}); van Genuchten air-water capillary retention parameter (α); and van Genuchten air-water capillary retention parameter (*n).* These were modeled as probabilistic inputs to propagate the effect of parameter variability through MOFAT. For these parameters, with the intent of minimizing parameter uncertainty, a comprehensive input parameter database was used to define parameter variability and correlations. Similarly to minimize scenario and model uncertainty an innovative site scenario based on sites scenarios used in the MOFAT validation studies was developed. The governing equations of MOFAT, input parameter database, simulation scenario, simulation setup and tools are presented in Chapter 3.

The applicability of various uncertainty analysis techniques for the uncertainty analysis of MOFAT was evaluated in this research. The complexity of MOFAT restricted the techniques that could be used to "simulation based" uncertainty analysis techniques. In addition to the benchmark Random Sampling Monte Carlo (RS-MC) technique, stratified sampling based and model replacement based techniques (Monte Carlo using Latin Hypercube sampling (LHS-MC), Monte Carlo using a Response Surface Methodology (RSM-MC) based replacement model and Monte Carlo using a Neural Network (NN-MC) based replacement model) were evaluated to test their efficiency and accuracy

against the benchmark RS-MC technique, which in itself required two years to execute. The effect of using different LHS sample sizes was also evaluated through the use of four different LHS samples of 35, 100, 300 and 500 respectively.

Cumulative density function (*cdf*) plots were used to assess the accuracy with which the uncertainty analysis techniques being evaluated were able to replicate the results of the benchmark RS-MC analysis. RS-MC and LHS-MC outputs were used to generate cumulative density function (*cdf*) plots for all 12 MOFAT outputs, which are the BTEX concentrations in the water, gas and solid phases. These *cdfs* have been presented in Chapter 4.

All four LHS-MC sample sizes were able to accurately replicate the *cdfs* generated by 10,000 RS-MC samples and thus LHS-MC analysis can be used as an accurate and extremely efficient (35 versus 10,000 samples) substitute for RS-MC uncertainty analysis of MOFAT. For higher cumulative probabilities the *cdfs* generated using the 100 sample LHS were more accurate than the *cdfs* generated using the smaller 35 sample LHS. Using a 300 sample LHS produces *cdfs* that display a much higher degree of convergence to the RS-MC *cdfs* than the 100 sample LHS *cdfs*. The use of a yet larger LHS sample size (such as the LHS sample size of 500 used in this study) over the LHS sample size of 300 does not provide any appreciable increase in convergence as the *cdfs* produced using a 300 sample LHS are already very similar to the RS-MC *cdfs*. The RSM and NN replacement models were not able to accurately and efficiently replace MOFAT for the

purpose of uncertainty analysis. RSM replacement models are not suitable for MOFAT as the factorial design is not able to accommodate the correlations between input parameters. Similarly NN replacement models are not efficient in replicating the results of RS-MC.

An extensive sensitivity analysis of MOFAT was also accomplished and is presented in Chapter 5. The use of LHS-MC as a substitute for RS-MC in uncertainty analysis positively impacts the sensitivity analysis process since the smaller samples associated with LHS-MC simulation are better for identifying important variables than the larger sample sizes associated with the RS-MC simulation.

Sensitive parameters were identified through the application of sampling based statistical measures on the set of LHS inputs and outputs. Scatter plots of each of the twelve MOFAT outputs versus the probabilistic input parameters indicated that all the outputs displayed a monotonic dependence on the inputs K_{sw}, α, and n. A slight dependence between all the outputs and the input S_m was also apparent. Since correlation is a quantification of the strength of the relationship between two variables, dependencies between input parameters and MOFAT outputs were also evaluated using four different measures of correlation (Pearson's r, Spearman's ρ, Partial Correlation Coefficient and Partial Rank Correlation Coefficient). While all the tests do not always concur, in general all the outputs are correlated with K_{sw}, α, n and to a lesser degree S_m. The variation in correlations as detected by the four different tests is a function of the different testing

powers of the tests, the complexity of MOFAT and the correlations between the probabilistic input parameters (where K_{sw} is positively correlated with S_m, α and n.)

As a part of the sensitivity analysis, the RSM models developed earlier for uncertainty analysis were used to provide valuable information on the interactions between the input parameters. As presented in Section 4.4.4, for all phases of the BTEX components there are interactions between K_{sw} and ϕ and between ϕ and α. The interaction between K_{sw} and α is significant for the gas phases of Benzene and Toluene and all phases of Ethyl-benzene and Xylene.

To assign priorities to the input variables for reducing uncertainties, the input variables were ranked on the relative size of the absolute value of the Partial Rank Correlation Coefficients (PRCC). They were also grouped into three categories of decreasing significance based on critical values of the PRCC analysis. Additionally, using a new approach developed in this study the input variables were first grouped into four groups on the basis of the critical values of the PRCC and then within each group they were relatively ranked based on the relative size of absolute value of the PRCC. The higher ranked inputs within the lower critical value groups will have the most influence on the calibration and predictions and should be the focus of field investigation and calibration efforts. The ranking and categorizations are presented in Chapter 5.

Drawing on the results of Chapter 3, 4 and 5 a comprehensive six-step framework for uncertainty and sensitivity analysis of MOFAT was developed and has been presented in Chapter 6. The six steps are:

Step 1: Specification of Parameter Uncertainty

Step 2: Selecting an Uncertainty Analysis Method

Step 3: Generating Correlated Probabilistic Samples and Assembling Input Files

Step 4: Propagating Parameter Uncertainty through MC-MOFAT

Step 5: Post Processing of MOFAT Output Files

Step 6: Sensitivity Analysis

The need for this MOFAT specific framework arises from the fact that for complex models like MOFAT the applicability and performance of various uncertainty analysis techniques is very model specific. A distinguishing feature of this framework is that not only does it lay out a methodology for uncertainty and sensitivity analysis for MOFAT but it also provides the tools required to conduct such an analysis. The framework and supporting tools developed will be very enabling for MOFAT users and will allow them to conduct comprehensive parametric uncertainty and sensitivity analysis of their simulation scenarios. This will provide them with better quantification of parametric uncertainties, with invaluable insight into the uncertainty associated with their simulations, and will help them meet growing regulatory requirements for uncertainty and sensitivity analysis. The framework developed is specific to MOFAT but can be

applied as a starting point for developing similar frameworks for other computationally demanding models.

7.2 Recommendations

The research presented in this research study is an important first step in filling the existing gap in the body of knowledge. The completion of this study and the tools developed in this study are important for undertaking further research on parametric uncertainties. The following recommendations with respect to further research are drawn from the experiences gained in executing this study:

7.2.1 Improvements to Input Covariance Matrix

As recommended in Section 6.1 including porosity in the input covariance matrices could strengthen the covariance matrices used to incorporate correlation between input parameters.

The Carsel and Parrish (1988) covariance matrices could be further improved if an attempt is made to use a transformation to obtain a normal distribution that does not need the estimation of the ranges of variation for each water retention parameter as was needed by the Johnson family of distributions[1].

[1] An attempt was made to implement this recommendation prior to the start of this research and R. F Carsel was contacted to obtain a copy of the soil database used to derive the covariance matrices. Unfortunately the database could not be located

7.2.2 Incorporation of Component Properties as Probabilistic Inputs

While the primary contributors to parameter variability are the soil properties, the variability of component properties should be researched further. This will help to better quantify and understand the contribution of the transport component input parameters to the uncertainty of MOFAT

Some of the components properties (such as the adsorption coefficients) are dependent on site-specific factors such as the organic mass fraction in the soil. This should be taken into account when planning the parametric study.

7.2.3 Applicability of SRSM-ADIFOR

An uncertainty technique that has been recently used for the uncertainty analysis of transport-transformation models is Stochastic Response Surface Method (SRSM). SRSM approximates uncertainties in model outputs through a series expansion in normal random variable. The unknown coefficients in the series expansions are calculated using a limited number of model simulations (Isukapalli, 1999; Isukapalli et. al., 2004). Further computational efficiency can be achieved by coupling the SRSM with Automatic DIfferentiation of FORtran (ADIFOR). ADIFOR is a computer algebra based method that reads the FORTRAN source code of a transport-transformation model and constructs the code that calculates first order partial derivatives of model outputs with respect to model inputs (Isukapalli, 1999; Isukapalli et. al., 2004).

Since MOFAT is implemented in a FORTRAN code this technique might be applicable and its efficiency and accuracy in comparison to LHS-MC should be researched further.

7.2.4 Study of Interactions

As presented in Section 4.4.4, for all phases of the BTEX components there are interactions between K_{sw} and ϕ and between ϕ and α. The interaction between K_{sw} and α is significant for the gas phases of Benzene and Toluene and all phases of Ethyl-benzene and Xylene.

An attempt to discuss the physical significance of these interactions was made in section in Section 5.2.3, but the physical significance of the negative interaction between ϕ and α and the positive interaction between K_{sw} and α, could not be analyzed due to the complexity of the governing equations of MOFAT. These interactions need to be researched further to understand these interactions and their physical significance.

7.2.5 Extension to Other Tier 3 RBCA Models

The parametric uncertainty analysis presented in this study should be extended to other multi-phase and multi-component fate and transport models that are being used in the Tier 3 RBCA of petroleum release sites. Candidate models for extending this study are MODFLOW coupled with RT3D and the TOUGH code TMVOC.

If the same simulation scenario, soil parameter database and assumptions are used for the parametric uncertainty studies with MODFLOW coupled with RT3D and the TOUGH code TMVOC, then these parametric uncertainty studies can be used as the basis for comparing these numerical models with MOFAT from the perspective of parametric uncertainty.

7.2.6 Scaling Up of Input Parameters and Uncertainty Analysis

This study has not looked at how scaling up of input parameters in the use of numerical models contributes to model output uncertainty. The effect of scaling up in the context of uncertainty analysis of MOFAT should be researched further.

The research could be planned by adapting the approach adopted by Wang and Bright (2004) to study the effect of small scale spatial variability of aquifer hydraulic conductivity on solute transport. They compared point concentrations from fine grid Monte Carlo simulations of a synthetic heterogeneous aquifer (representing actual soil heterogeneity) to those from coarse grid deterministic simulations of an equivalent homogeneous aquifer (representing numerical scaling up and deterministic modeling). For an uncertainty analysis of scaling up the coarse grid simulations would also be Monte Carlo based.

Chapter 8. Statement of Originality

Originality of the work presented in this research study can be viewed from the following accounts:

1. To allow for better quantification of parametric uncertainties, a comprehensive parametric uncertainty study on a complex Tier 3 RBCA multi-phase and multi-component fate and transport model has been undertaken in this research. This includes:

    a. a benchmark uncertainty analysis of MOFAT using Random Sampling based Monte Carlo.
    b. an uncertainty analysis of MOFAT using Latin Hypercube Sampling based Monte Carlo. The effect of LHS sample size was also simulated.

    No similar quantification of parametric uncertainties has been found in published literature. The tools used in this uncertainty study are not new but it is the first

comparative application of these tools to a complex multi-phase and multi-component petroleum release fate and transport model.

2. To identify sensitive parameters and to help prioritize input parameters for uncertainty analysis, a sensitivity study on a complex multi-phase and multi-component fate and transport finite element model that is used in the Tier 3 RBCA process has been undertaken in this study. No similar sensitivity study has been found in published literature. To prioritize input parameters for uncertainty analysis a new technique for grouping and ranking input parameters has been developed as a part of this study.

3. To provide guidance on how to undertake a parametric uncertainty and sensitivity analysis of MOFAT, a comprehensive framework has been developed in this study. No similar framework has been found in published literature.

4. In the course of undertaking this study a MC version of MOFAT was developed by modifying the FORTRAN code for MOFAT to allow batch processing. A set of pre and post processing tools were also developed as a part of this research. A FORTRAN pre-processing tool has been developed to allow automated generation of MOFAT input files from a text file listing all MC or LHS samples. A VBA based post-processing tool was also developed to automatically extract the results for a specified step and time step from MOFAT output files. These

tools had to be developed, as they were not found in literature. The MC version of MOFAT and the pre and post processing tools developed in this study are invaluable aids for MOFAT users wishing to undertake uncertainty and sensitivity analysis of their simulation scenarios.

5. To achieve better and more efficient quantification of parametric uncertainties, an attempt was made to replace a complex multi-phase and multi-component fate and transport model by a response surface model for the purpose of uncertainty analysis. No such application has been found in literature. The attempt to replace MOFAT by a response surface model successfully demonstrated that due to the correlated nature of MOFAT inputs and the non-linear behavior of MOFAT, MOFAT cannot be accurately replaced by a response surface model for the purpose of uncertainty analysis.

6. To achieve better and more efficient quantification of parametric uncertainties, an attempt was made to replace a complex multi-phase and multi-component fate and transport model by a neural network model for the purpose of uncertainty analysis. No such application has been found in literature. The attempt to replace MOFAT by a neural network model successfully demonstrated that due to the non-linear behavior of MOFAT, MOFAT cannot be efficiently (especially when compared to the efficiency of Latin Hypercube Sampling based Monte Carlo) replaced by a neural network model for the purpose of uncertainty analysis.

7. This is the first known study on MOFAT that has attempted to identify areas of additional research from the perspective of uncertainty so that uncertainty in MOFAT estimates can be better quantified.

8. This is the only known uncertainty analysis of a numerical fate and transport finite element model to study the effect of variability in seven soil properties while preserving their correlation structure. Studies on sensitive parameters are unfortunately limited in scope and most of the sensitivity studies reported in literature mainly concentrate on hydraulic conductivity. Amongst the various groundwater researchers who have studied the sensitivity of hydraulic conductivity and have modeled the hydraulic conductivity as input subject to uncertainty are Medina et al. (1989), Ahlfeld (1991), McLaughlin et al. (1993), and Huang and Mayer (1996). This is because, as stated by Freeze et al. (1990), in most advective transport analyses the input parameter with the largest uncertainty is the hydraulic conductivity.

References

Ahlfeld, D. 1991. Reliability of Model Prediction for Pump and Treat Strategies, Proceedings of Water Resources Planning and Management and Urban Water Resources, ASCE, NY, pp. 847-851.

Anderson, M.P., and W.W. Woessner. 1992. Applied Groundwater Modeling: Simulation of Flow and Advective Transport, Academic Press, San Diego, 381pp.

ASTM. 1995. Standard Guide for Risk Based Corrective Action Applied at Petroleum Release Sites, ASTM E 1739-95.

ASTM. 1998. RBCA Fate and Transport Models: Compendium and Selection Guidance. American Society for Testing and Materials, PA.

Baehr, A. L. 1987. Selective Transport of Hydrocarbons in the Unsaturated Zone due to Aqueous and Vapor Phase Partitioning, Water Resources Research, Vol. 23, No. 10, pp.1926-1938.

Bear, J. 1972. Dynamics of Fluids in Porous Media. American Elsevier publishing company Inc., New York.

Box, G.E.P., and K.G. Wilson. 1951. On Experimental Attainment of Optimum Conditions, Journal of the Royal Statistical Society, B, Vol. 13, pp. 1-45.

Brewer, K., T. Fogle, A. Stieve, and C. Barr. 2003. Uncertainty Analysis with Specific Groundwater Models: Experiences and Observations, ERD-EN-2003-0126, July 15, 2003, U.S. Department of Energy, Office of Scientific and Technical Information, TN, 6 pp.

Bright, J., F. Wang, and M. Close. 2002. Influence of the Amount of Available K Data on Uncertainty About Contaminant Transport Prediction, Ground Water, Vol. 40, No. 5, pp. 529-534.

Burmaster, D.E., and J.H. Lehr. 1991. It's Time to Make Risk Assessments Science, Groundwater Monit. Rev., X Summer Issue.

Campolongo, F., A. Saltelli, T. Sorenson, and S. Tarantola. 2000. Hitchhiker's Guide to Sensitivity Analysis. In *Sensitivity Analysis* (Saltelli, A., Chan, K., Scott, E.M., eds.), John Wiley & Sons: West Sussex, England, pp. 15-47.

Carsel, R. F., and R. S. Parrish. 1988. Developing Joint Probability Distributions of Soil Water Retention Characteristics, Water Resources Research, Vol. 24, No. 5, pp.755-769.

Carsel, R.F., R.S. Parrish, R.L. Jones, J.L. Hansen, and R.L. Lamb. 1988. Characterizing the Uncertainty of Pesticide Leaching in Agricultural Soils. Journal of Contaminant Hydrology, Vol. 2, No. 2, pp. 111-124.

Cawlfield, J. D. 2000. Reliability Algorithms: FORM and SORM Methods. In *Sensitivity Analysis* (Saltelli, A., Chan, K., Scott, E.M., eds.), John Wiley & Sons: West Sussex, England, pp. 155-165.

Chan, K., S. Tarantola, A. Saltelli, and I. M. Sobol. 2000. Variance Based Methods. In *Sensitivity Analysis* (Saltelli, A., Chan, K., Scott, E.M., eds.), John Wiley & Sons: West Sussex, England, pp. 167-197.

Clark, K. E., and M. G. Richardson. 1998. Fate and Exposure Models: Selecting the Appropriate Model for a Specific Application- Introduction, Journal of Soil Contamination, Vol. 7, No. 3, pp. 267-274.

Connor, J. A., J.P. Nevin, M. Malander, C. Stanley, and G. DeVaull. 1996. Tier 2 RBCA Guidance Manual for Risk-Based Corrective Action, Groundwater Services, Inc., Houston, Texas.

Cox, D. C., and P. Baybutt. 1981. Methods for Uncertainty Analysis: A Comparative Survey, Risk Analysis, Vol. 1, No. 4.

Dobermann, A., P. Goovaerts, and H.U. Neue. 1997. Scale-Dependent Correlations Among Soil Properties In Two Tropical Lowland Rice Fields, Soil Science Society of America Journal, Vol. 61, No. 5.

Fetter, C. W. 1992. Contaminant Hydrogeology, Macmillan Publishing Company, New York, New York.

Finkel, A.M. 1990. Confronting Uncertainty in Risk Management: A Guide for Decision-Makers, Center for Risk Management, Resources for the Future, Washington, DC.

Finkel, A.M. 1994. Stepping Out of Your Own Shadow: A Didactic Example of How Facing Uncertainty Can Improve Decision-Making, Risk Analysis, Vol. 14, pp. 751-761.

Finley B., V. Lau, and D. Paustenbach. 1992. Using an Uncertainty Analysis of Direct and Indirect Exposure to Contaminated Groundwater to Evaluate EPA's MCL and Health-Based Cleanup Goals, Journal of Hazardous Materials, Vol. 32, pp. 263-274.

Freeze, R. A., J. Massmann, L. Smith, T. Sperling, and B. James. 1990. Hydrogeological Decision Analysis 1. A Framework, Ground Water, Vol. 28, No. 5, pp. 739-766.

Goodrich, M. T., and J. T. McCord. 1995. Quantification of Uncertainty in Exposure Assessments at Hazardous Waste Sites, Ground Water, Vol. 33, No. 5, pp. 727-732.

Hamby, D. M. 1994. A Review of Techniques for Parameter Sensitivity Analysis of Environmental Models, Environmental Monitoring and Assessment, Vol. 32, pp. 135-154.

Hamed, M. M., and P. B. Bedient. 1997. On the Performance of Computational Methods for the Assessment of Risk from Ground-water Contamination, Ground Water, Vol. 35, No. 4, pp. 639-646.

Harter, T. 1998. Uncertainty and Risk Analysis of Contaminant Transport, California Water Resources Center Report, Vol. 95, University of California, Davis, pp. 97-107.

Hassan, A.E., and K. H. Hamed. 2001. Prediction of Plume Migration in Heterogeneous Media using Artificial Neural Networks, Water Resources Research, Vol. 37, No. 3, pp. 605-623.

Helton, J.C., and F.J. Davis. 2000. Sampling Based Methods. In *Sensitivity Analysis* (Saltelli, A., Chan, K., Scott, E.M., eds.), John Wiley & Sons: West Sussex, England, pp. 101-153.

Helton, J.C., and F.J. Davis. 2002. Illustration of Sampling Based Methods for Uncertainty and Sensitivity Analysis, Risk Analysis, Vol. 22, No. 3, pp. 591-622.

Helton, J.C., and F.J. Davis. 2003. Latin Hypercube Sampling and the Propagation of Uncertainty in Analyses of Complex Systems, Reliability Engineering and System Safety, Vol. 81, No. 1, pp. 23-69.

Helweg, O. J. 1992. Migration of Spilled Oil from Ruptured Underground Crude Oil Pipelines in the Memphis area, in proceedings of Lifeline Earthquake Engineering in the Central and Eastern US Conference, Nov 1992, n TCLEE5, pp. 140-152.

Hillier, F.S., and G.J. Lieberman. 1990. Introduction to Operation Research, 5th edition. McGraw-Hill, New York.

Hiramatsu, K., E. Ichion, T. Kawachi, and J. Takeuchi. 2001. ANN and GA Methods to Identify the Non-Point Contamination Flux to Groundwater, Progress in Water Resources, First International Conference on Water Resources Management, Sept. 24-26, Haldiki, Greece, pp. 291-299.

Huang, C., and A.S. Meyer. 1996. The Role of Uncertainty in the Optimization of Groundwater Remediation Systems, 11th International Conference on Computational Methods in Water Resources. Southampton, pp. 359-366.

Huyakorn, P. S., and Nikuha. 1979. Solution of Transient Transport Equation using an Upstream Finite Element Scheme, Applied Math. Modeling, Vol. 3, pp. 7-17.

Iman, R. L., and W.J. Conover. 1982. A Distribution Free Approach to Inducing Rank Correlations among Input Variables, Communications in Statistics, B11(3), pp. 311-334.

Iman, R. L., and M.J. Shortencarier. 1984. A FORTRAN 77 program and User's Guide for the Generation of Latin Hypercube and Random Samples for Use with Computer Models, Technical Report SAND83-2365. Sandia National Laboratories. NUREG/CR-3624.

Iman, R. L., and J. C. Helton. 1985. A Comparison of Uncertainty and Sensitivity Analysis Techniques for Computer Models, Technical Report SAND84-1461. Sandia National Laboratories. NUREG/CR-3904.

Iman R. L., and J. C. Helton. 1988. An investigation of Uncertainty and Sensitivity Analysis Techniques for Computer Models, Risk Analysis, Vol. 8, No.1.

Isukapalli, S. S. 1999. Uncertainty Analysis of Transport-Transformation Models. Ph.D. Thesis, The State University of New Jersey.

Isukapalli, S. S., S. Balakrishnana, and P. G. Georgopoulos. 2004. Computationally Efficient Uncertainty Propagation and Reduction using the Stochastic Response Surface Method, Proceedings of the 2004 43rd IEEE Conference on Decision and Control, December 14-17, 2004, Bahamas, Vol. 2, pp. 2237-2243.

Johnson, D. W., and J. D. Marx. 2003. The Importance of Multiphase and Multicomponent Modeling in Consequence and Risk Analysis, Journal of Hazardous Materials, Vol. 104, No. 1-3, pp. 51-64.

Kaluarachchi, J.J., and J.C. Parker. 1989. An Efficient Finite Element Method for Modeling Multiphase Flow in Porous Media, Water Resources Research. Vol. 25, pp. 43-54.

Kaluarachchi, J.J., and J.C. Parker. 1990. Modeling Multi-Component Organic Chemical Transport in Three Fluid Phase Porous Media, Journal of Contaminant Hydrology, Vol. 5, pp. 349-374.

Kaluarachchi, J.J., and J.C. Parker. 1992. Multiphase Flow with a Simplified Model for Oil Entrapment, Transport in Porous Media, Vol. 7, No. 1, pp. 1-14.

Katyal, A.K., J.J. Kaluarachchi, and J.C. Parker. 1991. MOFAT: A Two Dimensional Finite Element Program for Multi-phase Flow and Multi-component Transport, Program Documentation and User's Guide, Robert S. Kerr Environmental research Laboratory, Office of Research and Development, U.S. EPA, Ada, Oklahoma.EPA-600-2-91-020.

Keenan, R. E., B.L. Finley, and P.S. Price. 1994. Exposure assessment: Then, Now, and Quantum Leaps in the Future. Risk Analysis, Vol. 14, No. 3, pp. 225-230.

Kleijnen, J.P.C., and J.C. Helton. 1999a. Statistical Analysis of Scatterplots to Identify Important Factors in Large-Scale Simulations, 1: Review and Comparison of Techniques, Reliability Engineering and System Safety, Vol. 65, pp. 147-185.

Kleijnen, J.P.C., and J.C. Helton. 1999b. Statistical Analysis of Scatterplots to Identify Important Factors in Large-Scale Simulations, 2: Robustness of Techniques, Reliability Engineering and System Safety, Vol. 65, pp. 187-197.

Konikow, L.F., and J.D. Bredehoeft. 1992. Ground-Water Models Cannot Be Validated, Advances in Water Resources, Vol. 19, pp.75-83.

Krom, T.D., and D. Rosbjerg. 2000. Artificial neural networks: Development and Application in Groundwater pollution Remediation Design, Proceedings of ModelCARE'99 Conference, Sept. 20 –23, IAHS publication No. 265, pp. 34-40.

Land, C. S. 1968. Calculation of Imbibition Relative Permeability for Two and Three Phase Flow from Rock Properties, Trans. Am. Inst. Min. Metall. Pet. Eng., Vol. 243, pp. 149-156.

Lenhard R. J., M. Oostrom, and M.D. White. 1995. Modeling Fluid Flow and Transport in Variably Saturated Porous Media with the STOMP Simulator. 2. Verification and Validation, Advances in Water Resources, Vol. 18, No. 6, pp. 356-373.

Lenhard, R. J., J.C. Parker, and J.J. Kaluarachchi. 1988. Measurement and Simulation of One-Dimensional Transient Three-Phase Flow for Monotonic Liquid Drainage, Water Resources Research, Vol. 24, pp. 853-863.

Levy, J., 1993. A Field and Modeling Study of Atrazine Transport and Fate in Ground Water. Ph.D. Thesis, University of Wisconsin-Madison, Madison, WI, 561pp.

Lu, Z., and D. Zhang. 2003. On Importance Sampling Monte Carlo Approach to Uncertainty Analysis for Flow and Transport in Porous Media, Advances in Water Resources, Vol. 26, No. 11, pp. 1177-1188.

Maxim, L.D. 1989. Problems Associated with the Use of Conservative Assumptions in Exposure and Risk Analyis. in; D.J. Paustenbach (Ed.), The Risk Assessment of Environment and Human Health Hazards: A Textbook of Case Studies. Wiley. New York. Chapter 4.

McGrath, E.J., and D.C. Irving. 1975. Techniques for Efficient Monte Carlo Simulation Volume III: Variance Reduction, SAI-72-590-LJ, Oak Ridge National Laboratory, Tennessee.

McKay, M.D., Conover, W.J., and R.J. Beckman. 1979. A comparison of Three Methods for Selecting values of Input Variables in the Analysis of Output from a Computer Code, Technometrics, Vol. 21, No. 2, pp. 239-245.

McKone, T.E., and K. T. Bogen. 1991. Predicting the Uncertainties in Risk Assessment. Environmental Science and Technology, Vol. 25, No. 10, pp. 1674-1681.

McLaughlin, D., B. R. Lynn, L. Shu-Guang, and J. Hyman. 1993. A Stochastic Method for Characterizing Ground-Water Contamination, Ground Water, Vol. 31, No. 2, pp. 237-249.

Medina M. A. Jr, J. B. Butcher, and C. M. Martin.1989. Monte Carlo Analyses and Bayesian Decision Theory for Assessing the Effects of Waste Sites on Groundwater, II: Applications, Journal of Contaminant Hydrology, Vol. 5, pp. 15-31.

Meeks, Y. J., and A.M. Salhotra. 1990. Monte Carlo Approach to Exposure Assessment, in: Proceedings of the Specialty Conference on Environmental Engineering, Environmental Engineering Div., ASCE, NY, pp. 775-782.

Millington, R. J., and J.P. Quirk. 1959. Gas Diffusion In Porous Media, Science, Vol. 130, pp. 100-102.

Mishra, S., J.C. Parker, and N. Singhal.1989. Estimation of Soil Hydraulics Properties and their Uncertainty from Particle Size Distribution Data. Journal of Hydrology, Vol. 108, pp. 1-18.

Montgomery, D. C. 2001. Design and Analysis of Experiments, 5th Edition, John Wiley & Sons Ltd.

Moore, D.R.J., and B.J. Elliott. 1996. Should Uncertainty Be Quantified in Human and Ecological Risk Assessments Used for Decision-Making? Hum. Ecol. Risk Assessment, Vol. 2, pp. 11-24.

Morgan, M.G., and M. Henrion. 1990. Uncertainty: A Guide to Dealing with Uncertainty in Quantitative Risk and Policy Analysis, Cambridge University Press. 332 pp.

Morshed, J., and J. J. Kaluarachchi. 1998. Application of Neural Network and Genetic Algorithm in Flow and Transport Simulations, Advances in Water Resources, Vol. 22, No. 2, pp. 145-158.

Myers, R., and D. C. Montgomery. 1995. Response Surface Methodology: Process and Product Optimization Using Designed Experiments, John Wiley & Sons Inc.

National Research Council. 1990. Ground Water Models: Scientific and Regulatory Applications, National Academy Press, Washington, DC.252 pp.

Najjar, T. M., and I. A. Basheer. 1995. Spatial Mapping of Groundwater Contamination Using Neuronets, Intelligent Engineering Systems Through Artificial Neural Network,

Proceedings of the 1995 Artificial Neural Networks in Engineering, ANNIE'95, Vol. 5, pp. 817-822.

Palisade. 1992. @ RISK Risk Analysis and Simulation Ad-In For Microsoft Excel, Release 1.1 User's Guide, Palisade Corporation. NY USA 14867

Parker, J.C. 1989. Multi-phase Flow and Transport in Porous Media, Reviews of Geophysics, Vol. 27, pp. 311-328.

Parker, J.C., R.J. Lenhard, and T. Kuppusamy. 1987. A Parametric Model for Constitutive Properties Governing Multi-phase Flow in Porous Media, Water Resources Research. Vol. 23, pp.618-624.

Paustenbach, D.J (Ed.). 1989. The risk assessment of Environmental and Human health Hazards: A Textbook of Case Studies, Wiley, New York.

Paustenbach, D.J, D.M. Meyer, P.J. Sheehan, and V. Lau. 1991. An Assessment and Quantitative Uncertainty Analysis of the Health Risk to Workers Exposed to Chromium Contaminated Soils, Toxicol. Ind. Health, Vol. 7, pp. 159-196.

Picton, P. 1994. Introduction to Neural Networks, Macmillan Press Ltd., London.

Peck, A., S. Gorelick, G. de Marsily, S. Foster, and V. Kovalevsky. 1988. Consequences of Spatial Variability in Aquifer Properties and Data Limitations for Groundwater Modeling Practice, Intern. Assoc. Sci. Hydrology. Publ. No. 175.

Reckhow, K.H. 1994. Water Quality Simulation Modeling and Uncertainty Analysis for Risk Assessment and Decision-Making, Ecol. Model., Vol. 72, pp. 1-20.

Raiffa, H. 1982. Science and Policy: Their Separation and Integration in Risk Analysis. American Statistician, Vol. 36, pp. 225-231.

Rawls, W.J., and D.L. Brankensick. 1985. Prediction of Soil Water Properties for Hydrologic Modeling. Proceedings of Symposium on Watershed Management. American Society of Civil Engineers. New York. pp. 293-299.

Rojas, R. 1996. Neural networks: A Systematic Introduction, Springer-Verlag Berlin Heidelberg.

Rubinstein, R.Y. 1981. Simulation and The Monte Carlo Method, Wiley Series in Probability and Mathematical Statistics. 278pp.

Salhotra, A.M., Y.J. Meeks, R.T. Thorpe, T. McKone, and K. Bogen. 1991. Application of Monte Carlo Simulation To Estimate Probabilities Of Exposure And Human Health

Risks, In: Proceedings of the National Research and Development Conference on the Control of Hazardous Materials, Anaheim, CA, pp. 107-111.

Saltelli, A. 2000. What is Sensitivity Analysis?. In *Sensitivity Analysis* (Saltelli, A., Chan, K., Scott, E.M., eds.), John Wiley & Sons: West Sussex, England, pp. 3-13.

Saltelli, A., T. Stefano, F. Campolongo, and M. Ratto. 2004. Sensitivity In Practice: A Guide To Assessing Scientific Models, John Wiley & Sons Ltd, West Sussex, England.

Scientific Software Group. 2005. SoilPara. www.scientificsoftwaregroup.com

Scott, F., and W. T. Tucker. 2003. Reliability of Risk Analyses for Contaminated Groundwater, Groundwater Quality Modeling and Management under Uncertainty, Proceeding of the Symposium on Groundwater Management Under Uncertainty, June 23, Philadelphia, pp. 226-235.

Shevenell, L., and F.O. Hoffman. 1993. Necessity of Uncertainty Analyses in Risk Assessment, Journal of Hazardous Materials, Vol. 35, pp. 369-385.

Sleep, B.E., and J.F. Sykes. 1989. Modeling the Transport of Volatile Organics in Variably Saturated Media, Water Resources Research, Vol. 25, pp. 81-92.

Spitz, K., and J. Moreno. 1996. A Practical Guide to Groundwater and Solute Transport Modeling. John Wiley & Sons Inc.

Steffy, D.A., C. D. Johnston, and D.A. Barry. 1998. Numerical Simulations and Long-Column Tests of LNAPL Displacement and Trapping by a Fluctuating Water Table, Journal of Soil Contamination, Vol. 7, Issue 3, pp. 325-356.

Stein, M. 1987. Large Sample Properties of Simulations Using Latin Hypercube Sampling, Technometrics, Vol. 29, pp. 143-151.

Tansel, B., C. Jordahl, and I. Tansel. 1999. Mapping of Subsurface Contaminant Profiles by Neural Networks, Civil Engineering and Environmental Systems, Vol. 16, No. 1, pp. 37-50.

Thompson, K. M., D. E. Burmaster, and E.A. Crouch. 1992. Monte Carlo Techniques for Quantitative Uncertainty Analysis in Public Health Risk Assessment, Risk Analysis, Vol. 12, No. 1, pp. 53-63.

Tyagi, A. K., and J. Martell. 1993. Fate/transport Modeling of Immiscible LNAPL in Unsaturated Aquifers. Proceedings of the Symposium on Engineering Hydrology, San Francisco, CA, USA, pp. 701-705.

Uhl, V.W., and S.T. Sullivan. 1982. Uncertainty Analysis in the Appraisal of Capital Investment Projects. In Uncertainty Analysis for Engineers. V.W Uhl and W.E. Lowthian, eds., AIChE Symposium Series, Vol. 78, No. 220, American Institute of Chemical Engineers, New York, pp. 10-22.

U.S. EPA. 1989a. Risk Assessment Guidance for Superfund, Volume 11, Environmental Evaluation Manual, Washington, DC. EPA 540-1-89.

U.S. EPA. 1989b. Risk Assessment Guidance for Superfund, Volume 1, Human Health Evaluation Manual, Part A, Interim Final. Washington, DC. EPA 540-R-92-003.

U.S. EPA. 1991a. Risk Assessment Guidance for Superfund, Volume 1, Human Health Evaluation Manual; Supplemental Guidance Standard Default Exposure Factors, Washington, DC. OSWER Directive: 9285.6-03.

U.S. EPA. 1991b. Risk Assessment Guidance for Superfund, Volume 1, Human Health Evaluation Manual, Part B: Development of Risk-Based Preliminary Remediation Goals. Washington, DC. EPA 540-R-92-003.

U.S. EPA. 1996. Summary report for the Workshop on Monte Carlo Analysis, Superfund Today, September. EPA 630-R-96-010, 1-1.

U.S. EPA. 1997a. Policy for Use of Probabilistic Analysis in Risk Assessment at the U.S. Environmental Protection Agency, May 15.

U.S. EPA. 1997b. Guiding Principles for Monte Carlo Analysis. EPA 630-R-97-001.

U.S. EPA. 2003. Multimedia, Multipathway, and Multireceptor Risk Assessment (3MRA) Modeling System. Volume IV: Evaluating Uncertainty and Sensitivity. EPA 530-D-03-001d. July 2003.

van Genuchten, M. Th. 1980. A Closed Form Equation for Predicting the Hydraulic Conductivity of Unsaturated Soils, Soil Sci. Soc. Am., Vol. 44, pp. 892-898.

Vario, J.K. 1982. Statistical Determination of Effective Input Variables. Reactor Analysis and Safety Division, ANL-82-57, Argonne National laboratory, Argonne, Illinois.

Veneziano, D., R. Kulkarni, G. Luster, G. Rao, and A. Salhotra. 1989. Improving The Efficiency of Monte Carlo Simulation for Groundwater Transport. Proceedings of the conference on Geostatistical, Sensitivity, and Uncertainty Modeling. B.E. Buxton, ed., Battelle Press, Columbus, OH, pp. 155-172.

Walker, D.D., Z. Hubao, D. M. Peterson, and R. G. Knowlton , Jr. 1996. Probabilistic Screening Model of Volatile Contaminant Transport in the Saturated and Unsaturated

Zones. Proceedings of the ModelCARE 96 Conference. IAHS Publ. No. 237, pp. 597-606.

Wang, F., and J. Bright. 2004. Scale Effect and Calibration of Contaminant Transport Models, Ground Water, Vol. 42, No. 5, pp. 760-766.

Ward Systems Group, Inc. 1993. NeuroShell 2 – Users Manual. 2nd Edition, Frederick, MD

Weisstein, E. W. 1999. Positive Definite Matrix, from *MathWorld* –A Wolfram Web Resource. http://mathworld.wolfram.com/PositiveDefiniteMatrix.html

Yen, B. C. 2002. System and Component Uncertainties in Water Resources.In *Risk, Reliability, Uncertainty and Robustness of Water Resources Systems* (Bogardi, Janos J., Kundzewicz, Zbigniew W., eds), Cambridge University Press, Cambridge, pp. 133-142.

Zhang, Y., B. Seo, N. LoVanh, P. J.J. Alvarez, and R. Heathcote. 2001. Final Report-Evaluation of Computer Software Packages for RBCA Tier 3 Analysis, Submitted to Iowa Comprehensive Petroleum Underground Storage Tank Fund Board.

Zheng, C., and G. D. Bennett. 1995. Applied Contaminant Transport Modeling: Theory and Practice, van Nostrand Reinhold, New York.

Zou, R., W. Lung, and H. Guo. 2002. Neural Network Embedded Monte Carlo Approach for Water Quality Modeling under Input Information Uncertainty, Journal of Computing in Civil Engineering, Vol. 16, No. 2, pp. 135-142.

Appendix A. Summary Statistics

RS-MC

Benzene

water		*gas*		*solid*	
Mean	0.002414662	Mean	0.0005433	Mean	0.003333204
Standard Error	2.27E-05	Standard Error	5.10803E-06	Standard Error	3.13395E-05
Median	0.002512	Median	0.0005652	Median	0.0034675
Mode	0	Mode	0	Mode	0
Standard Deviation	0.002269999	Standard Deviation	0.000510803	Standard Deviation	0.003133953
Sample Variance	5.15289E-06	Sample Variance	2.6092E-07	Sample Variance	9.82166E-06
Kurtosis	874.1020853	Kurtosis	874.6772283	Kurtosis	874.9391754
Skewness	22.56901593	Skewness	22.57665719	Skewness	22.58007713
Range	0.1136	Range	0.02557	Range	0.1569
Minimum	0	Minimum	0	Minimum	0
Maximum	0.1136	Maximum	0.02557	Maximum	0.1569
Sum	24.14661515	Sum	5.432996317	Sum	33.33204115
Count	10000	Count	10000	Count	10000
Confidence Level(95.0%)	4.44966E-05	Confidence Level(95.0%)	1.00128E-05	Confidence Level(95.0%)	6.14318E-05

Toluene

water		*gas*		*solid*	
Mean	0.000673168	Mean	0.000184448	Mean	0.002677857
Standard Error	5.59145E-06	Standard Error	1.53203E-06	Standard Error	2.22423E-05
Median	0.00056315	Median	0.0001543	Median	0.0022405
Mode	0	Mode	0	Mode	0
Standard Deviation	0.000559145	Standard Deviation	0.000153203	Standard Deviation	0.002224226
Sample Variance	3.12643E-07	Sample Variance	2.34713E-08	Sample Variance	4.94718E-06
Kurtosis	11.39919764	Kurtosis	11.38480541	Kurtosis	11.37573815
Skewness	1.662523361	Skewness	1.661968003	Skewness	1.661599964
Range	0.01073	Range	0.002939	Range	0.04266
Minimum	0	Minimum	0	Minimum	0
Maximum	0.01073	Maximum	0.002939	Maximum	0.04266
Sum	6.731681752	Sum	1.844475158	Sum	26.77856685
Count	10000	Count	10000	Count	10000
Confidence Level(95.0%)	1.09604E-05	Confidence Level(95.0%)	3.00309E-06	Confidence Level(95.0%)	4.35993E-05

Ethylbenzene

water		*gas*		*solid*	
Mean	0.00022768	Mean	8.15096E-05	Mean	0.002078502
Standard Error	2.03512E-06	Standard Error	7.28572E-07	Standard Error	1.85786E-05
Median	0.0001693	Median	0.000060605	Median	0.0015455
Mode	0	Mode	0	Mode	0
Standard Deviation	0.000203512	Standard Deviation	7.28572E-05	Standard Deviation	0.001857857
Sample Variance	4.1417E-08	Sample Variance	5.30816E-09	Sample Variance	3.45163E-06
Kurtosis	2.031763571	Kurtosis	2.031813722	Kurtosis	2.031739605
Skewness	1.610190399	Skewness	1.610198554	Skewness	1.610182756
Range	0.001003	Range	0.0003592	Range	0.009159
Minimum	0	Minimum	0	Minimum	0
Maximum	0.001003	Maximum	0.0003592	Maximum	0.009159
Sum	2.276803884	Sum	0.815096187	Sum	20.78501984
Count	10000	Count	10000	Count	10000
Confidence Level(95.0%)	3.98924E-06	Confidence Level(95.0%)	1.42815E-06	Confidence Level(95.0%)	3.64177E-05

Xylene

water		*gas*		*solid*	
Mean	0.000190813	Mean	4.8085E-05	Mean	0.001901929
Standard Error	2.44722E-06	Standard Error	6.16702E-07	Standard Error	2.43925E-05
Median	0.00009919	Median	0.000025	Median	0.0009886
Mode	0	Mode	0	Mode	0
Standard Deviation	0.000244722	Standard Deviation	6.16702E-05	Standard Deviation	0.002439252
Sample Variance	5.98888E-08	Sample Variance	3.80321E-09	Sample Variance	5.94995E-06
Kurtosis	2.18879999	Kurtosis	2.18876561	Kurtosis	2.188635679
Skewness	1.802318988	Skewness	1.802317015	Skewness	1.802290055
Range	0.001089	Range	0.0002744	Range	0.01085
Minimum	0	Minimum	0	Minimum	0
Maximum	0.001089	Maximum	0.0002744	Maximum	0.01085
Sum	1.908130091	Sum	0.480850243	Sum	19.01929198
Count	10000	Count	10000	Count	10000
Confidence Level(95.0%)	4.79704E-06	Confidence Level(95.0%)	1.20886E-06	Confidence Level(95.0%)	4.78143E-05

Units = 1000 mg/L

MC with LHS

Benzene

water		gas		solid	
Mean	0.00233102	Mean	0.000524477	Mean	0.003217781
Standard Error	0.000147122	Standard Error	3.31014E-05	Standard Error	0.000203095
Median	0.002259	Median	0.0005082	Median	0.003118
Mode	0	Mode	0	Mode	0
Standard Deviation	0.001471218	Standard Deviation	0.000331014	Standard Deviation	0.00203095
Sample Variance	2.16448E-06	Sample Variance	1.0957E-07	Sample Variance	4.12476E-06
Kurtosis	0.879677858	Kurtosis	0.879382208	Kurtosis	0.879997432
Skewness	0.596361526	Skewness	0.596219175	Skewness	0.596518613
Range	0.007112	Range	0.0016	Range	0.009818
Minimum	0	Minimum	0	Minimum	0
Maximum	0.007112	Maximum	0.0016	Maximum	0.009818
Sum	0.23310195	Sum	0.05244765	Sum	0.32177812
Count	100	Count	100	Count	100
Confidence Level(95.0%)	0.000291922	Confidence Level(95.0%)	6.56804E-05	Confidence Level(95.0%)	0.000402985

Toluene

water		gas		solid	
Mean	0.000654769	Mean	0.000179406	Mean	0.002604598
Standard Error	5.65216E-05	Standard Error	1.54866E-05	Standard Error	0.000224836
Median	0.00053975	Median	0.0001479	Median	0.002147
Mode	0	Mode	0	Mode	0
Standard Deviation	0.000565216	Standard Deviation	0.000154866	Standard Deviation	0.002248363
Sample Variance	3.1947E-07	Sample Variance	2.39834E-08	Sample Variance	5.05514E-06
Kurtosis	1.266615393	Kurtosis	1.266459756	Kurtosis	1.266474039
Skewness	1.234844442	Skewness	1.234789287	Skewness	1.234818232
Range	0.002501	Range	0.0006852	Range	0.009948
Minimum	0	Minimum	0	Minimum	0
Maximum	0.002501	Maximum	0.0006852	Maximum	0.009948
Sum	0.06547694	Sum	0.017940588	Sum	0.26045976
Count	100	Count	100	Count	100
Confidence Level(95.0%)	0.000112151	Confidence Level(95.0%)	3.07287E-05	Confidence Level(95.0%)	0.000446124

Ethylbenzene

water		gas		solid	
Mean	0.000238793	Mean	8.4397E-05	Mean	0.002112956
Standard Error	2.37032E-05	Standard Error	8.05124E-06	Standard Error	0.00019545
Median	0.00016675	Median	0.000059695	Median	0.001522
Mode	0	Mode	0	Mode	0
Standard Deviation	0.000237032	Standard Deviation	8.05124E-05	Standard Deviation	0.001954497
Sample Variance	5.61843E-08	Sample Variance	6.48225E-09	Sample Variance	3.82006E-06
Kurtosis	4.742029474	Kurtosis	2.727596387	Kurtosis	2.497675267
Skewness	2.091990816	Skewness	1.799827641	Skewness	1.725519081
Range	0.0013	Range	0.0003563	Range	0.008857
Minimum	0	Minimum	0	Minimum	0
Maximum	0.0013	Maximum	0.0003563	Maximum	0.008857
Sum	0.023879268	Sum	0.008439704	Sum	0.21129559
Count	100	Count	100	Count	100
Confidence Level(95.0%)	4.70324E-05	Confidence Level(95.0%)	1.59754E-05	Confidence Level(95.0%)	0.000387815

Xylene

water		gas		solid	
Mean	0.000188504	Mean	4.80971E-05	Mean	0.001874179
Standard Error	2.48274E-05	Standard Error	6.37347E-06	Standard Error	0.000246799
Median	0.00009673	Median	0.000024375	Median	0.00096415
Mode	0	Mode	0	Mode	0
Standard Deviation	0.000248274	Standard Deviation	6.37347E-05	Standard Deviation	0.002467995
Sample Variance	6.164E-08	Sample Variance	4.06212E-09	Sample Variance	6.091E-06
Kurtosis	2.602331966	Kurtosis	2.430536975	Kurtosis	2.656755433
Skewness	1.882900338	Skewness	1.862801037	Skewness	1.892471392
Range	0.001003	Range	0.0002528	Range	0.009998
Minimum	0	Minimum	0	Minimum	0
Maximum	0.001003	Maximum	0.0002528	Maximum	0.009998
Sum	0.018850439	Sum	0.004809711	Sum	0.187417882
Count	100	Count	100	Count	100
Confidence Level(95.0%)	4.9263E-05	Confidence Level(95.0%)	1.26464E-05	Confidence Level(95.0%)	0.000489704

Units = 1000 mg/L

MC with LHS-s

Benzene

water		*gas*		*solid*	
Mean	0.002369	Mean	0.000533	Mean	0.003271
Standard Error	0.000234	Standard Error	5.26E-05	Standard Error	0.000322
Median	0.002564	Median	0.000577	Median	0.003539
Mode	0	Mode	0	Mode	0
Standard Deviation	0.001382	Standard Deviation	0.000311	Standard Deviation	0.001908
Sample Variance	1.91E-06	Sample Variance	9.67E-08	Sample Variance	3.64E-06
Kurtosis	-0.782024	Kurtosis	-0.782124	Kurtosis	-0.781844
Skewness	-0.207073	Skewness	-0.207398	Skewness	-0.207038
Range	0.004614	Range	0.001038	Range	0.006369
Minimum	0	Minimum	0	Minimum	0
Maximum	0.004614	Maximum	0.001038	Maximum	0.006369
Sum	0.082924	Sum	0.018657	Sum	0.114468
Count	35	Count	35	Count	35
Confidence Level(95.0%)	0.000475	Confidence Level(95.0%)	0.000107	Confidence Level(95.0%)	0.000655

Toluene

water		*gas*		*solid*	
Mean	0.000655	Mean	0.000179	Mean	0.002606
Standard Error	8.2E-05	Standard Error	2.25E-05	Standard Error	0.000326
Median	0.00061	Median	0.000167	Median	0.002428
Mode	0	Mode	0	Mode	0
Standard Deviation	0.000485	Standard Deviation	0.000133	Standard Deviation	0.001929
Sample Variance	2.35E-07	Sample Variance	1.77E-08	Sample Variance	3.72E-06
Kurtosis	-0.449609	Kurtosis	-0.449536	Kurtosis	-0.450102
Skewness	0.535421	Skewness	0.535658	Skewness	0.53539
Range	0.001725	Range	0.000473	Range	0.006862
Minimum	0	Minimum	0	Minimum	0
Maximum	0.001725	Maximum	0.000473	Maximum	0.006862
Sum	0.022925	Sum	0.006282	Sum	0.091198
Count	35	Count	35	Count	35
Confidence Level(95.0%)	0.000167	Confidence Level(95.0%)	4.56E-05	Confidence Level(95.0%)	0.000663

Ethylbenzene

water		*gas*		*solid*	
Mean	0.000214	Mean	7.67E-05	Mean	0.001956
Standard Error	2.89E-05	Standard Error	1.04E-05	Standard Error	0.000264
Median	0.00018	Median	6.43E-05	Median	0.001639
Mode	0.000236	Mode	0	Mode	0
Standard Deviation	0.000171	Standard Deviation	6.13E-05	Standard Deviation	0.001563
Sample Variance	2.93E-08	Sample Variance	3.76E-09	Sample Variance	2.44E-06
Kurtosis	0.895186	Kurtosis	0.896225	Kurtosis	0.895267
Skewness	1.19737	Skewness	1.197636	Skewness	1.197295
Range	0.000679	Range	0.000243	Range	0.006198
Minimum	0	Minimum	0	Minimum	0
Maximum	0.000679	Maximum	0.000243	Maximum	0.006198
Sum	0.007499	Sum	0.002685	Sum	0.06846
Count	35	Count	35	Count	35
Confidence Level(95.0%)	5.88E-05	Confidence Level(95.0%)	2.11E-05	Confidence Level(95.0%)	0.000537

Xylene

water		*gas*		*solid*	
Mean	0.000182	Mean	4.58E-05	Mean	0.00181
Standard Error	3.42E-05	Standard Error	8.62E-06	Standard Error	0.000341
Median	0.000109	Median	2.75E-05	Median	0.001088
Mode	0	Mode	0	Mode	0
Standard Deviation	0.000202	Standard Deviation	5.1E-05	Standard Deviation	0.002017
Sample Variance	4.09E-08	Sample Variance	2.6E-09	Sample Variance	4.07E-06
Kurtosis	0.649564	Kurtosis	0.65023	Kurtosis	0.649556
Skewness	1.314676	Skewness	1.314732	Skewness	1.314667
Range	0.000678	Range	0.000171	Range	0.00676
Minimum	0	Minimum	0	Minimum	0
Maximum	0.000678	Maximum	0.000171	Maximum	0.00676
Sum	0.006356	Sum	0.001602	Sum	0.063352
Count	35	Count	35	Count	35
Confidence Level(95.0%)	6.95E-05	Confidence Level(95.0%)	1.75E-05	Confidence Level(95.0%)	0.000693

Units = 1000 mg/L

MC with LHS-c

Benzene

water		gas		solid	
Mean	0.002251445	Mean	0.000506577	Mean	0.003107868
Standard Error	0.00014108	Standard Error	3.17442E-05	Standard Error	0.000194743
Median	0.002374	Median	0.0005342	Median	0.003277
Mode	0	Mode	0	Mode	0
Standard Deviation	0.001410799	Standard Deviation	0.000317442	Standard Deviation	0.001947429
Sample Variance	1.99035E-06	Sample Variance	1.0077E-07	Sample Variance	3.79248E-06
Kurtosis	0.062336921	Kurtosis	0.062932709	Kurtosis	0.062219827
Skewness	0.174275951	Skewness	0.174588731	Skewness	0.174240035
Range	0.006631	Range	0.001492	Range	0.009153
Minimum	0	Minimum	0	Minimum	0
Maximum	0.006631	Maximum	0.001492	Maximum	0.009153
Sum	0.22514445	Sum	0.050657736	Sum	0.31078682
Count	100	Count	100	Count	100
Largest(1)	0.006631	Largest(1)	0.001492	Largest(1)	0.009153
Smallest(1)	0	Smallest(1)	0	Smallest(1)	0
Confidence Level(95.0%)	0.000279933	Confidence Level(95.0%)	6.29875E-05	Confidence Level(95.0%)	0.000386412

Toluene

water		gas		solid	
Mean	0.00065208	Mean	0.000177202	Mean	0.002515739
Standard Error	5.59313E-05	Standard Error	1.47559E-05	Standard Error	0.000201929
Median	0.0005335	Median	0.0001462	Median	0.0021225
Mode	0	Mode	0	Mode	0
Standard Deviation	0.000559313	Standard Deviation	0.000147559	Standard Deviation	0.002019294
Sample Variance	3.12831E-07	Sample Variance	2.17736E-08	Sample Variance	4.07755E-06
Kurtosis	3.067905225	Kurtosis	1.563227151	Kurtosis	1.130033816
Skewness	1.507377934	Skewness	1.249248867	Skewness	1.101849334
Range	0.003014	Range	0.000678	Range	0.009089
Minimum	0	Minimum	0	Minimum	0
Maximum	0.003014	Maximum	0.000678	Maximum	0.009089
Sum	0.06520796	Sum	0.017720211	Sum	0.25157394
Count	100	Count	100	Count	100
Largest(1)	0.003014	Largest(1)	0.000678	Largest(1)	0.009089
Smallest(1)	0	Smallest(1)	0	Smallest(1)	0
Confidence Level(95.0%)	0.00011098	Confidence Level(95.0%)	2.92789E-05	Confidence Level(95.0%)	0.000400672

Ethylbenzene

water		gas		solid	
Mean	0.000234467	Mean	8.20526E-05	Mean	0.00202461
Standard Error	2.28252E-05	Standard Error	7.49716E-06	Standard Error	0.000175544
Median	0.00016895	Median	0.00006049	Median	0.001542
Mode	0	Mode	0	Mode	0
Standard Deviation	0.000228252	Standard Deviation	7.49716E-05	Standard Deviation	0.001755436
Sample Variance	5.20989E-08	Sample Variance	5.62074E-09	Sample Variance	3.08156E-06
Kurtosis	4.837988595	Kurtosis	2.343917896	Kurtosis	2.012710817
Skewness	2.075358197	Skewness	1.673625345	Skewness	1.553152021
Range	0.001255	Range	0.000344	Range	0.007965
Minimum	0	Minimum	0	Minimum	0
Maximum	0.001255	Maximum	0.000344	Maximum	0.007965
Sum	0.02344673	Sum	0.008205263	Sum	0.202461
Count	100	Count	100	Count	100
Largest(1)	0.001255	Largest(1)	0.000344	Largest(1)	0.007965
Smallest(1)	0	Smallest(1)	0	Smallest(1)	0
Confidence Level(95.0%)	4.52901E-05	Confidence Level(95.0%)	1.4876E-05	Confidence Level(95.0%)	0.000348317

Xylene

water		gas		solid	
Mean	0.000180177	Mean	4.61369E-05	Mean	0.001790147
Standard Error	2.36352E-05	Standard Error	6.03517E-06	Standard Error	0.000235178
Median	0.00009816	Median	0.000024735	Median	0.0009784
Mode	0	Mode	0	Mode	0
Standard Deviation	0.000236352	Standard Deviation	6.03517E-05	Standard Deviation	0.002351783
Sample Variance	5.58622E-08	Sample Variance	3.64232E-09	Sample Variance	5.53089E-06
Kurtosis	2.806182223	Kurtosis	2.499496569	Kurtosis	2.861236037
Skewness	1.90528425	Skewness	1.843145301	Skewness	1.918362936
Range	0.0009517	Range	0.0002398	Range	0.009486
Minimum	0	Minimum	0	Minimum	0
Maximum	0.0009517	Maximum	0.0002398	Maximum	0.009486
Sum	0.018017719	Sum	0.004613689	Sum	0.179014686
Count	100	Count	100	Count	100
Largest(1)	0.0009517	Largest(1)	0.0002398	Largest(1)	0.009486
Smallest(1)	0	Smallest(1)	0	Smallest(1)	0
Confidence Level(95.0%)	4.68973E-05	Confidence Level(95.0%)	1.19751E-05	Confidence Level(95.0%)	0.000466645

Units = 1000 mg/L

MC with LHS-p

Benzene

water		gas		solid	
Mean	0.002261998	Mean	0.000508951	Mean	0.003122506
Standard Error	0.00014417	Standard Error	3.24373E-05	Standard Error	0.000199011
Median	0.002383	Median	0.00053615	Median	0.0032895
Mode	0	Mode	0	Mode	0
Standard Deviation	0.001441703	Standard Deviation	0.000324373	Standard Deviation	0.001990111
Sample Variance	2.07851E-06	Sample Variance	1.05218E-07	Sample Variance	3.96054E-06
Kurtosis	0.84226785	Kurtosis	0.841759263	Kurtosis	0.841935075
Skewness	0.519676147	Skewness	0.519465346	Skewness	0.519579324
Range	0.007204	Range	0.001621	Range	0.009944
Minimum	0	Minimum	0	Minimum	0
Maximum	0.007204	Maximum	0.001621	Maximum	0.009944
Sum	0.22619981	Sum	0.050895146	Sum	0.31225064
Count	100	Count	100	Count	100
Confidence Level(95.0%)	0.000286065	Confidence Level(95.0%)	6.43627E-05	Confidence Level(95.0%)	0.000394881

Toluene

water		gas		solid	
Mean	0.000640146	Mean	0.000175394	Mean	0.002546438
Standard Error	5.51442E-05	Standard Error	1.5108E-05	Standard Error	0.000219358
Median	0.00056465	Median	0.0001547	Median	0.002246
Mode	0	Mode	0	Mode	0
Standard Deviation	0.000551442	Standard Deviation	0.00015108	Standard Deviation	0.00219358
Sample Variance	3.04088E-07	Sample Variance	2.28253E-08	Sample Variance	4.81179E-06
Kurtosis	1.659235719	Kurtosis	1.659253894	Kurtosis	1.660682695
Skewness	1.302579251	Skewness	1.302505506	Skewness	1.302839639
Range	0.002556	Range	0.0007003	Range	0.01017
Minimum	0	Minimum	0	Minimum	0
Maximum	0.002556	Maximum	0.0007003	Maximum	0.01017
Sum	0.064014636	Sum	0.017539352	Sum	0.25464377
Count	100	Count	100	Count	100
Confidence Level(95.0%)	0.000109418	Confidence Level(95.0%)	2.99776E-05	Confidence Level(95.0%)	0.000435254

Ethylbenzene

water		gas		solid	
Mean	0.000218377	Mean	7.8177E-05	Mean	0.001993511
Standard Error	2.02767E-05	Standard Error	7.25877E-06	Standard Error	0.000185106
Median	0.0001704	Median	0.000061	Median	0.0015555
Mode	0	Mode	0	Mode	0
Standard Deviation	0.000202767	Standard Deviation	7.25877E-05	Standard Deviation	0.001851061
Sample Variance	4.11145E-08	Sample Variance	5.26898E-09	Sample Variance	3.42643E-06
Kurtosis	3.222135768	Kurtosis	3.221939492	Kurtosis	3.221890099
Skewness	1.825618166	Skewness	1.825525865	Skewness	1.825584834
Range	0.0009883	Range	0.0003538	Range	0.009022
Minimum	0	Minimum	0	Minimum	0
Maximum	0.0009883	Maximum	0.0003538	Maximum	0.009022
Sum	0.02183765	Sum	0.007817698	Sum	0.1993511
Count	100	Count	100	Count	100
Confidence Level(95.0%)	4.02334E-05	Confidence Level(95.0%)	1.4403E-05	Confidence Level(95.0%)	0.000367291

Xylene

water		gas		solid	
Mean	0.000182648	Mean	4.60264E-05	Mean	0.001820555
Standard Error	2.48616E-05	Standard Error	6.26487E-06	Standard Error	0.000247814
Median	0.00010235	Median	0.00002579	Median	0.00102
Mode	0	Mode	0	Mode	0
Standard Deviation	0.000248616	Standard Deviation	6.26487E-05	Standard Deviation	0.002478136
Sample Variance	6.18098E-08	Sample Variance	3.92486E-09	Sample Variance	6.14116E-06
Kurtosis	3.054709141	Kurtosis	3.054179264	Kurtosis	3.055916824
Skewness	2.000725241	Skewness	2.000642624	Skewness	2.000911489
Range	0.001035	Range	0.0002608	Range	0.01032
Minimum	0	Minimum	0	Minimum	0
Maximum	0.001035	Maximum	0.0002608	Maximum	0.01032
Sum	0.018264813	Sum	0.004602644	Sum	0.182055495
Count	100	Count	100	Count	100
Confidence Level(95.0%)	4.93308E-05	Confidence Level(95.0%)	1.24309E-05	Confidence Level(95.0%)	0.000491716

Units = 1000 mg/L

Appendix B. Compact Disc (CDROM)

Contents

1. MC-MOFAT Code (Code modified to allow batch processing)
2. LHS code used (Ready for compiling on a Unix system)
3. Pre-Processor: - Fortran Code for Creating MC and LHS Input Files
4. Post–Processor: - Microsoft Word File with Visual Basic for Applications (VBA) Macro for Extracting Concentrations from Output Files

Appendix C. Scatter Plots

Scatter Plots for LHS Simulations

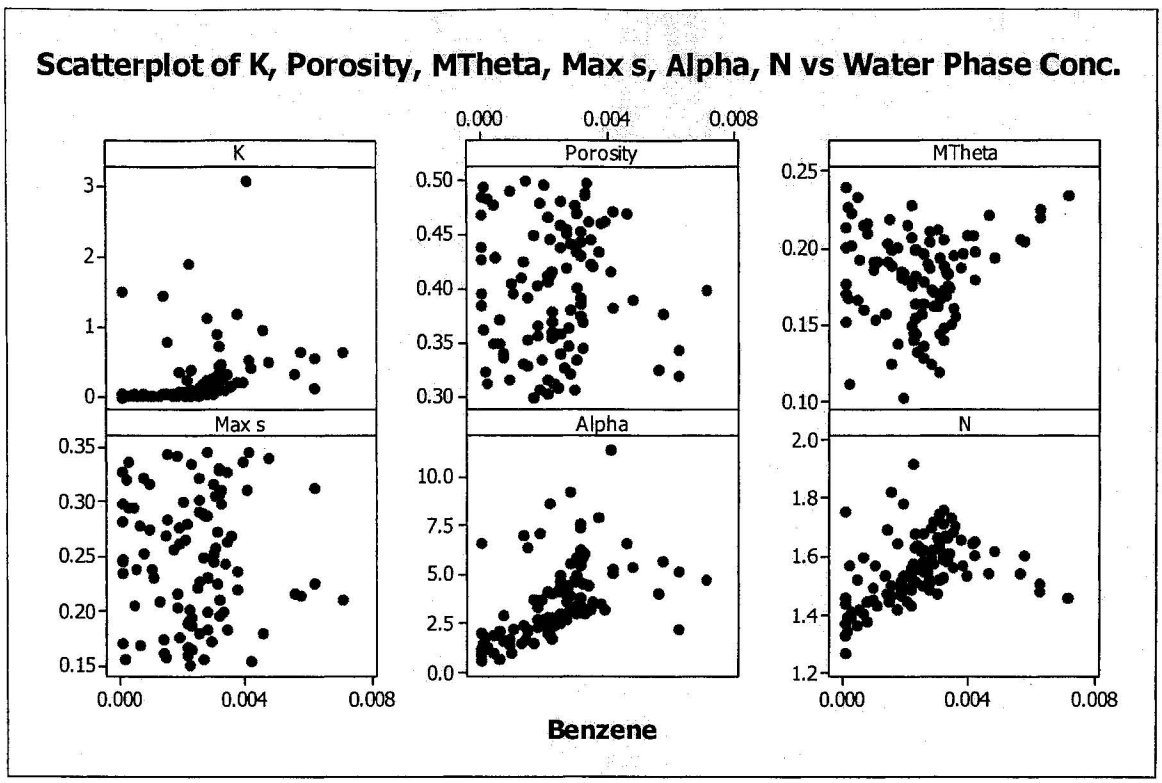
Scatterplot of K, Porosity, MTheta, Max s, Alpha, N vs Water Phase Conc.
K
Porosity
MTheta
Max s
Alpha
N
Benzene

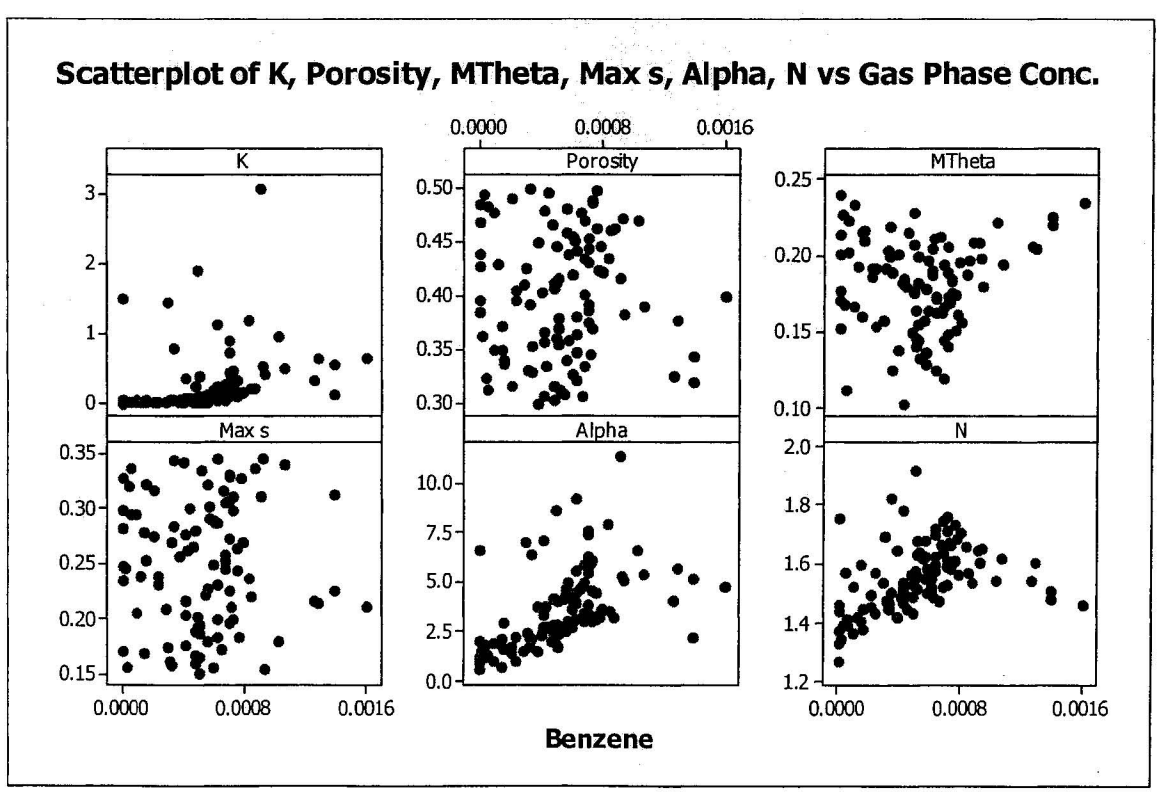
Scatterplot of K, Porosity, MTheta, Max s, Alpha, N vs Gas Phase Conc.
K
Porosity
MTheta
Max s
Alpha
N
Benzene

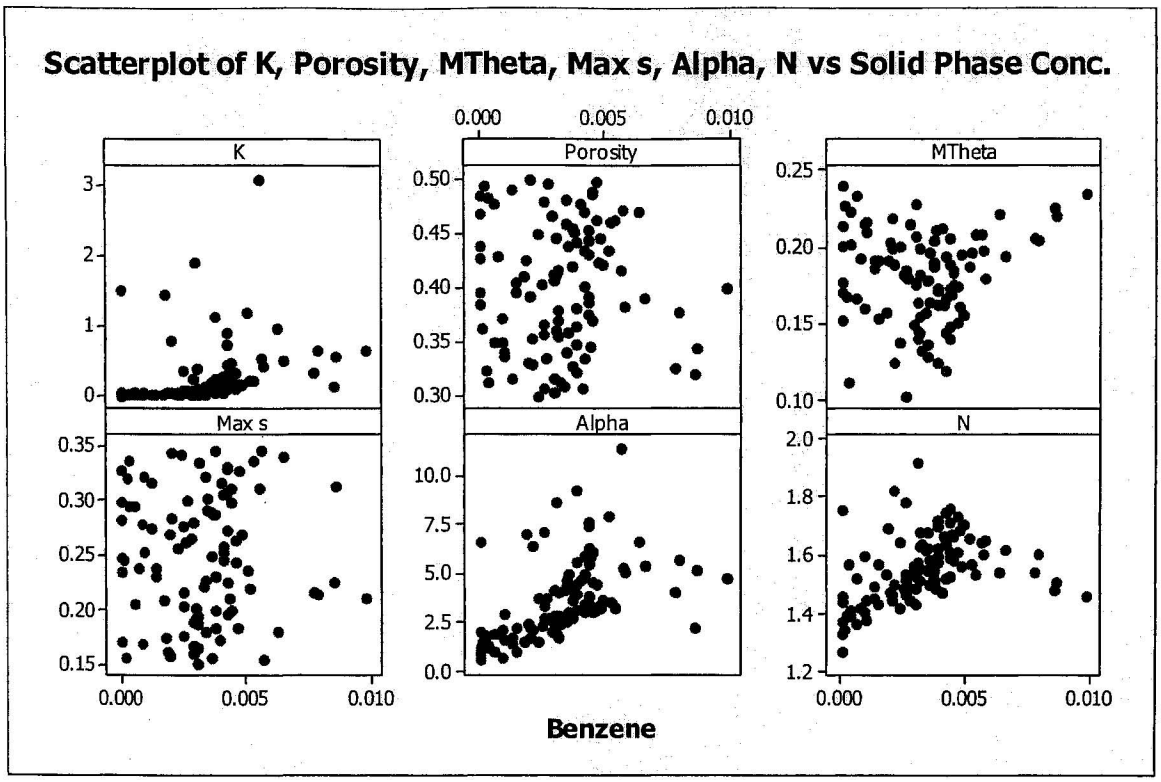
Scatterplot of K, Porosity, MTheta, Max s, Alpha, N vs Solid Phase Conc.
K
Porosity
MTheta
Max s
Alpha
N
Benzene

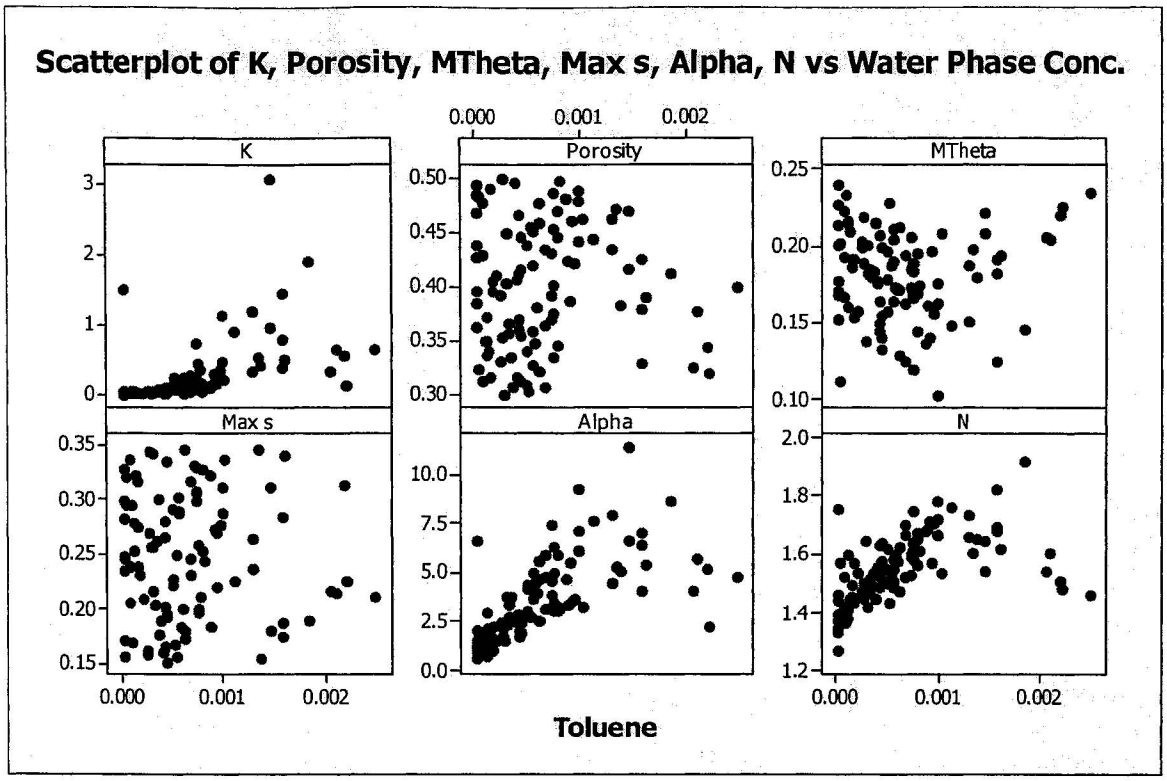
Scatterplot of K, Porosity, MTheta, Max s, Alpha, N vs Water Phase Conc.
K
Porosity
MTheta
Max s
Alpha
N
Toluene

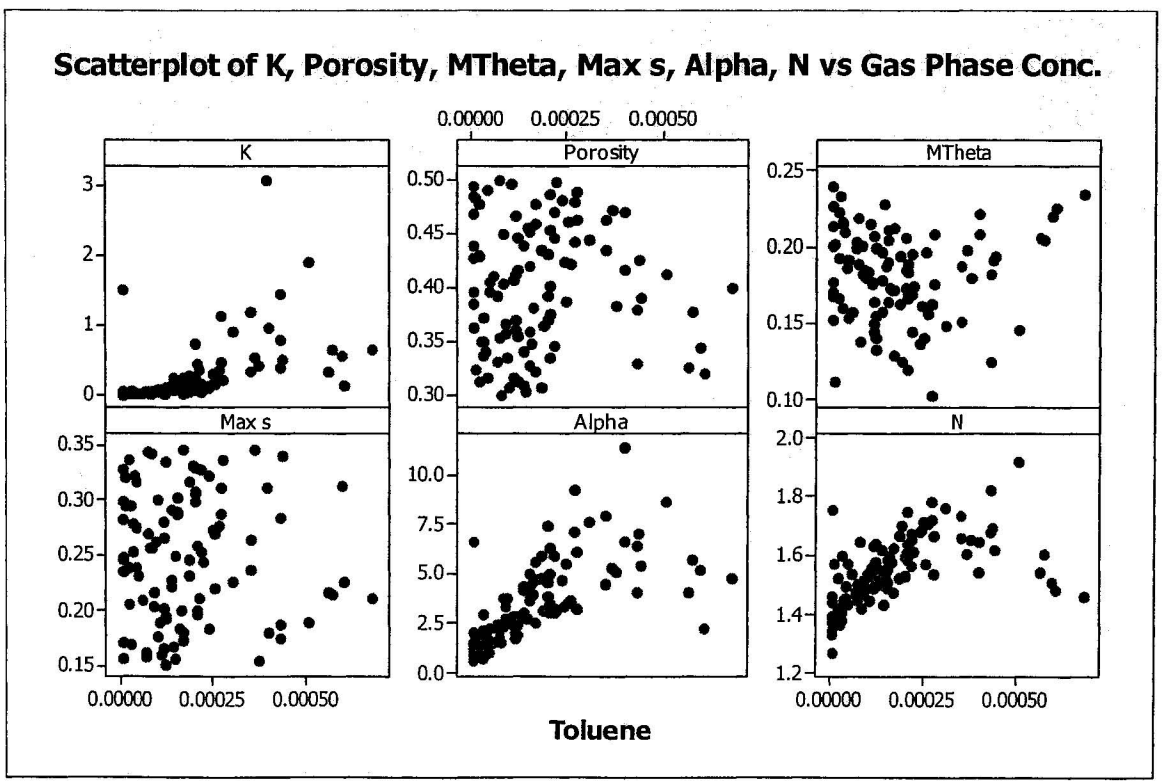
Scatterplot of K, Porosity, MTheta, Max s, Alpha, N vs Gas Phase Conc.
K
Porosity
MTheta
Max s
Alpha
N
Toluene

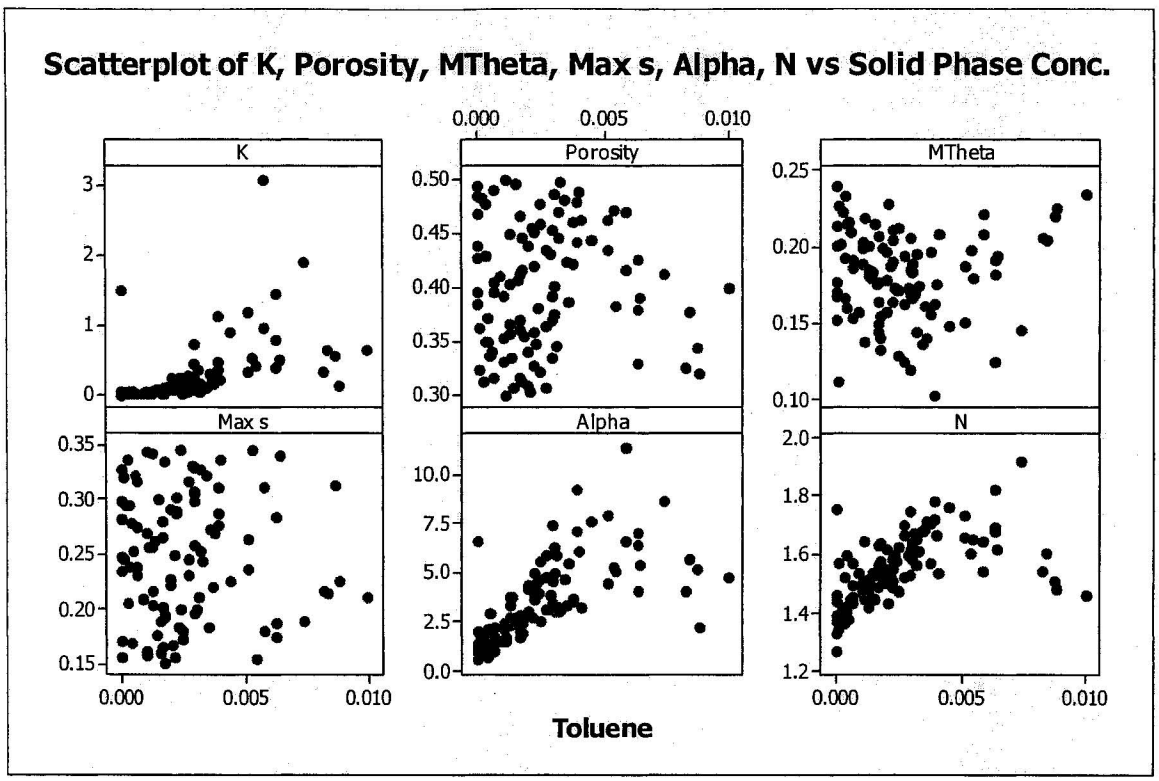
Scatterplot of K, Porosity, MTheta, Max s, Alpha, N vs Solid Phase Conc.
K
Porosity
MTheta
Max s
Alpha
N
Toluene

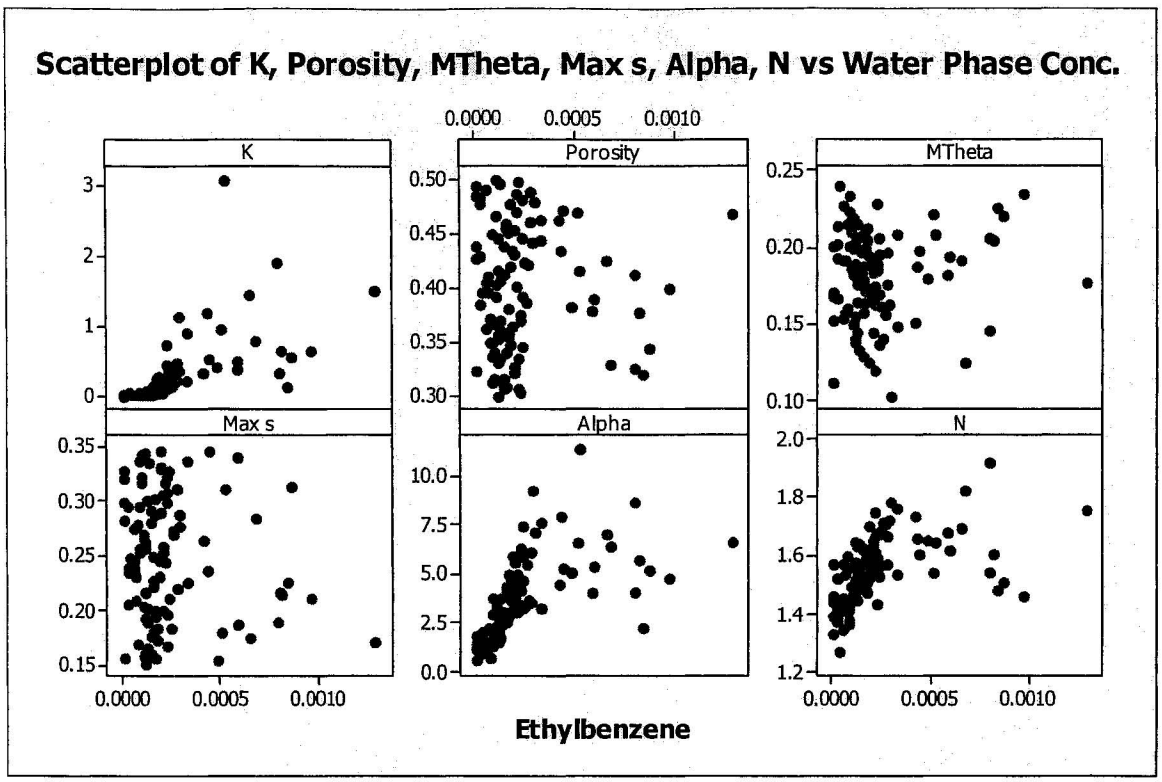
Scatterplot of K, Porosity, MTheta, Max s, Alpha, N vs Water Phase Conc.
K
Porosity
MTheta
Max s
Alpha
N
Ethylbenzene

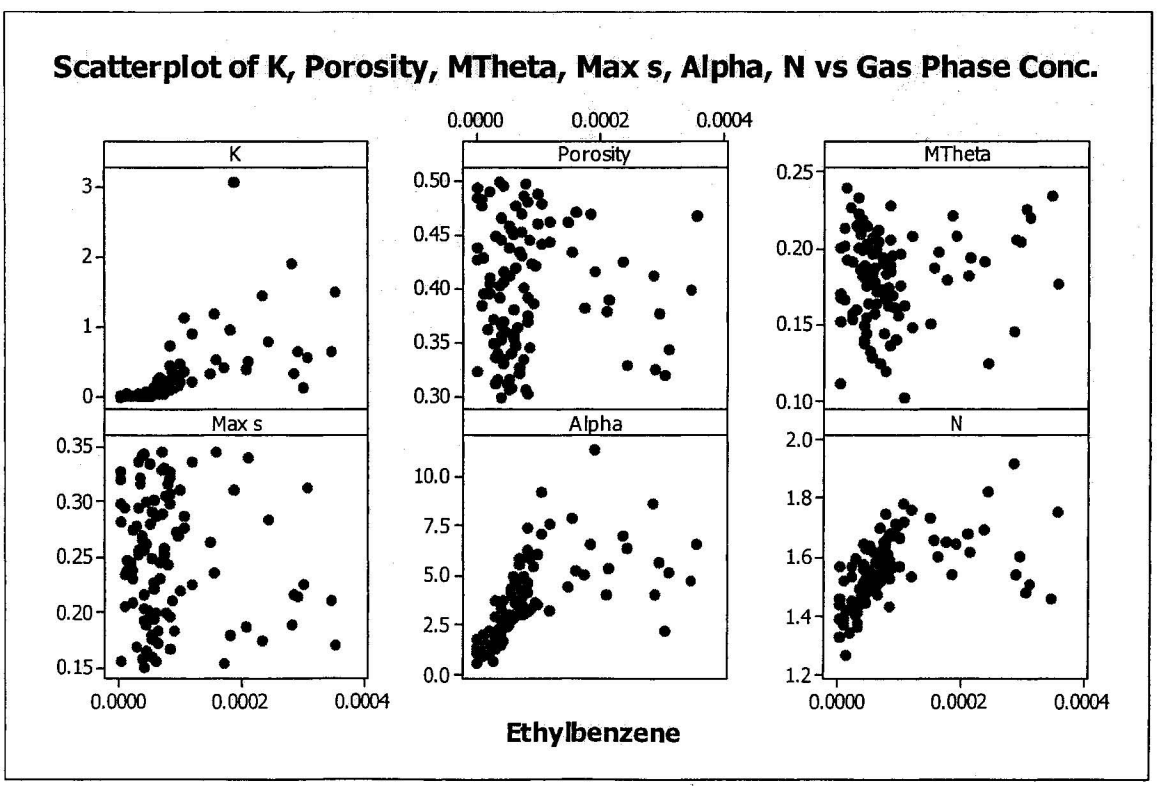
Scatterplot of K, Porosity, MTheta, Max s, Alpha, N vs Gas Phase Conc.
K
Porosity
MTheta
Max s
Alpha
N
Ethylbenzene

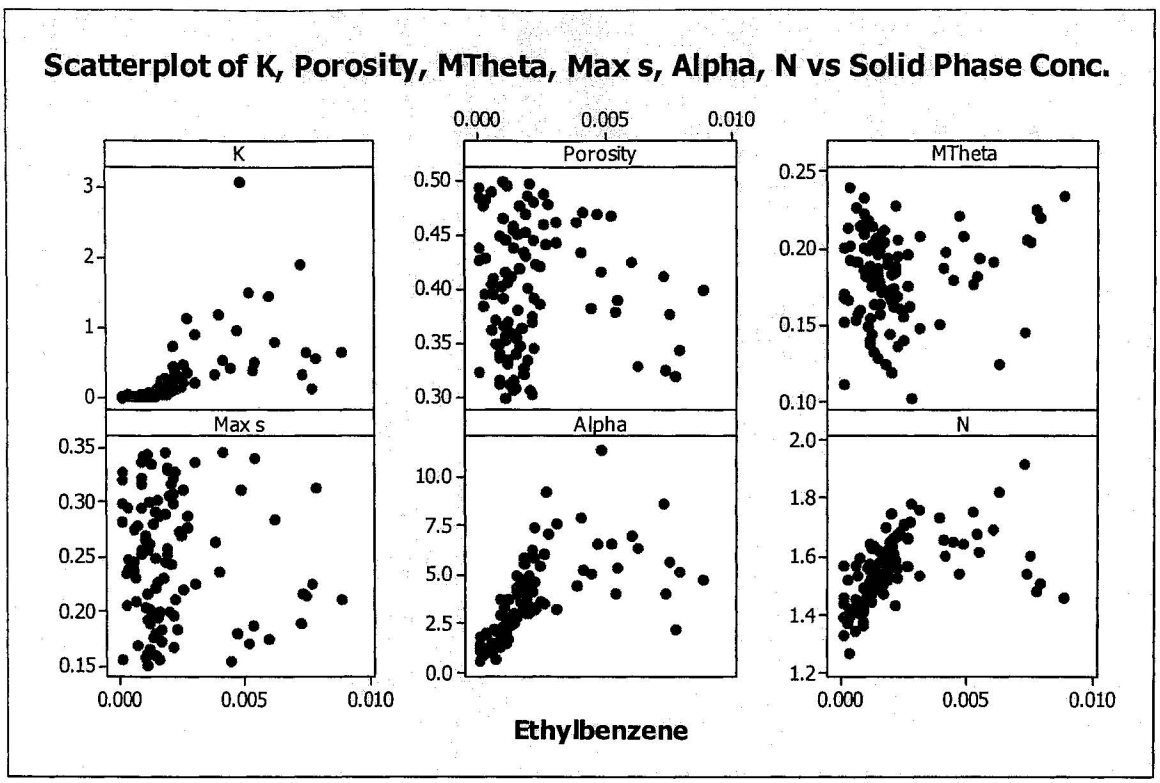
Scatterplot of K, Porosity, MTheta, Max s, Alpha, N vs Solid Phase Conc.
K
Porosity
MTheta
Max s
Alpha
N
Ethylbenzene

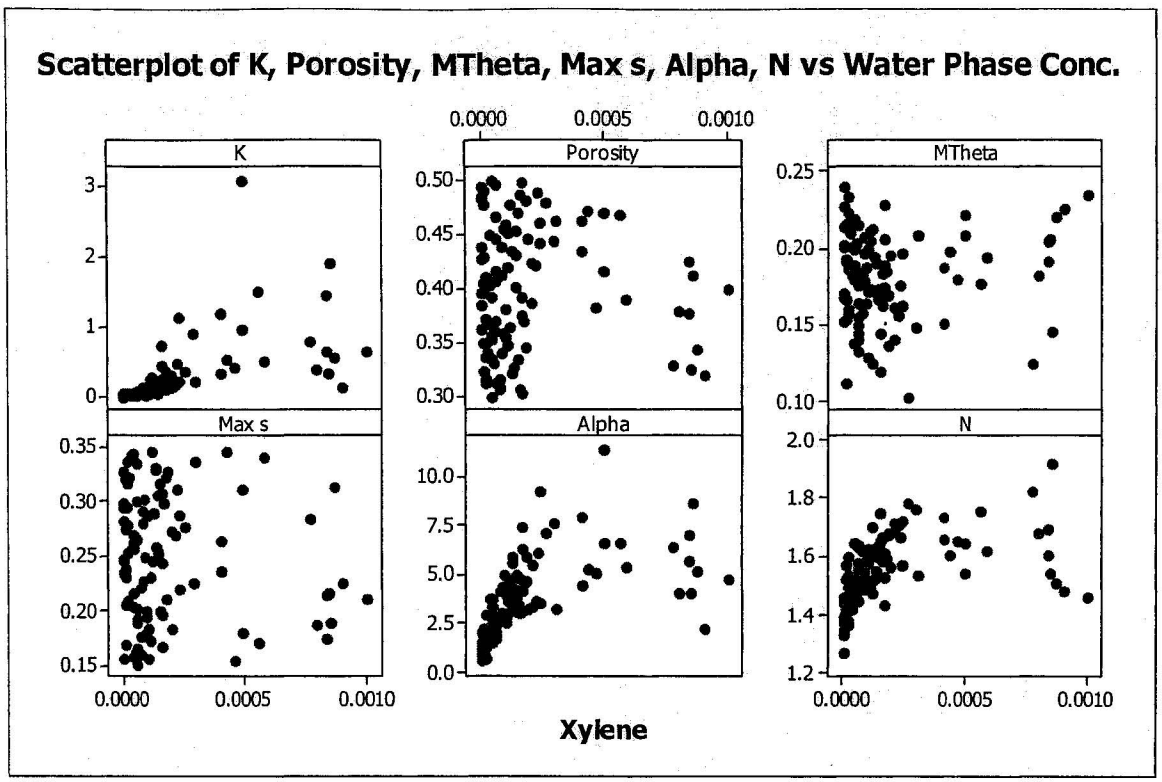
Scatterplot of K, Porosity, MTheta, Max s, Alpha, N vs Water Phase Conc.
K
Porosity
MTheta
Max s
Alpha
N
Xylene

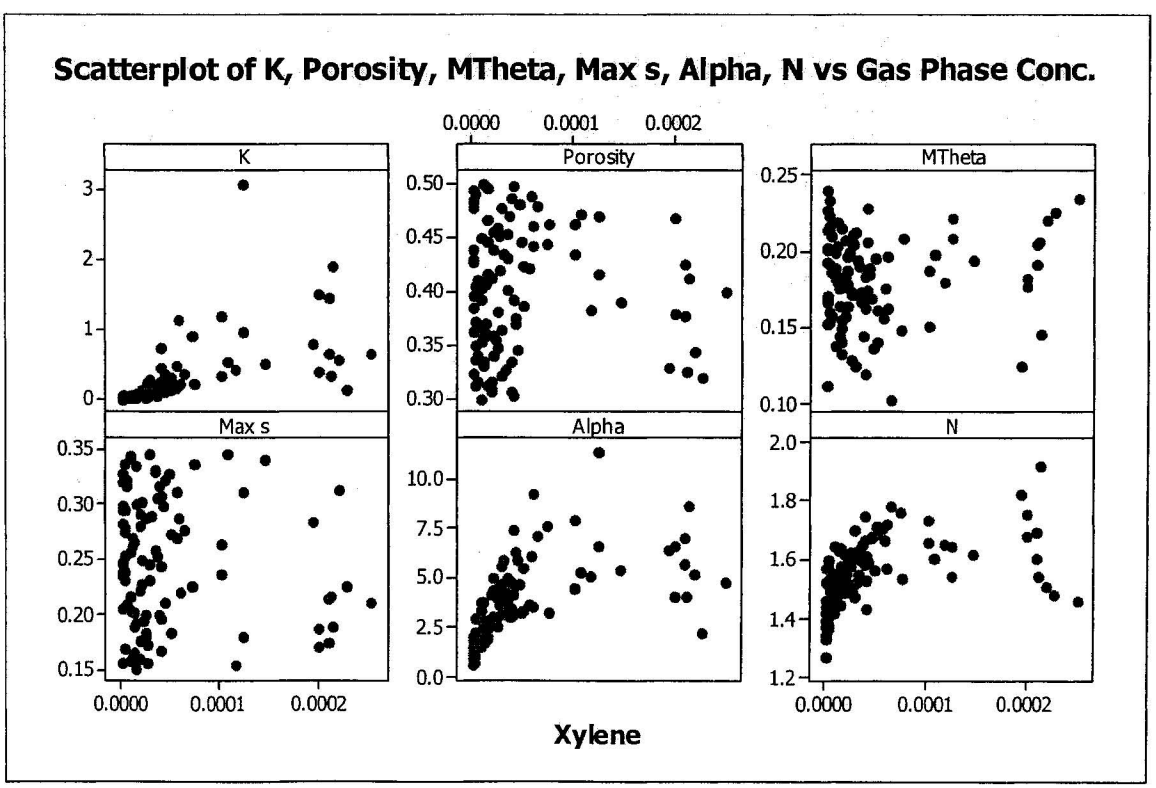
Scatterplot of K, Porosity, MTheta, Max s, Alpha, N vs Gas Phase Conc.
K
Porosity
MTheta
Max s
Alpha
N
Xylene

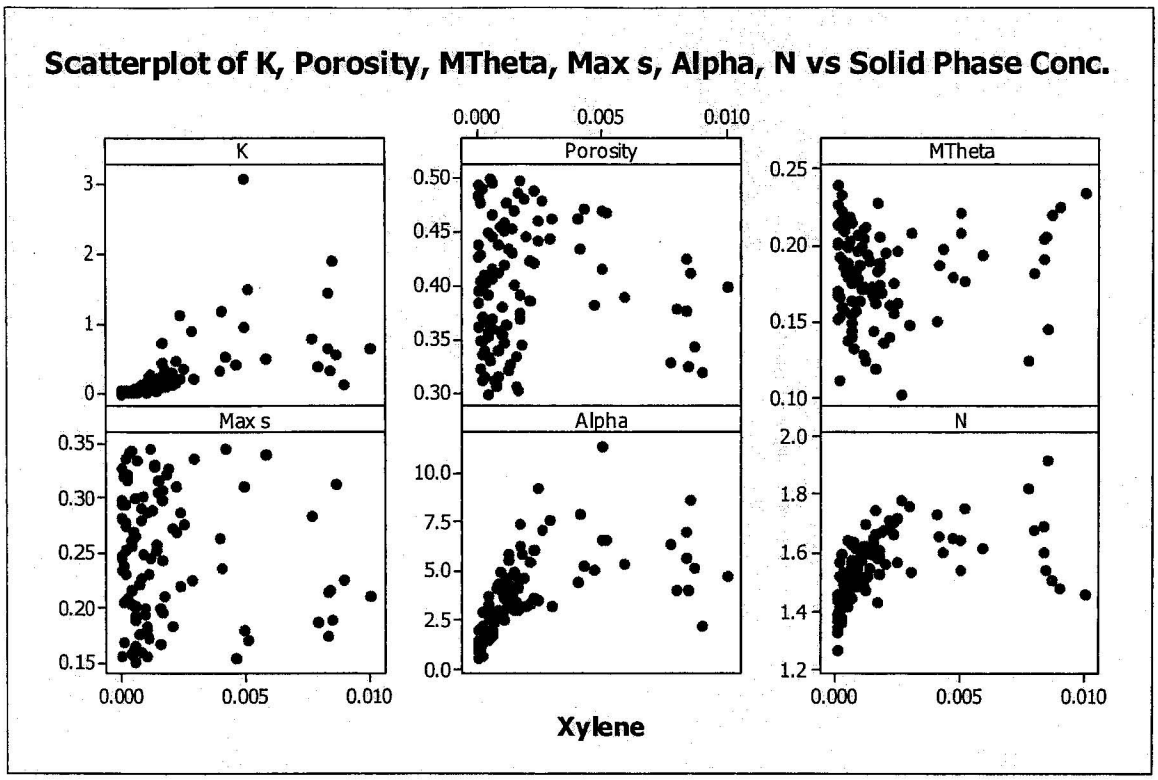
Scatterplot of K, Porosity, MTheta, Max s, Alpha, N vs Solid Phase Conc.
K
Porosity
MTheta
Max s
Alpha
N
0.000
0.005
0.010
Xylene

Scatter Plots for LHS-c Simulations

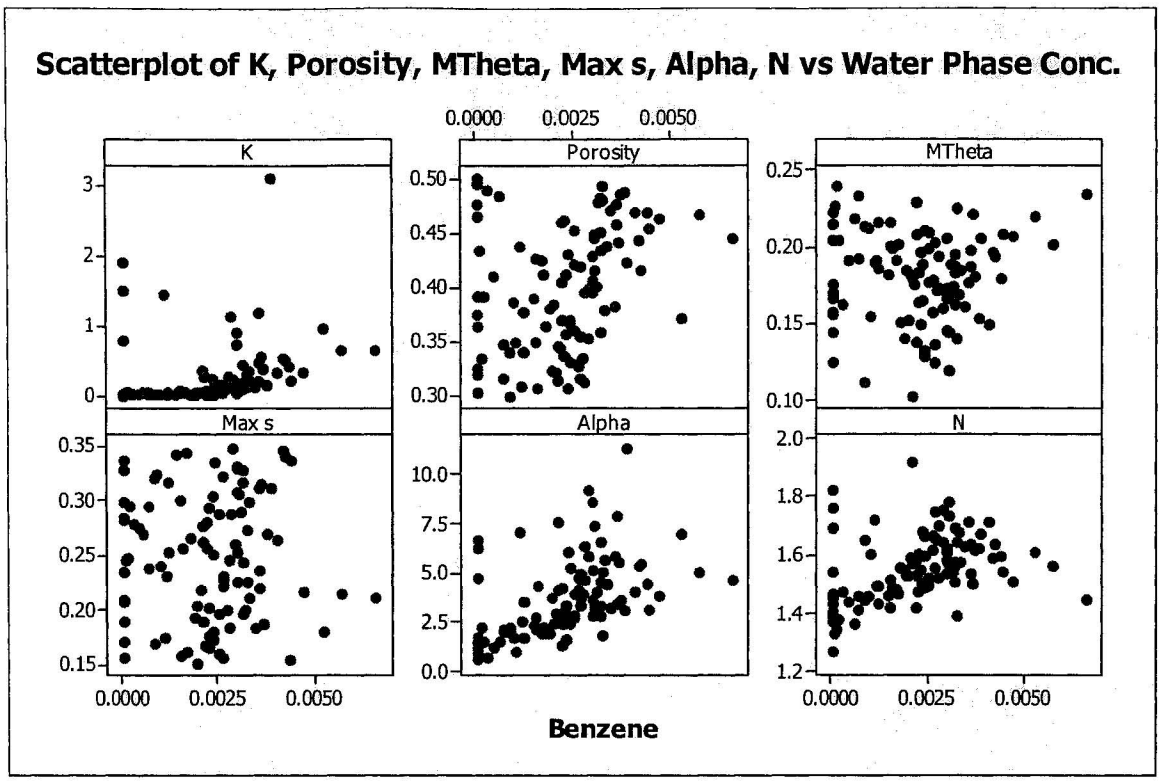
Scatterplot of K, Porosity, MTheta, Max s, Alpha, N vs Water Phase Conc.
K
Porosity
MTheta
Max s
Alpha
N
Benzene

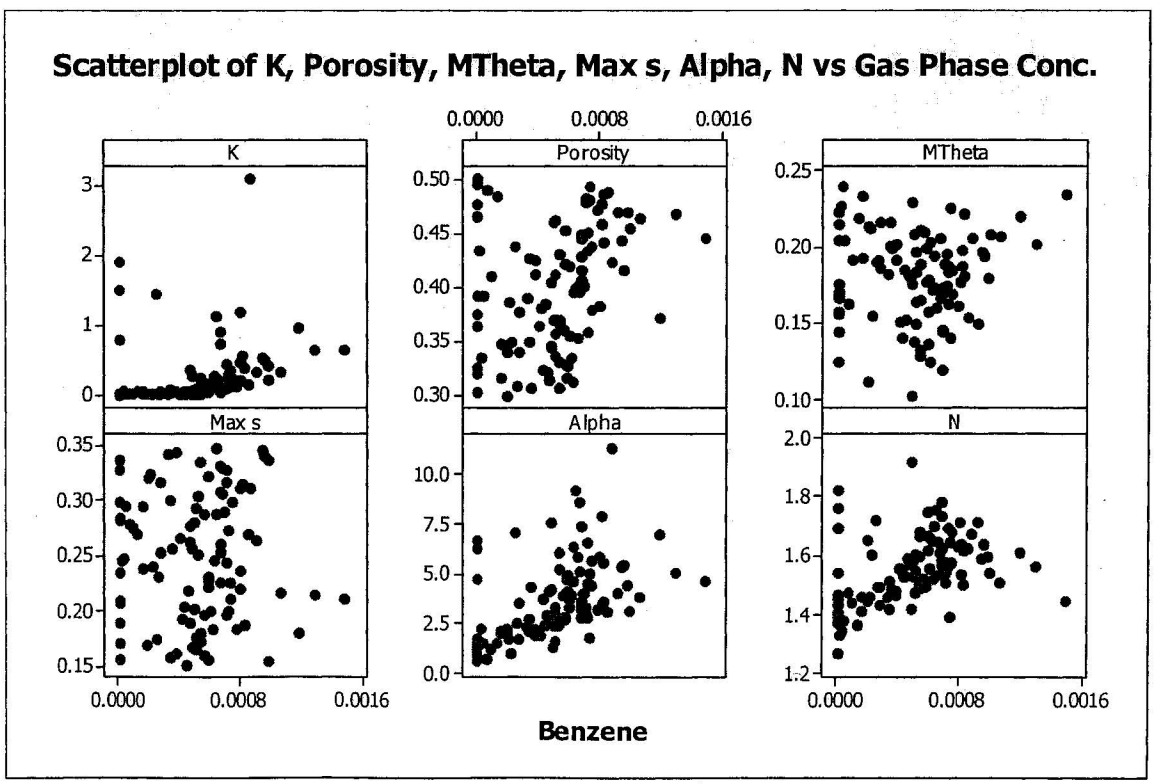
Scatterplot of K, Porosity, MTheta, Max s, Alpha, N vs Gas Phase Conc.
K
Porosity
MTheta
Max s
Alpha
N
Benzene

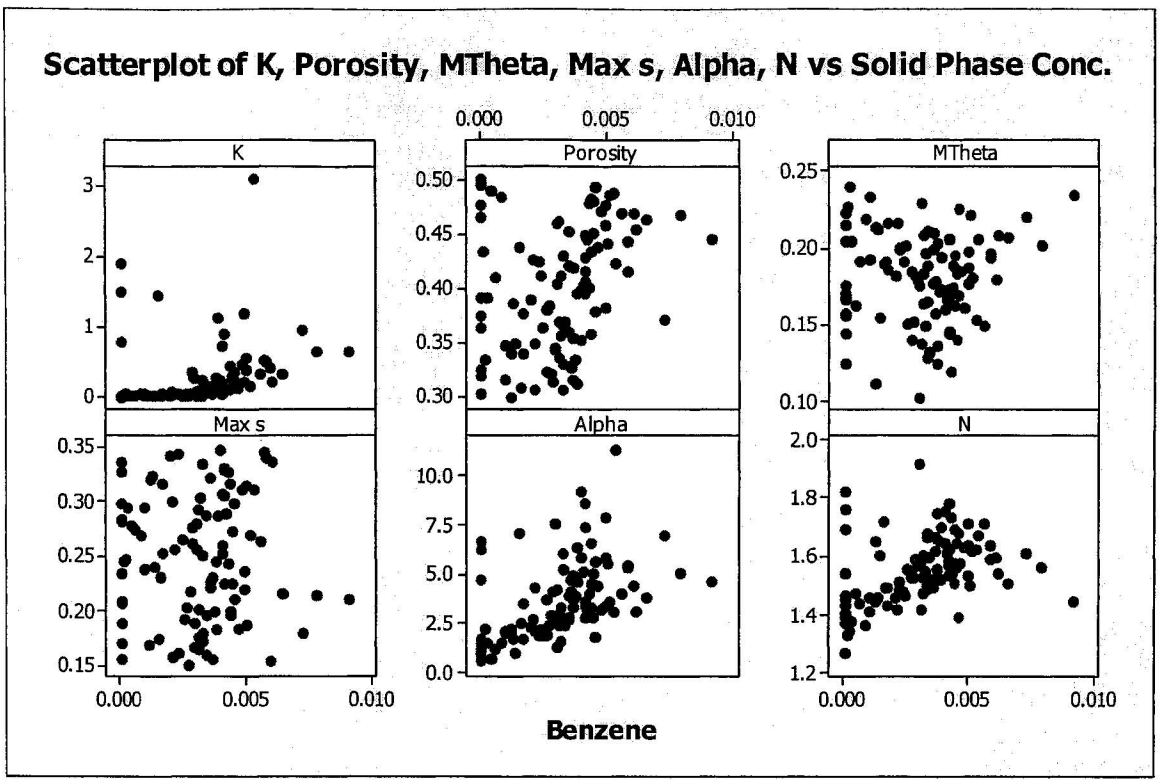
Scatterplot of K, Porosity, MTheta, Max s, Alpha, N vs Solid Phase Conc.
K
Porosity
MTheta
Max s
Alpha
N
Benzene

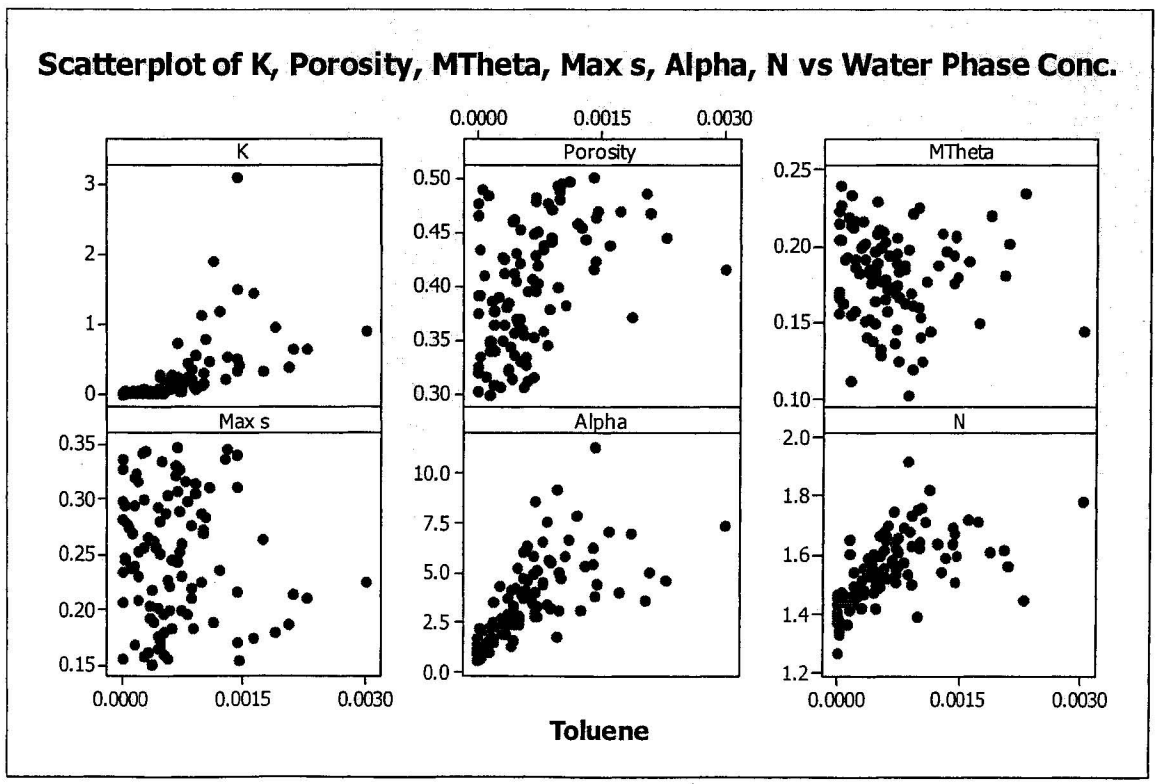
Scatterplot of K, Porosity, MTheta, Max s, Alpha, N vs Water Phase Conc.
K
Porosity
MTheta
Max s
Alpha
N
Toluene

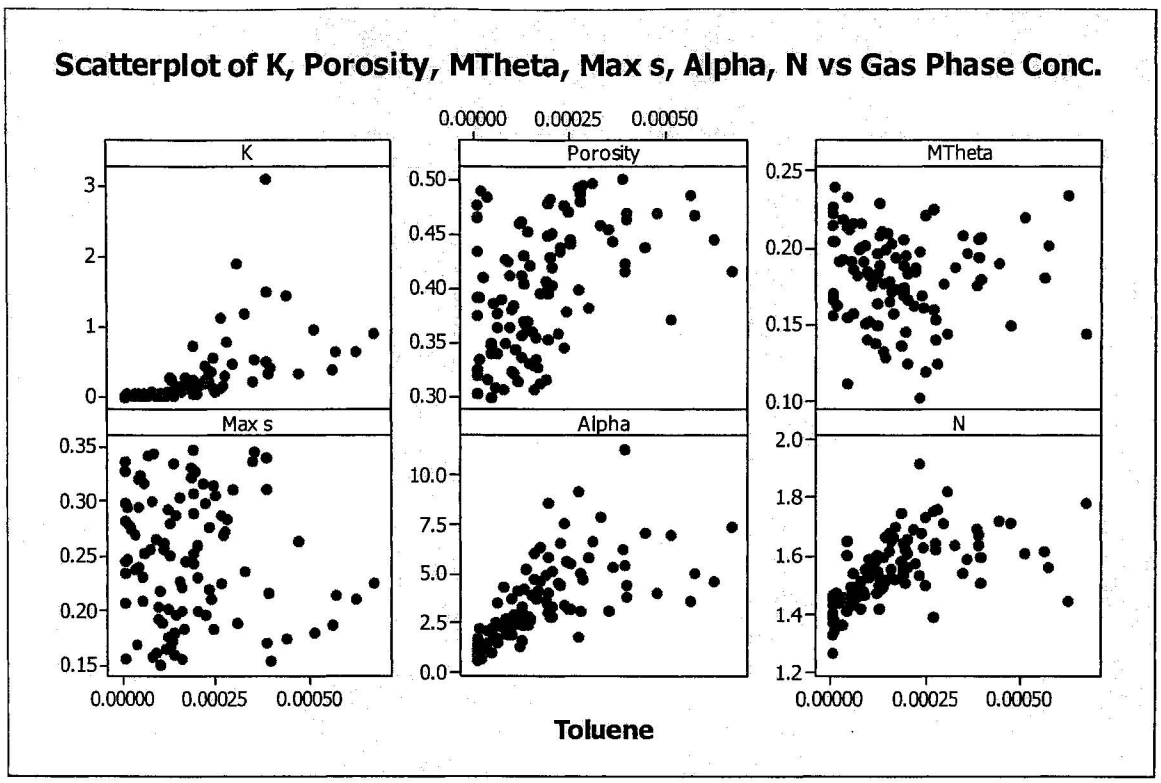
Scatterplot of K, Porosity, MTheta, Max s, Alpha, N vs Gas Phase Conc.
K
Porosity
MTheta
Max s
Alpha
N
Toluene

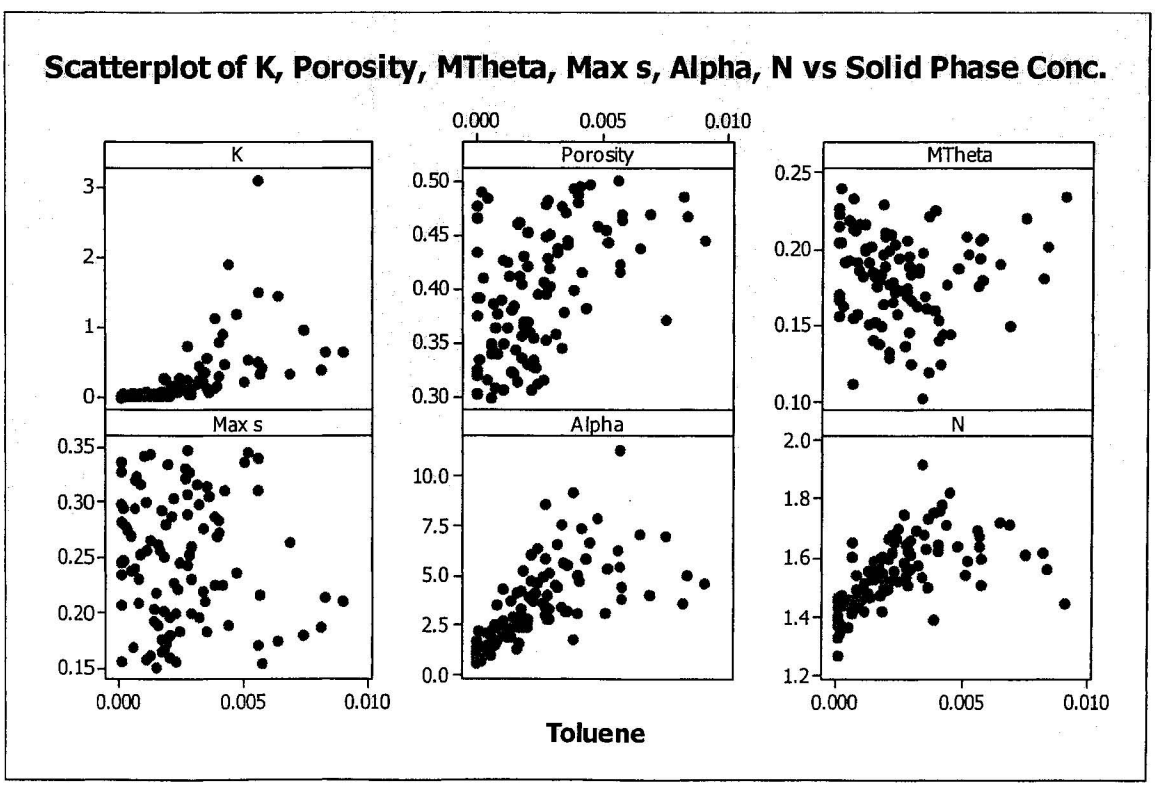
Scatterplot of K, Porosity, MTheta, Max s, Alpha, N vs Solid Phase Conc.
K
Porosity
MTheta
Max s
Alpha
N
Toluene

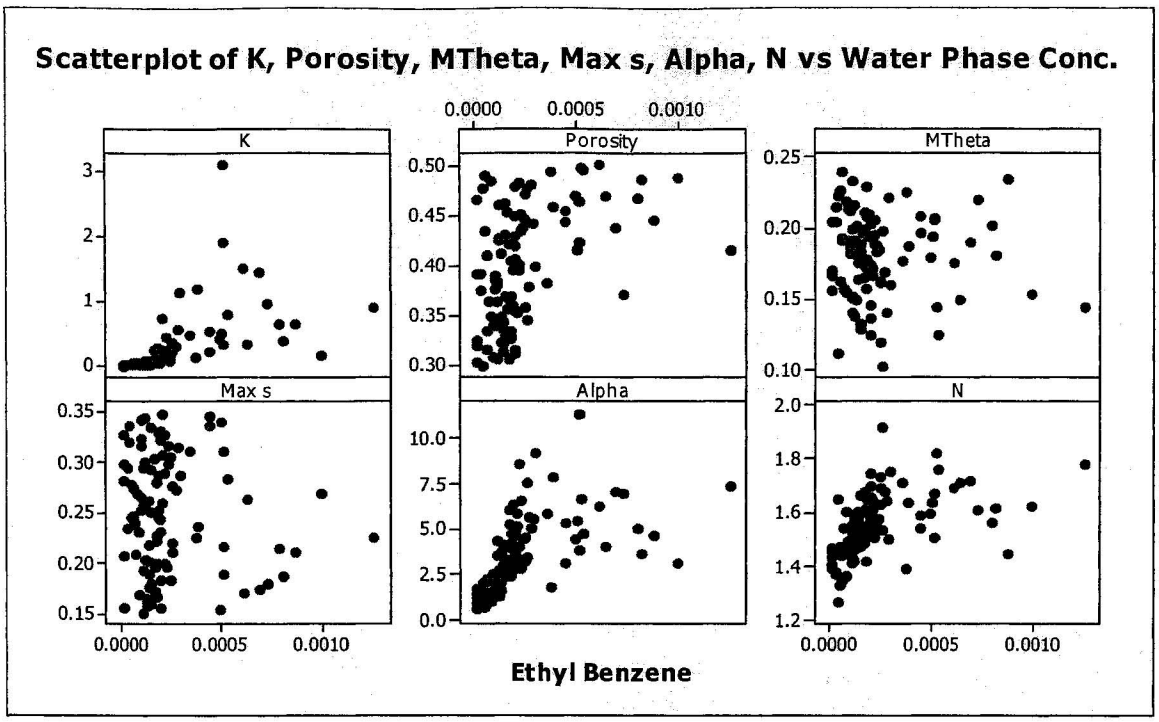
Scatterplot of K, Porosity, MTheta, Max s, Alpha, N vs Water Phase Conc.
K
Porosity
MTheta
Max s
Alpha
N
Ethyl Benzene

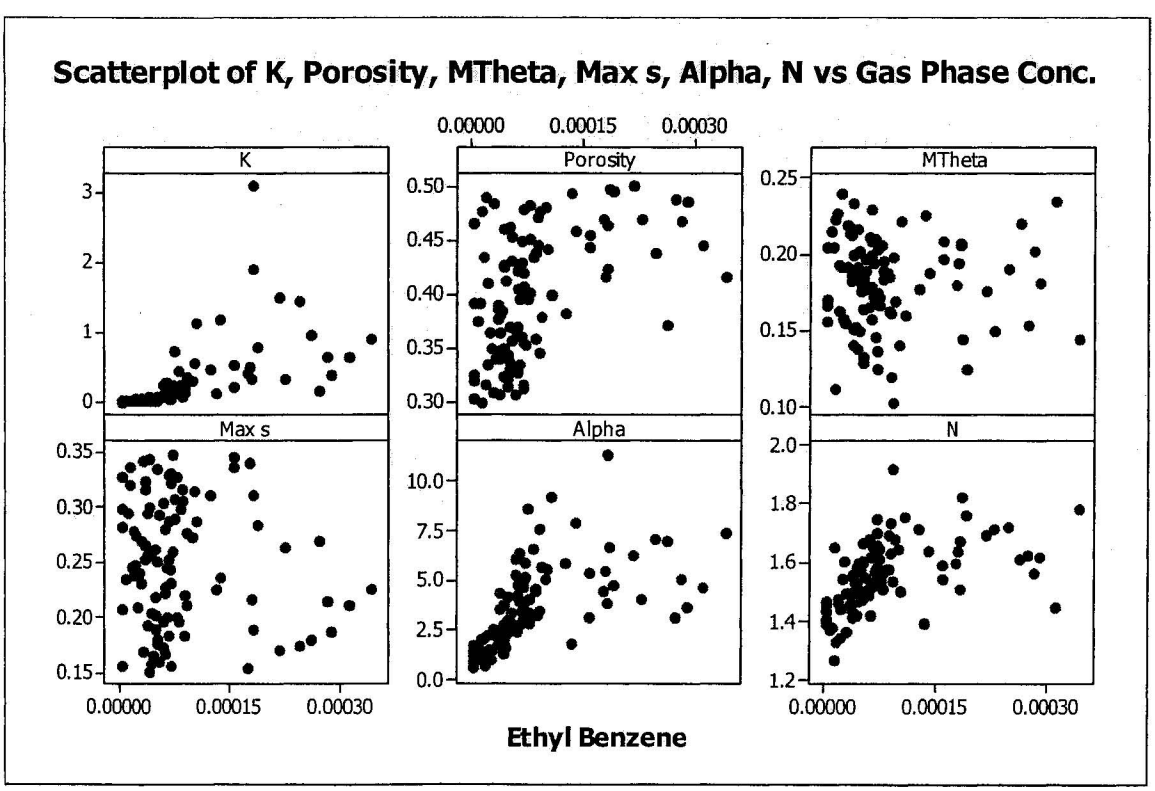
Scatterplot of K, Porosity, MTheta, Max s, Alpha, N vs Gas Phase Conc.
K
Porosity
MTheta
Max s
Alpha
N
Ethyl Benzene

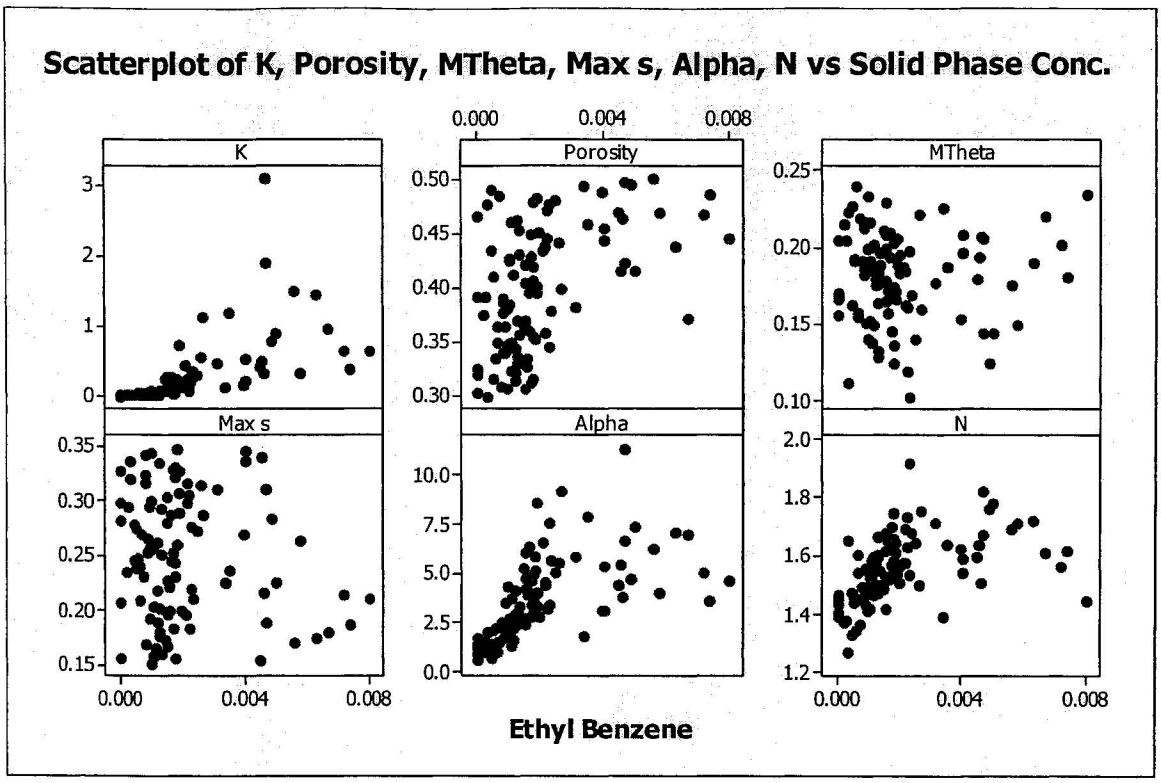
Scatterplot of K, Porosity, MTheta, Max s, Alpha, N vs Solid Phase Conc.
K
Porosity
MTheta
Max s
Alpha
N
Ethyl Benzene

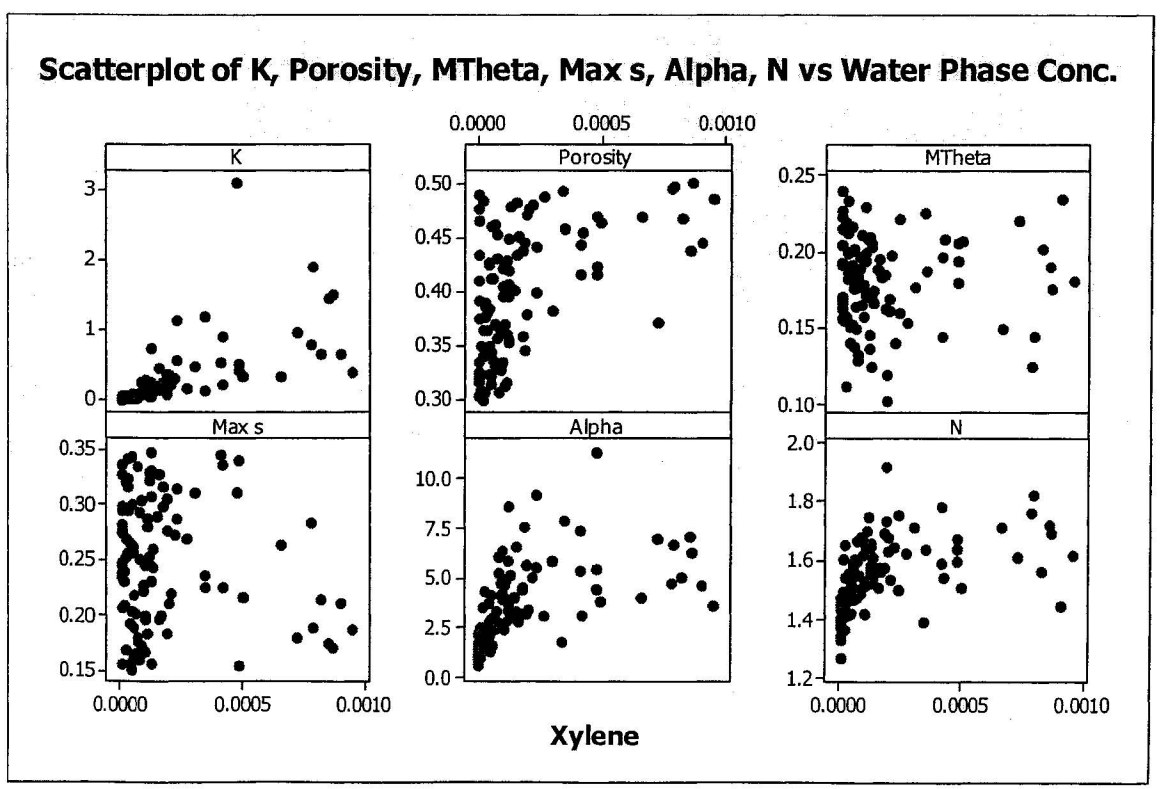
Scatterplot of K, Porosity, MTheta, Max s, Alpha, N vs Water Phase Conc.
K
Porosity
MTheta
Max s
Alpha
N
Xylene

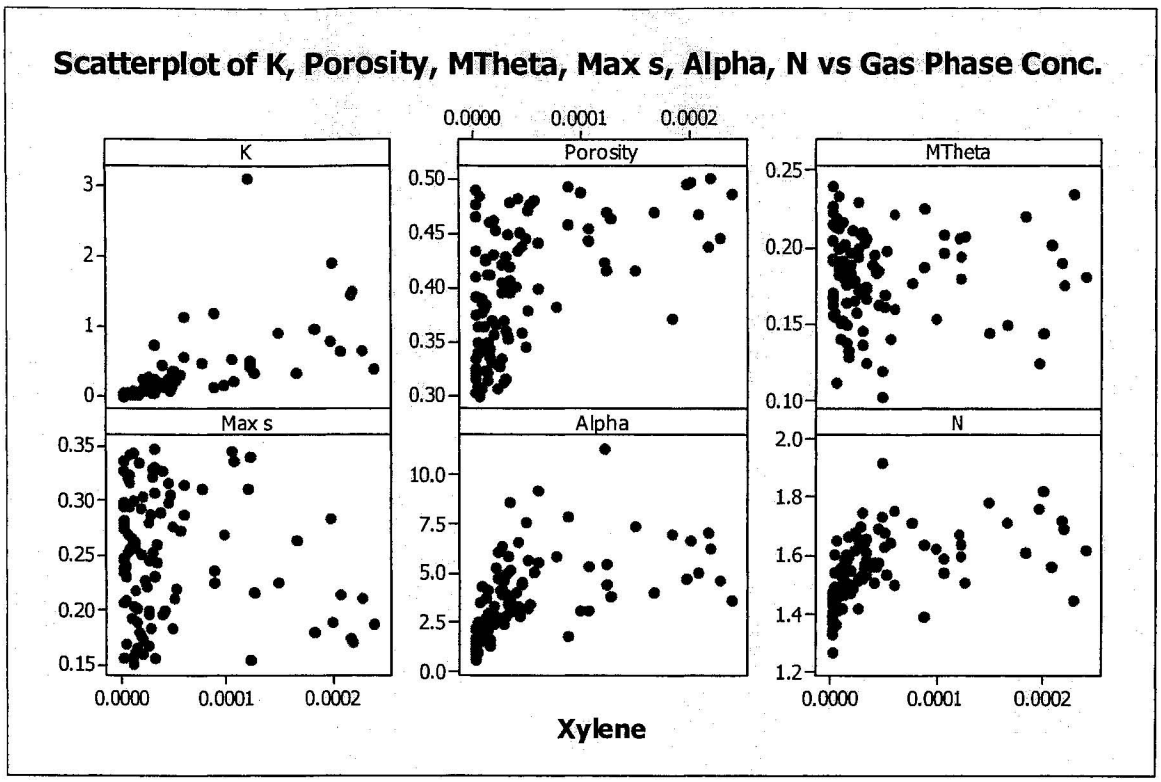
Scatterplot of K, Porosity, MTheta, Max s, Alpha, N vs Gas Phase Conc.
K
Porosity
MTheta
Max s
Alpha
N
Xylene

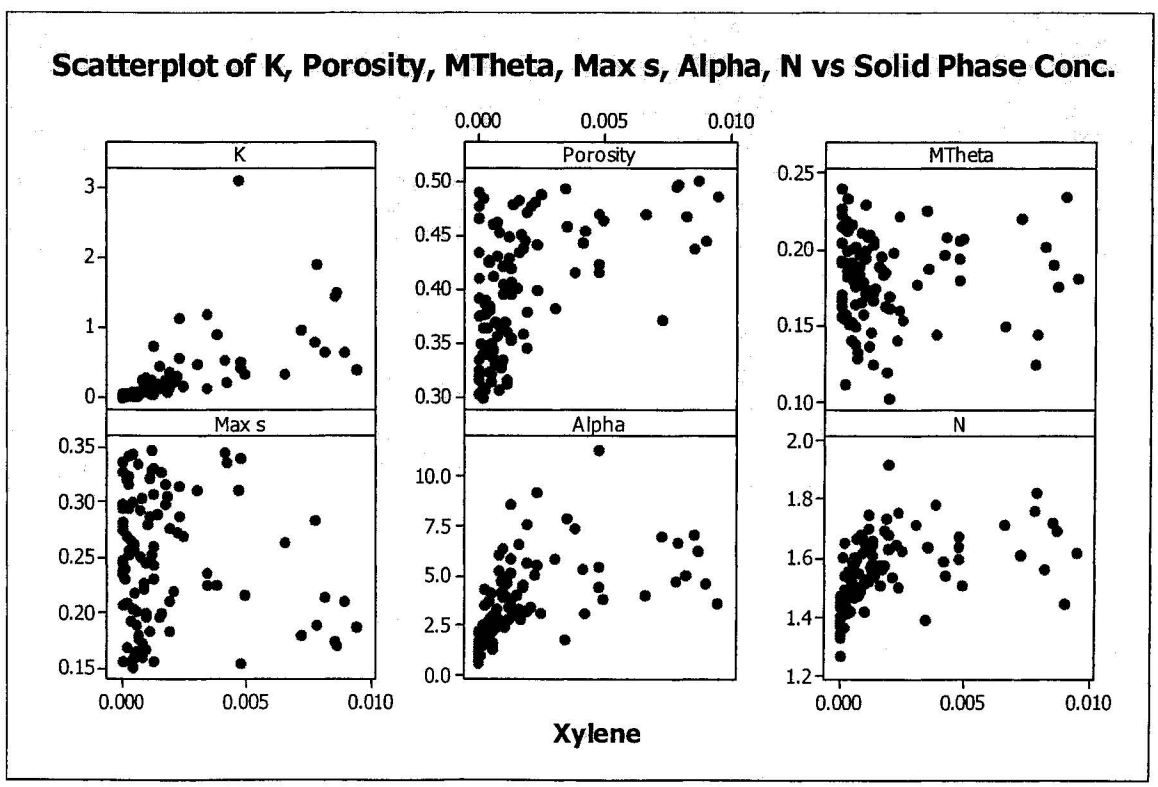
Scatterplot of K, Porosity, MTheta, Max s, Alpha, N vs Solid Phase Conc.
K
Porosity
MTheta
Max s
Alpha
N
Xylene

Scatter Plots for LHS-p Simulations

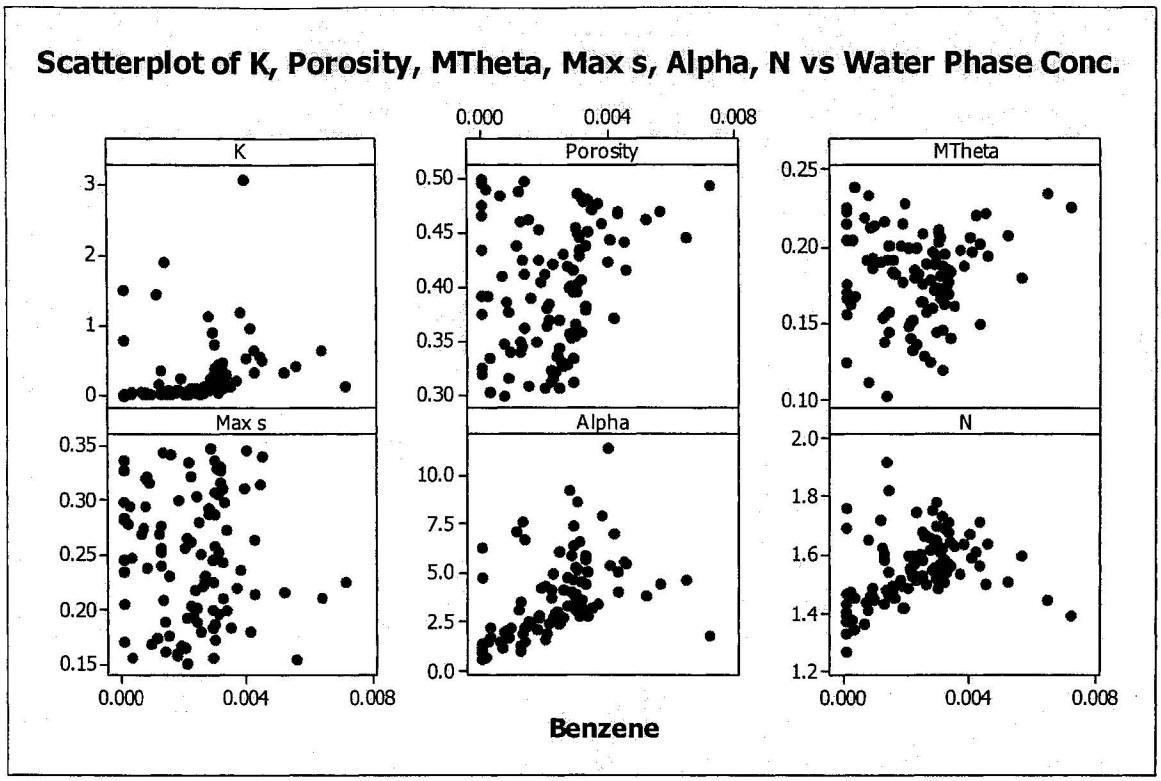
Scatterplot of K, Porosity, MTheta, Max s, Alpha, N vs Water Phase Conc.
K
Porosity
MTheta
Max s
Alpha
N
Benzene

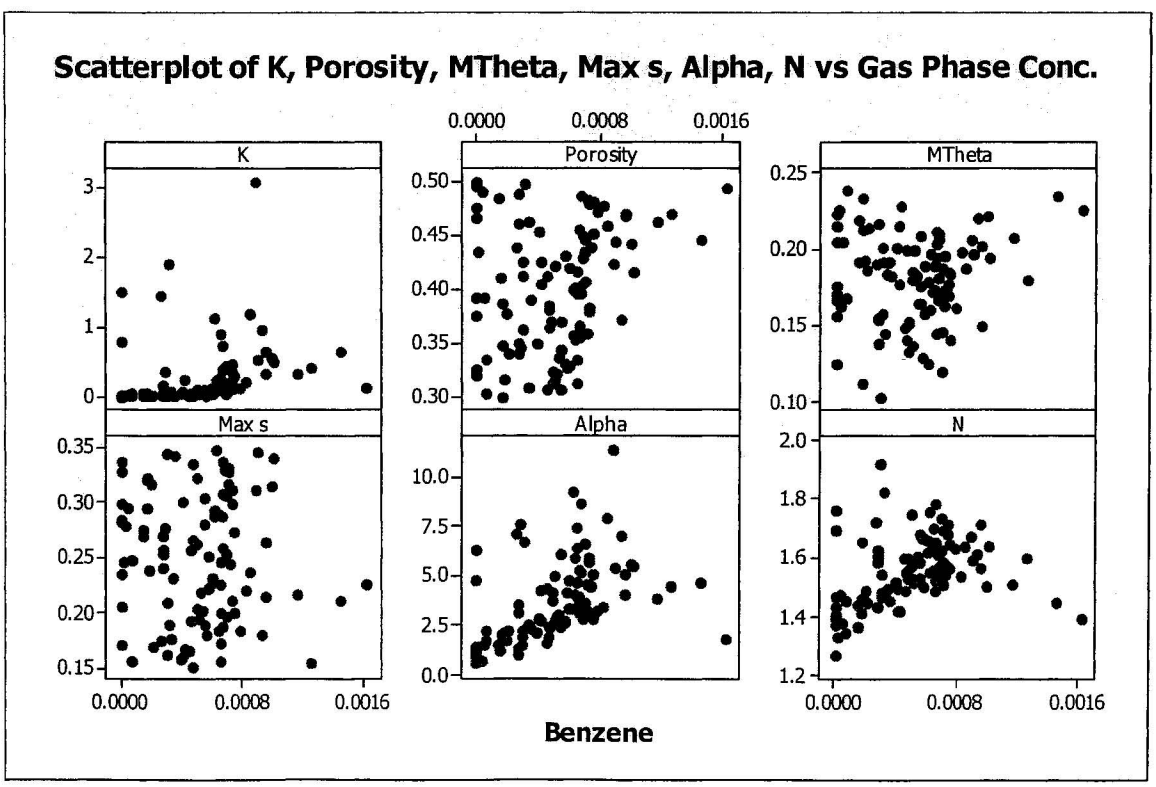
Scatterplot of K, Porosity, MTheta, Max s, Alpha, N vs Gas Phase Conc.
K
Porosity
MTheta
Max s
Alpha
N
Benzene

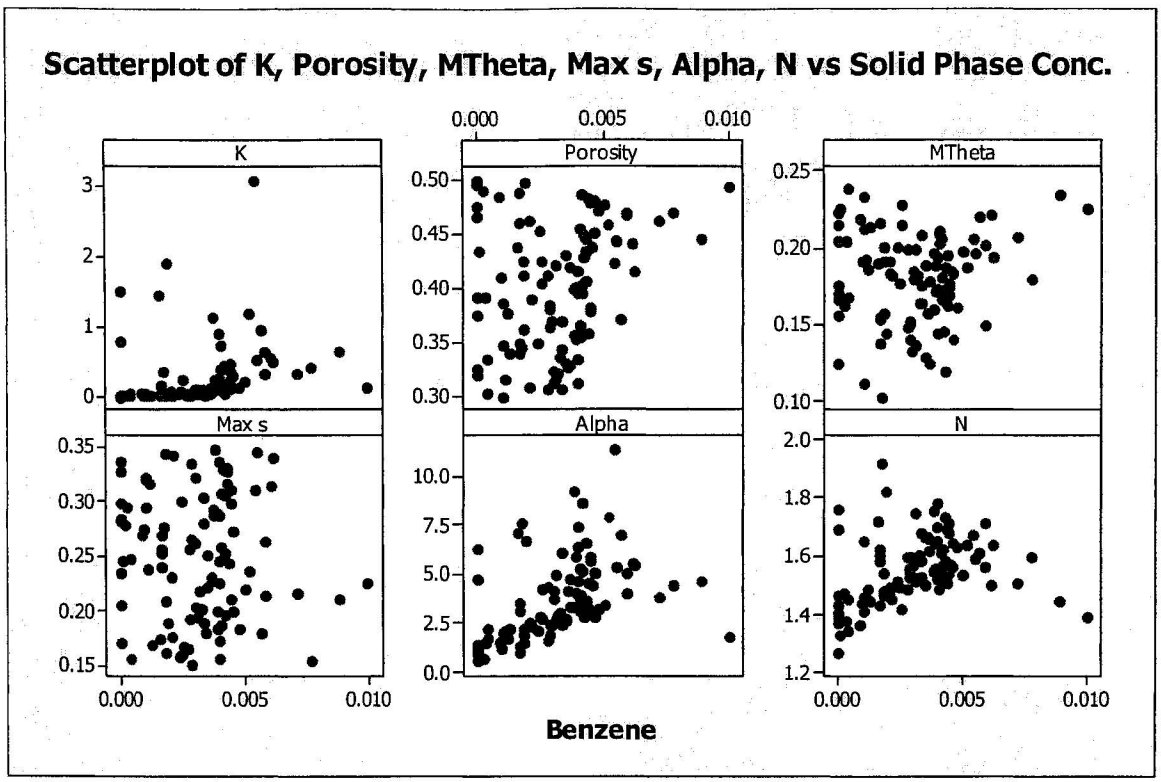
Scatterplot of K, Porosity, MTheta, Max s, Alpha, N vs Solid Phase Conc.
K
Porosity
MTheta
Max s
Alpha
N
Benzene

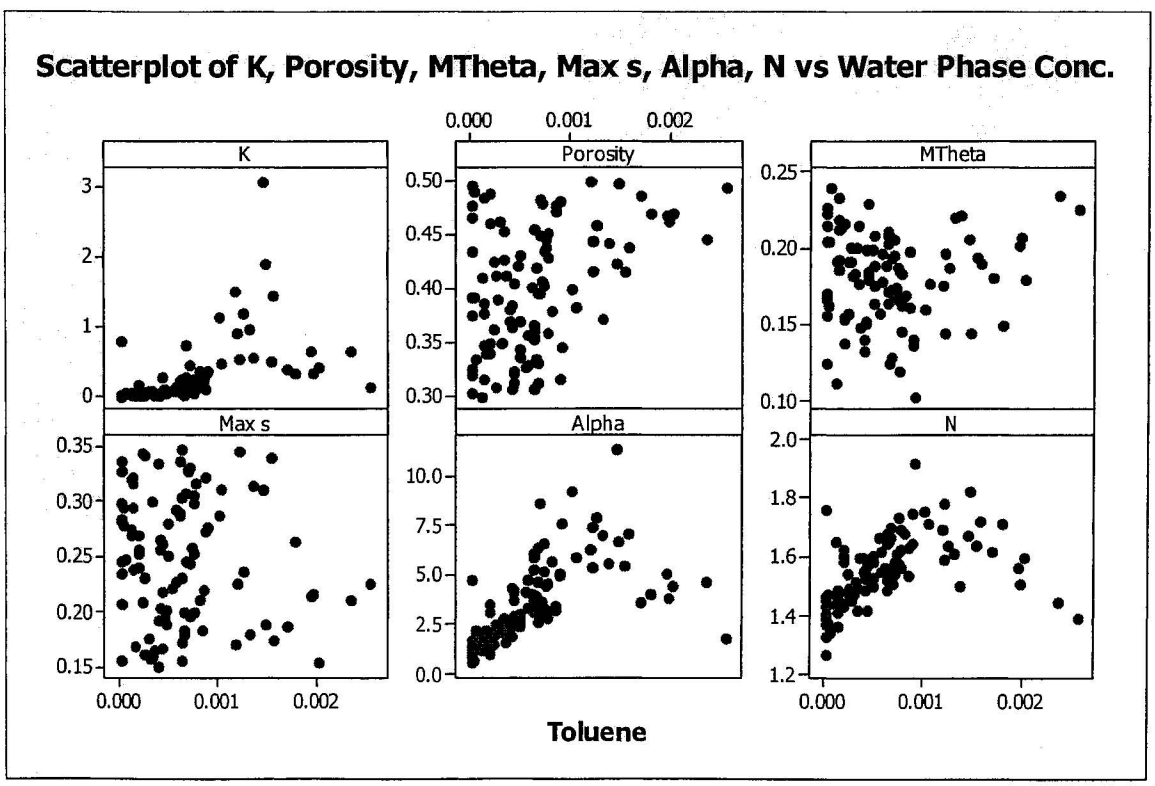
Scatterplot of K, Porosity, MTheta, Max s, Alpha, N vs Water Phase Conc.
K
Porosity
MTheta
Max s
Alpha
N
Toluene

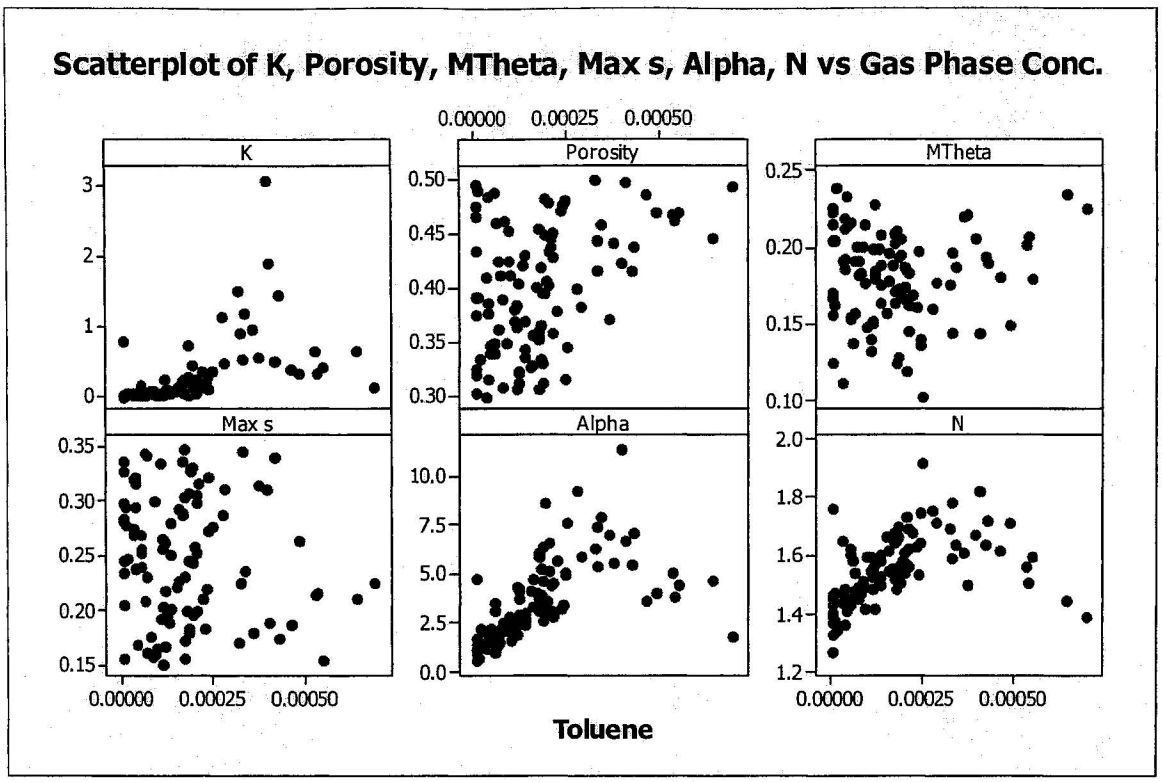
Scatterplot of K, Porosity, MTheta, Max s, Alpha, N vs Gas Phase Conc.
K
Porosity
MTheta
Max s
Alpha
N
0.00000 0.00025 0.00050
Toluene

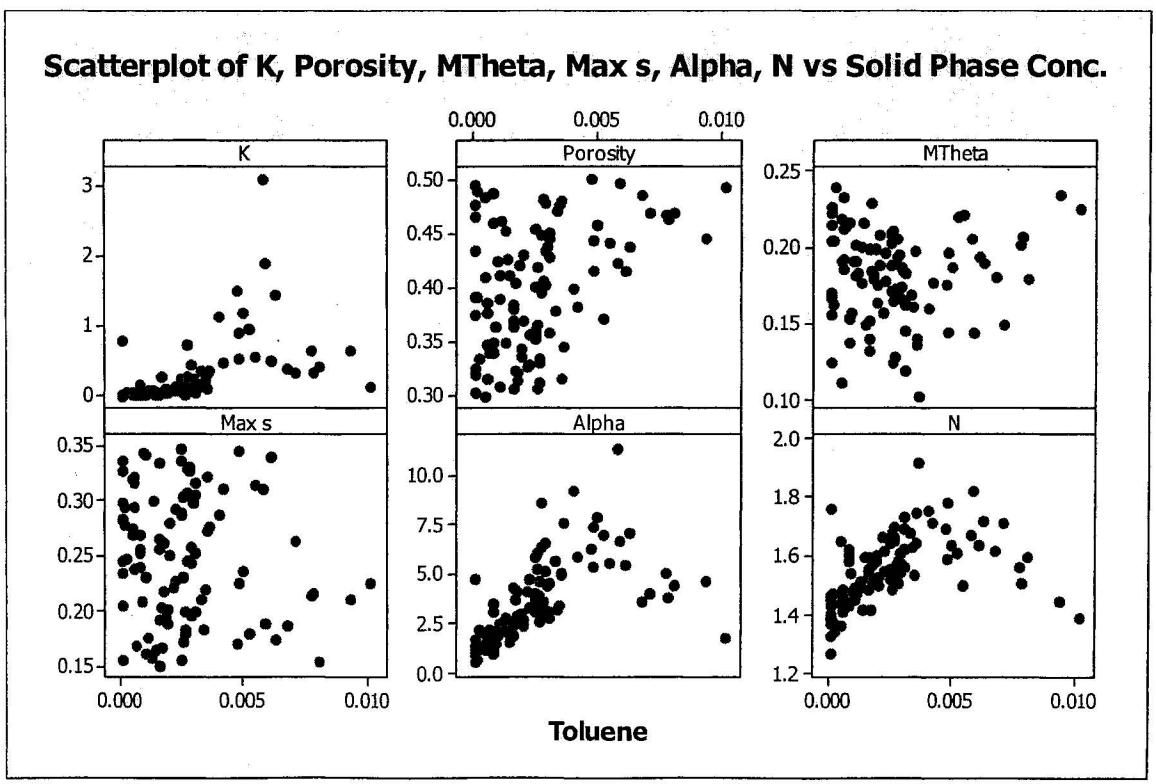
Scatterplot of K, Porosity, MTheta, Max s, Alpha, N vs Solid Phase Conc.
K
Porosity
MTheta
Max s
Alpha
N
0.000 0.005 0.010
Toluene

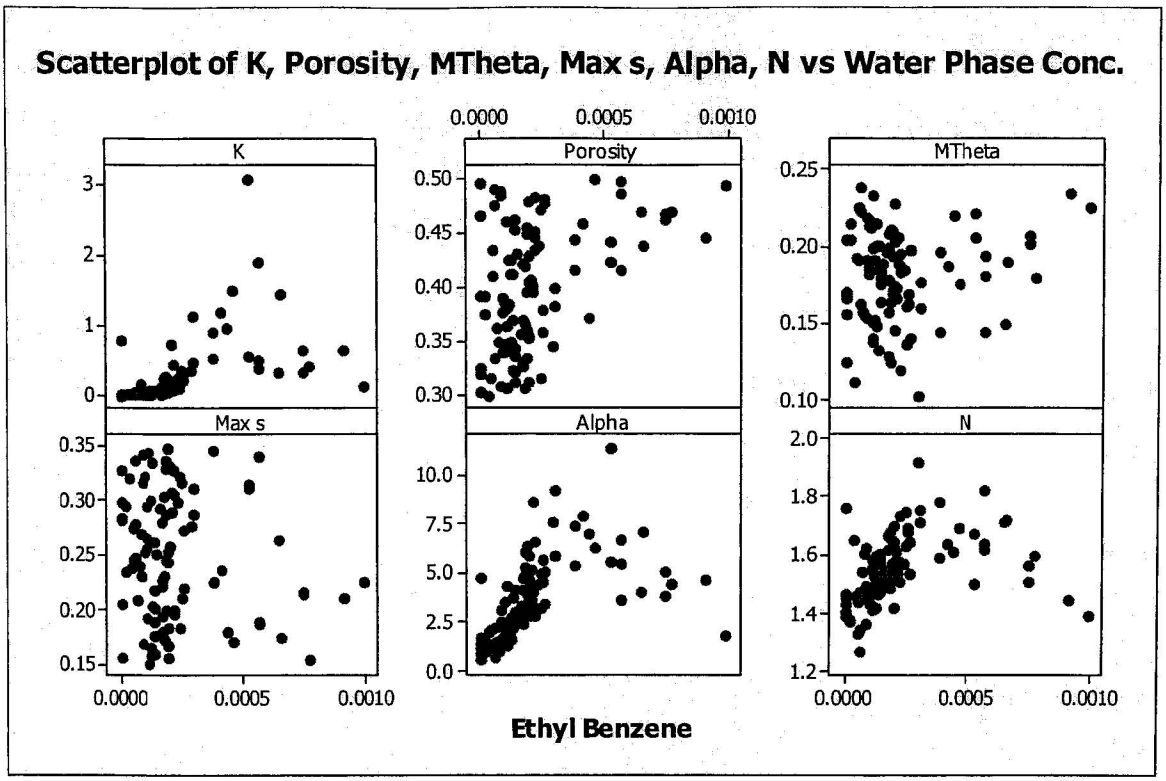
Scatterplot of K, Porosity, MTheta, Max s, Alpha, N vs Water Phase Conc.
K
Porosity
MTheta
Max s
Alpha
N
Ethyl Benzene

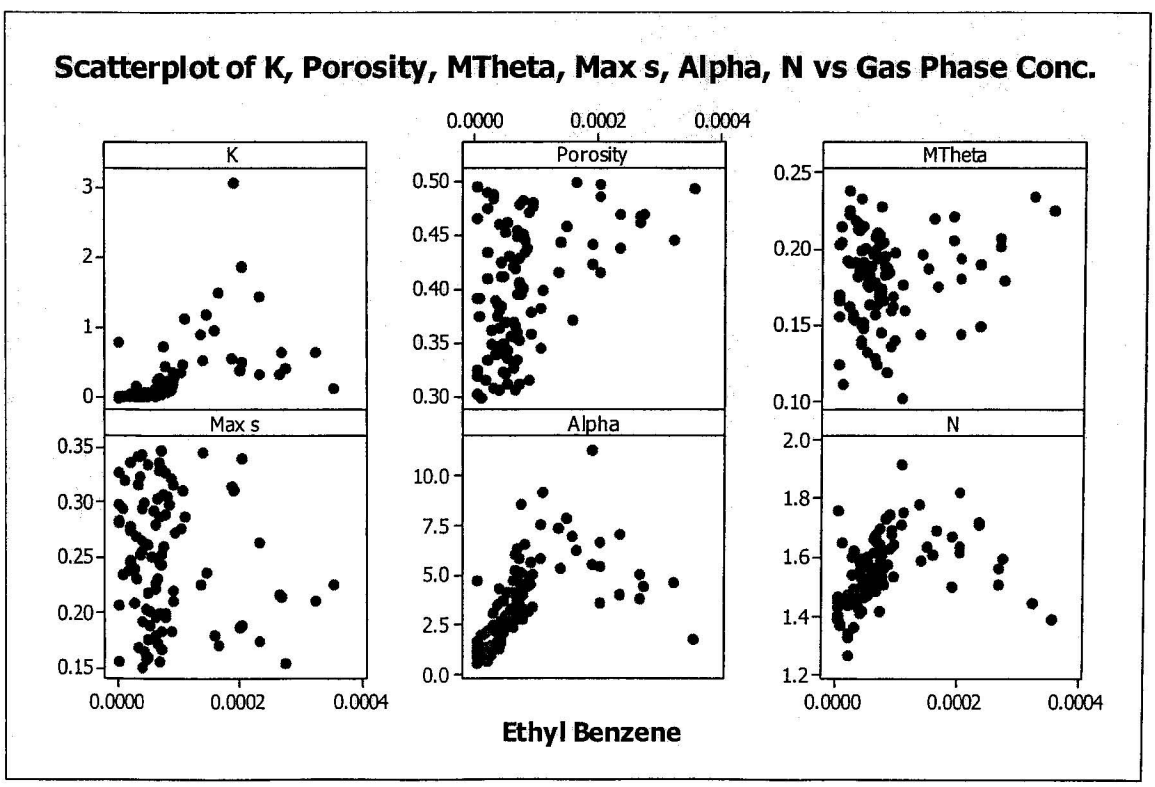
Scatterplot of K, Porosity, MTheta, Max s, Alpha, N vs Gas Phase Conc.
K
Porosity
MTheta
Max s
Alpha
N
Ethyl Benzene

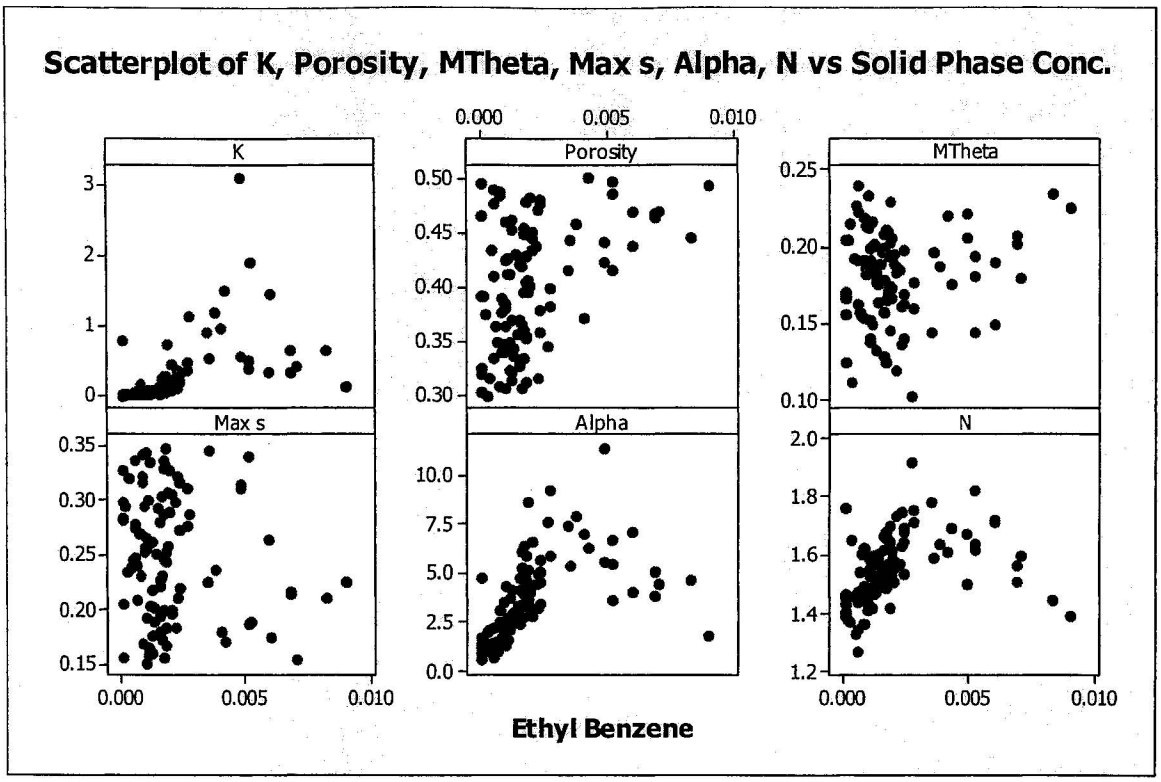
Scatterplot of K, Porosity, MTheta, Max s, Alpha, N vs Solid Phase Conc.
K
Porosity
MTheta
Max s
Alpha
N
Ethyl Benzene

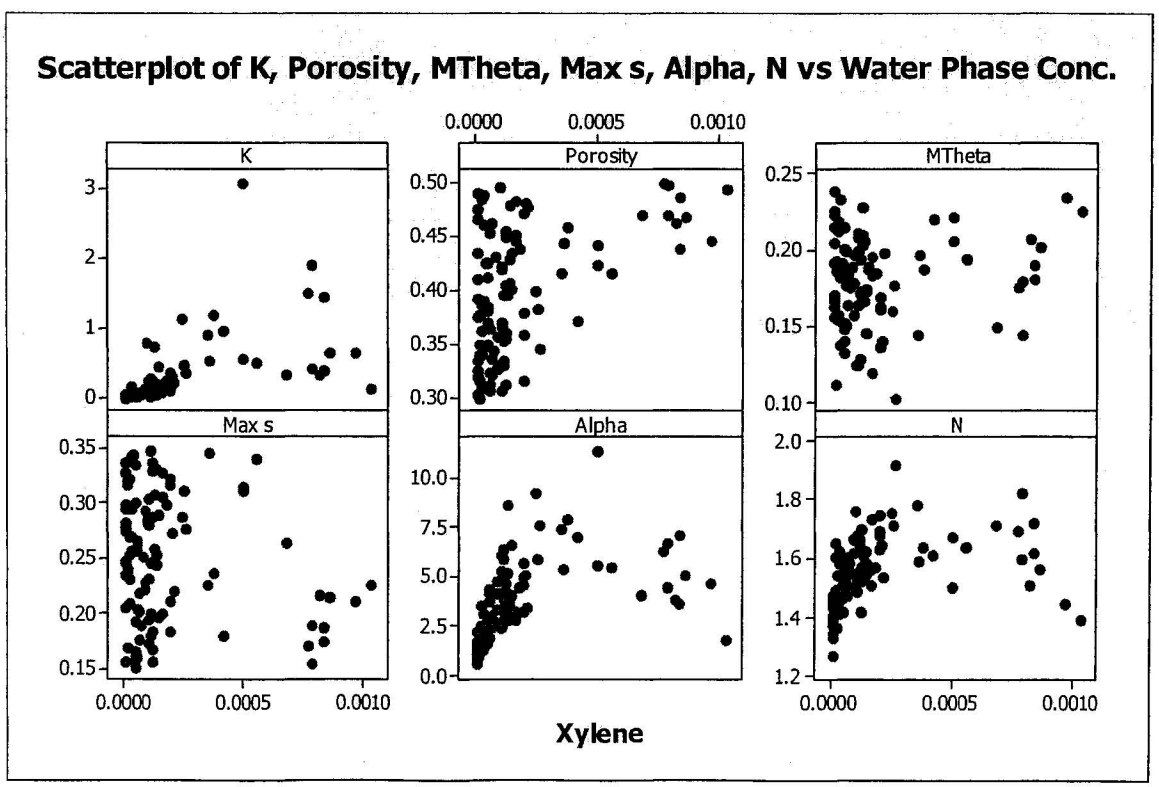
Scatterplot of K, Porosity, MTheta, Max s, Alpha, N vs Water Phase Conc.
K
Porosity
MTheta
Max s
Alpha
N
Xylene

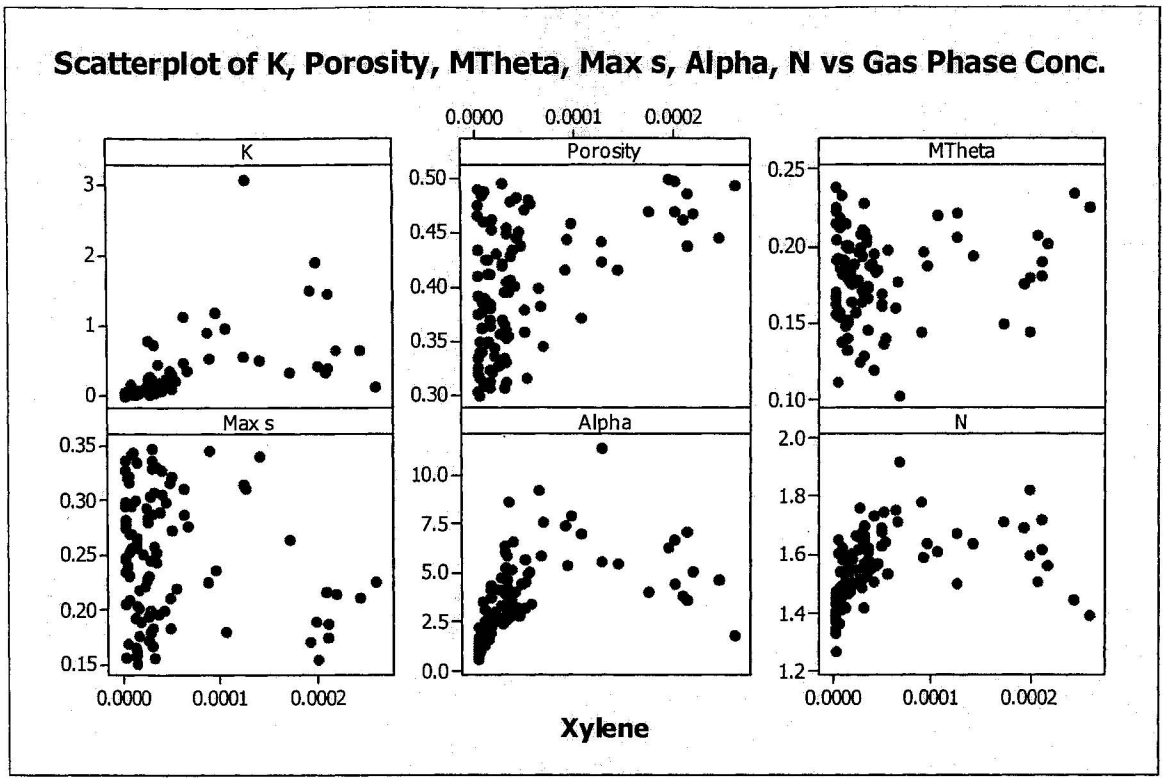
Scatterplot of K, Porosity, MTheta, Max s, Alpha, N vs Gas Phase Conc.
K
Porosity
MTheta
Max s
Alpha
N
Xylene

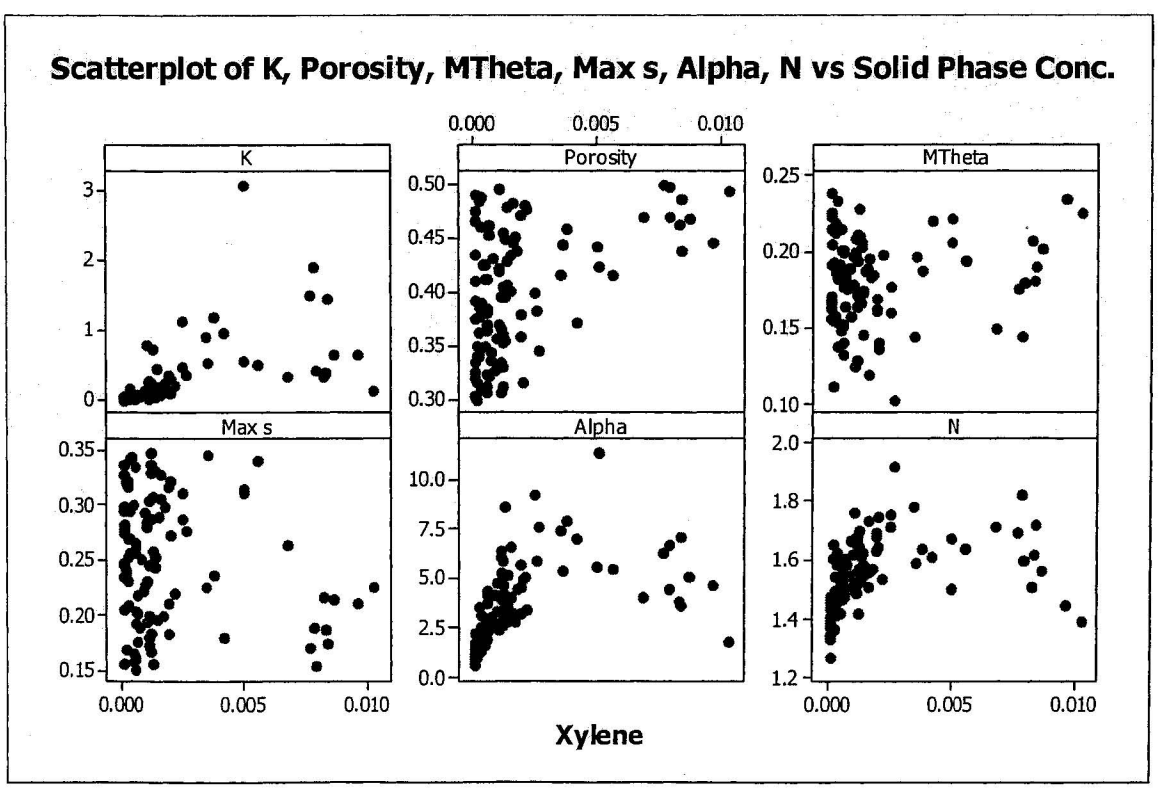
Scatterplot of K, Porosity, MTheta, Max s, Alpha, N vs Solid Phase Conc.
K
Porosity
MTheta
Max s
Alpha
N
Xylene